Automatic transcription of polyphonic music exploiting temporal evolution

Benetos, E

PhD thesis

Automatic Transcription of Polyphonic Music Exploiting Temporal Evolution

Emmanouil Benetos

School of Electronic Engineering and Computer Science
Queen Mary University of London

2012

I certify that this thesis, and the research to which it refers, are the product of my own work, and that any ideas or quotations from the work of other people, published or otherwise, are fully acknowledged in accordance with the standard referencing practices of the discipline. I acknowledge the helpful guidance and support of my supervisor, Dr Simon Dixon.

Abstract

Automatic music transcription is the process of converting an audio recording into a symbolic representation using musical notation. It has numerous applications in music information retrieval, computational musicology, and the creation of interactive systems. Even for expert musicians, transcribing polyphonic pieces of music is not a trivial task, and while the problem of automatic pitch estimation for monophonic signals is considered to be solved, the creation of an automated system able to transcribe polyphonic music without setting restrictions on the degree of polyphony and the instrument type still remains open.

In this thesis, research on automatic transcription is performed by explicitly incorporating information on the temporal evolution of sounds. First efforts address the problem by focusing on signal processing techniques and by proposing audio features utilising temporal characteristics. Techniques for note onset and offset detection are also utilised for improving transcription performance. Subsequent approaches propose transcription models based on shift-invariant probabilistic latent component analysis (SI-PLCA), modeling the temporal evolution of notes in a multiple-instrument case and supporting frequency modulations in produced notes. Datasets and annotations for transcription research have also been created during this work. Proposed systems have been privately as well as publicly evaluated within the Music Information Retrieval Evaluation eXchange (MIREX) framework. Proposed systems have been shown to outperform several state-of-the-art transcription approaches.

Developed techniques have also been employed for other tasks related to music technology, such as for key modulation detection, temperament estimation, and automatic piano tutoring. Finally, proposed music transcription models have also been utilized in a wider context, namely for modeling acoustic scenes.

Acknowledgements

First and foremost, I would like to thank my supervisor, Simon Dixon, for three years of sound advice, his cheerful disposition, for providing me with a great deal of freedom to explore the topics of my choice and work on the research areas that interest me the most. I would like to also thank Anssi Klapuri and Mark Plumbley for their extremely detailed feedback, and for their useful advice that helped shape my research.

A big thanks to the members (past and present) of the Centre for Digital Music who have made these three years easily my most pleasant research experience. Special thanks to Amélie Anglade, Matthias Mauch, Lesley Mearns, Dan Tidhar, Dimitrios Giannoulis, Holger Kirchhoff, and Dan Stowell for their expertise and help that has led to joint publications and work. Thanks also to Mathieu Lagrange for a very nice stay at IRCAM and to Arshia Cont for making it possible.

There are so many other people from C4DM that I am grateful to, including (but not limited to): Daniele Barchiesi, Mathieu Barthet, Magdalena Chudy, Alice Clifford, Matthew Davies, Joachim Ganseman, Steven Hargreaves, Robert Macrae, Boris Mailhé, Martin Morrell, Katy Noland, Ken O'Hanlon, Steve Welburn, and Asterios Zacharakis. Thanks also to the following non-C4DM people for helping me with my work: Gautham Mysore, Masahiro Nakano, Romain Hennequin, Piotr Holonowicz, and Valentin Emiya.

I would like to also thank the people from the QMUL IEEE student branch: Yiannis Patras, Sohaib Qamer, Xian Zhang, Yading Song, Ammar Lilamwala, Bob Chew, Sabri-E-Zaman, Amna Wahid, and Roya Haratian. A big thanks to Margarita for the support and the occasional proofreading! Many thanks finally to my family and friends for simply putting up with me all this time!

This work was funded by a Queen Mary University of London Westfield Trust Research Studentship.

Contents

List of Figures

List of Tables

List of Abbreviations

ALS	Alternating Least Squares
AMT	Automatic Music Transcription
ARMA	AutoRegressive Moving Average
ASR	Automatic Speech Recognition
BLSTM	Bidirectional Long Short-Term Memory
BOF	Bag-of-frames
CAM	Common Amplitude Modulation
CASA	Computational Auditory Scene Analysis
CQT	Constant-Q Transform
CRF	Conditional Random Fields
DBNs	Dynamic Bayesian Networks
DFT	Discrete Fourier Transform
EM	Expectation Maximization
ERB	Equivalent Rectangular Bandwidth
FFT	Fast Fourier Transform
GMMs	Gaussian Mixture Models
HMMs	Hidden Markov Models
HMP	Harmonic Matching Pursuit
HNNMA	Harmonic Non-Negative Matrix Approximation
HPS	Harmonic Partial Sequence
KL	Kullback-Leibler
MAP	Maximum A Posteriori
MCMC	Markov Chain Monte Carlo
MFCC	Mel-Frequency Cepstral Coefficient
MIR	Music Information Retrieval
ML	Maximum Likelihood
MP	Matching Pursuit

MUSIC	MUltiple Signal Classification
NHMM	Non-negative Hidden Markov Model
NMD	Non-negative Matrix Deconvolution
NMF	Non-negative Matrix Factorization
PDF	Probability Density Function
PLCA	Probabilistic Latent Component Analysis
PLTF	Probabilistic Latent Tensor Factorization
RTFI	Resonator Time-Frequency Image
SI-PLCA	Shift-Invariant Probabilistic Latent Component Analysis
STFT	Short-Time Fourier Transform
SVMs	Support Vector Machines
TCSI-PLCA	Temporally-constrained SI-PLCA
TDNNs	Time-Delay Neural Networks
VB	Variational Bayes

List of Variables

a	partial amplitude
$\alpha_t(q_t)$	forward variable
b_p	inharmonicity parameter for pitch p
B	RTFI segment for CAM feature
$\beta_t(q_t)$	backward variable
β	beta-divergence
$\boldsymbol{\mathcal{C}}$	Set of all possible f_0 combinations
δ_p	tuning deviation for pitch p
χ	exponential distribution parameter
$d_z(l, m)$	distance between acoustic scenes l and m for component z
$D(l, m)$	distance between two acoustic scenes l and m
$\Delta\phi$	phase difference
f_0	fundamental frequency
f	pitch impulse used in convolutive models
$f_{p,h}$	frequency for h-th harmonic of p-th pitch
γ	Euler constant
h	partial index
$\mathbf{H}$	activation matrix in NMF-based models
$HPS[p, h]$	harmonic partial sequence
j	spectral whitening parameter
λ	note tracking parameter
L	maximum polyphony level
μ	shifted log-frequency index for shift-invariant model
ν	time lag
$N[\omega, t]$	RTFI noise estimate
ω	frequency index
Ω	maximum frequency index

$\mathfrak{o}$	observation in HMMs for note tracking
p	pitch
$\mathfrak{p}$	chroma index
$\psi[p,t]$	Semitone-resolution filterbank for onset detection
$P(\cdot)$	probability
q	state in NHMM and variants for AMT
$\mathfrak{q}$	state in HMMs for note tracking
ρ	sparsity parameter in [Sma11]
ρ_1	sparsity parameter for source contribution
ρ_2	sparsity parameter for pitch activation
ϱ	peak scaling value for spectral whitening
s	Source index
S	Number of sources
$\mathcal{S}[p]$	pitch salience function
t	time index
T	Time length
τ	Shift in NMD model [Sma04a]
θ	floor parameter for spectral whitening
u	number of bins per octave
$\mathbf{V}$	spectrogram matrix in NMF-based models
$V_{\omega,t}$	spectrogram value at ω-th frequency and t-th frame
v	spectral frame
$\mathbf{W}$	basis matrix in NMF-based models
$x[n]$	discrete (sampled) domain signal
ξ	cepstral coefficient index
$X[\omega,t]$	Absolute value of RTFI
$Y[\omega,t]$	Whitened RTFI
z	component index
Z	number of components

Chapter 1

Introduction

The topic of this thesis is automatic transcription of polyphonic music exploiting temporal evolution. This chapter explains the motivations and aim (Section 1.1) of this work. Also, the structure of the thesis is provided (Section 1.2) along with the main contributions of this work (Section 1.3). Finally, publications associated with the thesis are listed in Section 1.4.

1.1 Motivation and aim

Automatic music transcription (AMT) is the process of converting an audio recording into a symbolic representation using some form of musical notation. Even for expert musicians, transcribing polyphonic pieces of music is not a trivial task [KD06], and while the problem of automatically transcribing monophonic signals is considered to be a solved problem, the creation of an automated system able to transcribe polyphonic music without setting restrictions on the degree of polyphony and the instrument type still remains open. The most immediate application of automatic music transcription is for allowing musicians to store and reproduce a *recorded performance* [Kla04b]. In the past years, the problem of automatic music transcription has gained considerable research interest due to the numerous applications associated with the area, such as automatic search and annotation of musical information, interactive music systems (e.g. computer participation in live human performances, score following, and rhythm tracking), as well as musicological analysis [Bel03, Got04, KD06].

The AMT problem can be divided into several subtasks, which include: pitch

estimation, onset/offset detection, loudness estimation, instrument recognition, and extraction of rhythmic information. The core problem in automatic transcription is the estimation of concurrent pitches in a time frame, also called multiple-F0 or multi-pitch estimation. As mentioned in [Cem04], automatic music transcription in the research literature is defined as the process of converting an audio recording into piano-roll notation, while the process of converting a piano-roll into a human readable score is viewed as a separate problem. The 1st process involves tasks such as pitch estimation, note tracking, and instrument identification, while the 2nd process involves tasks such as rhythmic parsing, key induction, and note grouping.

For an overview of transcription approaches, the reader is referred to [KD06], while in [dC06] a review of multiple fundamental frequency estimation systems is given. A more recent overview of multi-pitch estimation and transcription is given in [MEKR11], while [BDG+12] presents future directions in AMT research. A basic example of automatic music transcription is given in Fig. 1.1.

We identify two main motivations for research in automatic music transcription. Firstly, multi-pitch estimation methods (and thus, automatic transcription systems) can benefit from exploiting information on the temporal evolution of sounds, rather than analyzing each time frame or segment independently. Secondly, many applications in the broad field of music technology can benefit from automatic music transcription systems, although there are limited examples of such uses. Examples of transcription applications include the use of automatic transcription for improving music genre classification [LRPI07] and a karaoke application using melody transcription [RVPK08].

The aim of this work is to propose and develop methods for automatic music transcription which explicitly incorporate information on the temporal evolution of sounds, in an effort to improve transcription performance. The main focus of the thesis will be on transcribing Western classical and jazz music, excluding unpitched percussion and vocals. To that end, we utilize and propose techniques from music signal processing and analysis, aiming to develop a system which is able to transcribe music with a high level of polyphony and is not limited to pitched percussive instruments such as piano, but can accurately transcribe music produced by bowed string and wind instruments. Finally, we aim to exploit proposed automatic music transcription systems in various applications in computational musicology, music information retrieval, and audio processing, demonstrating the potential of automatic music transcription research in music and audio technology.

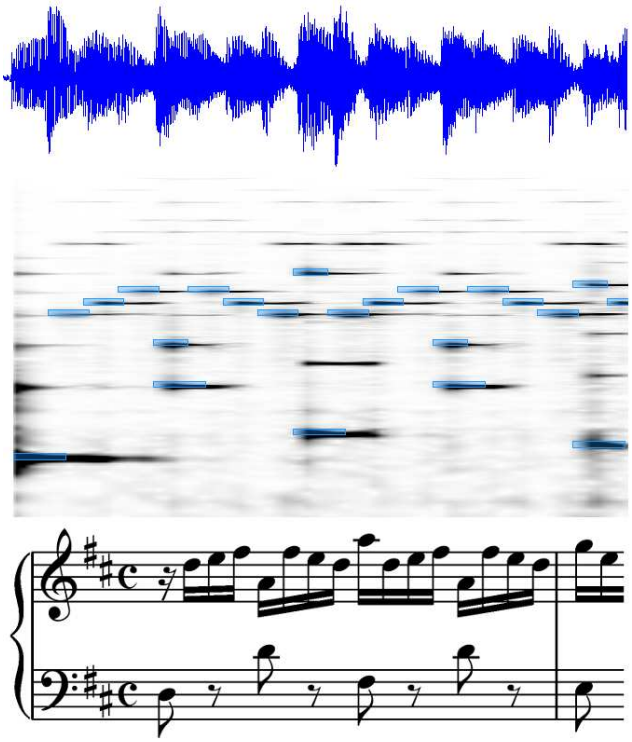

Figure 1.1: An automatic music transcription example. The top part of the figure contains a waveform segment from a recording of J.S. Bach's *Prelude in D major* from the *Well-Tempered Clavier Book I*, performed on a piano. In the middle figure, a time-frequency representation of the signal can be seen, with detected pitches in rectangles (using the transcription method of [DCL10]). The bottom part of the figure shows the corresponding score.

1.2 Thesis structure

Chapter 2 presents an overview of related work on automatic music transcription. It begins with a presentation of basic concepts from music terminology. Afterwards the problem of automatic music transcription is defined, followed by related work on single-pitch detection. Finally, a detailed survey on state-of-the-art automatic transcription methods for polyphonic music is presented.

Chapter 3 presents proposed methods for audio feature-based automatic music transcription. Preliminary work on multiple-F0 estimation on isolated piano chords is described, followed by an automatic music transcription

system for polyphonic music. The latter system utilizes audio features exploiting temporal evolution. Finally, a transcription system which also incorporates information on note onsets and offsets is given. Private and public evaluation results using the proposed methods are given.

Chapter 4 presents proposed methods for automatic music transcription which are based on spectrogram factorization techniques. More specifically, a transcription model which is based on shift-invariant probabilistic latent component analysis (SI-PLCA) is presented. Further work focuses on modeling the temporal evolution of sounds within the SI-PLCA framework, where a single-pitch model is presented followed by a multi-pitch, multi-instrument model for music transcription. Private and public evaluation results using the proposed methods are given.

Chapter 5 presents applications of proposed transcription systems. Proposed systems have been utilized in computational musicology applications, including key modulation detection in J.S. Bach chorales and temperament estimation in harpsichord recordings. A system for score-informed transcription has also been proposed, applied to automatic piano tutoring. Proposed transcription models have also been modified in order to be utilized for acoustic scene characterisation.

Chapter 6 concludes the thesis, summarizing the contributions of the thesis and providing future perspectives on further improving proposed transcription systems and on potential applications of transcription systems in music technology and audio processing.

1.3 Contributions

The principal contributions of this thesis are:

- Chapter 3: a pitch salience function in the log-frequency domain which supports inharmonicity and tuning changes.
- Chapter 3: A spectral irregularity feature which supports overlapping partials.
- Chapter 3: A common amplitude modulation (CAM) feature for suppressing harmonic errors.

- Chapter 3: A noise suppression algorithm based on a pink noise assumption.
- Chapter 3: Overlapping partial treatment procedure using harmonic envelopes of pitch candidates.
- Chapter 3: A pitch set score function incorporating spectral and temporal features.
- Chapter 3: An algorithm for log-frequency spectral envelope estimation based on the discrete cepstrum.
- Chapter 3: Note tracking using conditional random fields (CRFs).
- Chapter 3: Note onset detection which incorporates tuning and pitch information from the salience function.
- Chapter 3: Note offset detection using pitch-wise hidden Markov models (HMMs).
- Chapter 4: A convolutive probabilistic model for automatic music transcription which utilizes multiple-pitch and multiple-instrument templates and supports frequency modulations.
- Chapter 4: A convolutive probabilistic model for single-pitch detection which models the temporal evolution of notes.
- Chapter 4: A convolutive probabilistic model for multiple-instrument polyphonic music transcription which models the temporal evolution of notes.
- Chapter 5: The use of an automatic transcription system for the automatic detection of key modulations.
- Chapter 5: The use of a conservative transcription system for temperament estimation in harpsichord recordings.
- Chapter 5: A proposed algorithm for score-informed transcription, applied to automatic piano tutoring.
- Chapter 5: The application of techniques developed for automatic music transcription to acoustic scene characterisation.

1.4 Associated publications

This thesis covers work for automatic transcription which was carried out by the author between September 2009 and August 2012 at Queen Mary University of London. Work on acoustic scene characterisation (detailed in Chapter 5) was performed during a one-month visit to IRCAM, France in November 2011. The majority of the of the work presented in this thesis has been presented in international peer-reviewed conferences and journals:

Journal Papers

[i] E. Benetos and S. Dixon, "Joint multi-pitch detection using harmonic envelope estimation for polyphonic music transcription", *IEEE Journal on Selected Topics in Signal Processing*, vol. 5, no. 6, pp. 1111-1123, Oct. 2011.

[ii] E. Benetos and S. Dixon, "A shift-invariant latent variable model for automatic music transcription," *Computer Music Journal*, vol. 36, no. 4, pp. 81-94, Winter 2012.

[iii] E. Benetos and S. Dixon, "Multiple-instrument polyphonic music transcription using a temporally-constrained shift-invariant model," submitted.

[iv] E. Benetos, S. Dixon, D. Giannoulis, H. Kirchhoff, and A. Klapuri, "Automatic music transcription: challenges and future directions," submitted.

Peer-Reviewed Conference Papers

[v] E. Benetos and S. Dixon, "Multiple-F0 estimation of piano sounds exploiting spectral structure and temporal evolution", in Proc. *ISCA Tutorial and Research Workshop on Statistical and Perceptual Audition*, pp. 13-18, Sep. 2010.

[vi] E. Benetos and S. Dixon, "Polyphonic music transcription using note onset and offset detection", in Proc. *IEEE Int. Conf. Acoustics, Speech, and Signal Processing*, pp. 37-40, May 2011.

[vii] L. Mearns, E. Benetos, and S. Dixon, "Automatically detecting key modulations in J.S. Bach chorale recordings", in Proc. *8th Sound and Music Computing Conf.*, pp. 25-32, Jul. 2011.

[viii] E. Benetos and S. Dixon, "Multiple-instrument polyphonic music transcription using a convolutive probabilistic model", in Proc. *8th Sound and Music Computing Conf.*, pp. 19-24, Jul. 2011.

[ix] E. Benetos and S. Dixon, "A temporally-constrained convolutive probabilistic model for pitch detection", in Proc. *IEEE Workshop on Applications of Signal Processing to Audio and Acoustics*, pp. 133-136, Oct. 2011.

[x] S. Dixon, D. Tidhar, and E. Benetos, "The temperament police: The truth, the ground truth and nothing but the truth", in Proc. *12th Int. Society for Music Information Retrieval Conf.*, pp. 281-286, Oct. 2011.

[xi] E. Benetos and S. Dixon, "Temporally-constrained convolutive probabilistic latent component analysis for multi-pitch detection", in Proc. *Int. Conf. Latent Variable Analysis and Signal Separation*, pp. 364-371, Mar. 2012.

[xii] E. Benetos, A. Klapuri, and S. Dixon, "Score-informed transcription for automatic piano tutoring," *20th European Signal Processing Conf.*, pp. 2153-2157, Aug. 2012.

[xiii] E. Benetos, M. Lagrange, and S. Dixon, "Characterization of acoustic scenes using a temporally-constrained shift-invariant model," *15th Int. Conf. Digital Audio Effects*, pp. 317-323, Sep. 2012.

[xiv] E. Benetos, S. Dixon, D. Giannoulis, H. Kirchhoff, and A. Klapuri, "Automatic music transcription: breaking the glass ceiling," *13th Int. Society for Music Information Retrieval Conf.*, pp. 379-384, Oct. 2012.

Other Publications

[xv] E. Benetos and S. Dixon, "Multiple fundamental frequency estimation using spectral structure and temporal evolution rules", *Music Information Retrieval Evaluation eXchange (MIREX)*, Aug. 2010.

[xvi] E. Benetos and S. Dixon, "Transcription prelude", in *12th Int. Society for Music Information Retrieval Conference Concert*, Oct. 2011.

[xvii] E. Benetos and S. Dixon, "Multiple-F0 estimation and note tracking using a convolutive probabilistic model", *Music Information Retrieval Evaluation eXchange (MIREX)*, Oct. 2011.

It should be noted that for [vii] the author contributed in the collection of the dataset, the transcription experiments using the system of [vi], and the implementation of the HMMs for key detection. For [x], the author proposed and implemented a harpsichord-specific transcription system and performed transcription experiments. For [xiii], the author proposed a model for acoustic scene characterisation based on an existing evaluation framework by the second author. Finally in [iv, xiv], the author contributed information on state-of-the-art transcription, score-informed transcription, and insights on the creation of a complete transcription system. In all other cases, the author was the main contributor to the publications, under supervision by Dr Simon Dixon.

Finally, portions of this work have been linked to **Industry-related projects**:

1. A feasibility study on score-informed transcription technology for a piano tutor tablet application, in collaboration with AllegroIQ Ltd[1] (January and August 2011).

2. Several demos on automatic music transcription, for an automatic scoring/typesetting tool, in collaboration with DoReMIR Music Research AB[2] (March 2012 - today).

[1] `http://www.allegroiq.com/`
[2] `http://www.doremir.com/`

Chapter 2

Background

In this chapter, state-of-the-art methods on automatic transcription of polyphonic music are described. Firstly, some terms from music theory will be introduced, which will be used throughout the paper (Section 2.1). Afterwards, methods for single-pitch estimation will be presented along with monophonic transcription approaches (Section 2.2). The core of this chapter consists of a detailed review of polyphonic music transcription systems (Section 2.3), followed by a review of note tracking approaches (Section 2.4), commonly used evaluation metrics in the transcription literature (Section 2.5), and details on public evaluations of automatic music transcription methods (Section 2.6). Finally, a discussion on assumptions and design considerations made in creating automatic music transcription systems is made in Section 2.7. It should be noted that part of the discussion section has been published by the author in [BDG+12].

2.1 Terminology

2.1.1 Music Signals

A signal is called periodic if it repeats itself at regular time intervals, which is called the *period* [Yeh08]. The *fundamental frequency* (denoted f_0) of a signal is defined as the reciprocal of that period. Thus, the fundamental frequency is an attribute of periodic signals in the time domain (e.g. audio signals).

A *music signal* is a specific case of an audio signal, which is usually produced by a combination of several concurrent sounds, generated by different sources, where these sources are typically musical instruments or the singing

voice [Per10, Hai03]. The instrument sources can be broadly classified into two categories, which produce either pitched or unpitched sounds. Pitched instruments produce sounds with easily controlled and locally stable fundamental periods [MEKR11]. Pitched sounds can be described by a series of sinusoids (called harmonics or partials) which are harmonically-related, i.e. in the frequency domain the partials appear at integer multiples of the fundamental frequency. Thus, if the fundamental frequency of a certain harmonic sound is f_0, energy is expected to appear at frequencies hf_0, where $h \in \mathbb{N}$.

This fundamental frequency gives the perception of a musical note at a clearly defined pitch. A formal definition of pitch is given in [KD06], stating that "pitch is a perceptual attribute which allows the ordering of sounds on a frequency-related scale extending from low to high". As an example, Fig. 2.1 shows the waveform and spectrogram of a D3 piano note. In the spectrogram, the partials can be seen as occurring at integer multiples of the fundamental frequency (in this case it is 146.8 Hz).

It should be noted however that sounds produced by musical instruments are not strictly harmonic due to the very nature of the sources (e.g. a stiff string produces an inharmonic sound [JVV08, AS05]). Thus, a common assumption made for pitched instruments is that they are *quasi-periodic*. There are also cases of pitched instruments where the produced sound is completely inharmonic, where in practice the partials are not integer multiples of a fundamental frequency, such as idiophones (e.g. marimba, vibraphone) [Per10]. An example of an inharmonic sound is given in Fig. 2.2, where the spectrogram of a Marimba A3 note can be seen.

Finally, a musical instrument might also exhibit frequency modulations such as *vibrato*. In practice this means that the fundamental frequency changes slightly. One such example of frequency modulations can be seen in Fig. 2.3, where the spectrogram of a violin glissando followed by a vibrato is shown. At around 3 sec, the vibrato occurs and the fundamental frequency (with its corresponding partials) oscillates periodically over time. Whereas a vibrato denotes oscillations in the fundamental frequency, a tremolo refers to a periodic amplitude modulation, and can take place in woodwinds (e.g. flute) or in vocal sounds [FR98].

Notes produced by musical instruments typically can be decomposed into several temporal stages, denoting the temporal evolution of the sound. Pitched percussive instruments (e.g. piano, guitar) have an attack stage, followed by decay and release [BDA$^+$05]. Bowed string or woodwind instruments have a

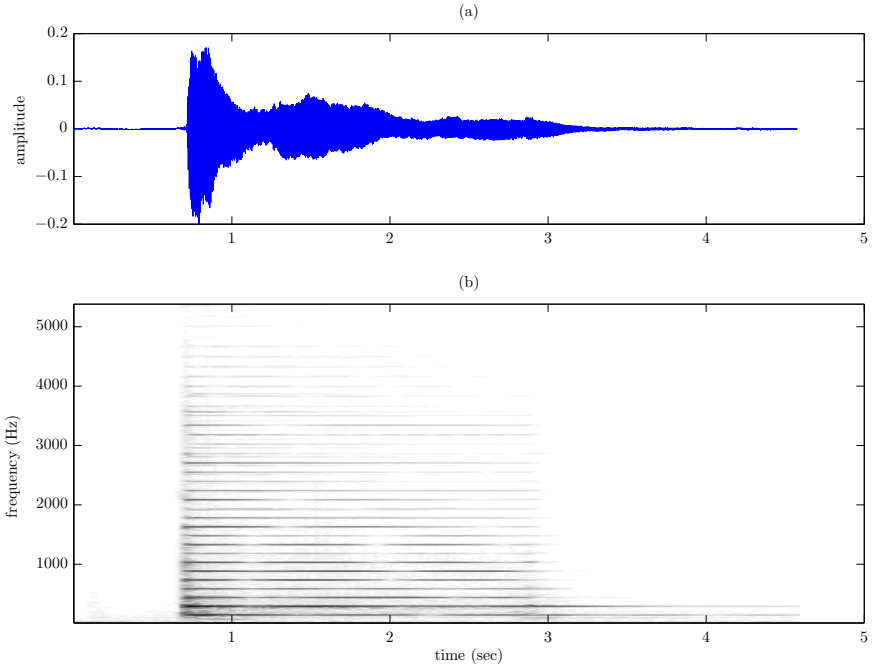

Figure 2.1: A D3 piano note (146.8 Hz). (a) The waveform of the signal. (b) The spectrogram of the signal. Harmonics occur at integer multiples of the fundamental frequency.

long sustain state [Per10]. Formally, the attack stage of a tone is the time interval during which the amplitude envelope increases [BDA+05]. An example of the attack and release states of a piano sound can be seen in Fig. 2.1, where at 0.7sec an attack region can be seen, whereas from 2-4 sec the tone decays before being released. It should finally be noted that the focus of the thesis is on transcribing music produced by pitched instruments, thus excluding percussion or audio effects. Human voice transcription is also not considered, although a transcription experiment using a singing voice excerpt is presented in the thesis (recording 12 in Table 3.1).

2.1.2 Tonality

Music typically contains combinations of notes organized in a way so that they please human listeners. The term *harmony* is used to the combination of concur-

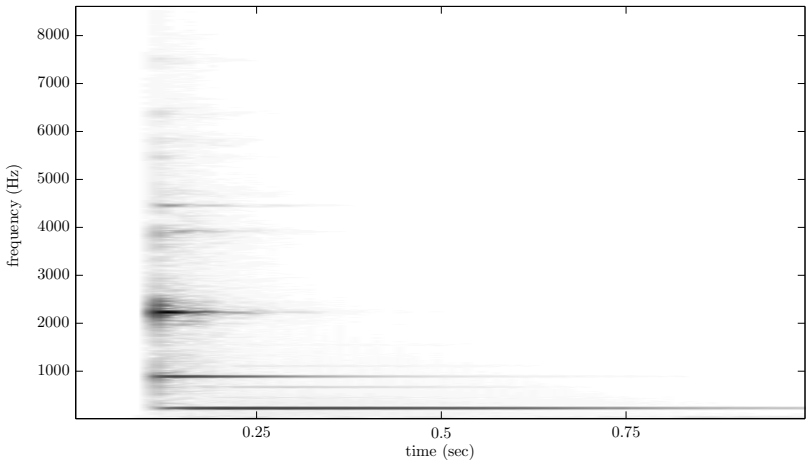

Figure 2.2: The spectrogram of an A3 marimba note.

rent pitches and the evolution of these note combinations over time. A *melodic interval* refers to the pitch relationship between two consecutive notes while a *melody* refers to a series of notes arranged in a musically meaningful succession [Sch11].

Research on auditory perception has shown that humans perceive as consonant musical notes whose ratio of fundamental frequencies (also called harmonic interval) is of the form $\frac{n+1}{n}$, where $n \leq 5$ [Ter77]. The most consonant harmonic intervals are $\frac{2}{1}$, which is called an octave, and $\frac{3}{2}$, which is called a perfect fifth. For the case of the octave, the partials of the higher note (which has a fundamental frequency of $2f_0$, where f_0 is the fundamental frequency of the lower note) appear at the same frequencies with the even partials of the lower note. Likewise, in the case of a perfect fifth, notes with fundamental frequencies f_0 and $\frac{3f_0}{2}$ will have in common every 3rd partial of f_0 (e.g. $3f_0, 6f_0$). These partials which appear in two or several concurrent notes are called *overlapping partials*.

In Western music, an octave corresponds to an interval of 12 semitones, while a perfect fifth to 7 semitones. A tone is an interval of two semitones. A note can be identified using a letter (A,B,C,D,E,F,G) and an octave number. Thus, A3 refers to note A in the 3rd octave. Also used are *accidentals*, which consist of sharps (♯) and flats (♭), shifting each note one semitone higher or lower,

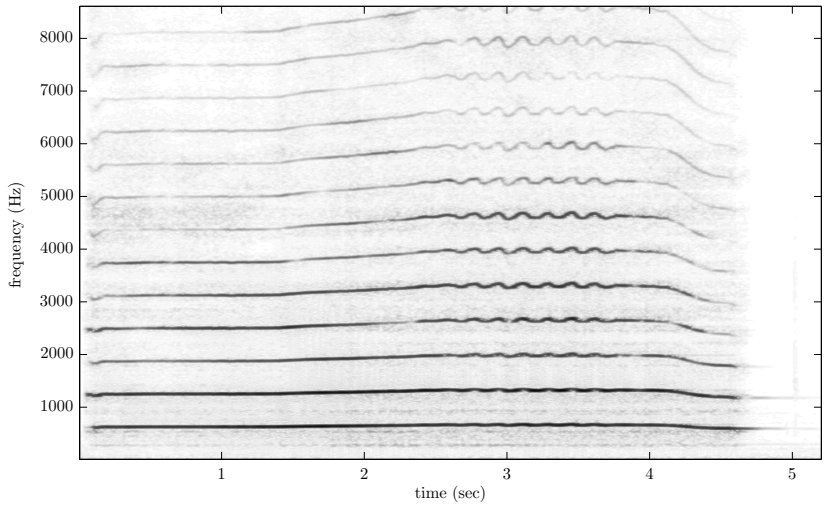

Figure 2.3: The spectrogram of a violin glissando. A vibrato can be seen around the 3 sec marker.

respectively. Although a succession of 7 octaves should result to the same note as a succession of 12 fifths, the ratio $(\frac{3}{2})^{12} : 2^7$ is approximately 1.0136, which is called a *Pythagorean comma*. Thus, some of the fifth intervals need to be adjusted accordingly. *Temperament* refers to the various methods of adjusting some or all of the fifth intervals (octaves are always kept pure) with the aim of reducing the dissonance in the most commonly used intervals in a piece of music [Bar51, Ver09].

One way of representing temperament is by the distribution of the Pythagorean comma around the cycle of fifths, as seen in Fig 2.4. The most common temperament is *equal temperament*, where each semitone is equal to one twelfth of an octave. Thus, all fifths are diminished by $\frac{1}{12}$ of a comma relative to the pure ratio of $\frac{3}{2}$. Typically, equal temperament is tuned using note A_4 as a reference note with a fundamental frequency of 440 Hz.

A *scale* is a sequence of notes in ascending order which forms a perceptually natural set [HM03]. The major scale follows the following pattern with respect to semitones: 2-2-1-2-2-2-1. An example of a C major scale using Western notation can be seen in Fig. 2.5. The natural minor scale has the pattern 2-1-2-2-1-2-2 and the harmonic minor scale has the pattern 2-1-2-2-1-3-1. The *key* of

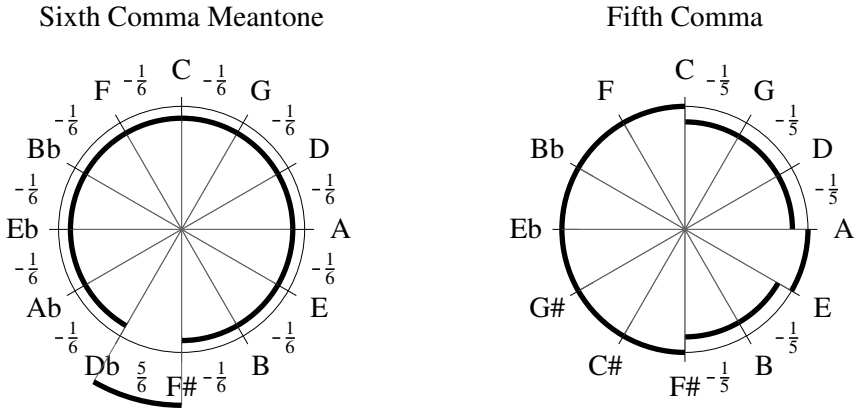

Figure 2.4: Circle of fifths representation for the 'Sixth comma meantone' and 'Fifth comma' temperaments. The deviation of each fifth from a pure fifth (the lighter cycle) is represented by the positions of the darker segments The fractions specify the distribution of the comma between the fifths (if omitted the fifth is pure). Fig. from [DTB11].

Figure 2.5: A C major scale, starting from C4 and finishing at C5.

a section of music is the scale which best fits the notes present. Using Western harmony rules, a set of concurrent notes which sound pleasant to most people is defined as a *chord*. A simple chord is the major triad (i.e. a three-note chord), which in equal temperament has a fundamental frequency ratio of 4:5:6. The consonance stems from the fact that these notes share many partials.

2.1.3 Rhythm

Rhythm describes the timing relationships between musical events within a piece [CM60]. A main rhythmic concept is the *metrical structure*, which consists of pulse sensations at different levels. Klapuri et al. [KEA06] consider three levels, namely the *tactus*, *tatum*, and *measure*.

The tatum is the lowest level, considering the shortest durational values which are commonly encountered in a piece. The tactus level consists of *beats*, which are basic time units referring to the individual elements that make up a

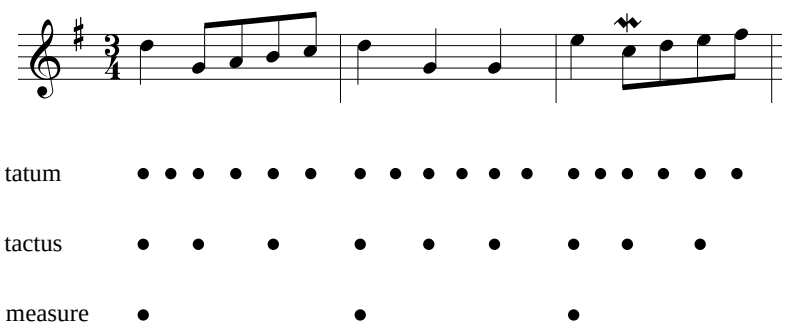

Figure 2.6: The opening bars of J.S. Bach's menuet in G major (BWV Anh. 114) illustrating the three metrical levels.

pulse. The *tempo* indicates the rate of the tactus. A pulse is a regularly spaced sequence of accents. Finally, the measure level consists of *bars*, which refers to the harmonic change rate or to the length of a rhythmic pattern [KEA06]. The three metrical levels are illustrated in Fig. 2.6 using J.S. Bach's menuet in G major. It should also be noted that in Western music notation rhythm is specified using a *time signature*, which specifies the number of beats in each measure (e.g. in Fig. 2.6 the time signature is 3/4, which means that each bar consists of 3 beats, with each beat corresponding to a crotchet).

2.1.4 MIDI Notation

A musical score can be stored in a computer in many different ways, however the most common computer music notation framework is the Musical Instrument Digital Interface (MIDI) protocol [MID]. Using the MIDI protocol, the specific pitch, onset, offset, and intensity of a note can be stored, along with additional parameters such as instrument type, key, and tempo.

In the MIDI protocol, each pitch is assigned a number (e.g. A_3=69). The equations which relate the fundamental frequency f_0 in Hz with the MIDI number n_{MIDI} are as follows:

$$\begin{aligned} n_{MIDI} &= 12 \cdot \log_2\left[\frac{f_0}{440}\right] + 69 \\ f_0 &= 440 \cdot 2^{\frac{n_{MIDI}-69}{12}} \end{aligned} \tag{2.1}$$

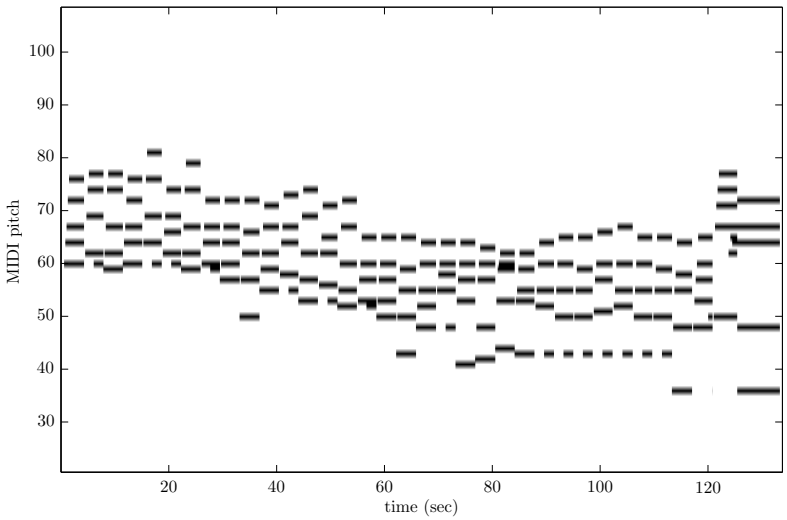

Figure 2.7: The piano-roll representation of J.S. Bach's prelude in C major from the Well-tempered Clavier, Book I.

Although MIDI has certain advantages regarding accessibility and simplicity, it has certain limitations, such as the storage of proper musical notation or expressive features. To that end, there are numerous protocols used for music notation in computers, such as MusicXML[1] or Lilypond[2]. Automatic transcription systems proposed in the literature usually convert an input recording into a MIDI file or a MIDI-like representation (returning a pitch, onset, offset).

One useful way to represent a MIDI score is a piano-roll representation, which depicts pitch in the vertical axis and time in the horizontal axis. An example of a piano-roll is given in Fig. 2.7, for J.S. Bach's prelude in C major, from the Well-tempered Clavier Book I.

2.2 Single-pitch Estimation

In this subsection, work on single-pitch and single-F0 detection for speech and music signals will be presented. Algorithms on single-F0 estimation assume that only one harmonic source is present in a specific instant within a signal. The

[1] `http://www.makemusic.com/musicxml`
[2] `http://lilypond.org/`

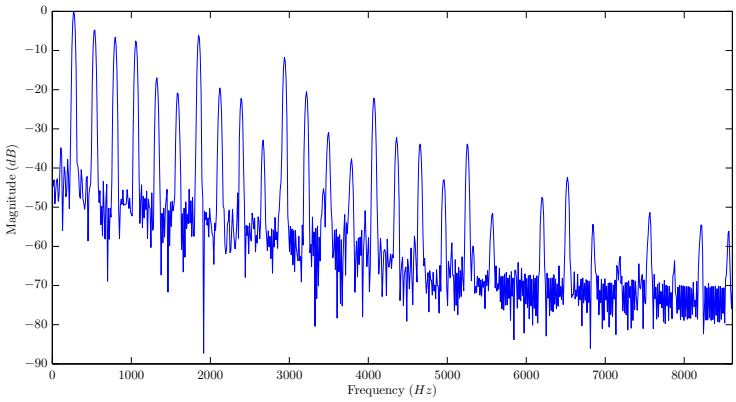

Figure 2.8: The spectrum of a C4 piano note (sample from MAPS database [EBD10]).

single-F0 estimation problem is largely considered to be solved in the literature, and a review on related methods can be found in [dC06]. In order to describe single-F0 estimation methods we will use the same categorization, i.e. separate approaches into spectral, temporal and spectrotemporal ones.

2.2.1 Spectral Methods

As mentioned in Section 2.1.1, the partials of a harmonic sound occur at integer multiples of the fundamental frequency of that sound. Thus, a decision on the pitch of a sound can be made by studying its spectrum. In Fig. 2.8 the spectrum of a C4 piano note is shown, where the regular spacing of harmonics can be observed.

The *autocorrelation function* can be used for detecting repetitive patterns in signals, since the maximum of the autocorrelation function for a harmonic spectrum corresponds to its fundamental frequency. Lahat et al. in [LNK87] propose a method for pitch detection which is based on flattening the spectrum of the signal and estimating the fundamental frequency from autocorrelation functions. A subsequent smoothing procedure using median filtering is also applied in order to further improve pitch detection accuracy.

In [Bro92], Brown computes the constant-Q spectrum [BP92] of an input sound, resulting in a log-frequency representation. Pitch is subsequently detected by computing the *cross-correlation* between the log-frequency spectrum

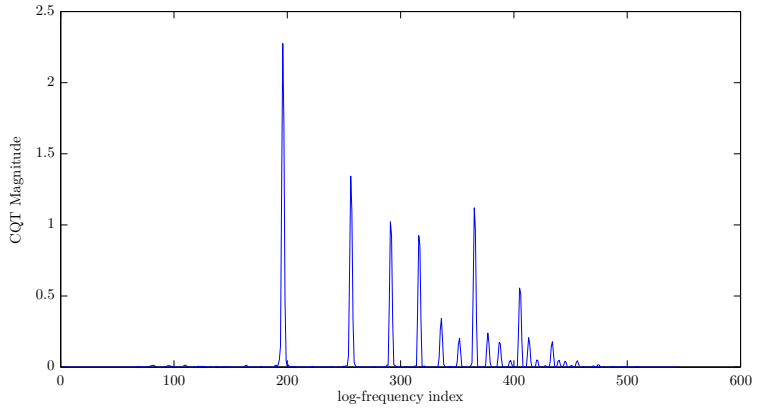

Figure 2.9: The constant-Q transform spectrum of a C4 piano note (sample from MAPS database [EBD10]). The lowest bin corresponds to 27.5 Hz and the frequency resolution is 60 bins/octave.

and an ideal spectral pattern, which consists of ones placed at the positions of harmonic partials. The maximum of the cross-correlation function indicates the pitch for the specific time frame. The advantage of using a harmonic pattern in log-frequency stems from the fact that the spacing between harmonics is constant for all pitches, compared to a linear frequency representation (e.g. the short-time Fourier transform). An example of a constant-Q transform spectrum of a C4 piano note (the same as in Fig. 2.8) can be seen in Fig. 2.9.

Doval and Rodet [DR93] proposed a maximum likelihood (ML) approach for fundamental frequency estimation which is based on a representation of an input spectrum as a set of sinusoidal partials. To better estimate the f_0 afterwards, a tracking step using hidden Markov models (HMMs) is also proposed.

Another subset of single-pitch detection methods uses *cepstral analysis*. The cepstrum is defined as the inverse Fourier transform of the logarithm of a signal spectrum. Noll in [Nol67] proposed using the cepstrum for pitch estimation, since peaks in the cepstrum indicate the fundamental period of a signal.

Finally, Kawahara et al. [KdCP98] proposed a spectrum-based F0 estimation algorithm called "TEMPO", which measures the instantaneous frequency at the output of a filterbank.

2.2.2 Temporal Methods

The most basic approach for time domain-based single-pitch detection is the use of the *autocorrelation function* using the input waveform [Rab77]. The autocorrelation function is defined as:

$$ACF[\nu] = \frac{1}{N} \sum_{n=0}^{N-\nu-1} x[n]x[n+\nu] \tag{2.2}$$

where $x[n]$ is the input waveform, N is the length of the waveform, and ν denotes the time lag. For a periodic waveform, the first major peak in the autocorrelation function indicates the fundamental period of the waveform. However it should be noted that peaks also occur at multiples of the period (also called subharmonic errors). Another advantage of the autocorrelation function is that it can be efficiently implemented using the discrete Fourier transform (DFT).

Several variants and extensions of the autocorrelation function have been proposed in the literature, such as the *average magnitude difference function* [RSC+74], which computes the city-block distance between a signal chunk and another chunk shifted by ν. Another variant is the *squared-difference function* [dC98], which replaced the city-block distance with the Euclidean distance:

$$SDF[\nu] = \frac{1}{N} \sum_{n=0}^{N-\nu-1} (x[n] - x[n+\nu])^2 \tag{2.3}$$

A normalized form of the squared-difference function was proposed by de Cheveigné and Kawahara for the YIN pitch estimation algorithm [dCK02]. The main improvement is that the proposed function avoids any spurious peaks near zero lag, thus avoiding any harmonic errors. YIN has been shown to outperform several pitch detection algorithms [dCK02] and is generally considered robust and reliable for fundamental frequency estimation [dC06, Kla04b, Yeh08, Per10, KD06].

2.2.3 Spectrotemporal Methods

It has been noted that spectrum-based pitch estimation methods have a tendency to introduce errors which appear in integer multiples of the fundamental frequency (harmonic errors), while time-based pitch estimation methods typically exhibit errors at submultiples of the f_0 (subharmonic errors) [Kla03]. Thus, it has been argued that a tradeoff between spectral and temporal meth-

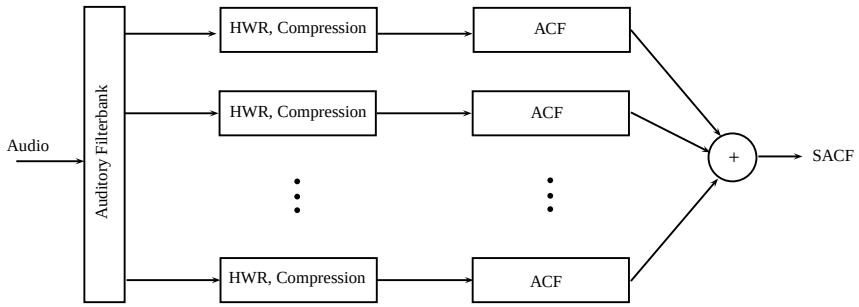

Figure 2.10: Pitch detection using the unitary model of [MO97]. HWR refers to half-wave rectification, ACF refers to the autocorrelation function, and SACF to the summary autocorrelation function.

ods [dC06] could potentially improve upon pitch estimation accuracy.

Such a tradeoff can be formulated by splitting the input signal using a filterbank, where each channel gives emphasis to a range of frequencies. Such a filterbank is the *unitary model* by Meddis and Hewitt [MH92] which was utilized by the same authors for pitch detection [MO97]. This model has links to human auditory models. The unitary model consists of the following steps:

1. The input signal is passed into a logarithmically-spaced filterbank.
2. The output of each filter is half-wave rectified.
3. Compression and lowpass filtering is performed to each channel.

the output of the model can be used for pitch detection by computing the autocorrelation for each channel and summing the results (summary autocorrelation function). A diagram showing the pitch detection procedure using the unitary model can be seen in Fig. 2.10. It should be noted however that harmonic errors might be introduced by the half-wave rectification [Kla04b]. A similar pitch detection model based on human perception theory which computes the autocorrelation for each channel was also proposed by Slaney and Lyon [SL90].

2.3 Multi-pitch Estimation and Polyphonic Music Transcription

In the polyphonic music transcription problem, we are interested in detecting notes which might occur concurrently and could be produced by several instru-

ment sources. The core problem for creating a system for polyphonic music transcription is thus multi-pitch estimation. For an overview on polyphonic transcription approaches, the reader is referred to [KD06], while in [dC06] a review of multiple-F0 estimation systems is given. A more recent overview on multi-pitch estimation and polyphonic music transcription is given in [MEKR11].

As far as the categorization of the proposed methods is concerned, in [dC06] multiple-F0 estimation methods are organized into three groups: temporal, spectral, and spectrotemporal methods. However, the majority of multiple-F0 estimation methods employ a variant of a spectral method; even the system by Tolonen [TK00] which depends on the summary autocorrelation function uses the FFT for computational efficiency. Thus, in this section, two different classifications of polyphonic music transcription approaches will be made; firstly, according to the time-frequency representation used and secondly according to various techniques or models employed for multi-pitch detection.

In Table 2.1, approaches for multi-pitch detection and polyphonic music transcription are organized according to the time-frequency representation employed. It can be clearly seen that most approaches use the short-time Fourier transform (STFT) as a front-end, while a number of approaches use filterbank methods, such as the equivalent rectangular bandwidth (ERB) gammatone filterbank, the constant-Q transform (CQT) [Bro91], the wavelet transform [Chu92], and the resonator time-frequency image [Zho06]. The gammatone filterbank with ERB channels is part of the unitary pitch perception model of Meddis and Hewitt and its refinement by Meddis and O'Mard [MH92, MO97], which compresses the dynamic level of each band, performs a non-linear processing such as half-wave rectification, and performs low-pass filtering. Another time-frequency representation that was proposed is *specmurt* [SKT$^+$08], which is produced by the inverse Fourier transform of a log-frequency spectrum.

Another categorization was proposed by Yeh in [Yeh08], separating systems according to their estimation type as joint or iterative. The iterative estimation approach extracts the most prominent pitch in each iteration, until no additional F0s can be estimated. Generally, iterative estimation models tend to accumulate errors at each iteration step, but are computationally inexpensive. In the contrary, joint estimation methods evaluate F0 combinations, leading to more accurate estimates but with increased computational cost. However, recent developments in the automatic music transcription field show that the vast majority of proposed approaches now falls within the 'joint' category.

Thus, the classification that will be presented in this thesis organises auto-

Time-Frequency Representation	Citation
Short-Time Fourier Transform	[Abd02, AP04, AP06, BJ05, BED09a, BBJT04, BBFT10, BBST11] [BKTB12, Bel03, BDS06, BMS00, BBR07, BD04, BS12, Bro06] [BG10, BG11, CLLY07, OCR+08, OCR+09b, OCR+09a] [OCQR10, OVC+11, CKB03, Cem04, CKB06, CSY+08] [CJAJ04, CJJ06, CJJ07, CSJJ07, CSJJ08, Con06, DG03, DGI06] [DCL10, Dix00, DR93, DZZS07, DHP09, DHP10, DPZ10] [DDR11, EBD07, EBD08, EBD10, FHAB10, FK11, FCC05] [Fon08, FF09, GBHL09, GS07a, GD02, GE09] [GE10, GE11, Gro08, GS07a, Joh03, Kla01, Kla03, Kla04b, Kla06] [Kla09a, Kla09b, KT11, LYLC10, LYC11, LYC12, LW07, LWB06] [Lu06, MSH08, NRK+10, NRK+11, NLRK+11] [NNLS11, NR07, Nie08, OKS12, OP11, ONP12] [OS03, OBBC10, BQ07, QRC+10, CRV+10, PLG07] [PCG10, PG11, Pee06, PI08, Per10, PI04] [PI05, PI07, PI08, Per10, PI12, PAB+02] [PEE+07, PE07a, PE07b, QCR+08, QCR+09] [QCRO09, QRC+10, CRV+10, CQRSVC+10, ROS09a] [ROS09b, RVBS10, Rap02, RFdVF08, RFF11, SM06] [ŞC10, ŞC11, SB03, Sma11, Sun00, TL05, VK02] [YSWJ10, WL06, Wel04, WS05] [Yeh08, YR04, YRR05, YRR10, YSWS05, ZCJM10]
ERB Filterbank	[BBV09, BBV10, KT99, Kla04b, Kla05, Kla08, RK05, Ryy08] [RK08, TK00, VR04, VBB07, VBB08, VBB10, ZLLX08]
Constant-Q Transform	[Bro92, CJ02, CPT09, CTS11, FBR11, KDK12] [Mar12, MS09, ROS07, Sma09, Wag03, WVR+11b, WVR+11a]
Wavelet Transform	[FCC05, KNS04, KNS07, MKT+07, NEOS09] [PHC06, SIOO12, WRK+10, YG10, YG12a]
Constant-Q Bispectral Analysis	[ANP11, NPA09]
Resonator Time-Frequency Image	[ZR07, ZR08, ZRMZ09, Zho06, BD10b, BD10a]
Multirate Filterbank	[CQ98, Got00, Got04]
Reassignment Spectrum	[HM03, Hai03, Pee06]
Modulation Spectrum	[CDW07]
Matching Pursuit Decomposition	[Der06]
Multiresolution Fourier Transform	[PGSMR12, KCZ09, Dre11]
Adaptive Oscillator Networks	[Mar04]
Modified Discrete Cosine Transform	[SC09]
Specmurt	[SKT+08]
High-resolution spectrum	[BLW07]
Quasi-Periodic Signal Extraction	[TS09]

Table 2.1: Multiple-F0 estimation approaches organized according to the time-frequency representation employed.

matic music transcription systems according to the core techniques or models employed for multi-pitch detection, as can be seen in Table 2.2. The majority of these systems employ signal processing techniques, usually for audio feature extraction, without resorting to any supervised or unsupervised learning procedures or classifiers for pitch estimation. Several approaches for note tracking have been proposed using spectrogram factorisation techniques, most notably non-negative matrix factorisation (NMF) [LS99]. NMF is a subspace analysis method able to decompose an input time-frequency representation into a basis matrix containing spectral templates for each component and a component activity matrix over time. Maximum likelihood (ML) approaches, usually employ-

ing the expectation-maximization (EM) algorithm [DLR77, SS04], have been also proposed in order to estimate the spectral envelope of candidate pitches or to estimate the likelihood of a set of pitch candidates. Other probabilistic methods include Bayesian models and networks, employing Markov Chain Monte Carlo (MCMC) methods for reducing the computational cost. Hidden Markov models (HMMs) [Rab89] are frequently used in a postprocessing stage for note tracking, due to the sequential structure offered by the models. Supervised training methods for multiple F0 estimation include support vector machines (SVMs) [CST00], artificial neural networks, and Gaussian mixture models (GMMs). Sparse decomposition techniques are also utilised, such as the K-SVD algorithm [AEB05], non-negative sparse coding, and multiple signal classification (MUSIC) [Sch86]. Least squares (LS) and alternating least squares (ALS) models have also been proposed. Finally, probabilistic latent component analysis (PLCA) [Sma04a] is a probabilistic variant of NMF which is also used in spectrogram factorization models for automatic transcription.

2.3.1 Signal Processing Methods

Most multiple-F0 estimation and note tracking systems employ methods derived from signal processing; a specific model is not employed, and notes are detected using audio features derived from the input time-frequency representation either in a joint or in an iterative fashion. Typically, multiple-F0 estimation occurs using a pitch salience function (also called pitch strength function) or a pitch candidate set score function [Kla06, PI08, YRR10]. In the following, signal processing-based methods related to the current work will be presented in detail.

In [Kla03], Klapuri proposed an iterative spectral subtraction method with polyphony inference, based on the principle that the envelope of harmonic sounds tends to be smooth. A magnitude-warped power spectrum is used as a data representation and a moving average filter is employed for noise suppression. The predominant pitch is estimated using a bandwise pitch salience function, which is able to handle inharmonicity [FR98, BQGB04, AS05]. Afterwards, the spectrum of the detected sound is estimated and smoothed before it is subtracted from the input signal spectrum. A polyphony inference method stops the iteration. A diagram showing the iterative spectral subtraction system of [Kla03] can be seen in Fig. 2.11. This method was expanded in [Kla08], where a variant of the unitary pitch model of [MO97] is used as a front-end, and the summary autocorrelation function is used for detecting the predomi-

Technique	Citation
Signal Processing Techniques	[ANP11, BBJT04, BBFT10, BBST11, BKTB12, BLW07, Bro06, Bro92] [CLLY07, OCR+08, OCR+09b, OCR+09a, Dix00, Dre11] [DZZS07, FHAB10, CQ98, FK11, Gro08, PGSMR12, HM03] [Hai03, Joh03, KT99, Kla01, Kla03] [Kla04b, Kla05, Kla06, Kla08, LRPI07, LWB06, NPA09] [BQ07, PHC06, PI07, PI08, Per10, PI12] [QCR+09, QCRO09, CQRSVC+10, SKT+08, SC09, TK00] [Wag03, WZ08, YSWJ10, WL06, WS05, YR04, YRR05] [Yeh08, YRR10, YSWS05, ZLLX08, Zho06, ZR07, ZR08, ZRMZ09]
Maximum Likelihood	[BED09a, DHP09, DPZ10, EBD07, EBD08, EBD10, FHAB10, Got00] [Got04, KNS04, KNS07, KT11, MKT+07, NEOS09, NR07] [Pee06, SIOO12, WRK+10, WVR+11b, WVR+11a, YG10, YG12b, YG12a]
Spectrogram Factorization	[BBR07, BBV09, BBV10, OVC+11, Con06, CDW07, CTS11] [DCL10, DDR11, FBR11, GE09, GE10, GE11, HBD10, HBD11a] [HBD11b, KDK12, Mar12, MS09, NRK+10, NRK+11, NLRK+11, Nie08] [OKS12, ROS07, ROS09a, ROS09b, SM06, SB03, Sma04b] [Sma09, Sma11, VBB07, VBB08, VBB10, VMR08]
Hidden Markov Models	[BJ05, CSY+08, EP06, EBD08, EBD10, LW07, OS03, PE07a, PE07b] [QRC+10, CRV+10, Rap02, Ryy08, RK05, ŞC10, ŞC11, VR04]
Sparse Decomposition	[Abd02, AP04, AP06, BBR07, BD04, OCQR10, CK11, Der06, GB03] [LYLC10, LYC11, LYC12, MSH08, OP11, ONP12, PAB+02, QCR+08]
Multiple Signal Classification	[CJAJ04, CJJ06, CSJJ07, CJJ07, CSJJ08, ZCJM10]
Support Vector Machines	[CJ02, CPT09, EP06, GBHL09, PE07a, PE07b, Zho06]
Dynamic Bayesian Network	[CKB03, Cem04, CKB06, KNKT98, ROS09b, RVBS10]
Neural Networks	[BS12, GS07a, Mar04, NNLS11, OBBC10, PI04, PI05]
Bayesian Model + MCMC	[BG10, BG11, DGI06, GD02, PLG07, PCG10, PG11, TL05]
Genetic Algorithms	[Fon08, FF09, Lu06, RFdVF08, RFF11]
Blackboard System	[BMS00, BDS06, Bel03, McK03]
Subspace Analysis Methods	[FCC05, VR04, Wel04]
Temporal Additive Model	[BDS06, Bel03]
Gaussian Mixture Models	[Kla09a, Mar07]
Least Squares	[Kla09b, KCZ09]

Table 2.2: Multiple-F0 and note tracking techniques organised according to the employed technique.

nant pitch. In [RK05] the system of [Kla03] was combined with a musicological model for estimating musical key and note transition probabilities. Note events are described using 3-state hidden Markov models (HMMs), which denote the attack, sustain, and noise/silence state of each sound. Also incorporated was information from an onset detection function. The system of [RK05] was also publicly evaluated in the MIREX 2008 multiple-F0 estimation and note tracking task [MIR] where competitive results were reported. Also, in [BKTB12], the system of [Kla08] was utilised for transcribing guitar recordings and also for extracting fingering configurations. An HMM was incorporated in order to model different fingering configurations, which was combined with the salience function of [Kla08]. Fingering transitions are controlled using a musicological model which was trained on guitar chord sequences.

Yeh et al. [YRR10] present a joint pitch estimation algorithm based on a

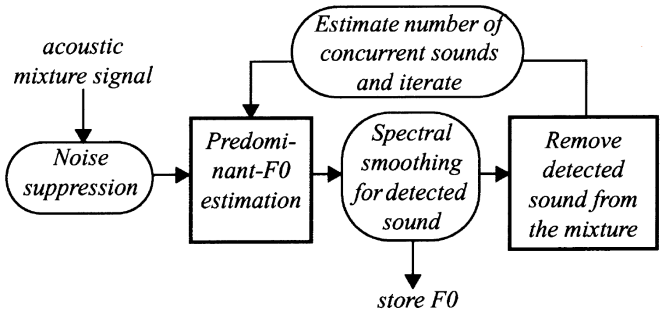

Figure 2.11: The iterative spectral subtraction system of Klapuri (figure from [Kla03]).

pitch candidate set score function. The front-end of the algorithm consists of a short-time Fourier transform (STFT) computation followed by an adaptive noise level estimation method based on the assumption that the noise amplitude follows a Rayleigh distribution. Given a set of pitch candidates, the overlapping partials are detected and smoothed according to the spectral smoothness principle [Kla03]. The weighted score function for the pitch candidate set consists of 4 features: harmonicity, mean bandwidth, spectral centroid, and synchronicity. A polyphony inference mechanism based on the score function increase selects the optimal pitch candidate set. The automatic transcription methods proposed by Yeh et al. [YRR05, Yeh08, YRR10] have been publicly evaluated in several MIREX competitions [MIR], where they rank first or amongst the first ones.

Pertusa and Iñesta [PI08, Per10, PI12] propose a computationally inexpensive method similar to Yeh's. The STFT of the input signal is computed, and a simple pitch salience function is computed. For each possible combination in the pitch candidate set, an overlapping partial treatment procedure is applied. Each harmonic partial sequence (HPS) is further smoothed using a truncated normalised Gaussian window, and a measure between the HPS and the smooth HPS is computed, which indicates the salience of the pitch hypothesis. The pitch candidate set with the greatest salience is selected for the specific time frame. In a postprocessing stage, minimum duration pruning is applied in order to eliminate local errors. In Fig. 2.12, an example of the Gaussian smoothing of [PI08] is given, where the original HPS can be seen along with the smoothed HPS.

Zhou et al. [ZRMZ09] proposed an iterative method for polyphonic pitch esti-

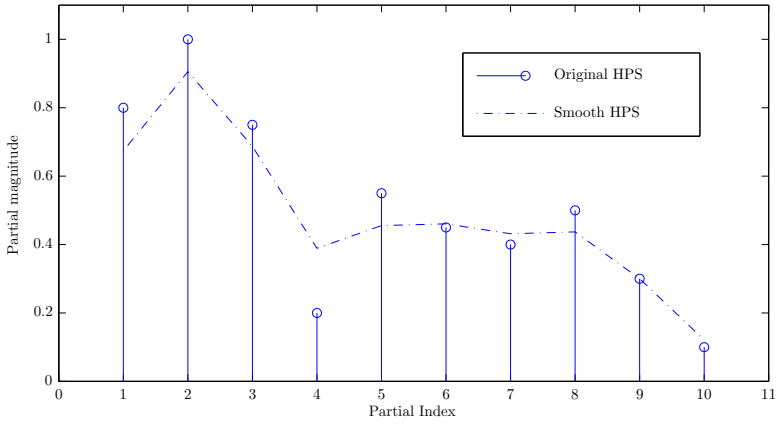

Figure 2.12: Example of the Gaussian smoothing procedure of [PI08] for a harmonic partial sequence.

mation using a complex resonator filterbank as a front-end, called the resonator time-frequency image (RTFI) [Zho06]. An example of the RTFI spectrum is given in Fig. 2.13. A mid-level representation is computed, called the pitch energy spectrum and pitch candidates are selected. Additional pitch candidates are selected from the RTFI using harmonic component extraction. These candidates are then eliminated in an iterative fashion using a set of rules based on features of the HPS. These rules are based on the number of harmonic components detected for each pitch and the spectral irregularity measure, which measures the concentrated energy around possibly overlapped partials from harmonically-related F0s. This method has been implemented as a real-time polyphonic music transcription system and has also been evaluated in the MIREX framework [MIR].

A mid-level representation along with a respective method for multi-pitch estimation was proposed by Saito et al. in [SKT+08], by using the inverse Fourier transform of the linear power spectrum with log-scale frequency, which was called *specmurt* (an anagram of cepstrum). The input spectrum (generated by a wavelet transform) is considered to be generated by a convolution of a common harmonic structure with a pitch indicator function. The deconvolution of the spectrum by the harmonic pattern results in the estimated pitch indicator function, which can be achieved through the concept of specmurt analysis. This

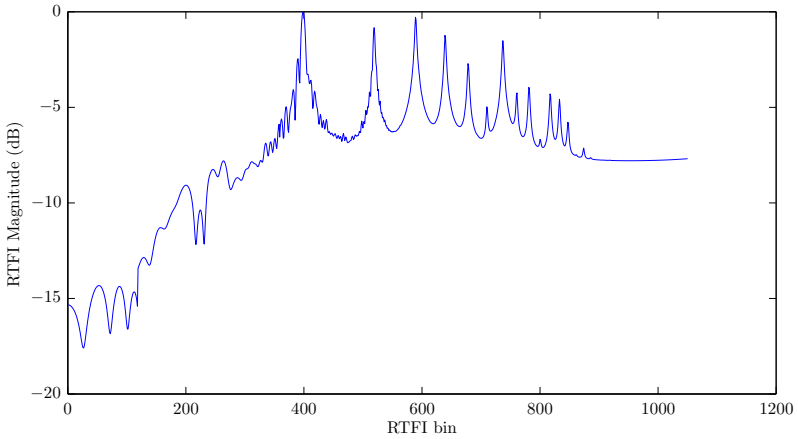

Figure 2.13: The RFTI spectrum of a C4 piano note (sample from MAPS databse [EBD10]). The lowest frequency is 27.5 Hz and the spectral resolution is 120 bins/octave.

process is analogous to deconvolution in the log-frequency domain with a constant harmonic pattern (see e.g. [Sma09]). Notes are detected by an iterative method which helps in estimating the optimal harmonic pattern and the pitch indicator function.

A system that uses a constant-Q and a bispectral analysis of the input audio signal was proposed by Argenti et al. in [ANP11, NPA09]. The processed input signal is compared with a two-dimensional pattern derived from the bispectral analysis, instead of the more common one-dimensional spectra, leading to improved transcription accuracy, as demonstrated by the lead ranking of the proposed system in the MIREX 2009 piano note tracking contest [MIR].

Cañadas-Quesada et al. in [QRC$^+$10] propose a frame-based multiple-F0 estimation algorithm which searches for F0 candidates using significant peaks in the spectrum. The HPS of pitch candidate combinations is extracted and a spectral distance measure between the observed spectrum and Gaussians centered at the positions of harmonics for the specific combination is computed. The candidate set that minimises the distance metric is finally selected. A post-processing step is also applied, using pitch-wise two-state hidden Markov models (HMMs), in a similar way to the method in [PE07a].

More recently, Grosche et al. [PGSMR12] proposed a method for automatic

transcription based on a mid-level representation derived from a multiresolution Fourier transform combined with an instantaneous frequency estimation. The system also combines onset detection and tuning estimation for computing frame-based estimates. Note events are afterwards detected using 2 HMMs per pitch, one for the *on* state and one for the *off* state.

2.3.2 Statistical Modelling Methods

Many approaches in the literature formulate the multiple-F0 estimation problem within a statistical framework. Given an observed frame v and a set $\boldsymbol{\mathcal{C}}$ of all possible fundamental frequency combinations, the frame-based multiple-F0 estimation problem can then be viewed as a maximum a posteriori (MAP) estimation problem [EBD10]:

$$\hat{\mathcal{C}} = \arg\max_{\mathcal{C} \in \boldsymbol{\mathcal{C}}} P(\mathcal{C}|v) \tag{2.4}$$

where $\hat{\mathcal{C}}$ is the estimated set of fundamental frequencies and $P(\cdot)$ denotes probability. If no prior information on the mixtures is specified, the problem can be expressed as a maximum likelihood (ML) estimation problem using Bayes' rule [CKB06, DPZ10, EBD10]:

$$\hat{\mathcal{C}} = \arg\max_{\mathcal{C} \in \boldsymbol{\mathcal{C}}} \frac{P(v|\mathcal{C})P(\mathcal{C})}{P(v)} = \arg\max_{\mathcal{C} \in \boldsymbol{\mathcal{C}}} P(v|\mathcal{C}) \tag{2.5}$$

Goto in [Got00, Got04] proposed an algorithm for predominant-F0 estimation of melody and bass line based on MAP estimation, called *PreFEst*. The input time-frequency representation (which is in log-frequency and is computed using instantaneous frequency estimation) is modelled using a weighted mixture of adapted tone models, which exhibit a harmonic structure. In these tone models, a Gaussian is placed in the position of each harmonic over the log-frequency axis. MAP estimation is performed using the expectation-maximization (EM) algorithm. In order to track the melody and bass-line F0s over time, a multiple-agent architecture is used, which selects the most stable F0 trajectory. An example of the tone model used in [Got04] is given in Fig. 2.14.

A Bayesian harmonic model was proposed by Davy and Godsill in [DG03], which models the spectrum as a sum of Gabor atoms with time-varying amplitudes with non-white residual noise, while inharmonicity is also considered. The unknown model parameters are estimated using a Markov chain Monte

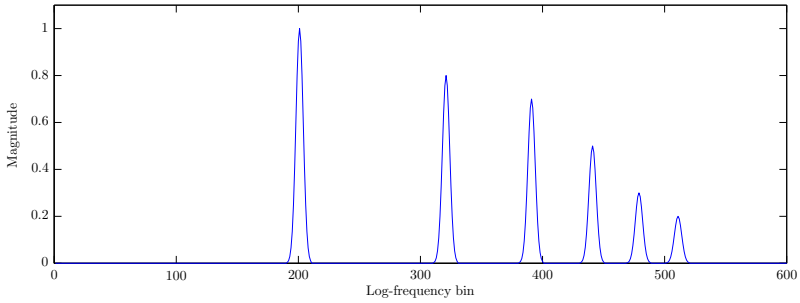

Figure 2.14: An example of the tone model of [Got04]. Each partial in the log-frequency domain is modelled by a Gaussian probability density function (PDF). The log-frequency resolution is 120 bins/octave.

Carlo (MCMC) method. The model was expanded in [DGI06], also including the extraction of dynamics, timbre, and instrument type.

An expansion of Goto's method from [Got04] was proposed by Kameoka et al. [KNS04, KNS07], called harmonic temporal structured clustering (HTC), which jointly estimates multiple fundamental frequencies, onsets, offsets, and dynamics. The input time-frequency representation is a wavelet spectrogram. Partials are modelled using Gaussians placed in the positions of partials in the log-frequency domain and the synchronous evolution of partials belonging to the same source is modelled by Gaussian mixtures. Time-evolving partials from the same source are then clustered. Model parameters are learned using the EM algorithm. The HTC algorithm was also used for automatic transcription in [MKT$^+$07], where rhythm and tempo are also extracted using note duration models with HMMs. A variant of the HTC algorithm was publicly evaluated for the MIREX competition [NEOS09], where an iterative version of the algorithm was used and penalty factors for the maximum number of active sources were incorporated into the HTC likelihood.

The HTC algorithm was also utilised in [WRK$^+$10] for instrument identification in polyphonic music, where for each detected note event harmonic temporal timbre features are computed and a support vector machine (SVM) classifier is used for instrument identification. The HTC algorithm was further extended by Wu et al. in [WVR$^+$11a], where each note event is separated into an attack and sustain state. For the attack states, an inharmonic model is used which is characterised by a spectral envelope and a respective power. For the sustain states, a harmonic model similar to [KNS07] is used. Instrument identification

is also performed using an SVM classifier, in a similar way to [WRK+10].

A maximum likelihood approach for multiple-F0 estimation which models spectral peaks and non-peak regions was proposed by Duan et al. in [DHP09, DPZ10]. The likelihood function of the model is composed of the peak region likelihood (probability that a peak is detected in the spectrum given a pitch) and the non-peak region likelihood (probability of not detecting any partials in a non-peak region), which are complementary. An iterative greedy F0 estimation procedure is proposed and priors are learned from monophonic and polyphonic training data. Polyphony inference, in order to control the number of iterations, is achieved by a threshold-based method using the likelihood function. A post-processing stage is performed using neighboring frames. Experiments were performed on the newly released Bach10 dataset[3], which contains multi-track recordings of Bach chorales. The methods in [DHP09, DPZ10] were also publicly evaluated in the MIREX 2009 and 2010 contests and ranked second best in the multiple-F0 estimation task.

Badeau et al. in [BED09a] proposed a maximum likelihood approach for multiple-pitch estimation which performs successive single-pitch and spectral envelope estimations. Inference is achieved using the expectation-maximization (EM) algorithm. As a continuation of the work of [BED09a], Emiya et al. in [EBD10] proposed a joint estimation method for piano notes using a likelihood function which models the spectral envelope of overtones using a smooth autoregressive (AR) model and models the residual noise using a low-order moving average (MA) model. The likelihood function is able to handle inharmonicity and the amplitudes of overtones are considered to be generated by a complex Gaussian random variable. The authors of [EBD10] also created a large database for piano transcription called MAPS, which was used for experiments. MAPS contains isolated notes and music pieces from synthesised and real pianos in different recording setups.

Raczynski et al. in [RVBS10] developed a probabilistic model for multiple pitch transcription based on dynamic Bayesian networks (DBNs) that takes into account temporal dependencies between musical notes and between the underlying chords, as well as the instantaneous dependencies between chords, notes and the observed note saliences. In addition, a front-end for obtaining initial note estimates was also used, which relied on the non-negative matrix factorization (NMF) algorithm.

[3] `http://music.cs.northwestern.edu`

Peeling and Godsill [PCG10, PG11] proposed a likelihood function for multiple-F0 estimation where for a given time frame, the occurrence of peaks in the frequency domain is assumed to follow an inhomogeneous Poisson process. This method was updated in [BG10, BG11], where in order to link detected pitches between adjacent frames, a model is proposed using Bayesian filtering and inference is achieved using the sequential MCMC algorithm. It should be noted however that the proposed likelihood function takes only into account the position of partials in f_0 candidates and not their amplitudes.

An extension of the *PreFEst* algorithm in [Got04] was proposed in [YG10, YG12a], where a statistical method called Infinite Latent Harmonic Allocation (iLHA) was proposed for detecting multiple fundamental frequencies in polyphonic audio signals, eliminating the problem of fixed system parameters. The proposed method assumes that the observed spectra are superpositions of a stochastically-distributed unbounded (theoretically infinite) number of bases. For inference, a modified version of the variational Bayes (VB) algorithm was used. In [YG12b], the method of [YG12a] was also used for unsupervised music understanding, where musicological models are also learned from the input signals. Finally, the iLHA method was improved by Sakaue et al. [SIOO12], where a corpus of overtone structures of musical instruments taken from a MIDI synthesizer was used instead of the prior distributions of the original iLHA algorithm.

Koretz and Tabrikian [KT11] proposed an iterative method for multi-pitch estimation, which combines MAP and ML criteria. The predominant source is expressed using a harmonic model while the remaining harmonic signals are modelled as Gaussian interference sources. After estimating the predominant source, it is removed from the spectrogram and the process is iterated, in a similar manner to the spectral subtraction method of [Kla03]. It should also be noted that the algorithm was also tested on speech signals in addition to music signals.

2.3.3 Spectrogram Factorization Methods

A large subset of recent automatic music transcription approaches employ *spectrogram factorization* techniques. These techniques are mainly non-negative matrix factorization (NMF) [LS99] and its probabilistic counterpart, probabilistic latent component analysis (PLCA) [SRS06]. Both of these algorithms will be presented in detail, since a large set of proposed automatic transcription

methods in this thesis are based on PLCA and NMF.

Non-negative Matrix Factorization

Subspace analysis seeks to find low dimensional structures of patterns within high-dimensional spaces. Non-negative matrix factorization (NMF) [LS99] is a subspace method able to obtain a parts-based representation of objects by imposing non-negative constraints. In music signal analysis, it has been shown to be useful in representing a spectrogram as a parts-based representation of sources or notes [MEKR11], thus the use of the term *spectrogram factorization*.

NMF was first introduced as a tool for music transcription by Smaragdis and Brown [SB03]. In NMF, an input matrix $\mathbf{V} \in \mathbb{R}_{+}^{\Omega \times T}$ can be decomposed as:

$$\mathbf{V} \approx \mathbf{WH} \tag{2.6}$$

where $\mathbf{H} \in \mathbb{R}_{+}^{Z \times T}$ is the atom activity matrix across T and $\mathbf{W} \in \mathbb{R}_{+}^{\Omega \times Z}$ is the atom basis matrix. In (2.6), Z is chosen as $\min(\Omega, T)$, as to reduce the data dimension. In order to achieve the factorization, a distance measure between the input $\mathbf{V}$ and the reconstruction $\mathbf{WH}$ is employed, with the most common being the Kullback-Leibler (KL) divergence or the Euclidean distance.

Thus, in the case of an input magnitude or power spectrogram $\mathbf{V}$, $\mathbf{H}$ is the atom activity matrix across time and $\mathbf{W}$ is the atom spectral basis matrix. In that case also, $t = 1, \ldots, T$ is the time index and $\omega = 1, \ldots, \Omega$ is the frequency bin index, while $z = 1, \ldots, Z$ is the atom/component index. An example of the NMF algorithm applied to a music signal is shown in Fig. 2.15, where the spectrogram of the opening bars of J.S. Bach's English Suite No. 5 is decomposed into note atoms $\mathbf{W}$ and atom activations $\mathbf{H}$.

In addition to [SB03], the standard NMF algorithm was also employed by Bertin et al. in [BBR07] where an additional post-processing step was presented, in order to associate atoms with pitch classes and to accurately detect note onsets and offsets.

Several extensions of NMF have been used for solving the automatic transcription problem. In [Con06], Cont has added sparseness constraints into the NMF update rules, in an effort to find meaningful transcriptions using a minimum number of non-zero elements in $\mathbf{H}$. In order to formulate the sparseness constraint into the NMF cost function, the l_ϵ norm is employed, which is approximated by the *tanh* function. An extension of the work in [Con06] was proposed in [CDW07], where the input time-frequency representation was

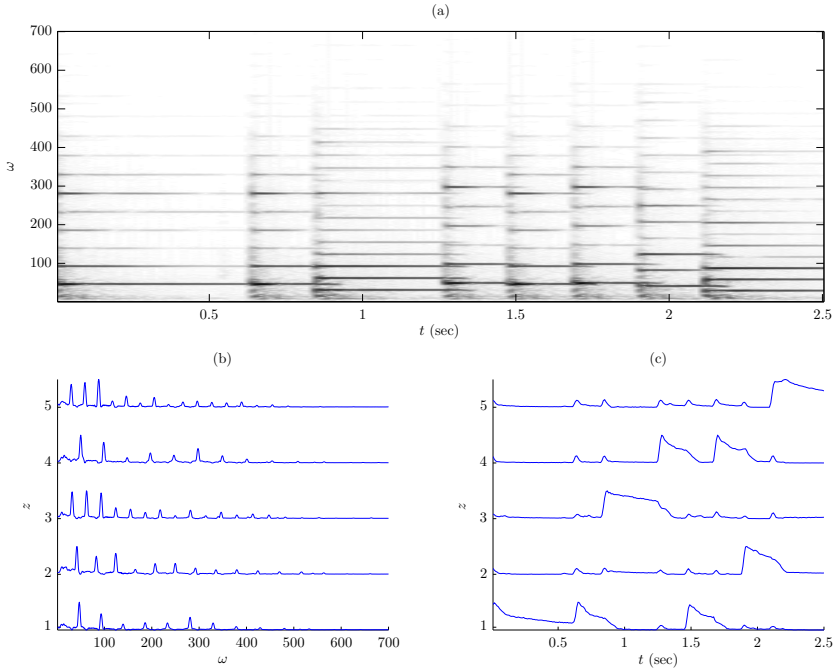

Figure 2.15: The NMF algorithm with $Z = 5$ applied to the opening bars of J.S. Bach's English Suite No. 5 (BWV 810 - recording from [Mar04]). (a) The STFT spectrogram of the recording using a 46ms Hanning window. (b) The computed spectral bases $\mathbf{W}$ (each basis corresponds to a different note). (c) The activation $\mathbf{H}$ for each basis.

a modulation spectrogram. The 2D representation of a time frame using the modulation spectrogram contains additional information which was also used for instrument identification.

Raczyński et al. in [ROS07] presented a harmonically-constrained variant of non-negative matrix approximation (which is a generalized version of NMF which supports different cost functions) for multipitch analysis, called harmonic non-negative matrix approximation (HNNMA). The spectral basis matrix $\mathbf{W}$ is initialized to have non-zero values in the overtone positions of each pitch and its structure is enforced with each iteration. Additional penalties in HNNMA include a sparsity constraint on $\mathbf{H}$ using the l_1 norm and a correlation measure for the rows of $\mathbf{H}$, in order to reduce the inter-row crosstalk. In [ROS09a], additional regularizations are incorporated into the NNMA model, for enforcing harmonicity and sparsity over the resulting activations.

Niedermayer in [Nie08] introduced a method aiming to incorporate prior knowledge about the pitch dictionary into the NMF algorithm. His approach was called non-negative matrix division, and it included a step for tone model learning before using a modified version of the unconstrained NMF with Euclidean distance in order to extract the transcription. As an input, the magnitude-warped power spectrum of [Kla03] was used.

Vincent et al. [VBB07, VBB08] incorporated harmonicity constraints in the NMF model, resulting in two algorithms; harmonic and inharmonic NMF. The model additionally constrains each basis spectrum to be expressed as a weighted sum of narrowband spectra, in order to preserve a smooth spectral envelope for the resulting basis functions. The inharmonic version of the algorithm is also able to support inharmonic spectra and tuning deviations. An ERB-scale time-frequency representation is used as input and a threshold-based onset/offset detection is performed in a post-processing step. The harmonic constraints and the post-processing procedure for note identification and onset/offset detection were further refined in [VBB10].

A model for automatic transcription of multiple-instrument recordings was proposed in [GE09], which extends the NMF algorithm to incorporate constraints on the basis vectors. Instrument models are incorporated using a grouping of spectral bases, called *eigeninstruments*.

Bertin et al. [BBV09, BBV10] expanded upon the work of [VBB08], proposing a Bayesian framework for NMF, which considers each pitch as a model of Gaussian components in harmonic positions. Spectral smoothness constraints are incorporated into the likelihood function and for parameter estimation the space alternating generalized EM algorithm (SAGE) is employed. Temporal smoothness of the detected notes is also enforced by using a Markov chain prior structure.

Nakano et al. [NRK+10] propose an NMF algorithm with Markov-chained basis for modelling the temporal evolution of music sounds. The goal of the system is to learn the time-varying sound states of musical instruments, such as attack, sustain, and decay, without any prior information. The proposed method is linked to the Viterbi algorithm using Factorial HMMs [GJ97].

In [DCL10], the NMF algorithm with β-divergence is utilised for piano transcription. β-divergence is a parametric family of distortion functions which can be used in the NMF cost function to influence the NMF update rules for $\mathbf{W}$ and $\mathbf{H}$. Essentially, $\beta = 0$ equally penalizes a bad fit of factorization for small and large coefficients while when $\beta > 0$, emphasis is given to components with

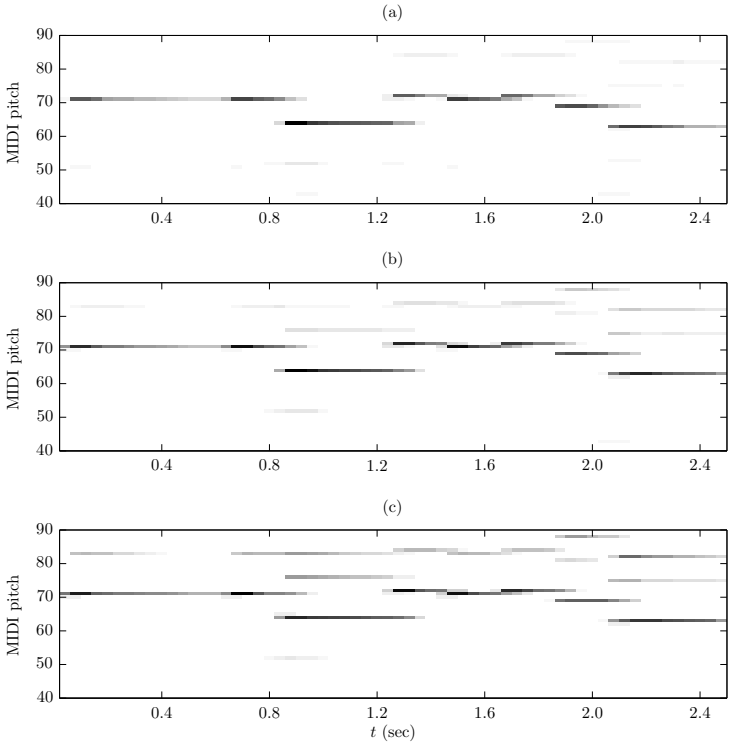

Figure 2.16: The activation matrix of the NMF algorithm with β-divergence applied to the monophonic melody of Fig. 2.15. (a) $\beta = 0$ (b) $\beta = 0.5$ (c) $\beta = 1$.

greater energy. A tradeoff between an equal penalization and a penalization of coefficients with high energy only has been shown to produce improved results for harmonic sounds (which typically have a strong fundamental and weaker harmonics). It should also be mentioned that the method of [DCL10] was publicly evaluated in the MIREX contest, giving good results in the piano-only note tracking task. An example of the use of parameter β for the transcription of the opening bars of J.S. Bach's English Suite No. 5 can be seen in Fig. 2.16.

Costantini et al. in [CTS11] employed a variant of the NMF algorithm with sparsity constraints for the activation matrix, using the constant-Q transform as a time-frequency representation. The system also incorporated an onset detector for splitting the input spectrogram into segments.

Hennequin et al. [HBD10, HBD11a] proposed an NMF-based algorithm for music signal analysis in order to model non-stationary note events. Since in a tone each harmonic decays with a different rate, the proposed model extends the NMF algorithm by including time-frequency activations based on autoregressive moving average (ARMA) modeling.

Carabias-Orti et al. [OVC+11] proposed a spectrogram factorization technique for automatic transcription as well as for musical instrument identification in polyphonic music. A harmonic comb-based excitation-filter model was incorporated into the NMF framework in order to model the excitation of different musical instruments.

Durrieu et al. [DDR11] proposed a mid-level representation which combines a source-filter model with the NMF algorithm in order to produce a pitch track which also contains timbral information. This mid-level representation was shown to be useful not only for multi-pitch detection, but also for melody extraction and lead instrument/accompaniment separation.

Marolt [Mar12] proposed a system for automatically transcribing bell chiming recordings using a modified version of the k-means algorithm for estimating the number of bells in the recording and the NMF algorithm for estimating the basis spectra of each bell. This system also incorporates an onset detector for improving transcription performance.

Ochiai et al. [OKS12] propose an algorithm for multi-pitch detection and beat structure analysis. The NMF objective function is constrained using information from the rhythmic structure of the recording, which helps improve transcription accuracy in highly repetitive recordings.

Non-negative Matrix Deconvolution

Another variant of the NMF algorithm changes the model from a linear to a *convolutive* one. Thus, two-dimensional bases can be learned from a time-frequency representation, where the 2-D atoms are convolved with atom activations. In [Sma04a, Sma04b], non-negative matrix deconvolution (NMD) is proposed, where $\mathbf{V}$ is considered to be the result of a convolution of time-varying spectra with their activity matrices. The NMD model can be formulated as:

$$\mathbf{V} \approx \sum_{\tau=0}^{\mathcal{T}-1} \mathbf{W}_\tau \cdot \overrightarrow{\mathbf{H}}^\tau \tag{2.7}$$

where $\mathbf{W}_\tau \in \mathbb{R}^{\Omega \times Z}$, $\mathbf{H} \in \mathbb{R}^{Z \times T}$, and $\overrightarrow{\mathbf{H}}^\tau$ denotes shifting the columns of $\mathbf{H}$ by τ spots to the right.

Schmidt and Mørup in [MS06, SM06] proposed an extension of NMD with sparsity constraints, called sparse non-negative matrix factor 2-D deconvolution (SNMF2D) for automatic transcription of polyphonic music. The method operates in the log-frequency domain, considering a constant shifted 2-D harmonic structure as a basis. In this case, the $l_{\frac{1}{2}}$ norm of $\mathbf{H}$ was used in order to control the sparseness, while non-negativity constraints on $\mathbf{W}_\tau$ and $\mathbf{H}$ are explicitly enforced for each iteration. It should also be noted that in [CŞS11], an alternative formulation of the NMD models is made, called probabilistic latent tensor factorization (PLTF).

In [KDK12], a method for semi-automatic music transcription is proposed which is based on a proposed model for shift-invariant NMD. The algorithm operates in the log-frequency domain and extracts a different instrument spectrum for each fundamental frequency under analysis. The term *semi-automatic transcription* refers to the user providing prior information about the polyphonic mixture or user transcribing some notes for each instrument in the mixture.

Probabilistic Latent Component Analysis

An alternative formulation of NMF was proposed by Smaragdis in [SRS06], called probabilistic latent component analysis (PLCA). It can be viewed as a probabilistic extension of the non-negative matrix factorization (NMF) algorithm [LS99] using the Kullback-Leibler cost function, providing a framework that is easy to generalize and interpret. PLCA can also offer a convenient way to incorporate priors over the parameters and control the resulting decomposition, for example using *entropic priors* [SRS08a]. In PLCA, the input spectrogram $V_{\omega,t}$ (ω denotes frequency, and t time), which must be scaled to have integer entries, is modeled as the histogram of the draw of N independent random variables (ω_n, t_n) which are distributed according to $P(\omega, t)$. $P(\omega, t)$ can be expressed by the product of a spectral basis matrix and a component activity matrix.

The asymmetric form of the PLCA model is expressed as:

$$P_t(\omega) = \sum_z P(\omega|z)P_t(z) \tag{2.8}$$

where z is the component index, $P(\omega|z)$ is the spectral template that corre-

sponds to the z-th component, and $P_t(z)$ is the activation of the z-th component.

The generative model for PLCA as presented in [Sha07] is as follows:

1. Choose z according to $P_t(z)$.
2. Choose ω according to $P(\omega|z)$.
3. Repeat the above steps V_t times ($V_t = \sum_\omega V_{\omega,t}$).

In order to estimate the unknown parameters $P(\omega|z)$ and $P_t(z)$, iterative update rules are applied, using the Expectation-Maximization (EM) algorithm [DLR77, SS04]. For the *E-step*, the a posteriori probability for the latent variable is derived using Bayes' theorem:

$$P_t(z|\omega) = \frac{P(\omega|z)P_t(z)}{\sum_z P(\omega|z)P_t(z)} \tag{2.9}$$

For the *M-step*, the expected complete data log-likelihood is maximised. The expected log-likelihood is given by [Sha07]:

$$\mathcal{L} = E_{\bar{z}|\bar{\omega};\Lambda} \log P(\bar{\omega}, \bar{z}) \tag{2.10}$$

where $\bar{\omega}, \bar{z}$ represent the set of all observations for ω, z and $\Lambda = \{P(\omega|z), P_t(z)\}$. The complete data likelihood $P(\bar{\omega}, \bar{z})$ can be written as:

$$P(\bar{\omega}, \bar{z}) = \prod_{j,t} P_t(z_j)P(\omega_j|z_j) \tag{2.11}$$

where ω_j, z_j are the values of ω, z in their j-th draw. Thus, $\mathcal{L}$ can be written as:

$$\mathcal{L} = \sum_{j,t,z} P(z|\omega_j) \log P_t(z) + \sum_{j,t,z} P(z|\omega_j) \log P(\omega_j|z) \tag{2.12}$$

By introducing Lagrange multipliers in (2.12) and maximising with respect to $P(\omega|z)$ and $P_t(z)$ leads to the following M-step equations:

$$P(\omega|z) = \frac{\sum_t V_{\omega,t} P_t(z|\omega)}{\sum_{\omega,t} V_{\omega,t} P_t(z|\omega)} \tag{2.13}$$

$$P_t(z) = \frac{\sum_\omega V_{\omega,t} P_t(z|\omega)}{\sum_{z,\omega} V_{\omega,t} P_t(z|\omega)} \tag{2.14}$$

The update rules of (2.9)-(2.14) are guaranteed to converge to a local min-

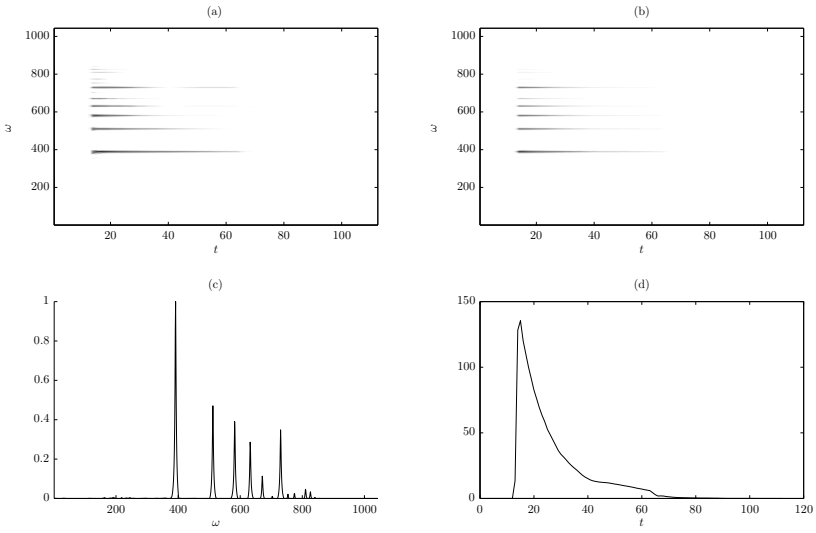

Figure 2.17: (a) The log-frequency spectrogram $P(\omega, t)$ of a C4 piano note (b) Approximation of the spectrogram using PLCA with $z = 1$ component (c) The spectral template $P(\omega|z)$ (d) The gain $P_t(z)$.

imum. In Fig. 2.17, an example of the application of the PLCA method to a log-frequency spectrogram of a piano note can be seen.

An extension of the asymmetric PLCA algorithm was used for multiple-instrument transcription in [GE10, GE11], where a system was proposed which supported multiple spectral templates for each pitch and instrument source. The notion of *eigeninstruments* was again utilised (as in [GE09]), by modeling the fixed spectral templates as a linear combination of basic instrument models in a training step. The model was expressed as:

$$P(\omega, t) = P(t) \sum_{s} \sum_{p} \sum_{z} P(\omega|p, z, s) P(z|s, p, t) P(s|p, t) P(p|t) \qquad (2.15)$$

In (2.15), p corresponds to pitch, s to the instrument source, and z to the index of pitch components per instrument. Thus, $P(\omega|p, z, s)$ is the spectral template that corresponds to the p-th pitch, s-th source, and z-th component. $P(p|t)$ is the transcription output and $P(t)$ is the signal energy (known quantity). Sparsity was enforced on the pitch activity matrix and the source contribution matrix by modifying the model update equations. Experiments were performed on J.S. Bach duets and on pairs of tracks from the multi-track MIREX multi-F0

woodwind recording [MIR], which is also used in this thesis.

Shift-Invariant Probabilistic Latent Component Analysis

Incorporating a shift-invariant model into the PLCA framework is practical since the sum of two random variables corresponds to a convolution of their distribution. Shift-invariant PLCA [SRS08b] was proposed for extracting shifted structures in non-negative data. It has been used in music signal processing applications using a normalized log-frequency spectrogram as an input, since a shift over log-frequency corresponds to a pitch change.

The shift-invariant PLCA (SI-PLCA) model can be defined as:

$$\begin{aligned} P(\omega, t) &= \sum_z P(z) P(\omega|z) *_\omega P(f, t|z) \\ &= \sum_z P(z) \sum_f P(\omega - f|z) P(f, t|z) \end{aligned} \tag{2.16}$$

where ω is the log-frequency index, z the component index, and f the shifting factor. $P(\omega - f|z) = P(\mu|f)$ denotes the spectral template for the z-th component, $P(f, t|z)$ the time-varying pitch shifting, and $P(z)$ the component prior. Again, the EM algorithm can be used for deriving update rules for the unknown parameters:

- **E Step**

$$P(f, z|\omega, t) = \frac{P(z) P(\omega - f|z) P(f, t|z)}{\sum_{z,f} P(z) P(\omega - f|z) P(f, t|z)} \tag{2.17}$$

- **M Step**

$$P(z) = \frac{\sum_{\omega,t,f} V_{\omega,t} P(f, z|\omega, t)}{\sum_{z,\omega,t,f} V_{\omega,t} P(f, z|\omega, t)} \tag{2.18}$$

$$P(\mu|z) = \frac{\sum_{f,t} V_{\omega,t} P(f, z|\omega, t)}{\sum_{\omega,f,t} V_{\omega,t} P(f, z|\omega, t)} \tag{2.19}$$

$$P(f, t|z) = \frac{\sum_{\omega} V_{\omega,t} P(f, z|\omega, t)}{\sum_{f,t,\omega} V_{\omega,t} P(f, z|\omega, t)} \tag{2.20}$$

An example of SI-PLCA applied to a music signal is given in Fig. 2.18, where the input log-frequency spectrogram of a cello melody is decomposed into a spectral template and a pitch impulse distribution.

Regarding applications of SI-PLCA, in [Sma09] the SI-PLCA model was used

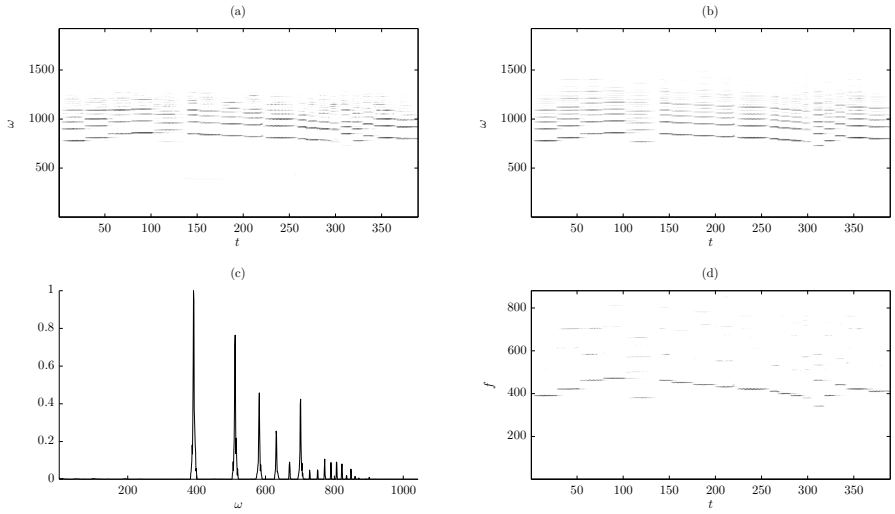

Figure 2.18: (a) The log-frequency spectrogram $P(\omega, t)$ of a cello melody (RWC-MDB-C-2001 No. 12 [GHNO03]) (b) Approximation of the spectrogram using SI-PLCA with $z = 1$ (c) The spectral template $P(\omega|z)$ (d) The pitch distribution $P(f, t|z)$.

for relative pitch tracking, where sparsity was enforced on the unknown matrices using an entropic prior. Mysore and Smaragdis [MS09] used the SI-PLCA model for multiple-instrument relative pitch tracking, tested on the MIREX multi-F0 recording [MIR]. For eliminating octave errors, a sliding-Gaussian Dirichlet prior was used in the model, while a temporal continuity constraint using a Kalman filter type smoothing was applied to $P(f, t|z)$ in order to extract a smooth pitch track.

More recently, an extension of the SI-PLCA algorithm was proposed for harmonic signals by Fuentes et al. [FBR11]. Each note is modeled as a weighted sum of narrowband log-spectra which are also shifted across log-frequency. This approach is a convolutive probabilistic formulation of the harmonic NMF algorithm proposed by Vincent [VBB10], with added time-dependence for the weights of the narrowband spectra. The harmonic SI-PLCA method was tested for single-pitch detection on isolated note samples and a model was proposed for multi-pitch detection. An asymmetric minimum variance prior was also incorporated into the parameter update rules in order to eliminate or reduce any harmonic errors.

Finally, a variant of PLCA was proposed for extracted scale-invariant struc-

tures from linear frequency spectrograms in [HBD11b], which is equivalent to extracting shift-invariant structures in log-frequency spectrograms. This *scale-invariant PLCA* is useful for detecting frequency shifts when a linear frequency representation such as the STFT is used. This can be useful for reconstructing individual sources, which might not be possible when a log-frequency representation is utilised.

Non-negative Hidden Markov Model

NMF and PLCA are not able to handle non-stationarity in signals. Their convolutive counterparts, NMD and SI-PLCA are able to extract 2-D structures from a time-frequency representation, which could assist in detecting non-stationary events. However, the dimensions of these 2-D structures are fixed, making the models not suitable for music signal analysis, where notes do not have a fixed duration. To that end, Mysore in [Mys10, MSR10] introduced temporal constraints into the PLCA model for music signal analysis and source separation. This *non-negative hidden Markov model* (NHMM) expressed each component using a set of spectral templates linked to a hidden state in an HMM. Thus, temporal constraints can be introduced in the NMF framework for modeling non-stationary events.

In the non-negative hidden Markov model, the input spectrogram $V_{\omega,t}$ is decomposed into a series of spectral templates per component and state, with corresponding time-varying mixture weights for the components. The model in terms of the observations is formulated as:

$$P_t(\omega_t|q_t) = \sum_{z_t} P_t(z_t|q_t)P(\omega_t|z_t, q_t) \tag{2.21}$$

where $P(\omega_t|z_t, q_t)$ denotes the spectral template for component z and state q, and $P_t(z_t|q_t)$ are the time-varying mixture weights. The use of subscript t in $P_t(\cdot)$ means that there is a separate distribution for each time frame. The subscript t in random variables z_t, ω_t, q_t refers to the value of the random variable for the specific time frame. $P_t(\omega_t|q_t)$ is the time-varying observation probability used in the HMM. Thus, the normalized spectrum of each time frame is approximated by:

$$P_t(\omega) = \sum_{q_t} P_t(\omega_t|q_t)P_t(q_t) \tag{2.22}$$

where $P_t(q_t)$ is the state activation, which can be computed using the HMM

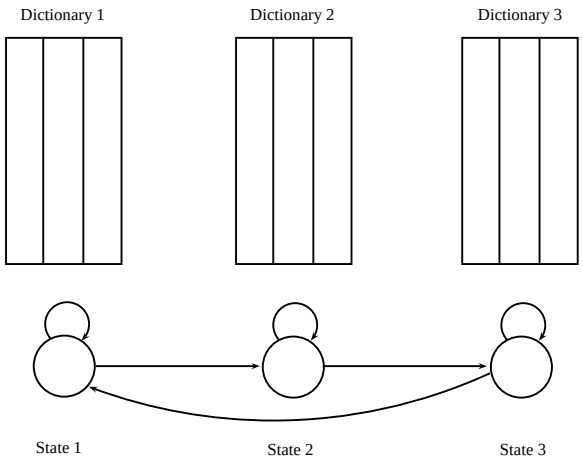

Figure 2.19: An example of a non-negative hidden Markov model using a left-to-right HMM with 3 states.

forward-backward procedure [Rab89]. Again, iterative update rules can be derived using the EM algorithm [DLR77]. An diagram of the NHMM using 3 states is shown in Fig. 2.19.

An extension of the NHMM for two sources was also proposed by Mysore [Mys10], which employed factorial HMMs [GJ97]. Factorial HMMs are used to model multiple time series data using a common observation. Thus, each source has its own transition matrix and state prior, but the observation probability is joint for all sources.

2.3.4 Sparse Methods

The basic concept of sparse coding [OF97] is similar to the aforementioned NMF model: we wish to express the observation $\mathbf{V}$ as a linear mixture of the matrices $\mathbf{W}$ (denoting the spectral basis) and $\mathbf{H}$ (the source weights). In sparse coding though, the sources are assumed to be non-active most of the time, resulting in a sparse $\mathbf{H}$; in order to derive the basis, ML estimation is performed.

In 2004, Blumensath and Davies [BD04] proposed an iterative reweighted least squares solution to the sparse coding problem for learning the basis functions in polyphonic piano music. Abdallah and Plumbley [AP04, AP06] used an ML approach for dictionary learning using non-negative sparse coding. Dictionary learning occurs directly from polyphonic samples, without requiring training on monophonic data, while the magnitude spectrum was used as input.

Convolutive sparse coding for sound source separation was presented by Virtanen in [Vir04], which is linked to non-negative matrix deconvolution presented in subsection 2.3.3. As in NMD, the resulting spectrum is considered to be produced by a convolution of source basis spectrograms and onset vectors. In addition, instead of a Euclidean distance-based cost function, a model fitting criterion based on loudness perception is proposed. Shift-invariant sparse coding, which is equivalent to convolutive sparse coding, was proposed in [MSH08] for automatic transcription in multi-instrument mixtures. In that case, the model extracts a spectral template per instrument source, which is shifted across log-frequency, as in SI-PLCA.

Derrien et al. [Der06] proposed a method for the decomposition of music spectrograms, based on the matching pursuit (MP) algorithm. A dictionary of atoms in the log-frequency scale was used and comparisons were made with the constant-Q spectrogram using a piano piece by Mozart.

Bertin et al. [BBR07] compared NMF with non-negative K-SVD, which is a sparse coding-like algorithm for image coding. The l_0 norm was used as a sparsity measure, and the algorithms' performance was found similar, although NMF is preferred due to its lower computational cost (even though in NMF sparsity is an uncontrolled side-effect).

Cañadas-Quesada et al. [QCR+08] proposed a note detection approach based on the harmonic matching pursuit (HMP) algorithm. The obtained atoms are further processed using an algorithm based on the spectral smoothness principle. Also, Carabias-Orti et al. [OCQR10] proposed an unsupervised process for learning spectral patterns of notes using the matching pursuit (MP) algorithm. Spectral patterns are learned using additional constraints on harmonicity, envelope smoothness, temporal continuity, and stability. The learned patterns are used in a note-event detection system, where the harmonic atoms are clustered according to the amplitude distribution of their spectral envelopes.

Sparse coding of Fourier coefficients was also used in [LYC11] for piano transcription. The sparse representation is solved by l_1 minimization, while a postprocessing step for note tracking is applied using pitch-wise hidden Markov models. This method was also publicly evaluated in [LYLC10] for the MIREX piano note tracking task. The model can be formulated as:

$$\widehat{\mathbf{h}}_t = \arg\min ||\mathbf{h}_t||_1, \quad \text{s.t. } \mathbf{v}_t = \mathbf{W}\mathbf{h}_t \tag{2.23}$$

where $\mathbf{v}_t$ is the input spectral vector at frame t, $\mathbf{W}$ is the dictionary matrix,

and $\mathbf{h}_t$ is the activation of the dictionary atoms. $||\cdot||_1$ refers to the l_1 norm. A method for automatic transcription using exemplar-based sparse representations was also proposed by the same authors in [LYC12]. In this method, a piano music segment is expressed as a linear combination of a small number of note exemplars from a dictionary. The drawback of this method is that it requires note samples from the same source as the recording (although it does not require as many samples as the note range of the instrument).

In [OP11] a method for structure-aware dictionary learning is proposed and applied to piano transcription, which takes into account harmonicity in music spectra. Modifications on the NMF and K-SVD algorithms were made by incorporating structure-awareness. More recently in [ONP12], structured sparsity (also called group sparsity) was applied to piano transcription. In group sparsity, groups of atoms tend to be active at the same time.

Finally in [Sma11], the notion of exemplars was also utilised for polyphonic pitch tracking. The method is formulated as a nearest subspace search problem. The input time-frequency representation is a normalized magnitude spectrogram, which as in the PLCA case, can exploit the l_2 norm for enforcing sparsity on the atom activations. The problem requires the minimization of the following cost function:

$$D[\mathbf{v}_t|\mathbf{W}\cdot\mathbf{h}_t] - \rho\sum_i h_{i,t}^2 \tag{2.24}$$

where $\mathbf{W}$ is the dictionary matrix, $\mathbf{v}_t$ the spectrum of the input signal, $\mathbf{h}_t$ is the atom activation for the t-th frame, $h_{i,t}$ the activation value for the i-th atom, and ρ is the sparsity parameter. In [Sma11], $D[\cdot]$ was set to be the Kullback-Leibler divergence.

2.3.5 Machine Learning Methods

A limited number of methods in the literature use standard machine learning techniques in order to estimate multiple F0s in frame-based systems. Chien and Jeng in [CJ02] proposed a signal processing-based system which solved the octave detection problem using a support vector machine (SVM) classifier. The constant-Q transform was used as input and the features used to train the SVM classifiers (one classifier for each pitch) were the partial amplitudes within a short period of time following an onset.

Marolt in [Mar04] performed a comparison of neural networks for note recognition, using as input features the output values of oscillator networks. A net-

work of adaptive oscillators was used for tracking the partials of each pitch. The best performance was reported for the time-delay neural networks (TDNNs).

Pertusa and Iñesta in [PI04, PI05] also used TDNNs for polyphonic music transcription, where the input consisted of pre-processed STFT bins. Poliner and Ellis [PE07a, PE07b] also used STFT bins for frame-level piano note classification using one-versus-all SVMs. In order to improve transcription performance, the classification output of the SVMs was fed as input to a hidden Markov model (HMM) for post-processing.

Giubin and Sheng [GS07a] proposed a transcription method which used a backpropagation neural network for classification. The input features were derived from an adaptive comb filter using an FFT as input. The system also supported the detection of onsets, repeated notes, as well as note duration and loudness estimation.

Zhou [Zho06] also used two-class SVMs for a comparative system for multiple-F0 estimation, using as features spectral peak amplitudes extracted from the RTFI representation. Gang et al. [GBHL09] employed a max-margin classifier for polyphonic music transcription, where features derived from partial amplitudes were used.

Costantini et al [CPT09] also employed SVMs for note classification and offset detection in piano recordings. The input time-frequency representation was the constant-Q transform (CQT). The CQT bins were used as features for the SVM classifier. It should be mentioned that this system performs classification at the time instants of each note onset, estimated from an onset detector.

Ortiz et al. [OBBC10] proposed a lightweight pitch detector to be used in embedded systems. A multilayer perceptron was used for classification, while the Goertzel Algorithm was employed for computing the frequency components of the signal on a log-frequency scale, which are used as features.

Nam et al. [NNLS11] employed deep belief networks for polyphonic piano transcription. Training was made using spectrogram bins as features and using both single notes and note combinations. For note tracking, the pitch-wise HMMs from [PE07a] were used.

Finally, Bock and Schedl [BS12] used recurrent neural networks for polyphonic piano transcription. Features consist of the output of two semitone filterbanks, one with short and one with a long window frame. A bidirectional long short-term memory (BLSTM) neural network is used for note classification and onset detection. In Fig. 2.20, the system diagram of the method proposed by [BS12] can be seen.

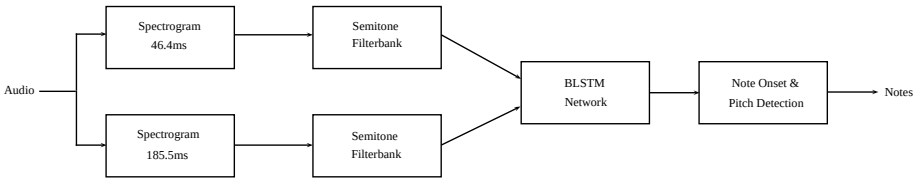

Figure 2.20: System diagram of the piano transcription method in [BS12].

2.3.6 Genetic Algorithm Methods

A radically different approach for automatic music transcription is the use of genetic algorithms. Essentially, a transcription is estimated which is mutated using a genetic algorithm until it matches some criterion. In the case of proposed approaches for transcription using genetic algorithms, this criterion is the similarity between the original signal and the synthesized signal from the estimated transcription.

In [Fon08, FF09], a possible piano-roll transcription is estimated from fragments defined by note onsets, is synthesized, and is compared with the original spectrogram. The procedure is iterated by mutating the piano-roll, until convergence is observed. In [Lu06], the same basic procedure is employed, although the features used for synthesizing the transcription are pitch, timbre and dynamics. Mutations employed by the proposed method in [Lu06] include a random note change, a change in note duration, note split, note reclassification, and note assimilation.

Finally, in [RFdVF08] a hybrid genetic algorithm based on gene fragment competition was proposed for polyphonic music transcription. The proposed method performs a quasi-global/quasi-local search by means of gene fragment evaluation and selection using as feature the STFT peaks of the original signal. A similar method was also publicly evaluated in the MIREX multiple-F0 and note tracking task by the same authors in [RFF11], where the current fitness function for the genetic algorithm is based on the log-spectral distance between the spectra of the original and synthesized recordings.

2.4 Note Tracking

Typically automatic transcription algorithms compute a time-pitch representation such as a pitch activation matrix, which needs to be further processed in order to detect note events (i.e. with note onsets and offsets). This procedure is

called *note tracking* or *note smoothing*. Most spectrogram factorization methods estimate the binary piano-roll representation from the pitch activation matrix using simple thresholding [GE11, Nie08, VBB08]. In [GE11] is is shown that the proposed PLCA-based algorithm is fairly robust to the choice of threshold.

One simple and fast solution for note tracking is minimum duration pruning [DCL10], which is applied after thresholding. Essentially, note events which have a duration smaller than a predefined value are removed from the final piano-roll. This method was also used in [BDS06], where more complex rules for note tracking were used, such as in the case where a small gap exists between two note events.

In [PE07a], a computationally inexpensive note tracking method was proposed, in order to post-process the non-binary posteriogram of SVM classifiers which were used for multi-pitch estimation. In this approach, pitch-wise hidden Markov models were used, where each HMM has two states, denoting note activity and inactivity. The HMM parameters (state transitions and priors) were learned directly from a ground-truth training set, while the observation probability is given by the posteriogram output for a specific pitch. The Viterbi algorithm [Rab89] is used for computing the optimal state sequence for each pitch, thus producing the final piano-roll. Given a pitch-wise state sequence $\mathcal{Q}^{(p)} = \{\mathfrak{q}_t^{(p)}\}, t = 1, \ldots, T$ and a sequence of observations $\mathcal{O}^{(p)} = \{\mathfrak{o}_t^{(p)}\}, t = 1, \ldots, T$, the optimal state sequence is achieved by maximizing:

$$\prod_t P(\mathfrak{o}_t^{(p)}|\mathfrak{q}_t^{(p)})P(\mathfrak{q}_t^{(p)}|\mathfrak{q}_{t-1}^{(p)}) \tag{2.25}$$

where $p = 1, \ldots, \mathcal{P}$ denotes pitch, $P(\mathfrak{q}_t^{(p)}|\mathfrak{q}_{t-1}^{(p)})$ is the state transition matrix for a given pitch, and $P(\mathfrak{o}_t^{(p)}|\mathfrak{q}_t^{(p)})$ is the pitch-wise observation probability. The graphical structure of the pitch-wise HMM proposed in [PE07a] can be seen in Fig. 2.21. An example of the note tracking procedure of [PE07a] can be seen in Fig. 2.22, where the pitch activation output of an NMF-based algorithm with β-divergence is used for HMM-based note tracking. This method has also been employed for other transcription systems, e.g. [QRC+10], where $P(\mathfrak{o}_t^{(p)}|\mathfrak{q}_t^{(p)})$ was computed using the pitch salience as input to an exponential probability density function (PDF). The note tracking method of [PE07a] was also used in [LYLC10].

A more complex HMM architecture was proposed in [EBD08] for note tracking, where each HMM state corresponds to note combinations (more specifically,

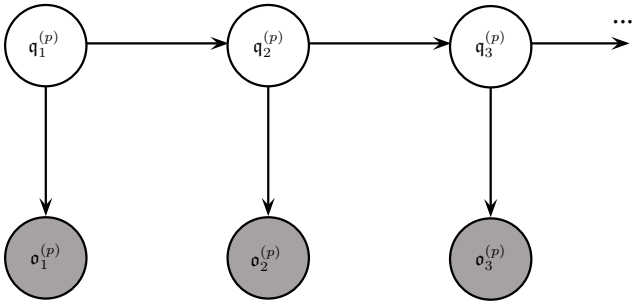

Figure 2.21: Graphical structure of the pitch-wise HMM of [PE07a].

chords). As in [PE07a], note combination transitions and priors were learned from MIDI data. However, it should be noted that the number of states is large: $\sum_{l=0}^{L} \binom{N_c}{L}$, where L is the maximum polyphony level and N_c is the set of pitch candidates.

Finally in [ROS09b], dynamic Bayesian networks (DBNs) were proposed for note tracking using as input the pitch activation of an NMF-based multipitch detection algorithm. The DBN has a note layer in the lowest level, followed by a note combination layer. Model parameters were learned using MIDI files from F. Chopin piano pieces.

2.5 Evaluation metrics

Evaluation of automatic transcription systems is typically done in two ways: frame-based evaluation and note-based evaluation.

2.5.1 Frame-based Evaluation

Frame-based evaluations are made by comparing the transcribed output and the ground-truth frame by frame typically using a 10 ms step, as in the MIREX multiple-F0 estimation task [MIR]. A commonly employed metric is the overall accuracy, defined by Dixon in [Dix00]:

$$Acc_1 = \frac{\sum_n N_{tp}[n]}{\sum_n N_{fp}[n] + N_{fn}[n] + N_{tp}[n]} \tag{2.26}$$

where $N_{tp}[n]$ is the number of correctly detected pitches at frame n, $N_{fn}[n]$ denotes the number of false negatives, and $N_{fp}[n]$ the number of false positives.

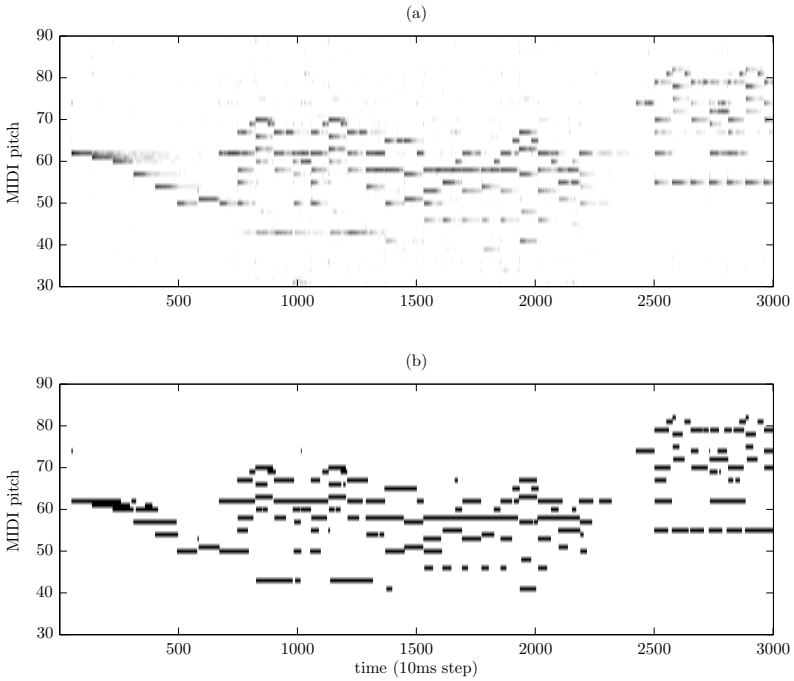

Figure 2.22: An example of the note tracking procedure of [PE07a]. (a) The NMF-based pitch activation of the first 30 sec of 'MAPS_MUS-alb_se2_ENSTDkCl' from the MAPS database [EBD10]. (b) The output of the HMM-based note tracking step.

In the MIREX task, a variant of Acc_1 is also used, called 'Chroma Accuracy' (Acc_{1c}), where the reference ground-truth and transcribed output are warped to one octave.

A second accuracy metric is also used for evaluation, proposed in [KNS07], which also takes into account pitch substitutions:

$$Acc_2 = \frac{\sum_n N_{ref}[n] - N_{fn}[n] - N_{fp}[n] + N_{subs}[n]}{\sum_n N_{ref}[n]} \tag{2.27}$$

where $N_{ref}[n]$ is the number of ground-truth pitches at frame n and $N_{subs}[n]$ is the number of pitch substitutions, given by $N_{subs}[n] = \min(N_{fn}[n], N_{fp}[n])$.

The frame-wise precision, recall, and F-measure metrics are also used for

evaluating transcription systems, defined in [VBB10] as:

$$Pre = \frac{\sum_n N_{tp}[n]}{\sum_n N_{sys}[n]} \quad Rec = \frac{\sum_n N_{tp}[n]}{\sum_n N_{ref}[n]} \quad \mathcal{F} = \frac{2 \cdot Rec \cdot Pre}{Rec + Pre} \tag{2.28}$$

where $N_{sys}[n]$ is the number of detected pitches for the n-th frame.

From the aforementioned definitions, several error metrics have been defined in [PE07a] that measure the substitution errors (E_{subs}), missed detection errors (E_{fn}), false alarm errors (E_{fp}), and the total error (E_{tot}):

$$\begin{aligned} E_{subs} &= \frac{\sum_n \min(N_{ref}[n], N_{sys}[n]) - N_{corr}[n]}{\sum_n N_{ref}[n]} \\ E_{fn} &= \frac{\sum_n \max(0, N_{ref}[n] - N_{sys}[n])}{\sum_n N_{ref}[n]} \\ E_{fp} &= \frac{\sum_n \max(0, N_{sys}[n] - N_{ref}[n])}{\sum_n N_{ref}[n]} \\ E_{tot} &= E_{subs} + E_{fn} + E_{fp} \end{aligned} \tag{2.29}$$

It should be noted that the aforementioned error metrics can exceed 100% if the number of false alarms is very high [PE07a].

2.5.2 Note-based Evaluation

For note-based evaluation, the output of a transcription system is typically in MIDI-like format, stating for each note event an onset, an offset, and the respective pitch. In this case, the evaluation is more straightforward. There are two ways of evaluating transcription algorithms using note-based metrics: firstly, by only utilizing information from note onsets and secondly by using information from onsets and offsets.

For onset-only evaluation, according to the MIREX [MIR] specifications, a note event is assumed to be correct if its onset is within a ± 50 ms range of a ground-truth onset and its F0 is within $\pm$ a quarter tone (3%) of the ground-truth pitch. For this case, metrics are defined in a similar way to (2.28), resulting in the onset-only note-based precision, recall, and F-measure, denoted as Pre_{on}, Rec_{on}, and $\mathcal{F}_{on}$, respectively.

For onset-offset evaluation, the same rules apply as in the onset-only evaluation, plus the offset of each note needs to be within 20% of ground-truth note's duration around the ground-truth note's offset value, or within 50 milliseconds of the ground-truth notes offset, whichever is larger [BED09b]. Again, preci-

sion, recall, and F-measure metrics are defined in a similar way to (2.28), being Pre_{off}, Rec_{off}, and $\mathcal{F}_{off}$, respectively.

2.6 Public Evaluation

Public evaluations of various multiple-F0 estimation and note tracking approaches are carried out as part of the Music Information Retrieval Evaluation eXchange (MIREX) framework [MIR]. Multiple-F0 estimation is evaluated in a frame-based manner, while the note tracking task performs evaluation for note-based events. For note tracking, two separate evaluations are made, one for multiple-instrument transcription and one for piano-only transcription. Results for the note tracking task are given using onset-only information, and using both note onsets and offsets.

Currently, the dataset used for evaluation consists of 30 recordings of 30 sec duration taken from a woodwind quintet recording of L. van Beethoven's Variations for String Quartet, Op.18 No. 5 and synthesized pieces from the RWC database [GHNO03]. The dataset also includes ten 30 sec recordings recorded from a Disklavier piano [PE07a]. A 5-track woodwind recording is used as a development dataset[4], which was annotated by the author and Graham Grindlay.

An overview of the results for the MIREX multiple-F0 estimation and note tracking tasks for 2007-2008 was made in [BED09b]. For these years, 16 algorithms from 12 labs and 11 algorithms from 7 labs were tested, respectively. For the multiple F0 estimation task, the best results were reported by the methods proposed by Yeh [Yeh08], Pertusa and Iñesta [PI08], Ryynänen and Klapuri [RK05], and Zhou and Reiss [ZR08]. All of the aforementioned approaches employ signal processing techniques for multiple-F0 estimation without any learning procedures or statistical models (Ryynänen's method employs HMMs in a post-processing step). For the note tracking task, the best results were also reported by the methods proposed by Yeh, Ryynänen and Klapuri, and Zhou and Reiss, followed by the SVM-based approach by Poliner and Ellis [PE07a]. As far as runtimes were concerned, the most efficient algorithm was the one by Zhou [ZR07], followed by the algorithm by Pertusa [PI08].

Best results for the multiple-F0 estimation task for years 2009-2011 are presented in Table 2.3. In 2009, the best results for the multiple-F0 estimation task were also reported by Yeh [Yeh08], followed by the statistical modelling method

[4] `http://www.music-ir.org/evaluation/MIREX/data/2007/multiF0/` (password required)

Participants	Metric	2009	2010	2011
Yeh and Röbel	Acc_1	0.69	0.69	0.68
	Acc_{1c}	0.71	0.71	0.70
Dressler	Acc_1	-	-	0.63
	Acc_{1c}	-	-	0.66
Cañadas-Quesada et al.	Acc_1	-	0.49	-
	Acc_{1c}	-	0.54	-
Benetos and Dixon	Acc_1	-	0.47	0.57
	Acc_{1c}	-	0.55	0.63
Duan, Han, and Pardo	Acc_1	0.57	0.55	-
	Acc_{1c}	0.61	0.59	-

Table 2.3: Best results for the MIREX Multi-F0 estimation task [MIR], from 2009-2011, using the accuracy and chroma accuracy metrics.

of Duan et al. [DHP09]. For the note tracking task, the best F-measure was reported by the system by Nakano et al. [NEOS09], which is based on the HTC algorithm by Kameoka et al. [KNS07]. The same rankings were reported for the piano-only note tracking task.

For 2010, the best multiple-F0 estimation results were reported by Yeh and Röbel [Yeh08], followed by Duan et al. [DHP09] and Cañadas-Quesada et al. [QRC$^+$10]. The same rankings were reported for the note tracking task.

For 2011, again the best results were reported by Yeh and Röbel [Yeh08], followed by Dressler [Dre11] and Benetos and Dixon [BD11b]. For note tracking, the best results were reported by Yeh and Röbel [Yeh08] followed by Benetos and Dixon [BD11b]. It should also be noted that the method by Dressler [Dre11] was by far the most computationally efficient.

It should be noted that results for the note tracking task are much inferior compared to the multiple-F0 estimation task, being in the range of 0.2-0.35 average F-measure with onset-offset detection and 0.4-0.55 average F-measure for onset-only evaluation.

2.7 Discussion

2.7.1 Assumptions

Most of the proposed methods for automatic transcription rely on several assumptions in order to solve the multiple-F0 estimation problem. The most basic assumption is *harmonicity*, which states that the frequency of partials of a har-

monic sequence are placed at integer multiples of the fundamental. In practice though, in certain instruments (e.g. piano) partials are slightly shifted upwards in frequency due to the inharmonicity phenomenon which needs to be taken into account [Kla04a]. Inharmonicity occurs due to string stiffness, where all partials of an inharmonic instrument have a frequency that is higher than their expected harmonic value [BQGB04].

A commonly used model for automatic transcription which supports inharmonicity considers a pitch p of a musical instrument sound with fundamental frequency $f_{p,0}$ and inharmonicity coefficient b_p. The partials for that sound are located at frequencies:

$$f_{p,h} = h f_{p,0} \sqrt{1 + (h^2 - 1) b_p} \tag{2.30}$$

where $h \geq 1$ is the partial index [KD06].

One of the most common assumptions used is *spectral smoothness* [BJ05, Cau99, EBD10, Kla03, PI08, Yeh08], which assumes that the spectral envelope of a pitched sound is smooth, although that assumption frequently does not appear to be valid. An example of that case can be seen in Figure 2.23, where the envelope of a trumpet sound forms a smooth contour, unlike the envelope of a clarinet sound, where even partials have lower amplitude compared to the odd ones.

Another assumption, which is implied for the spectral smoothness principle and is employed in subspace-based additive models is *power summation* [dC06], where it is assumed that the amplitude of two coinciding partials equals the sum of their respective amplitudes. In fact though, considering two coinciding partials with amplitudes a_1 and a_2, the resulting amplitude is given by $a = |a_1 + a_2 e^{i\Delta\phi}|$, where $\Delta\phi$ is their phase difference [Kla01]. This assumption can lead to estimation problems in the presence of harmonically-related pitches (pitches whose fundamental frequencies are in a rational number relation), which are frequently found in Western music. Also, when used explicitly in iterative approaches for multiple-F0 estimation (like [Kla03]), it can lead to signal corruption. In practice, the resulting amplitude is often considered to be the maximum of the two [dC06]. The power summation assumption is also implied in all spectrogram factorization approaches for automatic transcription, which use an additive model for representing a spectrum.

Other assumptions frequently encountered in multiple-F0 estimation systems include a constant spectral template for all pitches, as in [SKT+08]. Spectro-

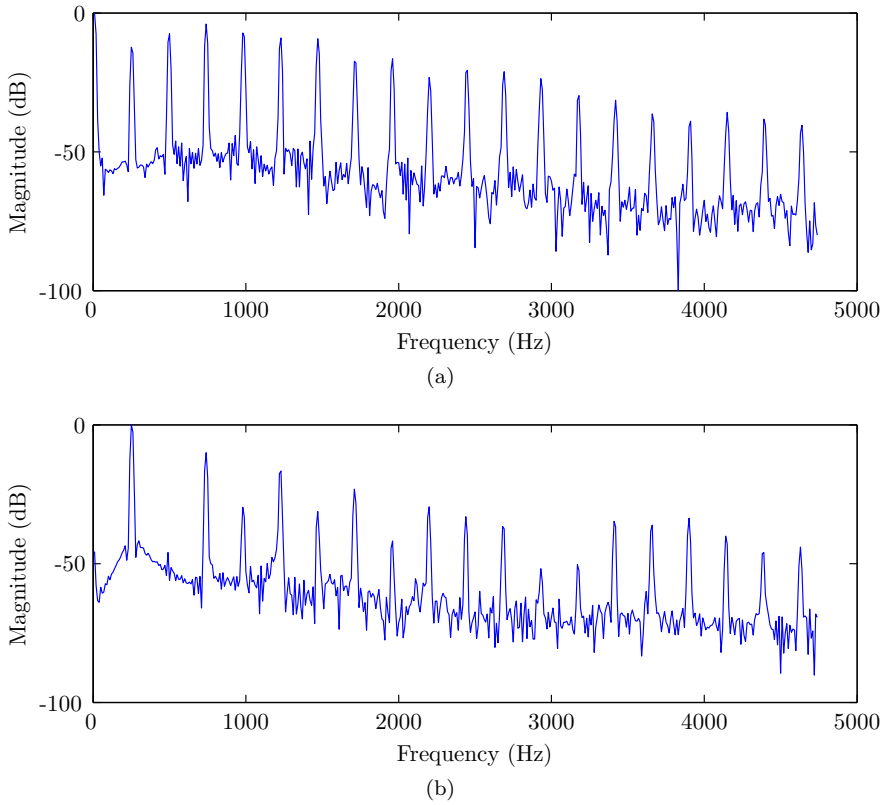

Figure 2.23: Trumpet (a) and clarinet (b) spectra of a C4 tone (261Hz). Overtones occur in positions determined by integer multiples of the fundamental frequency. In the trumpet case, the partial envelope produces a smooth contour, which is not the case for the clarinet.

gram factorization-based approaches usually consider one spectral template per pitch, which is however not sufficient for characterizing sounds produced by different instrument types, or even sounds produced by the same instrument at different conditions (instrument model, dynamics, articulation). These approaches also consider a similar decay model for all partials using a constant spectral template, when in fact higher partials decay more rapidly compared to lower partials. The problem of using a constant spectral template was addressed using non-negative matrix deconvolution [Sma04a, Sma04b] and convolutive sparse coding [Vir04], but a different issue arises because these algorithms use constant 2D templates with fixed note lengths, which is not the case in real-world music where notes have arbitrary durations.

2.7.2 Design Considerations

An overview of the design considerations that go into the development of a multiple-F0 estimation system will be given. The first decision to be made is selecting the time-frequency representation that will be used for the subsequent analysis. As shown in Section 2.3, most approaches use the short-time Fourier transform, due to its strong theoretic background and computational efficiency. There are however several drawbacks using the STFT, such as the constant frequency resolution which can create problems in detecting lower pitches. Using a log-frequency representation like the wavelet transform or the constant-Q representation of sounds has the advantage that the spacing between individual harmonics is the same for all pitches [Sma09], unlike the STFT. To that end, filterbank methods have been employed in the literature, trying to use an auditory front-end in an effort to produce improved estimation performance. The unitary model proposed by Meddis in [MH92, MO97] performs a non-linear transform into each filterbank input, which can assist pitch detection in the case of suppressed fundamentals, but can also create false spectral peaks in chord roots [TK00] due to the half-wave rectification, making the model useful for the monophonic case but problematic in the case of polyphonic western music, where harmonic relations are quite common. Another approach for computing a T/F representation for transcription is to increase the FFT resolution, using quadratic interpolation, parametric methods, or using non-stationary sinusoidal modelling techniques, such as the reassignment spectrum [Hai03], with the drawback of increased computational cost.

Another choice concerns the algorithm for multiple-F0 estimation. Signal processing methods for transcription (e.g. [Kla03, PI08, YRR10]) have proved to be quite robust and computationally inexpensive. However, they are difficult to generalize and to control, since their performance is mostly based on a combination of audio features and ad-hoc models. Spectrogram factorization models and sparse decomposition approaches ([VBB08, GE11, LYC12]) seem more appropriate for multi-pitch estimation, since they are based on a simple and transparent model which is easy to control and generalize. However, most spectrogram factorization-based approaches are computationally expensive and the results are sometimes not as high compared to signal processing-based approaches. Furthermore, spectrogram factorization-based approaches for multi-pitch detection are mostly based on the magnitude of the frequency or log-frequency bins of a spectrogram, thus ignoring any additional features from

audio processing which might improve transcription performance. Although machine learning methods have been shown to be appropriate for classification problems, problems have been reported regarding their generalization performance for the automatic transcription task (e.g. [PE07a]).

A third choice would be whether to perform multiple-F0 estimation on a frame-by-frame basis and afterwards form the notes using the frame-based pitch estimates or to jointly perform multipitch tracking. Only a few methods in the literature perform multiple-F0 estimation and note tracking in a joint fashion, due to the complexity of the problem. Such methods include the HTC algorithm by Kameoka [KNS07], the HMM-based model by Chang [CSY+08], the constrained clustering model proposed by Duan [DHP09], and the Poisson point process model for multi-pitch detection combined with a dynamical model for note transitions proposed by Bunch and Godsill [BG11]. Finally, another design consideration is whether the developed system is able to perform instrument identification along with multi-pitch detection (e.g. [GE11]).

2.7.3 Towards a Complete Transcription

Most of the aforementioned transcription approaches tackle the problems of multiple-F0 estimation and note onset and offset detection. However, in order to fully solve the AMT problem and have a system that provides an output that is equivalent to sheet music, additional issues need to be addressed, such as metre induction, rhythm parsing, key finding, note spelling, dynamics, fingering, expression, articulation and typesetting. Although there are approaches that address many of these individual problems, there exists no 'complete' AMT system to date.

Regarding typesetting, current tools produce readable scores from MIDI data only (e.g. Lilypond[5]), ignoring cues from the music signal which could also assist in incorporating additional information into the final score (e.g. expressive features for note phrasing). As far as dynamics are concerned, in [EM11] a method was proposed for estimating note intensities in a score-informed scenario. However, estimating note dynamics in an unsupervised way has not been tackled. Another issue would be the fact that most existing ground-truth does not include note intensities, which is difficult to annotate manually, except for datasets created using reproducing pianos (e.g. [PE07a]), which automatically contain intensity information such as MIDI note velocities.

[5] `http://lilypond.org/`

Recent work [BKTB12] addresses the problem of automatically extracting the fingering configurations for guitar recordings in an AMT framework. For computing fingering, information from the transcribed signal as well as instrument-specific knowledge is needed. Thus, a robust instrument identification system would need to be incorporated for computing fingerings in multi-instrument recordings.

For extracting expressive features, some work has been done in the past, mostly in the score-informed case. In [GBL+11] a framework for extracting expressive features both from a score-informed and an uninformed perspective is proposed. In the latter case, an AMT system is used prior to the extraction of expressive features. It should be mentioned though that the extracted features (e.g. auditory loudness, attack, pitch deviation) do not necessarily correspond to expressive notation. Thus, additional work needs to be done in order to provide a mapping between mid-level expressive features and the expressive markings in a final transcribed music score.

Chapter 3

Audio Feature-based Automatic Music Transcription

3.1 Introduction

This chapter presents proposed methods for multiple-F0 estimation of isolated sounds as well as for complete recordings using techniques from signal processing theory. Audio features are proposed which exploit the spectral structure and temporal evolution of notes. Firstly, an iterative multiple-F0 estimation method for isolated piano sounds is presented, which was published in [BD10a]. This method is also converted into a system for automatic music transcription, which was publicly evaluated in [BD10b].

Afterwards, a method for joint multiple-F0 estimation is proposed, which is based on a novel algorithm for spectral envelope estimation in the log-frequency domain. This method was published in [BD11a]. For this method, a novel note tracking procedure was also utilized using conditional random fields. An extension of the aforementioned system is also presented, which applies late fusion-based onset detection and hidden Markov model-based offset detection, which was published in [BD11d]. Finally, evaluation results are presented in this chapter for all proposed methods.

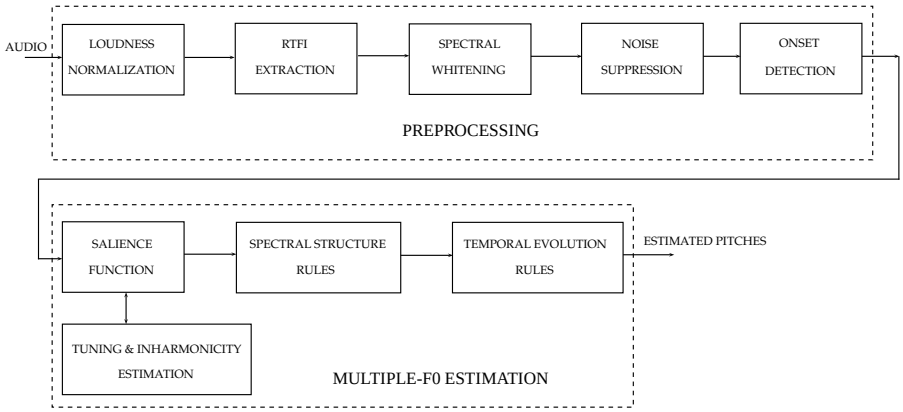

Figure 3.1: Diagram for the proposed multiple-F0 estimation system for isolated piano sounds.

3.2 Multiple-F0 Estimation of Piano Sounds

Initial research consists of a system for multiple-F0 estimation of isolated piano sounds which uses candidate selection and several rule-based refinement steps. The resonator time-frequency image (RTFI) is used as a data representation [ZRMZ09], and preprocessing steps for noise suppression, spectral whitening, and onset detection are utilized in order to make the estimation system robust to noise and recording conditions. A pitch salience function that is able to function in the log-frequency domain and utilizes tuning and inharmonicity estimation procedures is proposed and pitch candidates are selected according to their salience value. The set of candidates is refined using rules regarding the harmonic partial sequence of the selected pitches and the temporal evolution of the partials, in order to minimize errors occurring at multiples and sub-multiples of the actual F0s. For the spectral structure rules, a more robust formulation of the spectral irregularity measure [ZRMZ09] is proposed, taking into account overlapping partials. For the temporal evolution rules, a novel feature based on the common amplitude modulation (CAM) assumption [LWW09] is proposed in order to suppress estimation errors in harmonically-related F0 candidates. A diagram showing the stages of the proposed system is displayed in Figure 3.1.

3.2.1 Preprocessing

Resonator Time-Frequency Image

As a time-frequency representation, the resonator time-frequency image (RTFI) is used [ZRMZ09]. The RTFI selects a first-order complex resonator filter bank to implement a frequency-dependent time-frequency analysis. For the specific experiments, a RTFI with constant-Q resolution is selected for the time-frequency analysis, due to its suitability for music signal processing techniques, because the inter-harmonic spacing is the same for all pitches. The time interval between two successive frames is set to 40ms, which is typical for multiple-F0 estimation approaches [KD06]. The centre frequency difference between two neighbouring filters is set to 10 cents (the number of bins per octave is set to 120). The frequency range is set from 27.5Hz (A0) to 12.5kHz (which reaches up to the 3rd harmonic of C8). The employed absolute value of the RTFI will be denoted as $X[\omega, t]$, where t is the time frame and ω the log-frequency bin.

Spectral Whitening and Noise Suppression

Spectral whitening (or flattening) is a key preprocessing step applied in multiple-F0 estimation systems, in order to suppress timbral information and make the following analysis more robust to different sound sources. When viewed from an auditory perspective, it can be interpreted as the normalization of the hair cell activity level [TK00].

Here, a modified version of the real-time adaptive whitening method proposed in [SP07] is applied. Each band is scaled, taking into account the temporal evolution of the signal, while the scaling factor is dependent only on past frame values and the peak scaling value is exponentially decaying. The following iterative algorithm is applied:

$$\begin{aligned} Y[\omega, t] &= \begin{cases} \max(X[\omega, t], \theta, \varrho Y[\omega, t-1]), & t > 0 \\ \max(X[\omega, t], \theta), & t = 0 \end{cases} \\ X[\omega, t] &\leftarrow \frac{X[\omega, t]}{Y[\omega, t]} \end{aligned} \tag{3.1}$$

where $\varrho < 1$ is the peak scaling value and θ is a floor parameter.

In addition, a noise suppression approach similar to the one in [Kla09b] is employed, due to its computational efficiency. A half-octave span (60 bin) moving median filter is computed for $Y[\omega, t]$, resulting in noise estimate $N[\omega, t]$. After-

wards, an additional moving median filter $N'[\omega, t]$ of the same span is applied, but only including the RTFI bins whose amplitude is less than the respective amplitude of $N[\omega, t]$. This results in making the noise estimate $N'[\omega, t]$ robust in the presence of spectral peaks that could affect the noise estimate $N[\omega, t]$.

Onset Detection

In order to select the steady-state area of the piano tone (or tones), a spectral flux-based onset detection procedure is applied. The *spectral flux* measures the positive magnitude changes in each frequency bin, which indicate the attack parts of new notes [BDA+05]. It can be used effectively for onset detection of notes produced by percussive instruments such as the piano, but its performance decreases for the detection of soft onsets [Bel03]. For the RTFI, the spectral flux using the ℓ_1 norm can be defined as:

$$SF[t] = \sum_{\omega} HW(|Y[\omega, t]| - |Y[\omega, t-1]|) \tag{3.2}$$

where $HW(\cdot) = \frac{\cdot + |\cdot|}{2}$ is a half-wave rectifier. The resulting onset strength signal is smoothed using a median filter with a 3 sample span (120ms length), in order to remove spurious peaks. Onsets are subsequently selected from $SF[t]$ by a selection of local maxima, with a minimum inter-peak distance of 120 ms. Afterwards, the frames located between 100-300 ms after the onset are selected as the steady-state region of the signal and are averaged over time, in order to produce a robust spectral representation of the tones.

3.2.2 Multiple-F0 Estimation

Salience Function

In the linear frequency domain, considering a pitch p of a piano sound with fundamental frequency $f_{p,0}$ and inharmonicity coefficient b_p, partials are located at frequencies:

$$f_{p,h} = h f_{p,0} \sqrt{1 + (h^2 - 1) b_p} \tag{3.3}$$

where $h \geq 1$ is the partial index [KD06, BQGB04]. Consequently in the log-frequency domain, considering a pitch p at bin $\omega_{p,0}$, overtones are located at bins:

$$\omega_{p,h} = \omega_{p,0} + \left\lfloor u \cdot \log_2(h) + \frac{u}{2} \log_2\Big(1 + (h^2 - 1) b_p\Big) \right\rfloor \tag{3.4}$$

where $u = 120$ refers to the number of bins per octave and $\lceil \cdot \rfloor$ to the rounding operator.

A pitch salience function $\mathcal{S}[p, \delta_p, b_p]$ operating in the log-frequency domain is proposed, which indicates the strength of pitch candidates:

$$\mathcal{S}[p, \delta_p, b_p] = \sum_{h=1}^{H} \max_{m_h} \left\{ \sqrt{Y\left[\omega_{p,h} + \delta_p + \left\lceil um_h + \frac{u}{2}\log_2(1 + (h^2 - 1)b_p)\right\rfloor\right]} \right\} \tag{3.5}$$

where $Y[\omega]$ is the log-frequency spectrum for a specific time frame, $\delta_p \in [-4, \ldots, 4]$ is the tuning deviation for each pitch, and m_h specifies a search range around overtone positions, belonging to the interval (m_h^l, m_h^u), where:

$$\begin{aligned} m_h^l &= \left\lceil \frac{\log_2(h-1) + (M-1)\log_2(h)}{M} \right\rfloor \\ m_h^u &= \left\lceil \frac{(M-1)\log_2(h) + \log_2(h+1)}{M} \right\rfloor \end{aligned} \tag{3.6}$$

M is a factor controlling the width of the interval, which after experimentation was set to 60.

While the employed salience functions in the linear frequency domain (e.g. [Kla09b]) used a constant search space for each overtone, the proposed log-frequency salience function sets the search range around each partial to be inversely proportional to the partial index. The number of considered overtones H is set to 11 at maximum. A tuning search space of 50 cents is set around the ideal tuning frequency. The range of the inharmonicity coefficient b_p is set between 0 and $5 \cdot 10^{-4}$, which is typical for piano notes [BQGB04].

In order to accurately estimate the tuning factor and the inharmonicity coefficient for each pitch, a two-dimensional maximization procedure using exhaustive search is applied to $\mathcal{S}[p, \delta_p, b_p]$ for each pitch $p \in [21, \ldots, 108]$ in the MIDI scale (corresponding to a note range of A0-C8). This results in a pitch salience function estimate $\mathcal{S}'[p]$, a tuning deviation vector and an inharmonicity coefficient vector. Using the information extracted from the tuning and inharmonicity estimation, a harmonic partial sequence $HPS[p, h]$ for each candidate pitch and its harmonics (which contains the RTFI values at certain bin) is also stored for further processing.

An example of the salience function generation is given in Fig. 3.2, where the RTFI spectrum of an isolated F♯3 note played by a piano is seen, along with its corresponding salience $\mathcal{S}'[p]$. The highest peak in $\mathcal{S}'[p]$ corresponds to

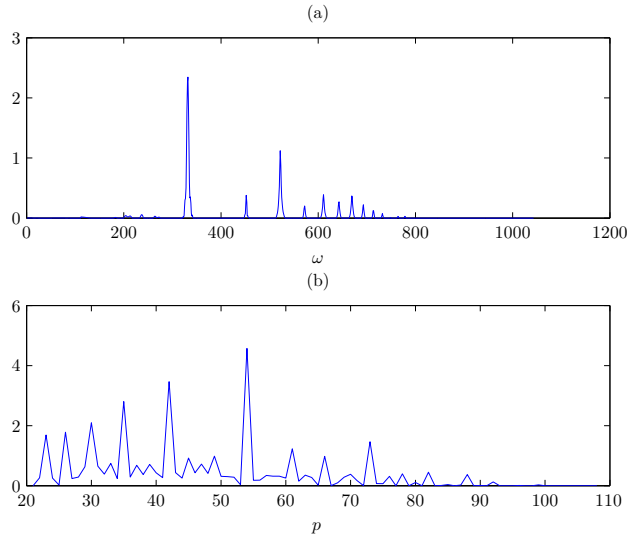

Figure 3.2: (a) The RTFI slice $Y[\omega]$ of an F♯3 piano sound. (b) The corresponding pitch salience function $\mathcal{S}'[p]$.

$p = 54$, thus F♯3.

Spectral Structure Rules

A set of rules examining the harmonic partial sequence structure of each pitch candidate is applied, which is inspired by work from [Bel03, Zho06]. These rules aim to suppress peaks in the salience function that occur at multiples and submultiples of the actual fundamental frequencies. In the semitone space, these peaks occur at $\pm\{12, 19, 24, 28, \ldots\}$ semitones from the actual pitch. The settings for the rules were made using a development set from the MAPS database [EBD10], as described in subsection 3.5.1.

A first rule for suppressing salience function peaks is setting a minimum number for partial detection in $HPS[p, h]$, similar to [Bel03, Zho06]. If $p < 47$, at least three partials out of the first six need to be present in the harmonic partial sequence (allowing for cases such as a missing fundamental). If $p \geq 47$, at least four partials out of the first six should be detected. A second rule concerns the salience value, which expresses the sum of the square root of the partial sequence amplitudes. If the salience value is below a minimum threshold (set to 0.2 using the development set explained in Section 3.5), this peak is suppressed. Another processing step in order to reduce processing time is the

reduction of the number of pitch candidates [EBD10], by selecting only the pitches with the greater salience values. In the current experiments, up to 10 candidate pitches are selected from $\mathcal{S}'[p]$.

Spectral flatness is another descriptor that can be used for the elimination of errors occurring in subharmonic positions [EBD10]. In the proposed system, the flatness of the first 6 partials of a harmonic sequence is used:

$$Fl[p] = \frac{\sqrt[6]{\prod_{h=1}^{6} HPS[p,h]}}{\frac{\sum_{h=1}^{6} HPS[p,h]}{6}} \tag{3.7}$$

The ratio of the geometric mean of $HPS[p]$ to its arithmetic mean gives a measure of smoothness; a high value of $Fl[p]$ indicates a partial sequence with a smooth envelope, while a lower value indicates fluctuations in the partial values, which could indicate the presence of a falsely detected pitch occurring in a sub-harmonic position. For the current experiments, the lower $Fl[p]$ threshold for suppressing pitch candidates was set to 0.1 after experimentation using the development set (described in Section 3.5).

In order to suppress candidate pitches occurring at multiples of the true fundamental frequency, a modified version of the *spectral irregularity* measure formulated in [ZRMZ09] is proposed. Considering a pitch candidate with fundamental frequency f_0 and another candidate with fundamental frequency lf_0, $l > 1$, spectral irregularity is defined as:

$$SI[p,l] = \sum_{h=1}^{3} HPS[p,hl] - \frac{HPS[p,hl-1] + HPS[p,hl+1]}{2} \tag{3.8}$$

The spectral irregularity is tested on pairs of harmonically-related candidate F0s. A high value of $SI[p,l]$ indicates the presence of the higher pitch with fundamental frequency lf_0, which is attributed to the higher energy of the shared partials between the two pitches compared to the energy of the neighbouring partials of f_0.

In this work, the SI is modified in order to make it more robust against overlapping partials that are caused by non-harmonically related F0s. Given the current set of candidate pitches from $\mathcal{S}'[p]$, the overlapping partials from non-harmonically related F0s are detected as in [Yeh08] and smoothed according to the *spectral smoothness* assumption, which states that the spectral envelope of harmonic sounds should form a smooth contour [Kla03]. For each overlap-

ping partial $HPS[p,h]$, an interpolated value $HPS_{interp}[p,h]$ is estimated by performing linear interpolation using its neighbouring partials. Afterwards, the smoothed partial amplitude $HPS'[p,h]$ is given by $\min(HPS[p,h], HPS_{interp}[p,h])$, as in [Kla03]. The proposed spectral irregularity measure, which now takes the form of a ratio in order to take into account the decreasing amplitude of higher partials, is thus formed as:

$$SI'[p,l] = \sum_{h=1}^{3} \frac{2 \cdot HPS'[p,hl]}{HPS'[p,hl-1] + HPS'[p,hl+1]} \tag{3.9}$$

For each pair of harmonically-related F0s (candidate pitches that have a pitch distance of $\pm\{12, 19, 24, 28, \ldots\}$) that are present in $\mathcal{S}'[p]$, the existence of the higher pitch is determined by the value of SI' (for the current experiments, a threshold of 1.2 was set using the development set).

Temporal Evolution Rules

Although the SI and the spectral smoothness assumption are able to suppress some harmonic errors, additional information needs to be exploited in order to produce more accurate estimates in the case of harmonically-related F0s. In [Yeh08], temporal information was employed for multiple-F0 estimation using the synchronicity criterion as a part of the F0 hypothesis score function. There, it is stated that the temporal centroid for a harmonic partial sequence should be the same for all partials. Thus, partials deviating from their global temporal centroid indicates an invalid F0 hypothesis. Here, we use the *common amplitude modulation* (CAM) assumption [GS07b, LWW09] in order to test the presence of a higher pitch in the case of harmonically-related F0s. CAM assumes that the partial amplitudes of a harmonic source are correlated over time and has been used in the past for note separation given a ground truth of F0 estimates [LWW09]. Thus, the presence of an additional source that overlaps certain partials (e.g. in the case of an octave where even partials are overlapped) causes the correlation between non-overlapped partials and the overlapped partials to decrease.

To that end, tests are performed for each harmonically-related F0 pair that is still present in $\mathcal{S}'[p]$, comparing partials that are not overlapped by any non-harmonically related F0 candidate with the partial of the fundamental. The

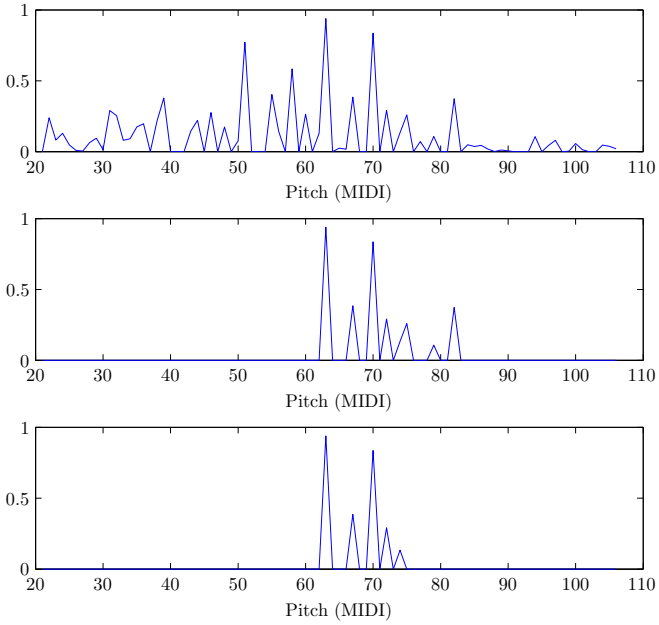

Figure 3.3: Salience function stages for an E♭4-G4-B♭4-C5-D5 piano chord. From top to bottom, the figures represent (i) The raw salience function (ii) The salience function after the spectral structure rules have been applied (iii) The salience function after the temporal evolution tests have been applied.

correlation coefficient is formed as:

$$Corr[p,h,l] = \frac{Cov(Y[\omega_{p,1},t], Y[\omega_{p,hl},t])}{\sqrt{Cov(Y[\omega_{p,1},t])\,Cov(Y[\omega_{p,hl},t])}} \tag{3.10}$$

where $\omega_{p,h}$ indicates the frequency bin corresponding to the h-th harmonic of pitch p, l the harmonic relation (eg. for octaves $l = 2$), and $Cov(\cdot)$ stands for the covariance measure. Tests are made for each pitch p and harmonics hl, using the same steady-state area used in subsection 3.2.1 as a frame range. If there is at least one harmonic where the correlation coefficient for a pitch is lower than a given value (in the experiments it was set to 0.8), then the hypothesis for the higher pitch presence is satisfied. In order to demonstrate the various refinement steps used in the salience function, Figure 3.3 shows the three basic stages of the multiple-F0 estimation system for a synthesized E♭4-G4-B♭4-C5-D5 piano chord.

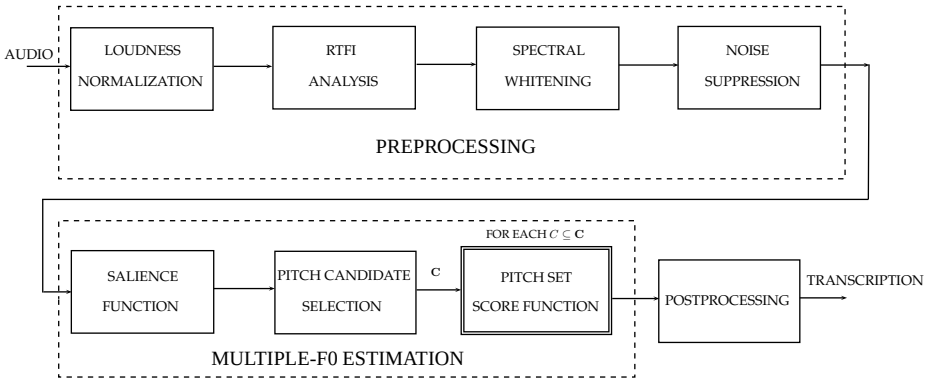

Figure 3.4: Diagram for the proposed joint multiple-F0 estimation system for automatic music transcription.

3.3 Joint Multiple-F0 Estimation for AMT

This automatic transcription system is an extension of the multiple-F0 estimation system of Section 3.2, but the estimation procedure is now joint instead of iterative, followed by note tracking. The constant-Q RTFI is used as a suitable time-frequency representation for music signals and a noise suppression method based on cepstral smoothing and pink noise assumption is proposed. For the multiple-F0 estimation step, a salience function is proposed for pitch candidate selection that incorporates tuning and inharmonicity estimation. For each possible pitch combination, an overlapping partial treatment procedure is proposed that is based on a novel method for spectral envelope estimation in the log-frequency domain, used for computing the harmonic envelope of candidate pitches. A score function which combines spectral and temporal features is proposed in order to select the optimal pitch set. Note smoothing is also applied in a postprocessing stage, employing HMMs and conditional random fields (CRFs) [LMP01] - the latter have not been used in the past for transcription approaches. A diagram of the proposed joint multiple-F0 estimation system can be seen in Fig. 3.4.

3.3.1 Preprocessing

Resonator Time-Frequency Image

As in the system of Section 3.2, the resonator time-frequency image was used as a time-frequency representation. The same settings were used, and the resulting

absolute value of the RTFI is denoted as $X[\omega, t]$.

Spectral Whitening

In this system, we employ a spectral whitening method similar to the one in [KD06], but modified for log-frequency spectra instead of linear frequency ones. For each frequency bin, the power within a subband of $\frac{1}{3}$ octave span multiplied by a Hann-window $W_{hann}[\omega]$ is computed. The square root of the power within each subband is:

$$\sigma[\omega] = \left(\frac{1}{\Omega} \sum_{l=\omega-\Omega/2}^{\omega+\Omega/2} W_{hann}[l] |X[l]|^2 \right)^{1/2} \tag{3.11}$$

where $\Omega = u/3 = 40$ bins and $X[\omega]$ is an RTFI spectrum. Afterwards, each bin is scaled according to:

$$Y[\omega] = (\sigma[\omega])^{j-1} X[\omega] \tag{3.12}$$

where j is a parameter which determines the amount of spectral whitening applied and $X[\omega]$ is the absolute value of the RTFI for a single time frame, and $Y[\omega]$ is the final whitened RTFI slice. As in [KD06], j was set to 0.33.

Noise Suppression

In [Yeh08], an algorithm for noise level estimation was proposed, based on the assumption that noise peaks are generated from a white Gaussian process, and the resulting spectral amplitudes obey a Rayleigh distribution. Here, an approach based on a pink noise assumption (elsewhere called $1/f$ noise or equal-loudness noise) is proposed. In pink noise, each octave carries an equal amount of energy, which corresponds well to the approximately logarithmic frequency scale of human auditory perception. Additionally, it occurs widely in nature, contrary to white noise and is also suitable for the employed time-frequency representation used in this work.

The proposed signal-dependent noise estimation algorithm is as follows:

1. Perform a two-stage median filtering procedure on $Y[\omega]$, in a similar way to [Kla09b], where a moving median average is calculated using the whitened spectrum. A second moving median average is calculated, including only the spectral bins that fall below the magnitude of the first moving average. The span of the filter is set to $\frac{1}{3}$ octave. The resulting noise representation $N[\omega]$ gives a rough estimate of the noise level.

2. Using the noise estimate, a transformation from the log-frequency spectral coefficients to cepstral coefficients is performed [Bro99]:

$$c_\xi = \sum_{\omega=1}^{\Omega'} \log(N[\omega]) \cos\left(\xi\left(\omega - \frac{1}{2}\right)\frac{\pi}{\Omega'}\right) \tag{3.13}$$

where $\Omega' = 1043$ is the total number of log-frequency bins in the RTFI and Ξ is the number of cepstral coefficients employed, $\xi = 0, \ldots, \Xi - 1$.

3. A smooth curve in the log-magnitude, log-frequency domain is reconstructed from the first D cepstral coefficients:

$$\log|N_c(\hat{\omega})| \approx \exp\left(c_0 + 2\sum_{\xi=1}^{D-1} c_\xi \cdot \cos(\xi\hat{\omega})\right) \tag{3.14}$$

4. The resulting smooth curve is mapped from $\hat{\omega}$ into ω. Assuming that the noise amplitude follows an exponential distribution, the expected value of the noise log amplitudes $E\{\log(|N_c(\hat{\omega})|)\}$ is equal to $\log(\lambda^{-1}) - \gamma$, where γ is the Euler constant (≈ 0.5772). Since the mean of an exponential distribution is equal to $\frac{1}{\lambda}$, the noise level in the linear amplitude scale can be described as:

$$\mathcal{L}_N(\hat{\omega}) = N_c(\hat{\omega}) \cdot e^\gamma \tag{3.15}$$

The analytic derivation of $E\{\log(|N_c(\hat{\omega})|)\}$ can be found in Appendix A.

In this work, the number of cepstral coefficients used was set to $D = 50$. Let $Z[\omega]$ stand for the whitened and noise-suppressed RTFI representation.

3.3.2 Multiple-F0 Estimation

In this subsection, multiple-F0 estimation, being the core of the proposed transcription system, is described. Performed on a frame-by-frame basis, a pitch salience function is generated, tuning and inharmonicity parameters are extracted, candidate pitches are selected, and for each possible pitch combination an overlapping partial treatment is performed and a score function is computed.

Salience Function

The same salience function that is proposed in the multiple-F0 estimation system of Section 3.2 is employed in this system. The final result of the salience

function computation stage is the pitch salience function estimate $\mathcal{S}'[p]$, a tuning deviation vector and an inharmonicity coefficient vector. Also, using the information extracted from the tuning and inharmonicity estimation, a harmonic partial sequence (HPS) $HPS[p, h]$, which contains magnitude information from $Y[\omega]$ for each harmonic of each candidate pitch, is also stored for further processing.

Pitch Candidate Selection

As in the multiple-F0 estimation system of Section 3.2, a set of conservative rules examining the harmonic partial sequence structure of each pitch candidate is applied, which is inspired by work from [Bel03, PI08]. For the present system, these rules aim to reduce the pitch candidate set for computational speed purposes.

A first rule for suppressing salience function peaks is setting a minimum number for partial detection in $HPS[p, h]$, similar to [Bel03]. At least three partials out of the first six need to be present in the harmonic partial sequence. A second rule discards pitch candidates with a salience value less than $0.1 \max(\mathcal{S}'[p])$, as in [PI08].

Finally, after spurious peaks in $\mathcal{S}'[p]$ have been eliminated, $\mathcal{C}_N = 10$ candidate pitches are selected from the highest amplitudes of $\mathcal{S}'[p]$ [EBD10]. The set of selected pitch candidates will be denoted as $\boldsymbol{\mathcal{C}}$. Thus, the maximum number of possible pitch candidate combinations that will be considered is 2^{10}, compared to 2^{88} if the aforementioned procedures were not employed.

Overlapping Partial Treatment

Current approaches in the literature rely on certain assumptions in order to recover the amplitude of overlapped harmonics. In [Kla03], it is assumed that harmonic amplitudes decay smoothly over frequency (*spectral smoothness*). Thus, the amplitude of an overlapped harmonic can be estimated from the amplitudes of neighboring non-overlapped harmonics. In [VK02], the amplitude of the overlapped harmonic is estimated through non-linear interpolation on the neighboring harmonics. In [ES06], each set of harmonics is filtered from the spectrum and in the case of overlapping harmonics, linear interpolation is employed.

In this system, an overlapping partial treatment procedure based on spectral envelope estimation of candidate pitches is proposed. The proposed spec-

tral envelope estimation algorithm for the log-frequency domain is presented in Appendix B. For each possible pitch combination $\mathcal{C} \subseteq \boldsymbol{\mathcal{C}}$, overlapping partial treatment is performed, in order to accurately estimate the partial amplitudes. The proposed overlapping partial treatment procedure is as follows:

1. Given a set $\mathcal{C}$ of pitch candidates, estimate a partial collision list.

2. For a given harmonic partial sequence, if the number of overlapped partials is less than N_{over}, then estimate the harmonic envelope $SE_p[\omega]$ of the candidate pitch using only amplitude information from non-overlapped partials.

3. For a given harmonic partial sequence, if the number of overlapped partials is equal to or greater than N_{over}, estimate the harmonic envelope using information from the complete harmonic partial sequence.

4. For each overlapped partial, estimate its amplitude using the harmonic envelope parameters of the corresponding pitch candidate (see Appendix B).

The output of the overlapping partial treatment procedure is the updated harmonic partial sequence $HPS[p, h]$ for each pitch set combination.

Pitch set score function

Having selected a set of possible pitch candidates and performed overlapping partial treatment on each possible combination, the goal is to select the optimal pitch combination for a specific time frame. In [Yeh08], Yeh proposed a score function which combined four criteria for each pitch: harmonicity, bandwidth, spectral centroid, and synchronicity. Also, in [PI08], a simple score function was proposed for pitch set selection, based on the smoothness of the pitch set. Finally, in [EBD10] a multipitch detection function was proposed, which employed the spectral flatness of pitch candidates along with the spectral flatness of the noise residual.

Here, a weighted pitch set score function is proposed, which combines spectral and temporal characteristics of the candidate F0s, and also attempts to minimize the noise residual to avoid any missed detections. Also, features which concern harmonically-related F0s are included in the score function, in order to suppress any harmonic errors. Given a candidate pitch set $\mathcal{C} \subseteq \boldsymbol{\mathcal{C}}$ with size $|\mathcal{C}|$,

the proposed pitch set score function is:

$$\mathcal{L}(\mathcal{C}) = \sum_{i=1}^{|\mathcal{C}|} (\mathcal{L}_{p(i)}) + \mathcal{L}_{res} \tag{3.16}$$

where $\mathcal{L}_{p(i)}$ is the score function for each candidate pitch $p(i) \in \mathcal{C}$, and $\mathcal{L}_{res}$ is the score for the residual spectrum. $\mathcal{L}_p$ and $\mathcal{L}_{res}$ are defined as:

$$\begin{aligned} \mathcal{L}_p &= w_1 Fl[p] + w_2 Sm[p] - w_3 SC[p] + w_4 PR[p] - w_5 AM[p] \\ \mathcal{L}_{res} &= w_6 Fl[Res] \end{aligned} \tag{3.17}$$

Features Fl, Sr, SC, PR, AM have been weighted by the salience function of the candidate pitch and divided by the sum of the salience function of the candidate pitch set, for normalization purposes. In order to train the weight parameters $w_i, i = 1, \ldots, 6$ of the features in (3.17), we used the Nelder-Mead search algorithm for parameter estimation [NM65]. The training set employed for experiments is described in Section 3.5. The pitch candidate set that maximizes the score function:

$$\hat{\mathcal{C}} = \arg\max_{\mathcal{C} \subseteq \boldsymbol{\mathcal{C}}} \mathcal{L}(\mathcal{C}) \tag{3.18}$$

is selected as the pitch estimate for the current frame.

$Fl[p]$ denotes the spectral flatness of the harmonic partial sequence:

$$Fl[p] = \frac{e^{[\sum_{h=1}^{H} \log(HPS[p,h])]/H}}{\frac{1}{H}\sum_{h=1}^{H} HPS[p,h]} \tag{3.19}$$

The spectral flatness is a measure of the 'whiteness' of the spectrum. Its values lie between 0 and 1 and it is maximized when the input sequence is smooth, which is the ideal case for an HPS. It has been used previously for multiple-F0 estimation in [PI08, EBD10]. Compared with (3.7), in (3.19) the definition is the one adapted by the MPEG-7 framework, which can be seen in [Uhl10].

$Sm[p]$ is the *smoothness* measure of a harmonic partial sequence, which was proposed in [PI08]. The definition of smoothness stems from the spectral smoothness principle and its definition stems from the definition of *sharpness*:

$$Sr[p] = \sum_{h=1}^{H} (SE_p[\omega_{p,h}] - HPS[p,h]) \tag{3.20}$$

Here, instead of a low-pass filtered HPS using a Gaussian window as in [PI08], the estimated harmonic envelope SE_p of each candidate pitch is employed for the smoothness computation. $Sr[p]$ is normalized into $\bar{Sr}[p]$ and the smoothness measure $Sm[p]$ is defined as: $Sm[p] = 1 - \bar{Sr}[p]$. A high value of $Sm[p]$ indicates a smooth HPS.

$SC[p]$ is the spectral centroid for a given HPS and has been used for the score function in [Yeh08]:

$$SC[p] = \sqrt{2 \cdot \frac{\sum_{h=1}^{H} h \cdot |HPS[p,h]|^2}{\sum_{h=1}^{H} |HPS[p,h]|^2}} \tag{3.21}$$

It indicates the center of gravity of an HPS; for pitched percussive instruments it is positioned at lower partials. A typical value for a piano note would be 1.5 denoting that the center of gravity of its HPS is between the 1st and 2nd harmonic.

$PR[p]$ is a novel feature, which stands for the harmonically-related pitch ratio. Here, harmonically-related pitches [Yeh08] are candidate pitches in $\boldsymbol{\mathcal{C}}$ that have a semitone difference of $\lceil 12 \cdot \log_2(l) \rfloor = \{12, 19, 24, 28, \ldots\}$, where $l > 1, l \in \mathbb{N}$. $PR[p]$ is applied only in cases of harmonically-related pitches, in an attempt to estimate the ratio of the energy of the smoothed partials of the higher pitch compared to the energy of the smoothed partials of the lower pitch. It is formulated as follows:

$$PR_l[p] = \sum_{h=1}^{3} \frac{HPS[p + \lceil 12 \cdot \log_2(l) \rfloor, h]}{HPS[p, l \cdot h]} \tag{3.22}$$

where p stands for the lower pitch and $p + \lceil 12 \cdot \log_2(l) \rfloor$ for the higher harmonically-related pitch. l stands for the harmonic relation between the two pitches ($f_{high} = l f_{low}$). In case of more than one harmonic relation between the candidate pitches, a mean value is computed: $PR[p] = \frac{1}{|N_{hr}|} \sum_{l \in N_{hr}} PR_l[p]$, where N_{hr} is the set of harmonic relations. A high value of PR indicates the presence of a pitch in the higher harmonically-related position.

Another novel feature applied in the case of harmonically-related F0s, measuring the amplitude modulation similarity between an overlapped partial and a non-overlapped partial frequency region, is proposed. The feature is based on the common amplitude modulation (CAM) assumption [LWW09] as in the temporal evolution rules of Section 3.2. Here, an extra assumption is made

that frequency deviations are also correlated over time. The time-frequency region of a non-overlapped partial is compared with the time-frequency region of the fundamental. In order to compare 2-D time-frequency partial regions, the normalized tensor scalar product [dL97] is used:

$$AM_l[p] = \sum_{h=1}^{3} \frac{\sum_{i,j} B_{ij} B_{ij}^h}{\sqrt{\sum_{i,j} B_{ij} B_{ij}^h} \cdot \sqrt{\sum_{i,j} B_{ij} B_{ij}^h}} \tag{3.23}$$

where

$$\begin{aligned} B &= Z[\omega_{p,1} - 4 : \omega_{p,1} + 4, \quad n_0 : n_1] \\ B^h &= Z[\omega_{p,hl} - 4 : \omega_{p,hl} + 4, \quad n_0 : n_1] \end{aligned} \tag{3.24}$$

where i, j denote the indexes of matrices B and B^h, and n_0 and $n_1 = n_0 + 5$ denote the frame boundaries of the time-frame region selected for consideration. The normalized tensor scalar product is a generalization of the cosine similarity measure, which compares two vectors, finding the cosine of the angle between them.

Res denotes the residual spectrum, which can be expressed in a similar way to the linear frequency version in [EBD10]:

$$Res = \left\{ Z[\omega] \Big/ \forall p, \forall h, \left| \omega - \omega_{p,h} \right| > \frac{\Delta_w}{2} \right\} \tag{3.25}$$

where $Z[\omega]$ is the whitened and noise-suppressed RTFI representation and Δ_w denotes the mainlobe width of the employed window w. In order to find a measure of the 'whiteness' of the residual, $1 - Fl[Res]$, which denotes the residual smoothness, is used.

3.3.3 Postprocessing

Although temporal information has been included in the frame-based multiple-F0 estimation system through the use of the CAM feature in the score function, additional postprocessing is needed in order to track notes over time, and eliminate any single-frame errors. In this system, two postprocessing methods were employed: the first using HMMs and the second using conditional random fields (CRFs), which to the author's knowledge have not been used before in music transcription research.

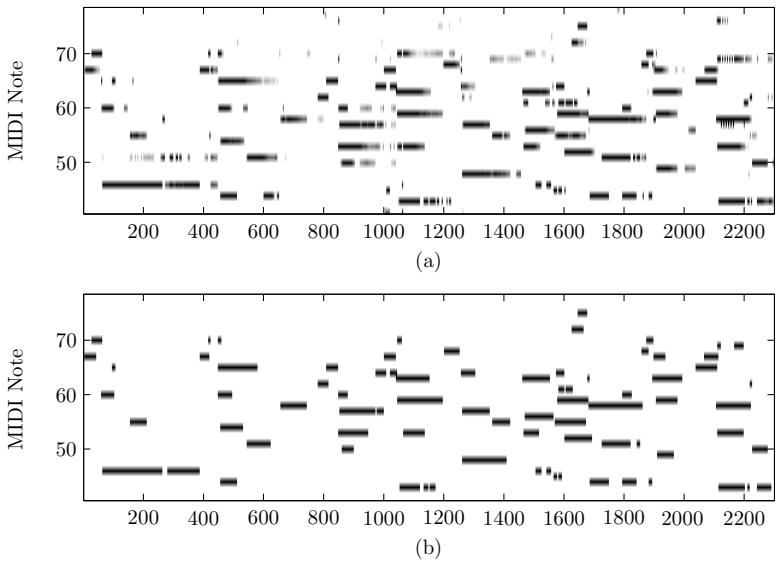

Figure 3.5: Transcription output of an excerpt of 'RWC MDB-J-2001 No. 2' (jazz piano) in a 10 ms time scale (a) Output of the multiple-F0 estimation system (b) Piano-roll transcription after HMM postprocessing.

HMM Postprocessing

In this work, each pitch $p = 1, \ldots, 88$ is modeled by a two-state HMM, denoting pitch activity/inactivity, as in [PE07a, QRC$^+$10]. The observation sequence is given by the output of the frame-based multiple-F0 estimation step for each pitch p: $\mathcal{O}^{(p)} = \{\mathfrak{o}_t^{(p)}\}$, $t = 1, \ldots, T$, while the state sequence is given by $\mathcal{Q}^{(p)} = \{\mathfrak{q}_t^{(p)}\}$. Essentially, in the HMM post-processing step, pitches from the multiple-F0 estimation step are tracked over time and their note activation boundaries are estimated using information from the salience function. In order to estimate the state priors $P(\mathfrak{q}_1^{(p)})$ and the state transition matrix $P(\mathfrak{q}_t^{(p)}|\mathfrak{q}_{t-1}^{(p)})$, MIDI files from the RWC database [GHNO03] from the classic and jazz subgenres were employed, as in [QRC$^+$10]. For each pitch, the most likely state sequence is given by:

$$\mathcal{Q}'^{(p)} = \arg\max_{\mathfrak{q}^{(p)}} \prod_t P(\mathfrak{q}_t^{(p)}|\mathfrak{q}_{t-1}^{(p)}) P(\mathfrak{o}_t^{(p)}|\mathfrak{q}_t^{(p)}) \tag{3.26}$$

In order to estimate the observation probabilities $P(\mathfrak{o}_t^{(p)}|\mathfrak{q}_t^{(p)})$, we employ a sigmoid curve which has as input the salience function of an active pitch from

the output of the multiple-F0 estimation step:

$$P(\mathfrak{o}_t^{(p)}|\mathfrak{q}_t^{(p)}=1)=\frac{1}{1+e^{-(\mathcal{S}'[p,t]-1)}} \tag{3.27}$$

where $\mathcal{S}'[p,t]$ denotes the salience function value at frame t. The output of the HMM-based postprocessing step is generated using the Viterbi algorithm. The transcription output of an example recording at the multiple-F0 estimation stage and after the HMM postprocessing is depicted in Fig. 3.5. In addition, in Fig. 3.6(a) the decoding process of the pitch-wise HMM is shown.

CRF Postprocessing

Although the HMMs have repeatedly proved to be an invaluable tool for smoothing sequential data, they suffer from the limitation that the observation at a given time frame depends only on the current state. In addition, the current state depends only on its immediate predecessor. In order to alleviate these assumptions, conditional random fields (CRFs) [LMP01] can be employed. CRFs are undirected graphical models that directly model the conditional distribution $P(\mathcal{Q}|\mathcal{O})$ instead of the joint probability distribution $P(\mathcal{Q},\mathcal{O})$ as in the HMMs. Thus, HMMs belong to the class of *generative* models, while the undirected CRFs are *discriminative* models. The assumptions concerning the state independence and the observation dependence on the current state which are posed for the HMMs are relaxed.

In this work, 88 linear-chain CRFs are employed (one for each pitch p), where the current state $\mathfrak{q}_t^{(p)}$ is dependent not only on the current observation $\mathfrak{o}_t^{(p)}$, but also on $\mathfrak{o}_{t-1}^{(p)}$, in order to exploit information not only from the current state, but from the past one as well. For learning, we used the same note priors and state transitions from the RWC database which were also utilized for the HMM post-processing. For inference, the most likely state sequence for each pitch is computed using a Viterbi-like recursion which estimates:

$$\mathcal{Q}'^{(p)}=\arg\max_{\mathcal{Q}^{(p)}} P(\mathcal{Q}^{(p)}|\mathcal{O}^{(p)}) \tag{3.28}$$

where $P(\mathcal{Q}^{(p)}|\mathcal{O}^{(p)})=\prod_t P(\mathfrak{q}_t^{(p)}|\mathcal{O}^{(p)})$ and the observation probability for a given state is given as a sum of two potential functions:

$$P(\mathcal{O}^{(p)}|\mathfrak{q}_t^{(p)}=1)=\frac{1}{1+e^{-(\mathcal{S}'[p,t]-1)}}+\frac{1}{1+e^{-(\mathcal{S}'[p,t-1]-1)}} \tag{3.29}$$

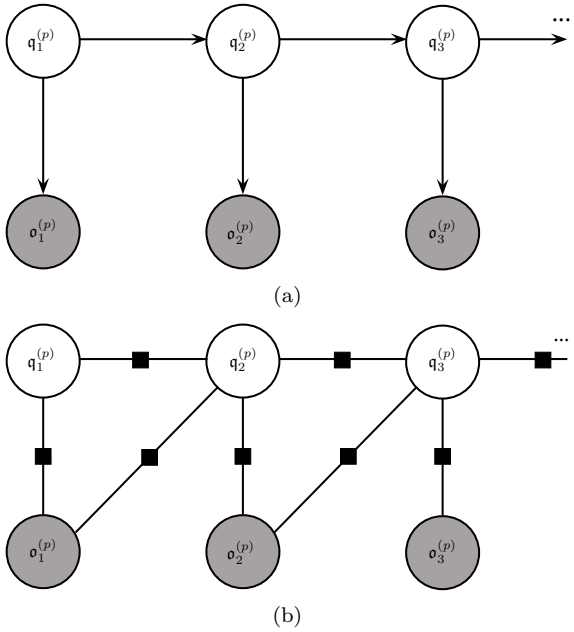

Figure 3.6: Graphical structure of the postprocessing decoding process for (a) HMM (b) Linear chain CRF networks.

It should be noted that in our employed CRF model we assume that each note state depends only on its immediate predecessor (like in the HMMs), while the relaxed assumption over the HMMs concerns the observation potentials. The graphical structure of the linear-chain CRF which was used in our experiments is presented in Fig. 3.6(b).

3.4 AMT using Note Onset and Offset Detection

The final system presented in this chapter is an extension of the joint multiple-F0 estimation system of Section 3.3, which explicitly incorporates information on note onsets and offsets. For onset detection, two novel descriptors are proposed which exploit information from the transcription preprocessing steps. The multiple-F0 estimation step is made using the same score function as in Section 3.3. Finally, a novel hidden Markov model-based offset detection procedure is proposed.

3.4.1 Preprocessing

Resonator Time-Frequency Image

As in the systems of Sections 3.2 and 3.3, the resonator time-frequency image was used as a time-frequency representation. The same settings were used, and the resulting absolute value of the RTFI is denoted as $X[\omega, t]$ while an RTFI slice is denoted as $X[\omega]$.

Spectral Whitening and Noise Suppression

In order to suppress timbral information and make the following analysis more robust to different sound sources, spectral whitening is performed using the same method described in Section 3.3, resulting in the whitened representation $Y[\omega, t]$. Afterwards, an algorithm for noise suppression is applied to the whitened RTFI, using the two-stage median filtering procedure presented in subsection 3.3.1.The result is a whitened and noise-suppressed RTFI representation $Z[\omega]$.

Salience Function

Using $Z[\omega]$, the log-frequency pitch salience function $\mathcal{S}[p]$ proposed in Section 3.2 is extracted, where $p \in [21, \ldots, 108]$ denotes MIDI pitch. Tuning and inharmonicity coefficients are also extracted. Using the extracted information, a harmonic partial sequence (HPS) $HPS[p, h]$ for each candidate pitch p and its harmonics $h = 1, \ldots, 13$ is also stored for further processing.

3.4.2 Onset Detection

In order to accurately detect onsets in polyphonic music, two onset descriptors which exploit information from the transcription preprocessing steps are proposed and combined using late fusion. Firstly, a novel spectral flux-based feature is defined, which incorporates pitch tuning information. Although spectral flux has been successfully used in the past for detecting hard onsets [BDA+05], false alarms may be detected for instruments that produce frequency modulations such as vibrato or portamento. Thus, a semitone-resolution filterbank is created from $Z[\omega, t]$, where each filter is centered at the estimated tuning position of each pitch:

$$\psi[p, t] = \left(\sum_{l=\omega_{p,0}+\delta_p-4}^{\omega_{p,0}+\delta_p+4} Z[l, t] \cdot W_p[l] \right)^{\frac{1}{2}} \tag{3.30}$$

where $\omega_{p,0}$ is the bin that ideally corresponds to pitch p and W_p is a 80 cent-span Hanning window centered at the pitch tuning position. Using the output of the filterbank, the novel spectral flux-based descriptor is defined as:

$$SF[t] = \sum_{p=21}^{108} HW(\psi[p,t] - \psi[p,t-1]) \tag{3.31}$$

where $HW(\cdot) = \frac{\cdot+|\cdot|}{2}$ is a half-wave rectifier. Afterwards, onsets can be detected by performing peak picking on $SF[t]$.

In order to detect soft onsets, which may not be indicated by a change in signal energy [BDA+05], a pitch-based descriptor is proposed which is based on the extracted salience function. The salience function $\mathcal{S}[p,t]$ is smoothed using a moving median filter with 120 ms span, in order to reduce any fluctuations that might be attributed to amplitude modulations (e.g. tremolo). The smoothed salience function $\bar{\mathcal{S}}[p,t]$ is then warped into a chroma-like representation:

$$Chr[\mathfrak{p},t] = \sum_{i=0}^{6} \bar{\mathcal{S}}[12 \cdot i + \mathfrak{p} + 20, t] \tag{3.32}$$

where $\mathfrak{p} = 1, \ldots, 12$ represents the pitch classes C, C♯,...,B. Afterwards, the half-wave rectified first-order difference of $Chr[\mathfrak{p},t]$ is used as a pitch-based onset detection function (denoted as salience difference SD):

$$SD[t] = \sum_{i=1}^{12} HW(Chr[i,t] - Chr[i,t-1]) \tag{3.33}$$

Accordingly, soft onsets are detected by peak picking on $SD[t]$.

In order to combine the onsets produced by the two aforementioned descriptors, late fusion is applied, as in [HS10]. From each of the two descriptors an onset strength signal is created, which contains either the value one at the instant of the detected onset or zero otherwise. The fused onset strength signal is created by summing and smoothing these two signals using a moving median filter of 40 ms length. Onsets are detected by performing peak picking on the fused signal by selecting peaks with a minimum 80 ms distance. For tuning onset detection parameters, a development set containing ten 30 sec classical recordings from the meter analysis data from Ghent University [VM07] was employed.

3.4.3 Multiple-F0 Estimation

We perform the same multiple-F0 estimation procedure described in subsection 3.4.3 using segments defined by two consecutive onsets instead of performing multiple-F0 estimation for each time frame.

Overlapping Partial Treatment

We extract segments defined by two consecutive onsets by using the mean $Z[\omega, t]$ of the first 3 frames after the onset. Using each segment, a salience function and HPS are extracted. A set of $\mathcal{C}_N$ candidate pitches is selected, based on the maximum values of the salience function $\mathcal{S}[p]$ (here, $\mathcal{C}_N$ is set to 10 as in [EBD10]). The pitch candidate set will be denoted as $\boldsymbol{\mathcal{C}}$.

In order to recover the amplitude of overlapped harmonics, we employ the proposed discrete cepstrum-based spectral envelope estimation algorithm described in subsection 3.3.2 and detailed in Appendix B. Firstly, given a subset $\mathcal{C}$ of pitch candidates, a partial collision list is computed. For a given HPS, if the number of overlapped partials is less than N_{over}, then the amplitudes of the overlapped partials are estimated from the spectral envelope $SE_p[\omega]$ of the candidate pitch using only amplitude information from non-overlapped partials. If the number of overlapped partials is equal or greater than N_{over}, the partial amplitudes are estimated using spectral envelope information from the complete HPS.

Pitch set score function

Having selected a set of possible pitch candidates and performed overlapping partial treatment on each possible combination, the goal is to select the optimal pitch combination for a specific time frame. A modified version of the pitch set score function presented in subsection 3.3.2 is employed, which combines spectral and temporal characteristics of the candidate F0s, and also attempts to minimize the noise residual to avoid any missed detections.

Given a candidate pitch set $\mathcal{C} \subseteq \boldsymbol{\mathcal{C}}$ with size $|\mathcal{C}|$, the proposed pitch set score function is given by (3.16), where in this case $\mathcal{L}_p$ is defined as:

$$\mathcal{L}_p = w_1 Fl[p] + w_2 Sm[p] - w_3 SC[p] + w_4 PR[p] \tag{3.34}$$

where $Fl[p], Sm[p], SC[p], PR[p]$ are defined in subsection 3.3.2.

In order to train the weight parameters $w_i, i = 1, \ldots, 4$ of the features in (3.34) as well as for the residual weight in (3.17), training was performed using the Nelder-Mead search algorithm for parameter estimation [NM65] with 100 classic, jazz, and random piano chords from the MAPS database [EBD10] as a training set. Trained weight parameters w_i were $\{1.3, 1.4, 0.6, 0.5, 25\}$. The pitch candidate set $\hat{\mathcal{C}}$ that maximizes the score function is selected as the pitch estimate for the current frame.

3.4.4 Offset Detection

In order to accurately detect note offsets we employ hidden Markov models (HMMs). HMMs have been used in the past for smoothing transcription results (e.g. [QRC+10]) but to the author's knowledge they have not been utilized for offset detection. As in the note tracking procedure of Subsection 3.3.1, each pitch is modeled by a two-state HMM, denoting pitch activity/inactivity. The observation sequence $\mathcal{O}^{(p)}$ is given by the output of the multiple-F0 estimation step for each pitch, while the state sequence is given by $\mathcal{Q}^{(p)}$. In order to estimate state priors $P(\mathfrak{q}_1^{(p)})$ and the state transition matrix $P(\mathfrak{q}_t^{(p)}|\mathfrak{q}_{t-1}^{(p)})$, MIDI files from the RWC database [GHNO03] from the classic and jazz genres were used.

In order to estimate the observation probabilities $P(\mathfrak{o}_t^{(p)}|\mathfrak{q}_t^{(p)})$, we employ a sigmoid curve which has as input the salience function of an active pitch from the output of the multiple-F0 estimation step:

$$P(\mathfrak{o}_t^{(p)}|\mathfrak{q}_t^{(p)} = 1) = \frac{1}{1 + e^{-(\mathcal{S}[p,t]-1)}} \tag{3.35}$$

where $\mathcal{S}[p, t]$ denotes the salience function value at frame t. The output of the HMM-based offset detection step is generated using the Viterbi algorithm. The note offset is detected as the time frame when an active pitch between two consecutive onsets changes from an active to an inactive state for the first time. Thus, the main difference between the present system and the system of Section 3.3 in terms of postprocessing is that for each active note event between two onsets, only one offset must be present; in the system of Section 3.3, a note event in an "off" state might move to an "on" state in the next frame. Thus, the present system explicitly models note offsets. An example for the complete transcription system, from preprocessing to offset detection, is given in Fig. 3.7 for a guitar recording from the RWC database.

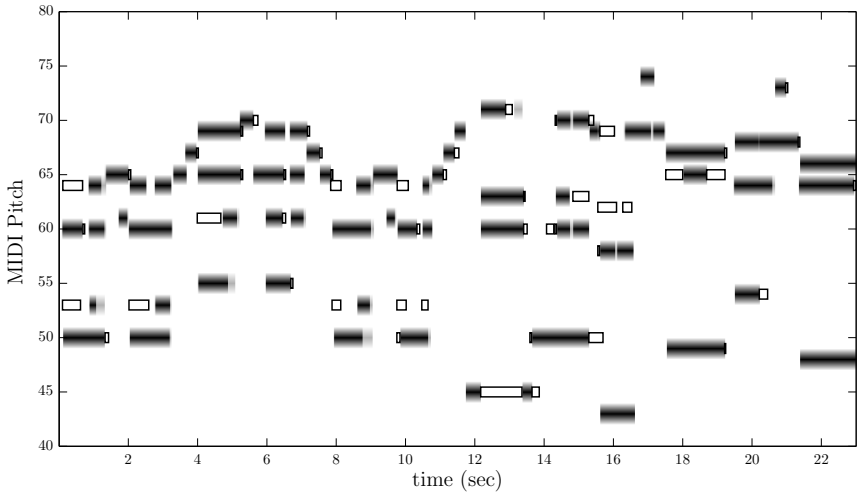

Figure 3.7: The transcription system of Section 3.4 applied to an excerpt from 'RWC MDB-J-2001 No. 9' (guitar). Black rectangles correspond to correctly detected pitches, gray rectangles to false alarms, and empty rectangles to missed detections.

3.5 Evaluation

3.5.1 Datasets

MAPS Database

The proposed multiple-F0 estimation system for isolated piano sounds of Section 3.2 is tested on the MIDI Aligned Piano Sounds (MAPS) database [EBD10]. MAPS contains real and synthesized recordings of isolated notes, musical chords, random chords, and music pieces, produced by 9 real and synthesized pianos in different recording conditions, containing around 10000 sounds in total. Recordings are stereo, sampled at 44100Hz, while MIDI files are provided as ground truth. For the current experiments, classic, jazz, and randomly generated chords (without any note progression) of polyphony levels between 1 and 6 are employed, while the note range is C2-B6, in order to match the experiments performed in [EBD10]. Each recording lasts about 4 seconds. A development set using 2 pianos (consisting of 1952 samples) is selected while the other 7 pianos (consisting of 6832 samples) are used as a test set.

For training the weight parameters for the score function in the transcription

systems of Sections 3.3 and 3.4, samples from the MAPS database are also used. Here, 103 samples from two piano types are employed for training[1]. For comparative experiments on isolated piano sounds using the transcription system of Section 3.3, it should be noted that the postprocessing stage was not employed for the MAPS dataset.

RWC Dataset

For the transcription experiments of systems presented in Sections 3.3 and 3.4, we use 12 excerpts from the RWC database [GHNO03], which have been used in the past to evaluate polyphonic music transcription approaches in [KNS07, SKT+08, QRC+10]. A list of the employed recordings along with the instruments present in each one is shown in the top half of Table 3.1. The recordings containing 'MDB-J' in their RWC ID belong to the jazz genre, while those that contain 'MDB-C' belong to the classic genre. For the recording titles and composer, the reader can refer to [SKT+08]. Five additional pieces are also selected from the RWC database, which have not yet been evaluated in the literature. These pieces are described in the bottom half of Table 3.1 (data 13-17).

As far as ground-truth for the RWC data 1-12 shown in Table 3.1, non-aligned MIDI files are provided along with the original 44.1 kHz recordings. However, these MIDI files contain several note errors and omissions, as well as unrealistic note durations, thus making them unsuitable for transcription evaluation. As in [KNS07, SKT+08, QRC+10], aligned ground-truth MIDI data has been created for the first 23s of each recording, using Sonic Visualiser [Son] for spectrogram visualization and MIDI editing. For the RWC data 13-17 in Table 3.1, the newly-released syncRWC ground truth annotations are utilized[2].

Disklavier Dataset

The test dataset developed by Poliner and Ellis [PE07a] is also used for transcription experiments. It contains 10 one-minute recordings from a Yamaha Disklavier grand piano, sampled at 8 kHz. Aligned MIDI ground truth using the Disklavier is also provided with the recordings. The list of music pieces that are contained in this dataset is shown in Table 3.2.

[1] Trained weight parameters for the system of Section 3.3 are $w_i = \{1.3, 1.4, 0.6, 0.5, 0.2, 25\}$.
[2] `http://staff.aist.go.jp/m.goto/RWC-MDB/AIST-Annotation/SyncRWC/`

	RWC ID	Instruments
1	RWC-MDB-J-2001 No. 1	Piano
2	RWC-MDB-J-2001 No. 2	Piano
3	RWC-MDB-J-2001 No. 6	Guitar
4	RWC-MDB-J-2001 No. 7	Guitar
5	RWC-MDB-J-2001 No. 8	Guitar
6	RWC-MDB-J-2001 No. 9	Guitar
7	RWC-MDB-C-2001 No. 30	Piano
8	RWC-MDB-C-2001 No. 35	Piano
9	RWC-MDB-J-2001 No. 12	Flute + Piano
10	RWC-MDB-C-2001 No. 12	Flute + String Quartet
11	RWC-MDB-C-2001 No. 42	Cello + Piano
12	RWC-MDB-C-2001 No. 49	Tenor + Piano
13	RWC-MDB-C-2001 No. 13	String Quartet
14	RWC-MDB-C-2001 No. 16	Clarinet + String Quartet
15	RWC-MDB-C-2001 No. 24a	Harpsichord
16	RWC-MDB-C-2001 No. 36	Violin (polyphonic)
17	RWC-MDB-C-2001 No. 38	Violin

Table 3.1: The RWC data used for transcription experiments.

MIREX MultiF0 Development Dataset

Finally, the full wind quintet recording from the MIREX multi-F0 development set is also used for experiments [MIR]. This recording is the fifth variation from L. van Beethoven's Variations from String Quartet Op.18 No.5. It consists of 5 individual instrument tracks (for bassoon, clarinet, flute, horn, and oboe) and a final mix, all sampled at 44.1 kHz. The multi-track recording has been evaluated in the literature in shorter segments [VBB10, PG11, GE11, OVC+11], or in pairs of tracks [MS09]. MIDI annotations for each instrument track have been created by the author and Graham Grindlay (the latter from LabROSA, Columbia University). The recording and the corresponding annotations can be found online[3].

[3] `http://www.music-ir.org/evaluation/MIREX/data/2007/multiF0/index.htm` (MIREX credentials required)

	Composer	Title
1	J. S. Bach	Prelude BWV 847
2	L. van Beethoven	Fur Elise WoO 59
3	L. van Beethoven	Sonata Op 13(3)
4	J. Brahms	Fantasia Op 116, No 6
5	F. Chopin	Etude Op 10, No 1
6	J. Haydn	Sonata XVI:40(2)
7	W. A. Mozart	Sonata KV 333(1)
8	F. Schubert	Fantasia D 760(4)
9	R. Schumann	Scenes from Childhood, Op 15(4)
10	P. I. Tchaikovsky	The Seasons, Op 37a(1)

Table 3.2: The piano dataset created in [PE07a], which is used for transcription experiments.

3.5.2 Results

MAPS Database

For the experiments performed on the isolated piano chords from the MAPS database [EBD10], we employed the precision, recall, and F-measure metrics for a single frame, as defined in (2.28). A comparison is made between the system presented in Section 3.2, the system of Section 3.3 using CRF postprocessing, the system by Emiya et al. [EBD10], as well as results found in [EBD10] for the system of Klapuri [Kla03]. We do not perform experiments using the system of Section 3.4, as the multiple-F0 estimation stage is the same as in the system 3.3 and the only difference is for the treatment of note onsets and offsets which does not apply in this specific experiment.

The performance of the proposed multiple-F0 estimation systems along with the systems in the literature is shown in Fig. 3.8, organized according to the polyphony level of the ground truth (experiments are performed with unknown polyphony).

For the system of Section 3.2, the mean $\mathcal{F}$ for polyphony levels $L = 1, \ldots, 6$ is 87.84%, 87.44%, 90.62%, 88.76%, 87.52%, and 72.96% respectively. It should be noted that the subset of polyphony level 6 consists only of 350 samples of random notes and not of classical and jazz chords. As far as precision is concerned, reported rates are high for polyphony levels 2-6, ranging from 91.11% to 95.83%. The lowest precision rate is 84.25% for $L = 1$, where some overtones were erroneously considered as pitches. Recall displays the opposite performance,

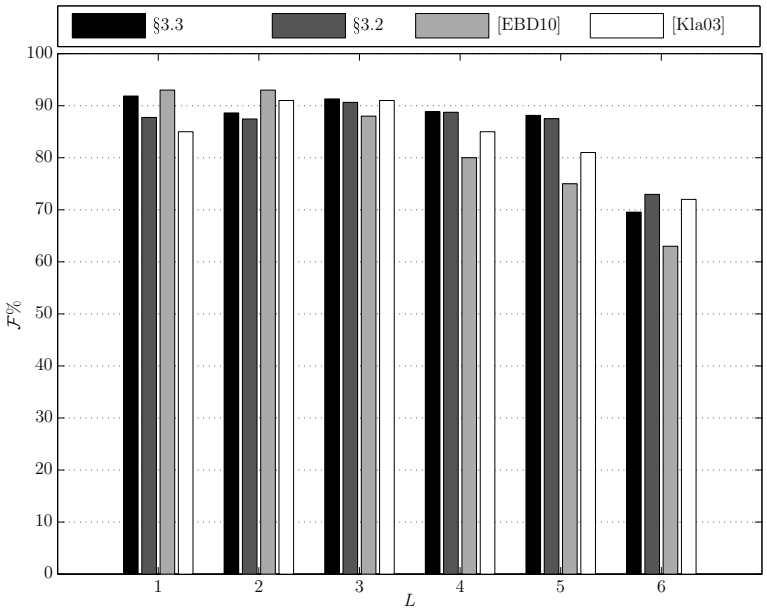

Figure 3.8: Multiple-F0 estimation results for the MAPS database (in F-measure) with unknown polyphony, organized according to the ground truth polyphony level L.

reaching 96.42% for one-note polyphony, and decreasing with the polyphony level, reaching 87.31%, 88.46%, 85.45%, and 82.35%, and 62.11% for levels 2-6.

For the system of Section 3.3 using CRF postprocessing, the mean $\mathcal{F}$ for polyphony levels $L = 1, \ldots, 6$ is 91.86%, 88.61%, 91.30%, 88.83%, 88.14%, and 69.55% respectively. As far as precision is concerned, reported rates are high for all polyphony levels, ranging from 89.88% to 96.19%, with the lowest precision rate reported for $L = 1$. Recall displays the opposite performance, reaching 96.40% for one-note polyphony, and decreasing with the polyphony level, reaching 86.53%, 88.65%, 85.00%, and 83.14%, and 57.44% for levels 2-6.

In terms of a general comparison between all systems, the global F-measure for all sounds is used, where the system of Section 3.3 outperforms all other approaches, reaching 88.54%. The system of Section 3.2 reports 87.47%, the system in [EBD10] 83.70%, and finally the algorithm of [Kla03] reaches 85.25%.

Concerning the statistical significance of the proposed methods' performance compared to the methods in [EBD10, Kla03], the recognizer comparison technique described in [GMSV98] is employed. The number of pitch estimation errors of the two methods is assumed to be distributed according to the binomial

law and the errors are assumed to be independent and identically distributed (i.i.d.). Although the independence assumption does not necessarily hold, the samples present in the test set do belong from different piano models and the employed statistical significance test gives an indication of what recogniser difference could be considered to be significant. It should be noted that a discussion on the importance of statistical significance tests in MIR research was made in [UDMS12], where it was suggested that indicators of statistical significance are eventually of secondary importance. The error rate of the method of Section 3.2 is $\hat{\epsilon}_1 = 0.1252$; for Section 3.3 it is $\hat{\epsilon}_2 = 0.1146$; for [EBD10] it is $\hat{\epsilon}_3 = 0.1630$ and for [Kla03] it is $\hat{\epsilon}_4 = 0.1475$. Taking into account that the test set size $N_{test} = 6832$ and considering 95% confidence ($\alpha_c = 0.05$), it can be seen that $\hat{\epsilon}_i - \hat{\epsilon}_j \geq z_{\alpha_c}\sqrt{2\hat{\epsilon}/N_{test}}$, where $i \in \{1, 2\}$, $j \in \{3, 4\}$, z_{α_c} can be determined from tables of the Normal law ($z_{0.05} = 1.65$), and $\hat{\epsilon} = \frac{\hat{\epsilon}_i + \hat{\epsilon}_j}{2}$. This indicates that the performance of the proposed multiple-F0 systems is significantly better when compared with the methods in [EBD10, Kla03]. Likewise, it can be shown that the method of Section 3.3 is significantly better compared to the method of Section 3.2 with 95% confidence.

Another issue for comparison is the matter of computational speed, where the algorithm in [EBD10] requires a processing time of about 150×real time, while the system of Section 3.2 is able to estimate pitches faster than real time (implemented in Matlab), with the bottleneck being the RTFI computation; all other processes are almost negligible regarding computation time. This makes the proposed approach attractive as a potential application for automatic polyphonic music transcription. The system of Section 3.3 requires a processing time of about 40×real time, with the bottleneck being the computation of the score function for all possible pitch candidate combinations.

RWC Dataset

Transcription results using the RWC recordings 1-12 for the proposed system of Section 3.2, the system of Section 3.3 using CRF postprocessing and the one in Section 3.4 can be found in Table 3.3. A comparison is made using several reported results in the literature for the same files [QRC+10, SKT+08, KNS07], where the proposed methods from Sections 3.3 and 3.4 report improved mean Acc_2. It should be noted that for the system in Section 3.3, results using the CRF postprocessing technique are displayed in Table 3.3. It should also be noted that the systems in Sections 3.3 and 3.4 demonstrate impressive results

	§3.4	§3.3	§3.2	[QRC+10]	[SKT+08]	[KNS07]
1	60.0%	60.2%	61.0%	63.5%	59.0%	64.2%
2	73.6%	75.0%	64.9%	72.1%	63.9%	62.2%
3	62.5%	57.9%	53.8%	58.6%	51.3%	63.8%
4	65.2%	66.8%	51.8%	79.4%	68.1%	77.9%
5	53.4%	54.8%	46.3%	55.6%	67.0%	75.2%
6	76.1%	74.4%	54.6%	70.3%	77.5%	81.2%
7	68.5%	64.0%	62.3%	49.3%	57.0%	70.9%
8	60.1%	58.9%	48.4%	64.3%	63.6%	63.2%
9	50.3%	53.9%	47.2%	50.6%	44.9%	43.2%
10	72.4%	74.1%	66.2%	55.9%	48.9%	48.1%
11	56.2%	50.0%	43.0%	51.1%	37.0%	37.6%
12	33.0%	35.7%	31.0%	38.0%	35.8%	27.5%
Mean	**61.2%**	**60.5%**	**52.5%**	**59.1%**	**56.2%**	**59.6%**
Std.	11.2%	11.5%	10.2%	11.5%	12.9%	16.9%

Table 3.3: Transcription results (Acc_2) for the RWC recordings 1-12.

for some recordings compared to the state-of-the-art (e.g. in file 11, which is a cello-piano duet) while in other cases they fall behind. In file 4 for example, results are inferior compared to state-of-the-art, which could be attributed to the digital effects applied in the recording (the present system was created mostly for transcribing classical and jazz music). As far as the standard deviation of the Acc_2 metric is concerned, the systems in Sections 3.3 and 3.4 reports 11.5% and 11.2% respectively, which is comparable to the state-of-the-art approaches in Table 3.3, although it is worth noting that the lowest standard deviation is reported for the method of Section 3.2.

For the RWC recordings 13-17, transcription results comparing all proposed methods from Sections 3.4, 3.3, and 3.2, can be found in Table 3.4. It should be noted that no results have been published in the literature for these recordings. In general, it can be seen that bowed string transcriptions are more accurate than woodwind transcriptions. Compared to RWC recordings 1-12, the system in Section 3.3 performs better compared to the one in Section 3.4, which can be attributed to the soft onsets found in the pitched non-percussive sounds found in recordings 13-17.

Additional insight into the proposed systems' performance for all 17 RWC recordings is given in Table 3.5, where the error metrics of Section 2.5 are presented. Results using three different configurations are shown for the system of Section 3.3: without any note smoothing, with HMM-based note smoothing,

	§3.4	§3.3	§3.2
13	60.3%	48.2%	37.7%
14	47.7%	41.8%	41.0%
15	57.8%	66.8%	50.6%
16	60.1%	70.7%	61.7%
17	52.0%	75.2%	58.3%
Mean	**55.5%**	**60.5%**	**49.9%**
Std.	5.5%	14.7%	10.5%

Table 3.4: Transcription results (Acc_2) for RWC recordings 13-17.

and with CRF-based note smoothing. For the system of Section 3.4, two different configurations are evaluated, using the complete system for onset and offset detection, as well as a variant of the system performing only onset detection for each segment defined by two onsets. It can be seen that for the system of Section 3.3, there is a significant accuracy improvement when a postprocessing technique is employed. In specific, the note postprocessing procedures mainly decrease the number of false alarms (as can be seen in E_{fp}), at the expense however of missed detections (E_{fn}). Especially for the HMM postprocessing, a large number of missed detections have impaired the system's performance.

As for the MAPS dataset, the recognizer comparison technique described in [GMSV98] was employed. Even though the independence assumption does not necessarily hold for time frames within a recording, it can be argued that performing statistical significance tests between multi-pitch detection rates on entire pieces (as in the MIREX evaluations) is an over-simplification, especially given that the problem of detecting multiple pitches out of 88 classes makes the problem space quite big. This is one of the reasons why to the author's knowledge no statistical significance tests take place in the transcription literature. Thus, considering 95% confidence, the performance of the transcription system of Section 3.3 using CRF postprocessing is significantly better when compared with the methods in [QRC$^+$10, SKT$^+$08, KNS07] and the systems of Sections 3.2 and 3.4 (the latter using both onset and offset detection). It should also be noted that the significance threshold was only just surpassed when comparing the system of Section 3.3 with the method of [KNS07] and the system in Section 3.4. For the system of Section 3.3, the accuracy improvement of the CRF postprocessing step over the HMM one is statistically significant with 95% confidence. Specifically, the significance threshold for this experiment was

Method	$\mathcal{F}_{on}$	Acc_1	Acc_2	E_{tot}	E_{subs}	E_{fn}	E_{fp}
§3.2	44.1%	50.9%	51.8%	48.2%	7.8%	33.9%	6.5%
§3.3 No Post.	33.8%	55.6%	54.5%	45.4%	11.3%	18.5%	15.7%
§3.3 HMM Post.	47.1%	58.5%	59.4%	40.5%	4.7%	31.7%	4.1%
§3.3 CRF Post.	48.2%	60.3%	60.5%	39.5%	6.0%	25.1%	8.4%
§3.4 onset only	46.1%	57.1%	56.9%	43.1%	9.0%	22.2%	11.9%
§3.4 onset+offset	51.1%	59.3%	59.6%	40.4%	7.3%	23.5%	9.6%

Table 3.5: Transcription error metrics for the proposed method using RWC recordings 1-17.

Removed feature	none	Fl	Sm	SC	PR	AM	$Fl[Res]$
Acc_2	60.5%	56.3%	59.2%	58.6%	53.5%	59.4%	29.1%

Table 3.6: Transcription results (Acc_2) for the RWC recordings 1-12 using the method in §3.3, when features are removed from the score function (3.17).

found to be 0.72% in terms of the error rate, which is surpassed by the CRF postprocessing (being 1.1%).

In order to test the contribution of each feature in the pitch set score function (3.17) to the performance of the transcription system of Section 3.3, experiments were made on RWC recordings 1-12. For each experiment, the weight $w_i,\ i = 1, \ldots, 6$ in the score function that corresponds to each feature was set to 0. Results are shown in Table 3.6, where it can clearly be seen that the most crucial feature is $Fl[Res]$, which is the residual flatness. For each experiment, the weight $w_i,\ i = 1, \ldots, 6$ in the score function that corresponds to each feature was set to 0. Results are shown in Table 3.6, where it can clearly be seen that the most crucial feature is $Fl[Res]$, which is the residual flatness.

When testing the contribution of the inharmonicity estimation in the salience function which is used in all proposed systems, a comparative experiment using RWC recordings 1-12 took place with the system of Section 3.3 using CRF postprocessing, where inharmonicity search is disabled. This results in $Acc_2 = 59.7\%$. By employing the statistical significance test of [GMSV98], the performance improvement when inharmonicity estimation is enabled is significant with 90% confidence. It should be noted however that the contribution of the inharmonicity estimation procedure depends on the instrument sources that are present in the signal. In addition, by disabling the overlapping partial treatment procedure for the same experiment, it was shown that $Acc_2 = 38.0\%$, with $E_{fp} = 20.4\%$, which indicates that additional false alarms from the over-

Method	§3.4	§3.3	§3.2	[PE07a]	[RK05]	[Mar04]
Acc_1	47.1%	49.4%	42.5%	56.5%	41.2%	38.4%

Table 3.7: Mean transcription results (Acc_1) for the recordings from [PE07a].

lapped peaks are introduced. The 22.5% difference in terms of accuracy for the overlapping partial treatment is shown to be statistically significant with 95% confidence, using the method in [GMSV98].

Finally, concerning the performance of the proposed noise suppression algorithm of Section 3.3, comparative experiments were performed using the 2-stage noise suppression procedure that was proposed for multiple-F0 estimation in [Kla09b], using RWC recordings 1-12. The noise suppression procedure of [Kla09b] consists of median filtering on the whitened spectrum, followed by a second median filtering which does not take into account spectral peaks. Experiments with CRF postprocessing showed that transcription accuracy using the 2-state noise suppression algorithm was $Acc_2 = 56.0\%$, compared to the 60.5% of the proposed method.

Disklavier Dataset

Transcription results using the 10 Disklavier recording test set created by Poliner and Ellis [PE07a] can be found in Table 3.7, along with results from other state-of-the-art approaches reported in [PE07a]. It can be seen that the best results in terms of Acc_1 are reported for the method in [PE07a] while the proposed system of Section 3.3 is second-best, although it should be noted that the training set for the method by Poliner and Ellis used data from the same source as the test set. In addition, the method in [PE07a] has displayed poor generalization performance when tested on different datasets, as can be seen from results shown in [PE07a] and [QRC$^+$10].

In Table 3.8, several error metrics are displayed for the Disklavier dataset for the three proposed systems. It is interesting to note that although the best performing system in terms of frame-based metrics is the one from Section 3.3, the best performing system in terms of the note-based F-measure is the one in Section 3.4. This can be attributed to the specific treatment of onsets in the system of Section 3.4. Since the present recordings are piano-only, capturing hard onsets is a considerably easier task compared to the soft onsets from the RWC recordings 13-17. As expected, the majority of errors for all

Method	$\mathcal{F}_{on}$	Acc_1	Acc_2	E_{tot}	E_{subs}	E_{fn}	E_{fp}
§3.2	39.1%	42.5%	42.3%	57.6%	14.2%	32.8%	10.6%
§3.3	48.9%	49.4%	49.8%	50.2%	10.1%	31.4%	8.6%
§3.4	53.8%	47.1%	47.2%	52.8%	10.7%	33.6%	8.5%

Table 3.8: Transcription error metrics using the recordings from [PE07a].

Method	$\mathcal{F}_{on}$	Acc_1	Acc_2	E_{tot}	E_{subs}	E_{fn}	E_{fp}
§3.2	40.4%	35.0%	39.9%	60.1%	16.2%	42.7%	1.2%
§3.3	35.9%	35.4%	41.3%	58.6%	25.9%	27.6%	5.2%
§3.4	35.9%	35.5%	41.0%	58.9%	19.5%	37.5%	1.9%

Table 3.9: Transcription error metrics using the MIREX multiF0 recording.

systems consists of missed detections, which typically are middle notes in dense harmonically-related note combinations.

MIREX MultiF0 Development Dataset

Transcription results for the MIREX woodwind quintet recording [MIR] for the three proposed methods of this chapter can be seen in Table 3.9. Again, for the method of Section 3.3 we consider the CRF postprocessing version, and for the method of Section 3.4 we consider the version with onset and offset detection. In terms of frame-based metrics, the system of Section 3.3 outperforms the other two systems, with the method of Section 3.4 falling slightly behind. This is the only case where the system of Section 3.2 outperforms the other ones, at least in terms of the onset-based F-measure. This can be attributed to the fast tempo of the piece, which makes the note smoothing procedure less robust for notes with small duration compared to the frame-based method of Section 3.2.

The MIREX recording has been used for evaluation in the literature, namely in [PG11, VBB10, GE11] using the frame-based F-measure ($\mathcal{F}$). The achieved $\mathcal{F}$ for the methods in Section 3.2, 3.3, and 3.4, is respectively 52.3%, 52.9%, and 52.9%. For the methods in [PG11, VBB10, GE11], it is 59.6%, 62.5%, and 65.0%, respectively. It should be noted that the first 30 sec of the recording were used for evaluation in [PG11, VBB10] and the first 23 sec in [GE11]. The first 30 sec were used to produce the results reported in Table 3.9. This discrepancy in performance can be attributed to the fact that the proposed systems were trained on piano samples instead of woodwind samples or multiple-instrument

	Accuracy	**Precision**	**Recall**
Results	0.468	0.716	0.485
Chroma results	0.545	0.830	0.567

Table 3.10: MIREX 2010 multiple-F0 estimation results for the submitted system.

Participants	Acc	Acc_c
Yeh and Roebel	0.692	0.71
Duan et al.	0.553	0.594
Cañadas-Quesada et al.	0.49	0.544
Benetos and Dixon	0.468	0.545
Dessein et al.	0.457	0.524
Lee et al.	0.373	0.457
Wu et al.	0.361	0.473
Nakano et al.	0.06	0.109

Table 3.11: MIREX 2010 multiple-F0 estimation results in terms of accuracy and chroma accuracy for all submitted systems.

templates as in [VBB10, GE11].

Public Evaluation

The transcription system of Section 3.2 was also submitted to the MIREX 2010 Multiple-F0 estimation public evaluation task [MIR, BD10b]. The system was evaluated using 40 test files from 3 different sources, consisting of several instrument types with maximum polyphony level 5. Results are displayed in Table 3.10, where it can be seen that the chroma accuracy is increased compared to the note accuracy by 8% (implying octave errors). The system produces very few false alarms and most of the errors consist of missed detections. Overall, the system ranked 4th out of the 8 groups that submitted for the task considering the accuracy measure (Acc) and 3rd using the chroma accuracy (Acc_c), as shown in Table 3.11. It should be noted that the system was trained only on piano chords and that no note tracking procedure took place. Results for individual files can be found online[4].

[4] `http://www.music-ir.org/mirex/wiki/2010:MIREX2010_Results`

3.6 Discussion

This chapter presented several approaches for multiple-F0 estimation and automatic music transcription based on signal processing-based techniques and audio features. All proposed systems have been published in international conferences and a journal paper. One system was also publicly evaluated in the MIREX 2010 contest.

Contributions of this work include a pitch salience function in the log-frequency domain which supports inharmonicity and tuning changes; audio features for multiple-F0 estimation which aim to reduce octave errors and to incorporate temporal information; a noise suppression algorithm based on a pink noise assumption; an overlapping partial treatment procedure using a novel harmonic envelope estimation algorithm; a pitch set score function for joint multi-pitch estimation; note tracking using conditional random fields; onset detection incorporating tuning and inharmonicity information; and offset detection using HMMs.

Multiple-F0 estimation and automatic transcription results showed that proposed systems outperform state-of-the-art algorithms in many cases. Specifically, the proposed algorithms display robust results in multi-pitch detection of piano sounds and piano transcription, even in the case where the training and testing datasets originate from different sources. It was shown that the joint multiple-F0 estimation algorithm performs better than the iterative multiple-F0 estimation algorithm. Also, in cases where hard onsets were present, explicitly incorporating note onset information helped in improving results. The main drawback of a joint multi-pitch detection method is computational complexity. Finally, it was shown that note smoothing significantly improves transcription performance.

Although signal processing-based techniques presented in this chapter provided competitive results with relatively low computational cost, the algorithms still exhibit a considerable number of missed note detections. Also, expanding audio feature-based algorithms is not straightforward, since these algorithms depend on an ever expanding number of sub-modules (e.g. noise suppression, envelope estimation, score function) that are difficult to isolate and improve. Moreover, incorporating instrument-specific settings and performing instrument identification in polyphonic music is not straightforward in audio feature-based approaches. In order to incorporate more elaborate temporal continuity constraints and to support instrument-specific transcription, in the next section we

will investigate spectral factorization-based approaches for multi-pitch detection.

Chapter 4

Spectrogram Factorization-based Automatic Music Transcription

4.1 Introduction

This chapter presents methods for automatic music transcription and monophonic pitch estimation using spectrogram factorization techniques. All proposed models are based on probabilistic latent component analysis (PLCA) [SRS06], which was presented in detail in subsection 2.3.3. PLCA was selected because it offers a spectrogram factorization model which is easy to generalise and interpret; thus it can be used for proposing complex models for multiple-instrument automatic transcription and at the same time to control these models using temporal or sparsity constraints. The end goal of this chapter is to build upon PLCA-based approaches for transcription in order to create a multiple-instrument AMT system which is able to model the temporal evolution of sounds.

Firstly, a system for automatic music transcription is presented which extends the shift-invariant PLCA (SI-PLCA) model [SRS08b] for supporting templates from multiple instrument sources and at the same time to model fre-

quency modulations and tuning changes by exploiting shift-invariance in the log-frequency domain. This model was published in [BD11c, BD12a] and was publicly evaluated in the MIREX 2011 multiple-F0 estimation and note tracking task in [BD11b].

Afterwards, a model is proposed for pitch detection which incorporates temporal continuity constraints in order to model the temporal evolution of notes. The time-frequency representation of a tone is expressed by the model as a temporal sequence of spectral templates which can also be shifted over log-frequency. The temporal sequence of the templates is controlled using hidden Markov models (HMMs) [Rab89]. This model was published in [BD11e].

Finally, a system for multiple-instrument AMT modelling the temporal evolution of sounds is proposed, which is based on the aforementioned models. This model supports templates for multiple sound states for each note of a set of instruments. The order of the sound state templates is controlled using pitch-wise HMMs. This system was published in [BD12b]. Finally, evaluation results for pitch detection, multi-pitch detection, and instrument assignment are presented in this chapter using the proposed spectrogram factorization-based models.

4.2 AMT using a Convolutive Probabilistic Model

The goal of this section is to propose an automatic transcription model which expands PLCA techniques and is able to support the use of multiple spectral templates per pitch, as well as per musical instrument. In addition, the model should also be able to exploit shift-invariance across log-frequency for detecting tuning changes and frequency modulations, unlike other PLCA- and NMF-based transcription approaches [GE10, DCL10]. Finally, the contribution of each source should be time- and pitch-dependent, contrary to the relative pitch tracking method of [MS09]. As in the transcription systems of Chapter 3, note smoothing is performed using hidden Markov models trained on MIDI data from the RWC database [GHNO03]. The output of the system is a semitone resolution pitch activity matrix and a higher resolution time-pitch representation; the latter can also be used for pitch content visualization purposes. A diagram of the proposed transcription system can be seen in Fig. 4.1.

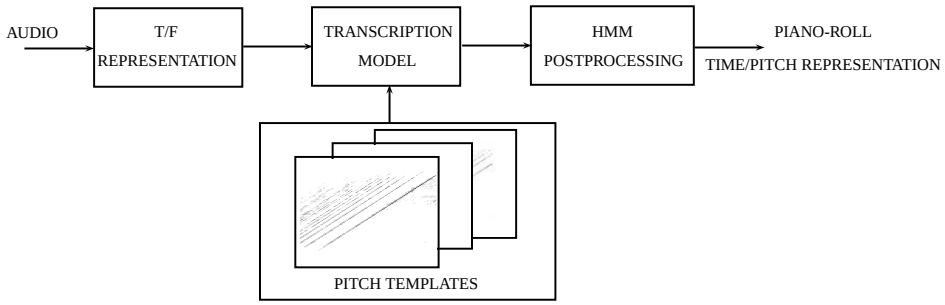

Figure 4.1: Diagram for the proposed automatic transcription system using a convolutive probabilistic model.

4.2.1 Formulation

The model takes as input a log-frequency spectrogram $V_{\omega,t}$, where ω denotes log-frequency and t time, and approximates it as a joint time-frequency distribution $P(\omega, t)$. This distribution can be expressed as a factorization of the spectrogram energy $P(t)$ (which is known) and the conditional distribution over the log-frequency bins $P_t(\omega) = P(\omega|t)$. By introducing p as a latent variable for pitch, the model can be expressed as:

$$P(\omega, t) = P(t) \sum_{p} P_t(\omega|p) P_t(p) \tag{4.1}$$

where $P_t(p)$ is the time-varying pitch activation and $P_t(\omega|p)$ denotes the spectral template for pitch p at the t-th frame. The model of (4.1) is similar to the standard PLCA model, albeit with time-dependent observed spectra. By introducing latent variables for instrument sources and for pitch shifting across log-frequency, the proposed model can be formulated as:

$$P(\omega, t) = P(t) \sum_{p,s} P(\omega|s, p) *_{\omega} P_t(f|p) P_t(s|p) P_t(p) \tag{4.2}$$

where p is the pitch index, s denotes the source, and f the shifting factor. In (4.2), $P(\omega|s, p)$ denotes the spectral templates for a given pitch and instrument source, while $P_t(f|p)$ is the time-dependent log-frequency shift for each pitch, convolved with $P(\omega|s, p)$ across ω. $P_t(s|p)$ is the time-dependent source contribution for each pitch and finally $P_t(p)$ is the time-dependent pitch contribution, which can be viewed as the transcription matrix.

By removing the convolution operator in (4.2), the model becomes:

$$P(\omega, t) = P(t) \sum_{p,f,s} P(\omega - f|s, p) P_t(f|p) P_t(s|p) P_t(p) \tag{4.3}$$

where $P(\omega - f|s, p) = P(\mu|s, p)$ denotes the shifted spectral template for a given pitch and source. It should be noted that as a time-frequency representation, we employ the constant-Q transform (CQT) with a spectral resolution of 120 bins per octave [SK10]. In order to utilise each spectral template $P(\omega|s, p)$ for detecting a single pitch, we constrain f to a range of one semitone. Thus, f has a length of 10.

4.2.2 Parameter Estimation

In order to estimate the unknown parameters in the model we employ the Expectation-Maximization algorithm [DLR77]. Given the input spectrogram $V_{\omega,t}$, the log-likelihood of the model given the data is:

$$\mathcal{L} = \sum_{\omega,t} V_{\omega,t} \log\big(P(\omega, t)\big) \tag{4.4}$$

For the *Expectation* step, we compute the contribution of latent variables p, f, s over the complete model reconstruction using Bayes' theorem:

$$P_t(p, f, s|\omega) = \frac{P(\omega - f|s, p) P_t(f|p) P_t(s|p) P_t(p)}{\sum_{p,f,s} P(\omega - f|s, p) P_t(f|p) P_t(s|p) P_t(p)} \tag{4.5}$$

For the *Maximization* step, we utilise the posterior of (4.5) for maximizing the log-likelihood of (4.4), resulting in the following update equations:

$$P(\omega|s, p) = \frac{\sum_{f,t} P_t(p, f, s|\omega + f) V_{\omega+f,t}}{\sum_{\omega,t,f} P_t(p, f, s|\omega + f) V_{\omega+f,t}} \tag{4.6}$$

$$P_t(f|p) = \frac{\sum_{\omega,s} P_t(p, f, s|\omega) V_{\omega,t}}{\sum_{f,\omega,s} P_t(p, f, s|\omega) V_{\omega,t}} \tag{4.7}$$

$$P_t(s|p) = \frac{\sum_{\omega,f} P_t(p, f, s|\omega) V_{\omega,t}}{\sum_{s,\omega,f} P_t(p, f, s|\omega) V_{\omega,t}} \tag{4.8}$$

$$P_t(p) = \frac{\sum_{\omega,f,s} P_t(p, f, s|\omega) V_{\omega,t}}{\sum_{p,\omega,f,s} P_t(p, f, s|\omega) V_{\omega,t}} \tag{4.9}$$

Equations (4.5-4.9) are iterated until convergence (the algorithm is guaranteed to converge to a local minimum). By keeping the spectral templates $P(\omega|s,p)$ fixed (using pre-extracted templates in a training step), the model converges quickly, requiring about 10-20 iterations. For the present experiments, we have set the number of iterations to 15. The runtime for the proposed system is about 50 times real-time. We set $p = 1, \ldots, 89$, where the first 88 indices correspond to notes A0-C8, and the 89th index corresponds to a residual template (which is also shifted). The spectral template update rule of eq. (4.6) is applied only to the 89th template, while all the other pitch templates remain fixed. The residual template is updated in order to learn the possible noise shape of the recording, or any other artifacts that might occur in the music signal.

The output of the transcription model is a MIDI-scale pitch activity matrix and a higher-resolution pitch activation tensor, respectively given by:

$$\begin{aligned} P(p,t) &= P(t)P_t(p) \\ P(f,p,t) &= P(t)P_t(p)P_t(f|p) \end{aligned} \tag{4.10}$$

By stacking together slices of $P(f,p,t)$ for all pitch values, we can create a 10-cent resolution time-pitch representation:

$$P(f',t) = [P(f,21,t) \cdots P(f,108,t)] \tag{4.11}$$

where $f' = 1, \ldots, 880$. The time-pitch representation $P(f',t)$ is useful for pitch content visualization and for the extraction of tuning information.

In Fig. 4.2, the pitch activity matrix $P(p,t)$ for an excerpt of a guitar recording from the RWC database can be seen, along with the corresponding pitch ground truth. Also, in Fig. 4.3, the time-pitch representation $P(f',t)$ of an excerpt of the 'RWC MDB-C-2001 No. 12' (string quartet) recording is shown, where vibrati in certain notes are visible. It should be noted that these vibrati would not be captured in a non-shift-invariant model.

4.2.3 Sparsity constraints

Since the proposed model in its unconstrained form is overcomplete (i.e. it contains more information than the input), especially due to the presence of the convolution operator and its commutativity property, it would be useful to enforce further constraints in order to regulate the potential increase of information

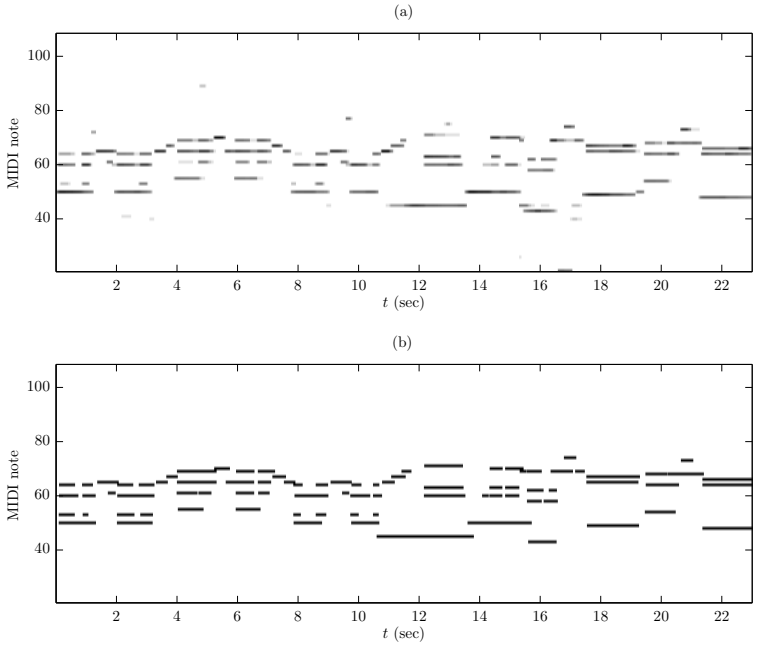

Figure 4.2: (a) The pitch activity matrix $P(p,t)$ of the first 23s of of 'RWC MDB-J-2001 No. 9' (guitar). (b) The pitch ground truth of the same recording.

from input to output [Sma09]. To that end, sparsity is enforced on the piano-roll matrix $P(p|t)$ and the source contribution matrix $P(s|p,t)$. This can be explained intuitively, since we expect that for a given time frame only few notes should be active, while each pitch for a time frame is produced from typically one or few instrument sources.

In [Sma09], sparsity was enforced in the shift-invariant PLCA model by using an entropic prior, while in the PLSA model of [Hof99], a scaling factor to select update equations was applied, which is related to the *Tempered EM* algorithm. This approach was used for automatic transcription in [GE10] and is used in this work as well, since it is simpler and easier to control. Essentially, equations (4.8) and (4.9) are modified as follows:

$$P_t(s|p) = \frac{\Big(\sum_{\omega,f} P_t(p,f,s|\omega)V_{\omega,t}\Big)^{\rho_1}}{\sum_s \Big(\sum_{\omega,f} P_t(p,f,s|\omega)V_{\omega,t}\Big)^{\rho_1}} \tag{4.12}$$

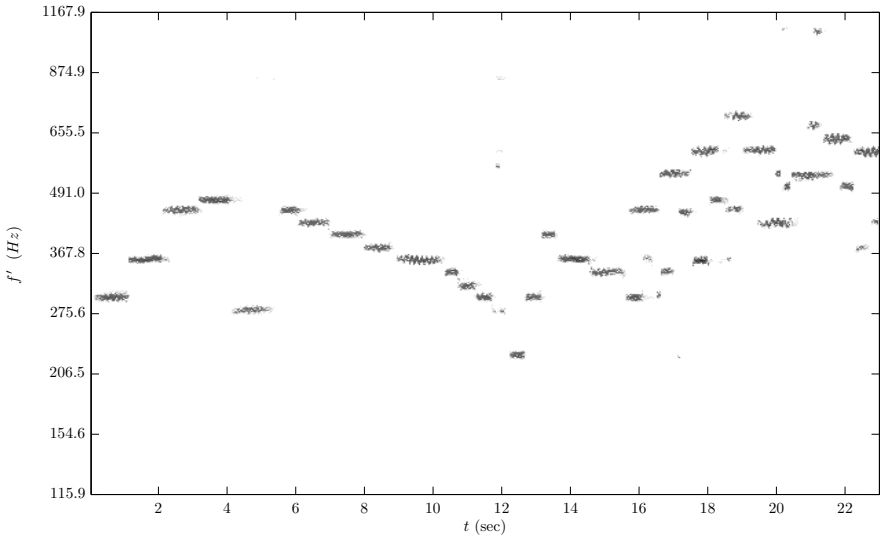

Figure 4.3: The time-pitch representation $P(f', t)$ of the first 23s of 'RWC MDB-C-2001 No. 12' (string quartet).

$$P_t(p) = \frac{\Big(\sum_{\omega,f,s} P_t(p, f, s|\omega) V_{\omega,t}\Big)^{\rho_2}}{\sum_p \Big(\sum_{\omega,f,s} P_t(p, f, s|\omega) V_{\omega,t}\Big)^{\rho_2}} \tag{4.13}$$

As mentioned in [GE10], when ρ_1 and ρ_2 are greater than 1, the probability distributions $P_t(s|p)$ and $P_t(p)$ are "sharpened" and their entropy is lowered. This leads to fewer weights being close to 1 and keeping most near 0, thus achieving sparsity.

Concerning sparsity parameters, after experimentation, the sparsity for the instrument contribution matrix was set to $\rho_1 = 1.1$, while the sparsity coefficient for the piano-roll transcription matrix was set to $\rho_2 = 1.3$. Although the optimal value of ρ_1 is 1 when $\rho_2 = 1$, the combination of these two parameters after experimentation yielded the optimal value of $\rho_1 = 1.1$.

4.2.4 Postprocessing

The output of spectrogram factorization techniques for automatic transcription is typically a non-binary pitch activation matrix (e.g. see Fig. 4.2(a)) which needs to be converted into a series of note events, listing onsets and offsets. Most spectrogram factorization-based approaches extract the final note events

by simply thresholding the pitch activation matrix, e.g. [GE10, DCL10]. As in the audio feature-based transcription methods of Chapter 3, we employ hidden Markov models (HMMs) [Rab89] for performing note smoothing and tracking. Here, we apply note smoothing on the pitch activity matrix $P(p,t)$.

As in Chapter 3, the activity/inactivity of each pitch p is modeled by a 2-state, on/off HMM. MIDI files from the RWC database [GHNO03] from the classic and jazz genres were employed in order to estimate the pitch-wise state priors and transition matrices. For estimating the time-varying observation probability for each active pitch $P(\mathfrak{o}_t^{(p)}|\mathfrak{q}_t^{(p)}=1)$, we use a sigmoid curve which has as input the piano-roll transcription matrix $P(p,t)$:

$$P(\mathfrak{o}_t^{(p)}|\mathfrak{q}_t^{(p)}=1)=\frac{1}{1+e^{-P(p,t)-\lambda}} \tag{4.14}$$

where λ controls the smoothing as in the postprocessing methods of the previous chapter. The result of the HMM postprocessing step is a binary piano-roll transcription which can be used for evaluation. An example of the postprocessing step is given in Fig. 4.4, where the transcription matrix $P(p,t)$ of a piano recording is seen along with the output of the HMM smoothing.

4.3 Pitch Detection using a Temporally-constrained Convolutive Probabilistic Model

In this section, a temporally-constrained shift-invariant model for pitch detection will be presented. The model expresses the evolution of monophonic music sounds as a sequence of sound state templates, shifted across log-frequency. The motivation behind it is to address drawbacks of current pitch detection approaches by: i) explicitly modeling sound states instead of using a constant spectral template for a complete note event, as in [Sma09, MS09, GE11] and the system of Section 4.2 ii) incorporating shift-invariance into the model in order to support the detection of notes which exhibit frequency modulations and tuning changes, extending the work done in [Mys10, NRK$^+$10]. Finally, compared to the NMF-based work in [NRK$^+$10], the parameters for the temporal constraints are learned from a hidden Markov model instead of being pre-defined.

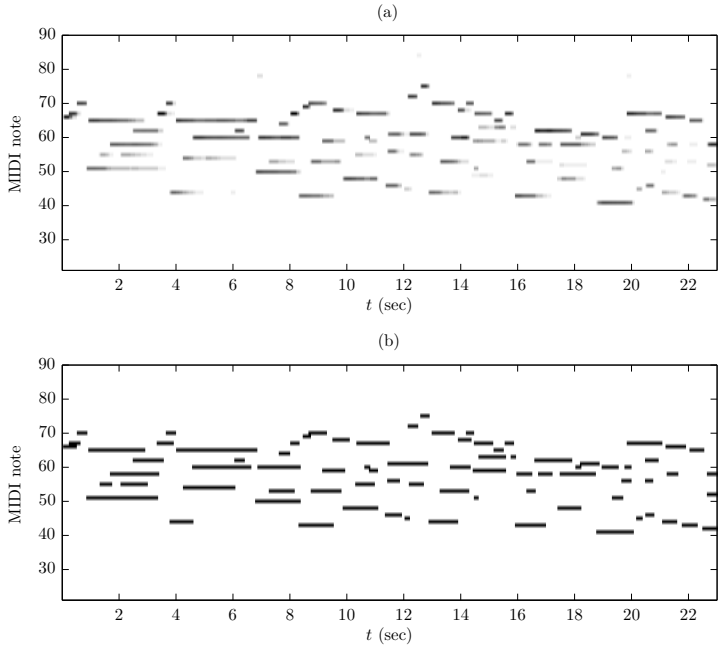

Figure 4.4: (a) The pitch activity matrix $P(p,t)$ of the first 23s of 'RWC MDB-C-2001 No. 30' (piano). (b) The piano-roll transcription matrix derived from the HMM postprocessing step.

4.3.1 Formulation

The proposed method can be named as HMM-constrained SI-PLCA. The notion is that the input log-frequency spectrogram[1] $V_{\omega,t}$ is decomposed as a sum of sound state spectral templates that are shifted across log-frequency, producing a pitch track. Each sound state q is constrained using an HMM. Here, $\omega \in [1, \Omega]$ is the log-frequency index and $t \in [1, T]$ the time index. The model in terms of the observations is defined as:

$$P(\bar{\omega}) = \sum_{\bar{q}} \left(P(q_1) \prod_t P(q_{t+1}|q_t) \right) \left(\prod_t P(\bar{\omega}_t|q_t) \right) \tag{4.15}$$

where $\bar{\omega}$ is the complete sequence of draws for all time frames (observable via $V_{\omega,t}$), $\bar{q}$ is the sequence of draws of q, $P(q_1)$ is the sound state prior distribution, $P(q_{t+1}|q_t)$ is the state transition matrix, $P(\bar{\omega}_t|q_t)$ is the observation probability

[1] As in [Mys10], a magnitude spectrogram can be scaled as to yield integer entries.

given a state, and $\bar{\omega}_t$ is the sequence of draws of ω at the t-th frame.

The observation probability is calculated as:

$$P(\bar{\omega}_t|q_t) = \prod_{\omega_t} P_t(\omega_t|q_t)^{V_{\omega,t}} \tag{4.16}$$

since $V_{\omega,t}$ represents the number of times ω has been drawn at time t. $P_t(\omega_t|q_t)$ is decomposed as:

$$P_t(\omega_t|q_t) = \sum_{f_t} P(\omega_t - f_t|q_t)P_t(f_t|q_t) \tag{4.17}$$

Eq. (4.17) denotes the spectrum reconstruction for a given state. $P(\omega - f|q) = P(\mu|q)$ are the shifted sound state templates and $P_t(f|q)$ is the time-dependent pitch shifting factor for each state ($f \in [1, F]$). The subscript t in f_t, ω_t, q_t denotes the values of the random variables f, ω, q taken at frame t. It should also be noted that the observation probability of (4.16) is computed in the log-domain in order to avoid any underflow errors.

Thus, the generative process for the proposed model is as follows:

1. Choose an initial state according to $P(q_1)$.
2. Set $t = 1$.
3. Repeat the following steps V_t times ($V_t = \sum_\omega V_{\omega,t}$):
   (a) Choose μ according to $P(\mu_t|q_t)$.
   (b) Choose f according to $P_t(f_t|q_t)$.
   (c) Set $\omega_t = \mu_t + f_t$.
4. Choose a new state q_{t+1} according to $P(q_{t+1}|q_t)$.
5. Set $t = t + 1$ and go to step 3 if $t < T$.

4.3.2 Parameter Estimation

The unknown parameters $P(\mu_t|q_t)$ and $P_t(f_t|q_t)$ can be estimated by maximizing the log-likelihood of the data, using the EM algorithm [DLR77]. The update equations are a combination of the SI-PLCA update rules and the HMM forward-backward algorithm [Rab89]. The posterior distribution of the model is

given by $P(\bar{f}, \bar{q}|\bar{\omega})$, where $\bar{f}$ is the sequence of draws of f. Analytical derivations for the proposed model are presented in Appendix C.

For the *Expectation* step, we compute the contribution of the latent variables f, q over the complete model reconstruction:

$$P_t(f_t, q_t|\bar{\omega}) = \frac{P_t(f_t|\bar{\omega}, q_t)P_t(\bar{\omega}, q_t)}{P(\bar{\omega})} = P_t(f_t|\omega_t, q_t)P_t(q_t|\bar{\omega}) \tag{4.18}$$

where

$$P_t(f_t|\omega_t, q_t) = \frac{P(\omega_t - f_t|q_t)P_t(f_t|q_t)}{\sum_{f_t} P(\omega_t - f_t|q_t)P_t(f_t|q_t)} \tag{4.19}$$

$$P_t(q_t|\bar{\omega}) = \frac{P_t(\bar{\omega}, q_t)}{\sum_{q_t} P_t(\bar{\omega}, q_t)} = \frac{\alpha_t(q_t)\beta_t(q_t)}{\sum_{q_t} \alpha_t(q_t)\beta_t(q_t)} \tag{4.20}$$

Equation (4.18) is the posterior of the hidden variables over the observations and is computed using the fact that $P_t(f_t|\bar{\omega}, q_t) = P_t(f_t|\omega_t, q_t)$. Equation (4.19) is computed using Bayes' rule and the notion that $P(\omega_t|f_t, q_t) = P(\omega_t - f_t|q_t)$. Equation (4.20) is the time-varying contribution of each sound state and is derived from the following:

$$\begin{aligned} P_t(\bar{\omega}, q_t) &= P(\bar{\omega}_1, \bar{\omega}_2, \ldots, \bar{\omega}_t, q_t)P(\bar{\omega}_{t+1}, \bar{\omega}_{t+2}, \ldots, \bar{\omega}_T|q_t) \\ &= \alpha_t(q_t)\beta_t(q_t) \end{aligned} \tag{4.21}$$

where T is the total number of frames and $\alpha_t(q_t)$, $\beta_t(q_t)$ are the HMM forward and backward variables [Rab89], respectively.

The forward variable $\alpha_t(q_t)$ can be computed recursively using the forward-backward algorithm as follows:

$$\begin{aligned} \alpha_1(q_1) &= P(\bar{\omega}_1|q_1)P(q_1) \\ \alpha_{t+1}(q_{t+1}) &= \left(\sum_{q_t} P(q_{t+1}|q_t)\alpha_t(q_t)\right) \cdot P(\bar{\omega}_{t+1}|q_{t+1}) \end{aligned} \tag{4.22}$$

while the backward variable $\beta_t(q_t)$ can be computed as:

$$\begin{aligned} \beta_T(q_T) &= 1 \\ \beta_t(q_t) &= \sum_{q_{t+1}} \beta_{t+1}(q_{t+1})P(q_{t+1}|q_t)P(\bar{\omega}_{t+1}|q_{t+1}) \end{aligned} \tag{4.23}$$

The posterior for the sound state transition matrix is given by:

$$P_t(q_t, q_{t+1}|\bar{\omega}) = \frac{P_t(\bar{\omega}, q_t, q_{t+1})}{\sum_{q_t}\sum_{q_{t+1}} P_t(\bar{\omega}, q_t, q_{t+1})} = \frac{\alpha_t(q_t)P(q_{t+1}|q_t)\beta_{t+1}(q_{t+1})P(\bar{\omega}_{t+1}|q_{t+1})}{\sum_{q_t,q_{t+1}} \alpha_t(q_t)P(q_{t+1}|q_t)\beta_{t+1}(q_{t+1})P(\bar{\omega}_{t+1}|q_{t+1})} \quad (4.24)$$

For the *Maximization* step, we derive the update equations for the unknown parameters $P(\mu|q)$, $P_t(f_t|q_t)$, $P(q_{t+1}|q_t)$, and $P(q_1)$ using the computed posteriors:

$$P(\mu|q) = \frac{\sum_{f,t} V_{\omega,t} P_t(f, q|\bar{\omega})}{\sum_{\omega,f,t} V_{\omega,t} P_t(f, q|\bar{\omega})} \quad (4.25)$$

$$P_t(f_t|q_t) = \frac{\sum_{\omega_t} V_{\omega,t} P_t(f_t, q_t|\bar{\omega})}{\sum_{f_t,\omega_t} V_{\omega,t} P_t(f_t, q_t|\bar{\omega})} \quad (4.26)$$

$$P(q_{t+1}|q_t) = \frac{\sum_t P_t(q_t, q_{t+1}|\bar{\omega})}{\sum_{q_{t+1}}\sum_t P_t(q_t, q_{t+1}|\bar{\omega})} \quad (4.27)$$

$$P(q_1) = P_1(q_1|\bar{\omega}) \quad (4.28)$$

After estimating the unknown parameters, the activation of each sound state is given by:

$$P_t(q_t|\bar{\omega}) \sum_{\omega} V_{\omega,t} \quad (4.29)$$

An example of the single-source model is given in Fig. 4.5, where the 10-cent resolution log-frequency spectrogram of a B1 piano note from the MAPS database [EBD10] is used as input. Here, a 4-state left-to-right HMM is used. The temporal succession of spectral templates can be seen in Fig. 4.5(d).

4.4 AMT using a Temporally-constrained Convolutive Probabilistic Model

In this Section, the single-source model of Section 4.3 is extended for supporting multiple sources, as well as multiple components per source. The goal is to create a multi-pitch detection system for multiple instruments, supporting also multiple sets of sound state templates per source. At the same time, the model will be able to support tuning changes and frequency modulations using a shift-invariant formulation. For modeling the temporal evolution of the sound state templates, one HMM will be linked with each pitch. Sparsity will also

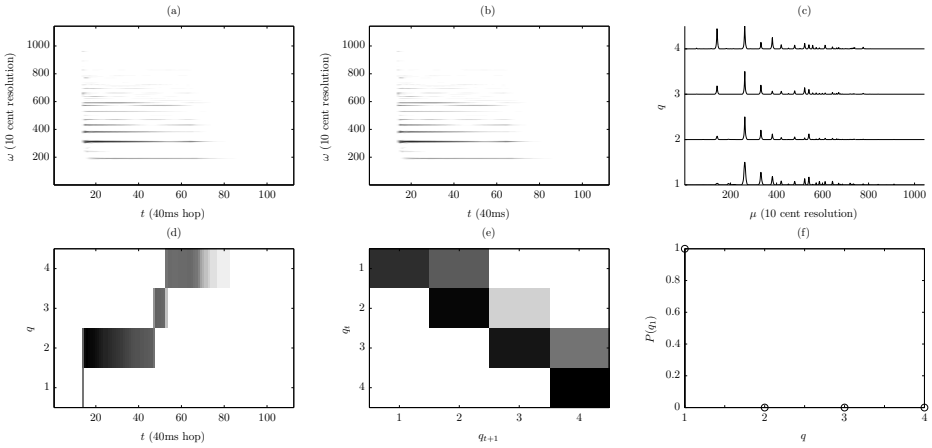

Figure 4.5: (a) Log-frequency spectrogram $V_{\omega,t}$ of a B1 piano note (b) Approximation of the spectrogram using estimated parameters from the single-source model (c) Spectral templates $P(\mu|q)$; the first template corresponds to the attack state, the second and third to the sustain states, and the fourth to the release state (d) Sound state activation $P_t(q_t|\bar{\omega})\sum_\omega V_{\omega,t}$ (e) Sound state transition matrix $P(q_{t+1}|q_t)$ (f) Sound state priors $P(q_1)$

be enforced on certain distributions, as in [GE11], for further constraining the solution. All of the above features will allow for an informative representation of the input music signal, addressing some drawbacks of current multi-pitch detection systems.

4.4.1 Formulation

This model decomposes an input log-frequency spectrogram $V_{\omega,t}$ as a series of sound state templates per source and pitch, a shifting parameter per pitch, a pitch activation, a source activation, and a sound state activation. The sound state sequence for each pitch $p = 1, \ldots, 88$ (denoting notes A0 to C8) is constrained using a corresponding HMM. The proposed model can be given in terms

of the observations as:

$$P(\bar{\omega}) = \sum_{\bar{q}^{(1)}} \cdots \sum_{\bar{q}^{(88)}} P(q_1^{(1)}) \cdots P(q_1^{(88)}) \left(\prod_t P(q_{t+1}^{(1)} | q_t^{(1)}) \right) \cdots \left(\prod_t P(q_{t+1}^{(88)} | q_t^{(88)}) \right) \left(\prod_t P(\bar{\omega}_t | q_t^{(1)}, \ldots, q_t^{(88)}) \right) \quad (4.30)$$

where $\bar{q}^{(p)}$ refers to the state sequences for a given pitch, $P(q_1^{(p)})$ is the sound state prior distribution for pitch p, $P(q_{t+1}^{(p)} | q_t^{(p)})$ is the sound state transition matrix, and $P(\bar{\omega}_t | q_t^{(1)}, \ldots, q_t^{(88)})$ is the observation probability.

The observation probability is calculated as:

$$P(\bar{\omega}_t | q_t^{(1)}, \ldots, q_t^{(88)}) = \prod_{\omega_t} P_t(\omega_t | q_t^{(1)}, \ldots, q_t^{(88)})^{V_{\omega,t}} \quad (4.31)$$

where

$$P_t(\omega_t | q_t^{(1)}, \ldots, q_t^{(88)}) = \sum_{s_t, p_t, f_t} P_t(p_t) P_t(s_t | p_t) P(\omega_t - f_t | s_t, p_t, q_t^{(p_t)}) P_t(f_t | p_t) \quad (4.32)$$

In (4.32), s denotes the instrument sources, f is the log-frequency pitch shifting parameter, and $q^{(p)}$ is the sound state sequence linked to pitch p. $P_t(p)$ is the pitch activity matrix (which is the output of the transcription system), and $P_t(s|p)$ is the contribution of each instrument source for each pitch across time. $P(\omega - f | s, p, q^{(p)}) = P(\mu | s, p, q^{(p)})$ denotes a spectral template for the q-th sound state, p-th pitch and s-th source, and $P_t(f|p)$ is the time- and pitch-dependent log-frequency shifting distribution. For computing (4.32), we exploit the fact that $P(\omega_t - f_t | s_t, p_t, q_t^{(1)}, \ldots, q_t^{(88)}) = P(\omega_t - f_t | s_t, p_t, q_t^{(p_t)})$. In order to constrain the pitch shifting f so that each sound state template is associated with a single pitch, the shifting occurs in a semitone range around the ideal position of each pitch. Due to memory and computational speed issues, we are using a log-frequency representation with a spectral resolution of 60 bins per octave instead of 120 as in the system of Section 4.2. Thus, $f \in [-2, 2]$.

Thus, the generative process for the multi-pitch model is as follows:

1. Choose initial states for each p according to $P(q_1^{(p)})$.

2. Set $t = 1$.

3. Repeat the following steps V_t times ($V_t = \sum_\omega V_{\omega,t}$):

   (a) Choose p according to $P_t(p_t)$.

   (b) Choose s according to $P_t(s_t|p_t)$.

   (c) Choose f according to $P_t(f_t|p_t)$.

   (d) Choose μ according to $P(\mu_t|s_t, p_t, q_t^{(p_t)})$.

   (e) Set $\omega_t = \mu_t + f_t$.

4. Choose new states $q_{t+1}^{(p)}$ for each p according to $P(q_{t+1}^{(p)}|q_t^{(p)})$.

5. Set $t = t + 1$ and go to step 3 if $t < T$.

4.4.2 Parameter Estimation

As in Section 4.3, the unknown model parameters can be estimated using the EM algorithm [DLR77]. For the *Expectation* step, the posterior of all hidden variables is given by:

$$\begin{aligned} &P_t(f_t, s_t, p_t, q_t^{(1)}, \ldots, q_t^{(88)}|\bar{\omega}) = \\ &P_t(q_t^{(1)}, \ldots, q_t^{(88)}|\bar{\omega}) P_t(f_t, s_t, p_t|\omega_t, q_t^{(1)}, \ldots, q_t^{(88)}) \end{aligned} \tag{4.33}$$

Since we are using independent HMMs, the joint probability of all pitch-wise sound states over the observations is given by:

$$P_t(q_t^{(1)}, \ldots, q_t^{(88)}|\bar{\omega}) = \prod_{p=1}^{88} P_t(q_t^{(p)}|\bar{\omega}) \tag{4.34}$$

where

$$P_t(q_t^{(p)}|\bar{\omega}) = \frac{P_t(\bar{\omega}, q_t^{(p)})}{\sum_{q_t^{(p)}} P_t(\bar{\omega}, q_t^{(p)})} = \frac{\alpha_t(q_t^{(p)})\beta_t(q_t^{(p)})}{\sum_{q_t^{(p)}} \alpha_t(q_t^{(p)})\beta_t(q_t^{(p)})} \tag{4.35}$$

and $\alpha_t(q_t^{(p)})$, $\beta_t(q_t^{(p)})$ are the forward and backward variables for the p-th HMM [Rab89], which can be computed recursively using equations (4.22)-(4.23). The second term of (4.33) can be computed using Bayes' theorem and the indepen-

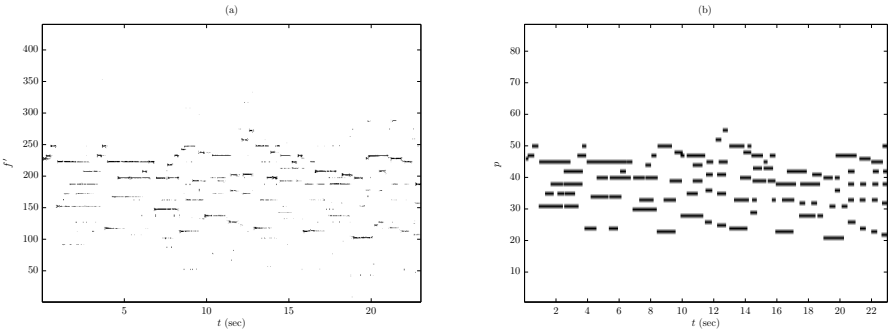

Figure 4.6: (a) Time-pitch representation $P(f', t)$ of an excerpt of "RWC-MDB-J-2001 No. 7" (guitar). (b) The pitch ground truth of the same recording.

dence of the pitch-wise HMMs as:

$$P_t(f_t, s_t, p_t|\omega_t, q_t^{(1)}, \ldots, q_t^{(88)}) = P_t(f_t, s_t, p_t|\omega_t, q_t^{(p_t)}) = \frac{P_t(p_t)P(\omega_t - f_t|s_t, p_t, q_t^{(p_t)})P_t(f_t|p_t)P_t(s_t|p_t)}{\sum_{p_t} P_t(p_t) \sum_{s_t, f_t} P(\omega_t - f_t|s_t, p_t, q_t^{(p_t)})P_t(f_t|p_t)P_t(s_t|p_t)} \tag{4.36}$$

Finally, the posterior probability for the p-th pitch transition matrix is given by:

$$P_t(q_{t+1}^{(p)}, q_t^{(p)}|\bar{\omega}) = \frac{\alpha_t(q_t^{(p)})P(q_{t+1}^{(p)}|q_t^{(p)})\beta_{t+1}(q_{t+1}^{(p)})P(\bar{\omega}_{t+1}|q_{t+1}^{(p)})}{\sum_{q_t^{(p)}} \sum_{q_{t+1}^{(p)}} \alpha_t(q_t^{(p)})P(q_{t+1}^{(p)}|q_t^{(p)})\beta_{t+1}(q_{t+1}^{(p)})P(\bar{\omega}_{t+1}|q_{t+1}^{(p)})} \tag{4.37}$$

$P(\bar{\omega}_t|q_t^{(p)})$ is given from $\overline{\sum}_{q_t^{(p)}} P(\bar{\omega}_t|q_t^{(1)}, \ldots, q_t^{(88)})\ P(q_t^{(1)}, \ldots, q_t^{(p-1)}, q_t^{(p+1)}, \ldots, q_t^{(88)})$, where $\overline{\sum}_{q_t^{(p)}} = \sum_{q_t^{(1)}} \cdots \sum_{q_t^{(p-1)}} \sum_{q_t^{(p+1)}} \cdots \sum_{q_t^{(88)}}$.

For the *Maximization* step, the unknown parameters in the model can be computed using the following update equations:

$$P(\mu|s, p, q^{(p)}) = \frac{\sum_{f,s,t} \overline{\sum}_{q_t^{(p)}} V_{\omega,t} P_t(f, s, p, q^{(1)}, \ldots, q^{(88)}|\bar{\omega})}{\sum_{\omega,f,s,t} \overline{\sum}_{q_t^{(p)}} V_{\omega,t} P_t(f, s, p, q^{(1)}, \ldots, q^{(88)}|\bar{\omega})} \tag{4.38}$$

$$P_t(f_t|p_t) = \frac{\sum_{\omega_t, s_t} \sum_{q_t^{(1)}} \cdots \sum_{q_t^{(88)}} V_{\omega,t} P_t(f_t, s_t, p_t, q_t^{(1)}, \ldots, q_t^{(88)}|\bar{\omega})}{\sum_{f_t, \omega_t, s_t} \sum_{q_t^{(1)}} \cdots \sum_{q_t^{(88)}} V_{\omega,t} P_t(f_t, s_t, p_t, q_t^{(1)}, \ldots, q_t^{(88)}|\bar{\omega})} \tag{4.39}$$

$$P_t(s_t|p_t) = \frac{\sum_{\omega_t,f_t} \sum_{q_t^{(1)}} \cdots \sum_{q_t^{(88)}} V_{\omega,t} P_t(f_t, s_t, p_t, q_t^{(1)}, \ldots, q_t^{(88)}|\bar{\omega})}{\sum_{s_t,\omega_t,f_t} \sum_{q_t^{(1)}} \cdots \sum_{q_t^{(88)}} V_{\omega,t} P_t(f_t, s_t, p_t, q_t^{(1)}, \ldots, q_t^{(88)}|\bar{\omega})} \quad (4.40)$$

$$P_t(p_t) = \frac{\sum_{\omega_t,f_t,s_t} \sum_{q_t^{(1)}} \cdots \sum_{q_t^{(88)}} V_{\omega,t} P_t(f_t, s_t, p_t, q_t^{(1)}, \ldots, q_t^{(88)}|\bar{\omega})}{\sum_{p_t,\omega_t,f_t,s_t} \sum_{q_t^{(1)}} \cdots \sum_{q_t^{(88)}} V_{\omega,t} P_t(f_t, s_t, p_t, q_t^{(1)}, \ldots, q_t^{(88)}|\bar{\omega})} \quad (4.41)$$

$$P(q_{t+1}^{(p)}|q_t^{(p)}) = \frac{\sum_t P_t(q_t^{(p)}, q_{t+1}^{(p)}|\bar{\omega})}{\sum_{q_{t+1}^{(p)}} \sum_t P_t(q_t^{(p)}, q_{t+1}^{(p)}|\bar{\omega})} \quad (4.42)$$

$$P(q_1^{(p)}) = P_1(q_1^{(p)}|\bar{\omega}) \quad (4.43)$$

We should note that the proposed multi-pitch transcription system uses pre-extracted sound state templates using the single-pitch model of Section 4.3, thus the spectral template update rule of (4.38) is not utilised, but is included here for completeness. The runtime for the proposed system is about 100 times real-time. After convergence using the update equations from the EM steps, the output of the system is a semitone resolution pitch activity matrix and a pitch activity tensor in the resolution of the input time-frequency representation, given respectively by:

$$\begin{aligned} &P_t(p) \sum_{\omega} V_{\omega,t} \\ &P_t(p) P_t(f|p) \sum_{\omega} V_{\omega,t} \end{aligned} \quad (4.44)$$

A time-pitch representation can be created by stacking together matrix slices of tensor $P_t(p)P_t(f|p)\sum_\omega V_{\omega,t}$ for all pitch values. We will denote this time-pitch representation as $P(f',t)$, which can be used for pitch visualization purposes or for extracting tuning information. An example from the proposed model is given in Fig. 4.6, where the output time-pitch representation $P(f',t)$ and the MIDI ground-truth of a guitar recording can be seen.

4.4.3 Sparsity constraints

The multi-pitch model can be further constrained using sparsity restrictions. Sparsity was enforced in the shift-invariant models of [Sma09, MS09], using an entropic prior. However, those models were completely unconstrained, since the spectral templates were not pre-extracted. Since we know that for a transcription problem few notes are active at a given time frame and that few instrument

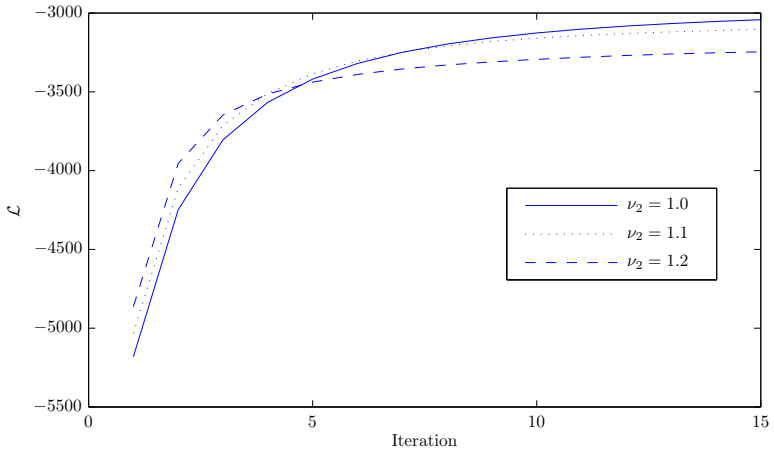

Figure 4.7: Log-likelihood evolution using different sparsity values for 'RWC-MDB-J-2001 No.1' (piano).

sources are responsible for creating a note event at a time frame, we impose sparsity on the pitch activity matrix $P_t(p_t)$ and the pitch-wise source contribution matrix $P_t(s_t|p_t)$. This is achieved in a similar way to [GE10] and the shift-invariant model in Section 4.2, by modifying update equations (4.40) and (4.41):

$$P_t(s_t|p_t) = \frac{\left(\sum_{\omega_t, f_t, q_t^{(1)}, \ldots, q_t^{(88)}} V_{\omega,t} P_t(f_t, s_t, p_t, q_t^{(1)}, \ldots, q_t^{(88)}|\bar{\omega})\right)^{\rho_1}}{\sum_{s_t}\left(\sum_{\omega_t, f_t, q_t^{(1)}, \ldots, q_t^{(88)}} V_{\omega,t} P_t(f_t, s_t, p_t, q_t^{(1)}, \ldots, q_t^{(88)}|\bar{\omega})\right)^{\rho_1}} \quad (4.45)$$

$$P_t(p_t) = \frac{\left(\sum_{\omega_t, f_t, s_t, q_t^{(1)}, \ldots, q_t^{(88)}} V_{\omega,t} P_t(f_t, s_t, p_t, q_t^{(1)}, \ldots, q_t^{(88)}|\bar{\omega})\right)^{\rho_2}}{\sum_{p_t}\left(\sum_{\omega_t, f_t, s_t, q_t^{(1)}, \ldots, q_t^{(88)}} V_{\omega,t} P_t(f_t, s_t, p_t, q_t^{(1)}, \ldots, q_t^{(88)}|\bar{\omega})\right)^{\rho_2}} \quad (4.46)$$

By setting $\rho_1, \rho_2 > 1$, the entropy in matrices $P_t(s|p)$ and $P_t(p)$ is lowered and sparsity is enforced [GE10]. It should be mentioned that this solution does not guarantee convergence, although it is observed in practice. In Fig. 4.7, the evolution of log-likelihood $\mathcal{L} = \sum_{\omega,t} V_{\omega,t} \log\left(\sum_{p_t, q_t^{(p_t)}} P_t(\omega_t|q_t^{(p)}) P_t(q_t^{(p_t)}|\bar{\omega}) \sum_\omega V_{\omega,t}\right)$ can be seen when using different values for sparsity parameter ρ_2, for the piano piece 'RWC-MDB-J-2001 No.1'. It can be seen that by enforcing sparsity convergence is still observed, although a higher sparsity value might result in a worse approximation.

4.4.4 Postprocessing

The same postprocessing technique as the one used in subsection 4.2.4 is employed for the temporally-constrained multi-pitch model. Here, for the pitch-wise two-state HMMs we use as observations the pitch activation $P_t(p)\sum_\omega V_{\omega,t}$. Thus, we define the observation probability for an active note event as:

$$P(\mathfrak{o}_t^{(p)}|\mathfrak{q}_t^{(p)}=1)=\frac{1}{1+e^{-P_t(p)\sum_\omega V_{\omega,t}-\lambda}} \tag{4.47}$$

As in subsection 4.2.4, eq. (4.47) is a sigmoid curve with $P_t(p)\sum_\omega V_{\omega,t}$ as input. Parameter λ controls the smoothing (a high value will discard pitch candidates with low probability). Essentially, in a case of high values in the pitch activation for a given note, where a gap might occur due to an octave error, a high self-transition probability in an active state would help filling in that gap, thus performing note smoothing. The output of the postprocessing step is a piano-roll transcription, which can be used for evaluation. An example of the HMM-based note tracking step for the proposed model is given in Fig. 4.8, where the input pitch activity matrix and the output transcription piano-roll of a string quartet recording can be seen.

4.5 Evaluation

4.5.1 Training Data

For the transcription systems of Section 4.2, spectral templates are extracted for various orchestral instruments, using their complete note range. The standard PLCA model of (2.8) using only one component z is employed in order to extract a single spectral template. For extracting piano templates, the MAPS database is employed [EBD10], where templates from three different piano models were extracted. In addition, note templates are extracted for bassoon, cello, clarinet, flute, guitar, harpsichord, horn, oboe, pipe organ, and violin using isolated notes from the RWC musical instrument samples database [GHNO03]. In total, source parameter s has a size of 13 (3 sets of templates from the piano and 10 for the rest of the instruments). The note range of each instrument used for sound state template extraction can be seen in Table 4.1. As a time-frequency representation, the CQT with 120 bins per octave is used [SK10].

For demonstrating the potential of the temporally-constrained pitch detection system of Section 4.3, sound state templates are extracted for piano, cello,

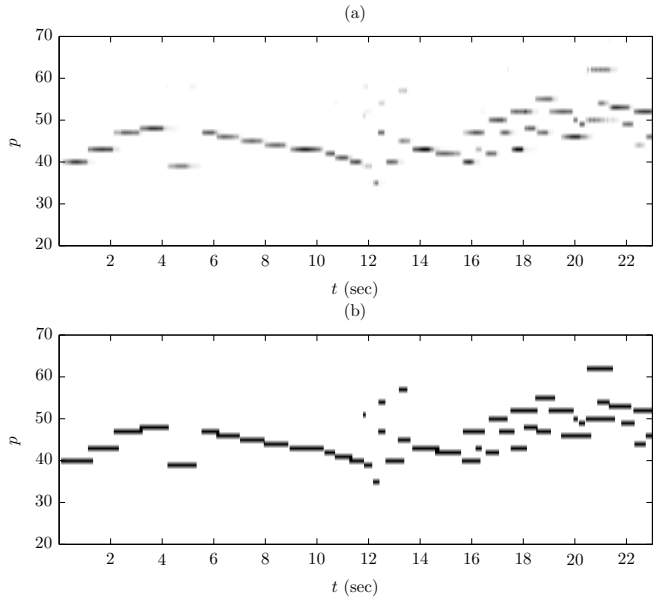

Figure 4.8: (a) The pitch activity matrix $P_t(p) \sum_\omega V_{\omega,t}$ of the first 23s of 'RWC-MDB-C-2001 No. 12' (string quartet) (b) The piano-roll transcription output of the note tracking step.

and oboe, using samples for note C4 from the RWC Musical Instrument Sound database [GHNO03]. The time-frequency representation that is employed for analysis is the resonator time-frequency image (RTFI) [Zho06] using a spectral resolution of 120 bins/octave. The reason the RTFI is selected instead of the more common CQT is because it provides a more accurate temporal resolution in lower frequencies, which is attributed to the use of an exponential decay factor in the filterbank analysis. For extracting the templates, the model in (4.17) is employed, using left-to-right HMMs with $Q = 4$ hidden sound states.

Finally, for the automatic transcription system of Section 4.4, sound state templates are extracted for the same list of instruments as in the transcription system of Section 4.2, using their complete note range as shown in Table 4.1. Ground-truth labels were given for each note and instrument type, but the sound state templates for each note segment are computed in an unsupervised manner, where the model learns the templates using the single-pitch model of Section 4.3. Three sound states were set in the model of equation (4.17). As a time-frequency representation, the constant-Q transform with 60 bins/octave was used [SK10]. The reason for using 60 bins/octave instead of 120 bins/octave

Instrument	Lowest note	Highest note
Bassoon	34	72
Cello	26	81
Clarinet	50	89
Flute	60	96
Guitar	40	76
Harpsichord	28	88
Horn	41	77
Oboe	58	91
Pipe Organ	36	91
Piano	21	108
Violin	55	100

Table 4.1: MIDI note range of the instruments employed for note and sound state template extraction.

is due to computational speed and memory issues.

4.5.2 Test Data

For testing the transcription systems of Sections 4.2 and 4.4, the same recordings that were used for transcription experiments in Section 3.5 are used, namely the 17 RWC recordings [GHNO03], the 10 Disklavier recordings from [PE07a], and the MIREX multiF0 development dataset [MIR]. It should be noted that the system of Section 4.4 is also evaluated for instrument identification experiments in polyphonic music (also called *instrument assignment* [GE11]) using the multi-track MIREX recording.

For testing the temporally-constrained pitch detection system of 4.3, three monophonic excerpts are utilised: a piano melody from the beginning of J.S. Bach's Chromatic Fugue synthesized using the Native Instruments soundfonts[2], a cello melody from the RWC database [GHNO03] (RWC-MDB-C-2001 No. 12), and an oboe melody from the MIREX multi-F0 development set [MIR].

4.5.3 Results

Monophonic Excerpts

For the pitch detection experiments, the update rules in (4.18) - (4.27) were used, excluding the update rule for the spectral templates in (4.25), since the

[2]Available at: `http://www.eecs.qmul.ac.uk/~emmanouilb/WASPAA.html`

patterns for each sound state were considered fixed. The detected pitch for the recordings is summed from the pitch distribution for each sound state:

$$\sum_{q_t} P_t(q_t|\bar{\omega}) P_t(f|q_t) \sum_{\omega} V_{\omega,t} \tag{4.48}$$

Using the detected pitch track, a piano-roll representation was created by summing every 10 pitch bins (which make for one semitone). The output piano-roll representation was compared against existing MIDI ground truth for the employed recordings. In Fig. 4.9, an excerpt of the employed piano melody can be seen along with the weighted sound state transitions using the employed model with a left-to-right HMM. For each tone, the transition from the attack state to two sustain states, followed by a brief decay state can clearly be seen. For evaluation, the frame-based transcription metrics presented in Section 2.5 are utilised, namely the overall accuracy (Acc), the total error (E_{tot}), the substitution error (E_{subs}), missed detection error (E_{fn}), and false alarm error (E_{fp}). For comparative purposes, the shift-invariant PLCA method in [Sma09] is also employed for transcription. In this case, one spectral template per source is employed, using the same training data as in the proposed method.

Pitch detection results using the proposed model are displayed for each recording in Table 4.2. Experiments using the proposed method are performed using left-to-right and ergodic HMMs (where all possible transitions between states were allowed). Although the use of an ergodic model might not be ideal in cases where the sound evolves clearly between the attack, transient, sustain, and decay states, it might be useful for instruments where different sustain states alternate (e.g. tremolo). It can be seen that in all cases, the proposed temporally-constrained convolutive model outperforms the shift-invariant PLCA method in terms of overall transcription accuracy. Also, the accuracy is relatively high for the piano and cello recordings, but significantly lower for the oboe recording. This can be attributed to the fact that the spectral pattern of oboe notes is not constant for all pitches, but in fact changes drastically. Most of the missed detections are located in the decay states of tones, whereas most false alarms are octave errors occurring in the attack part of notes. Finally, when comparing the HMM topologies, it can be seen that the ergodic model slightly outperforms the left-to-right one.

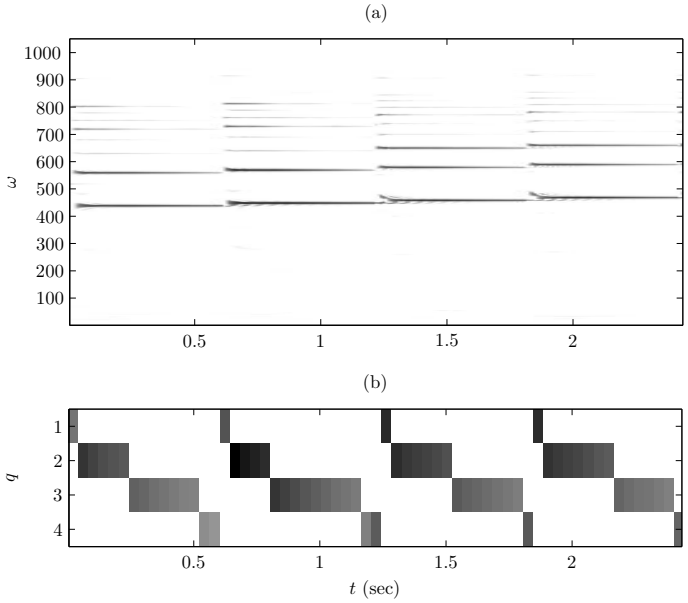

Figure 4.9: (a) Log-frequency spectrogram of a segment of the piano melody employed for experiments (b) Weighted state transitions $P_t(q_t|\bar{\omega}) \sum_{\omega} V_{\omega,t}$.

RWC Dataset

Transcription results using the 12 excerpts from the RWC database [GHNO03] are shown in terms of Acc_2 in Table 4.3, for the polyphonic transcription methods presented in this chapter. Comparisons are also made with the proposed audio feature-based methods of Chapter 3. It should be noted that for the method of Section 4.2, the input T/F representation has a resolution of 120 bins/octave, while for the method of Section 4.4, the resolution is 60 bins/octave. For the latter case, this was done due to computational speed and memory purposes, since the system supports sound state templates for multiple pitches and instruments. From Table 4.3, it can clearly be seen that the proposed spectrogram factorization methods outperform the proposed audio feature-based methods. In addition, all proposed methods outperform state-of-the-art results for the same dataset, for the GMM-based method of [QRC$^+$10], the *specmurt* method of [SKT$^+$08], and the HTC method of [KNS07] (detailed results for the aforementioned methods can be seen in Table 3.3).

In terms of specific recordings, the lowest performance of all systems is reported for recording 12, which is a piano-tenor duet. On the other hand, the best

Method	Instrument	Acc	E_{tot}	E_{subs}	E_{fn}	E_{fp}
§4.3 (LtR)	Piano	81.5%	17.8%	2.2%	9.8%	5.8%
	Cello	80.3%	22.1%	8.3%	5.6%	15.7%
	Oboe	55.0%	39.1%	13.3%	22.6%	3.2%
§4.3 (ergodic)	Piano	82.2%	16.9%	2.2%	9.5%	5.2%
	Cello	80.5%	22.2%	5.6%	5.4%	16.2%
	Oboe	55.6%	37.5%	14.9%	19.3%	3.2%
SI-PLCA	Piano	80.1%	20.2%	1.6%	10.7%	7.9%
	Cello	75.0%	28.5%	1.2%	9.2%	18.0%
	Oboe	54.1%	41.9%	13.7%	20.5%	7.7%

Table 4.2: Pitch detection results using the proposed method of Section 4.3 with left-to-right and ergodic HMMs, compared with the SI-PLCA method.

performance for the spectrogram factorization systems is reported for recording 10, which was performed by a string quartet. This demonstrates that this method can well support the transcription of recordings of non-ideally tuned instruments which also exhibit vibrati, which is not as well supported by signal processing-based methods. In addition, results using RWC recordings 13-17, which have not been evaluated by other methods in the literature, can be seen in Table 4.4. Again, the temporally-constrained system outperforms all other proposed systems.

Additional transcription metrics for RWC recordings 1-17 using the system of Section 4.4 along with two variants of the system of Section 4.2 (with a frequency resolution of 60 and 120 bins per octave) can be seen in Table 4.5. By comparing the two systems with a frequency resolution of 60 bins per octave, it can be seen that incorporating temporal constraints for the evolution of notes significantly improves transcription accuracy. Octave errors counting as note substitutions have been diminished in the temporally-constrained system due to modeling the decay state of tones, where in some cases the higher harmonics might be suppressed (e.g. piano). It can also be seen that a greater spectral resolution helps improve performance. In all three cases, the most common errors occurring in the system are missed detections, usually occurring in dense chords, where only the root note is detected and the higher notes are considered as harmonics. Another source of missed detections in the frame-based evaluation also occurs when the decay part of a note is not recognised due to low energy. Given the fact that estimating note durations is a challenging task even for a human annotator, missed detections due to different note durations are not considered as serious as e.g. octave errors. Note substitutions can also be

	§4.4	§4.2	§3.4	§3.3
1	65.1%	65.9%	60.0%	60.2%
2	65.0%	66.7%	73.6%	75.0%
3	65.3%	66.2%	62.5%	57.9%
4	66.8%	67.3%	65.2%	66.8%
5	57.1%	61.0%	53.4%	54.8%
6	76.6%	78.1%	76.1%	74.4%
7	67.0%	67.3%	68.5%	64.0%
8	67.9%	63.6%	60.1%	58.9%
9	50.4%	49.7%	50.3%	53.9%
10	80.7%	76.9%	72.4%	74.1%
11	57.6%	57.2%	56.2%	50.0%
12	34.0%	30.4%	33.0%	35.7%
Mean	**62.8%**	**62.5%**	**61.2%**	**60.5%**
Std.	12.1%	12.6%	11.2%	11.5%

Table 4.3: Transcription results (Acc_2) for the RWC recordings 1-12.

	§4.4	§4.2	§3.4	§3.3
13	61.2%	58.5%	60.3%	48.2%
14	51.3%	50.4%	47.7%	41.8%
15	66.2%	64.2%	57.8%	66.8%
16	60.4%	59.6%	60.1%	70.7%
17	69.2%	70.0%	52.0%	75.2%
Mean	**61.7%**	**60.6%**	**55.5%**	**60.5%**
Std.	6.8%	7.2%	5.5%	14.7%

Table 4.4: Transcription results (Acc_2) for RWC recordings 13-17.

octave errors when the lower note is missing, or can be semitone errors when an instrument might be severely untuned or might momentarily change pitch.

A comparative experiment was made by disabling the convolution operator in the system of Section 4.4, resulting in a non-shift-invariant system. For RWC recordings 1-12, the resulting $Acc_2 = 58.6\%$, which indicates that by including shift-invariance a more reliable transcription can be achieved. Most of the additional errors introduced by the non-shift-invariant system note substitutions, with the majority being semitone errors due to the inability of the non-shift-invariant model to estimate fine tuning or frequency modulations. It should be noted though that the improvement of a shift-invariant model over a linear one is also dependent on the overall tuning of a dataset; it is expected that tran-

Method	$\mathcal{F}_{on}$	Acc_1	Acc_2	E_{tot}	E_{subs}	E_{fn}	E_{fp}
§4.4 60 bins/octave	47.7%	62.0%	62.5%	37.5%	7.8%	19.4%	10.2%
§4.2 60 bins/octave	46.8%	60.4%	60.2%	39.8%	9.3%	16.7%	13.8%
§4.2 120 bins/octave	47.0%	61.3%	61.9%	38.1%	8.4%	19.0%	10.6%

Table 4.5: Transcription error metrics for the proposed methods using RWC recordings 1-17.

scribing an untuned dataset will cause additional errors in a non-shift-invariant transcription model.

In order to test the effect of the HMM-based postprocessing step, a comparative experiment is made which replaces the smoothing procedure with simple thresholding on the pitch activity matrix $P(p,t)$. Using the set of 12 RWC recordings, the best result for the system of Section 4.2 is $Acc_2 = 61.9\%$, which is 0.7% worse compared to the HMM postprocessing step. For the system of Section 4.4, $Acc_2 = 61.9\%$, which again shows that the HMM-based postprocessing helps achieve improved performance compared to simple thresholding.

Regarding sparsity parameters ρ_1 and ρ_2, the accuracy rates for the RWC recordings 1-12 using different sparsity values for the two parameters are presented in Figs. 4.10 and 4.11 for systems of Sections 4.2 and 4.4 respectively. It can be seen that with increased source contribution sparsity the accuracy of the system diminishes, while enforcing sparsity on the pitch activation leads to a significant improvement. However, after experimentation the optimal combination of sparsity parameters was found to be $\rho_1 = 1.1$ and $\rho_2 = 1.4$ for the system of Section 4.4, due to the interaction between parameters. For the system of Section 4.2 the combination of sparsity parameters was found to be $\rho_1 = 1.1$ and $\rho_2 = 1.3$.

Concerning the statistical significance of the accuracy improvement of the proposed system compared to the other reported systems from the literature, the same recogniser comparison technique of [GMSV98] that was used in Chapter 3 was used. For the experiments using the RWC dataset, the significance threshold with 95% confidence is 0.72% in terms of Acc_2, which makes the improvement significant for the spectrogram factorization-based systems compared to the audio feature-based systems. Although the 0.3% improvement for the temporally-constrained system of Section 4.4 over the system of Section 4.2 is not significant, the inclusion of the temporal constraints using the same T/F representation is actually significant, as can be seen from Table 4.5.

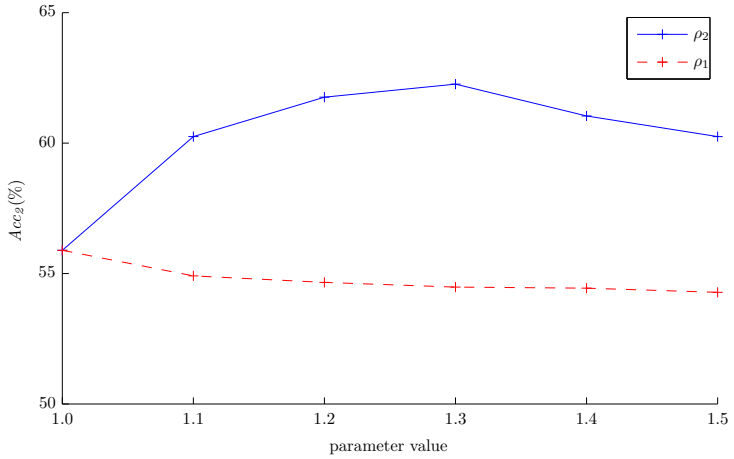

Figure 4.10: Transcription results (Acc_2) for the system of Section 4.2 for RWC recordings 1-12 using various sparsity parameters (while the other parameter is set to 1.0).

Method	§4.4 60 b/o	§4.2 120 b/o	§4.2 60 b/o	[PE07a]	[RK05]
Acc_1	58.2%	58.9%	57.6%	56.5%	41.2%

Table 4.6: Mean transcription results (Acc_1) for the piano recordings from [PE07a].

Disklavier Dataset

Transcription results using the Disklavier dataset from [PE07a] are presented in Table 4.6. For that case, the proposed spectrogram factorization systems of Sections 4.2 and 4.4 utilised only the sets of piano templates extracted from the MAPS database [EBD10]. It can be seen that both proposed spectrogram factorization-based systems outperform the methods in [PE07a] and [RK05], as well as the proposed audio feature-based methods (results shown in Table 3.7). The best accuracy is reported for the system of Section 4.2 with a CQT of 120 bins/octave, although the temporally-constrained system still outperforms the non-temporally-constrained system with the same CQT resolution.

Additional metrics for the Disklavier dataset are presented in Table 4.7, where a similar trend can be seen when using the note-based F-measure for the proposed spectrogram factorization-based systems. Another experiment using the Disklavier dataset was reported for the sparse coding system of [LYC11]

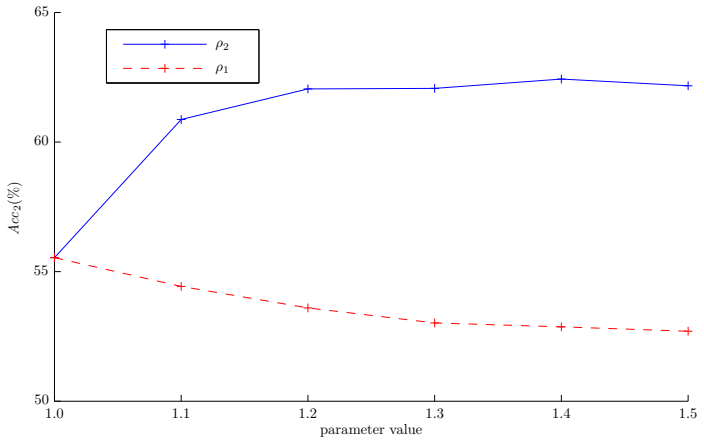

Figure 4.11: Transcription results (Acc_2) for the system of Section 4.4 for RWC recordings 1-12 using various sparsity parameters (while the other parameter is set to 1.0).

Method	$\mathcal{F}_{on}$	Acc_1	Acc_2	E_{tot}	E_{subs}	E_{fn}	E_{fp}
§4.4 60 b/o	55.5%	58.2%	57.7%	42.3%	9.8%	18.6%	13.9%
§4.2 120 b/o	60.3%	58.9%	58.2%	41.8%	9.6%	17.7%	14.5%
§4.2 60 b/o	55.0%	57.6%	56.7%	43.3%	10.9%	16.9%	15.5%

Table 4.7: Transcription error metrics for the piano recordings in [PE07a].

using the frame-based F-measure as a metric. In that case, the reported $\mathcal{F}$ from [LYC11] was 70.2%, while for the system of Section 4.4 it reaches $\mathcal{F} = 73.1\%$. For the Disklavier dataset the statistical significance threshold with 95% confidence is 0.44% in terms of Acc_1, which makes the performance difference of proposed systems compared to the state-of-the-art significant (cf. discussion on statistical significance in Subsection 3.5.2). As far as the choice of templates is concerned, comparative experiments were made using the full template set for the Disklavier recordings. For the system of Section 4.4, the full set produced $Acc_1 = 59.4\%$ and $Acc_2 = 57.8\%$, which outperforms the results using only the piano templates. This can be attributed by the fact that by the model can utilise additional templates from different instruments in order to better approximate the input sounds.

Method	§4.4 60 b/o	§4.2 120 b/o	§4.2 60 b/o	[PG11]	[VBB10]
$\mathcal{F}$	65.9%	60.5%	63.7%	59.6%	62.5%

Table 4.8: Frame-based $\mathcal{F}$ for the first 30 sec of the MIREX woodwind quintet, comparing the proposed methods with other approaches.

MIREX MultiF0 Development Dataset

Results using the MIREX 2007 woodwind quintet recording are shown in Tables 4.8 and 4.9. In Table 4.8, results using the first 30 sec of the recording are reported using the frame-based F-measure, compared with the harmonic NMF method of [VBB10], and the likelihood search method using a Poisson process in [PG11]. The proposed method of Section 4.4 outperforms other methods in the literature, including the non-temporally-constrained proposed method of Section 4.2. It should be noted that the corresponding precision and recall for the system of Section 4.4 are $Pre = 63.7\%$ and $Rec = 68.7\%$. Perhaps surprisingly, the system of Section 4.2 with 60 bins per octave outperforms the same system with a CQT of 120 bins per octave, which can be attributed to convergence issues due to the larger matrix sizes.

Experiments using the MIREX recording were also made in [GE11], where the authors employed the first 23 sec of the piece and reached an F-measure of 65.0%. Using the first 23 sec of the MIREX recording, the system of Section 4.4 reaches $\mathcal{F} = 65.8\%$. It should be noted that additional results are reported in [GE11] when the *eigeninstrument* matrices that are employed in that model are initialised to their optimal values, which are not directly comparable to the unsupervised experiments in the present work.

Additional transcription metrics for the proposed spectrogram factorization systems using the complete 54 sec recording are shown in Table 4.9. From these metrics it can clearly be seen that the proposed spectrogram factorization systems outperform the proposed audio feature-based systems, for which results can be seen in Table 3.8. A similar trend as with the RWC dataset can be seen, where the number of missed detections is significantly greater than the number of false alarms.

In addition, the first 30 sec of the piece were also utilised in [OVC$^+$11], resulting in $\mathcal{F}_n = 66.9\%$. However, in the case of [OVC$^+$11] the number of instruments present in the signal is known in advance, making again the experimental procedure not directly comparable with the present one. It should

Method	$\mathcal{F}_n$	Acc_1	Acc_2	E_{tot}	E_{subs}	E_{fn}	E_{fp}
§4.4 60 b/o	58.4%	47.8%	51.5%	48.5%	23.7%	12.7%	12.2%
§4.2 120 b/o	51.3%	42.2%	47.1%	52.8%	27.6%	13.5%	11.6%
§4.2 60 b/o	57.3%	45.2%	50.9%	49.2%	18.5%	25.7%	5.0%

Table 4.9: Transcription error metrics for the complete MIREX woodwind quintet.

be noted that for the MIREX quintet $\mathcal{F}_n$ is much higher than the frame-based accuracy measures, while the opposite occurs for the RWC database. This can be attributed to the fact that the majority of the tones in the MIREX recording are flute trills (with extremely short duration) that are successfully detected by the system.

Finally, as far as the choice of templates is concerned, we also transcribe the MIREX recording using only woodwind templates in the temporally-constrained system of Section 4.4. The frame-based F-measure reaches 65.2%, which is about 1% lower compared to the full set of templates. This indicates that having a large set of templates that might include instruments not present in the recording does in fact improve transcription accuracy, since the combination of different instrument templates might better approximate the spectra of the tones.

Instrument Assignment

An evaluation on the performance of the systems in Sections 4.2 and 4.4 for instrument identification in polyphonic music is also performed, using the first 30 sec of the MIREX woodwind quintet recording. In this *instrument assignment* task, a pitch is only considered correct if it occurs at the correct time and is assigned to the proper instrument source [GE11]. Two variants of the system are utilised, one using templates from the instruments that are present in the signal (bassoon, clarinet, flute, horn, and oboe) and another using the complete set of instrument templates. The instrument-specific output is given by $P(s = i, p, t) = P_t(p)P_t(s = i|p)\sum_\omega V_{\omega,t}$, where i is the index for the selected instrument. Postprocessing using the HMM-based methods described in Sections 4.2 and 4.4 is applied to each instrument-pitch activation in order to produce a binary piano-roll, which is compared to the MIDI ground truth of the specific instrument track.

Results for the non-temporally-constrained system of Section 4.2 are pre-

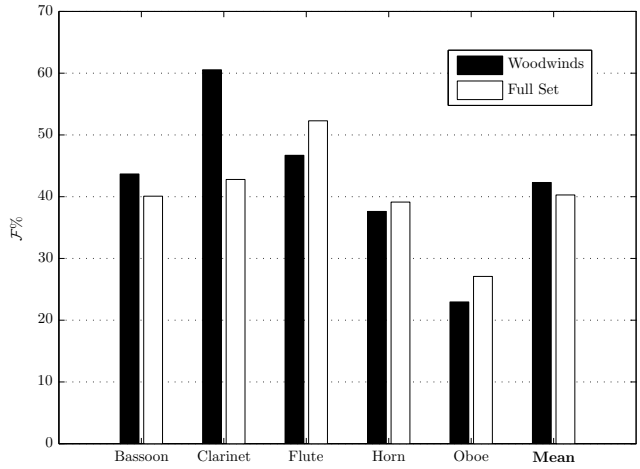

Figure 4.12: Instrument assignment results ($\mathcal{F}$) for the method of Section 4.2 using the first 30 sec of the MIREX woodwind quintet.

sented in Fig. 4.12, while results for the temporally-constrained system of Section 4.4 are presented in Fig. 4.13. It can be seen that the temporally-constrained system outperforms the non-temporally-constrained one for instrument assignment, for both variants of the system. In the case of the temporally-constrained system, using the complete set of templates has a higher instrument identification accuracy compared to the system that uses only woodwind templates (a similar trend was reported in [GE11]). This can be attributed to the fact that combining several instrument templates can help in better approximating tones. In both systems, clarinet and flute are more accurately transcribed compared to the rest of the instruments, which might be attributed to the spectral shape of the clarinet templates and the pitch range of the flute (where the specific flute notes in the recording were mostly outside the pitch range of the other woodwind instruments).

The same segment was also evaluated in [OVC+11] where $\mathcal{F} = 37.0\%$ in the case where the instrument sources are known. A 22 sec segment of the same recording was also evaluated in [GE11], where for the proposed system the F-measure using the woodwind templates is 43.85% and rises to 45.49% for the complete template set. For the method in [GE11], the reported F-measure for the complete set of templates was 40.0% and the performance for

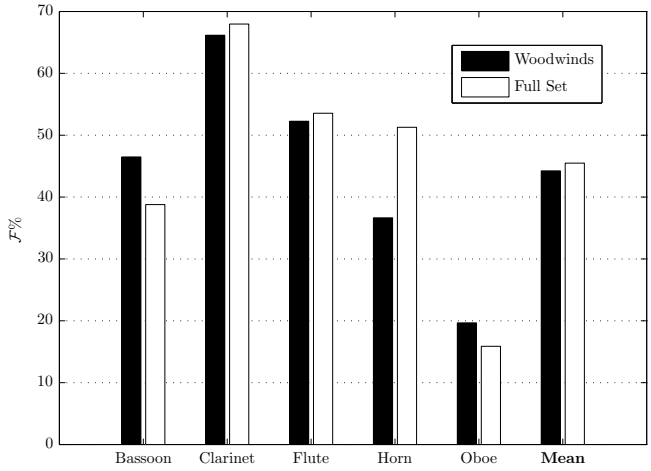

Figure 4.13: Instrument assignment results ($\mathcal{F}$) for the method of Section 4.4 using the first 30 sec of the MIREX woodwind quintet.

the instrument-specific transcription case drops to 35.0%. Thus, the proposed systems show promising results for instrument assignment in polyphonic music.

Public Evaluation

The transcription system of Section 4.2 was submitted to the MIREX 2011 Multiple-F0 estimation and Note Tracking public evaluation task [MIR, BD11b], using an input T/F representation of 60 bins/octave, for computational speed purposes. As in the MIREX 2010 evaluation for the system of Section 3.2, the evaluation was made using 40 test files from 3 different sources, consisting of several instrument types with maximum polyphony level 5. Results for individual files can be found online[3].

Multiple-F0 estimation results are displayed in Table 4.10, where it can be seen that the chroma accuracy is 5.5% greater than the frame-based pitch accuracy. The precision and recall of the system are fairly balanced compared to the system of Section 3.2. Overall, the system ranked 3rd out of the 5 groups that submitted for the Multiple-F0 estimation task, as shown in Table 4.11. Compared to the public evaluation of the system of Section 3.2 however, there

[3] `http://www.music-ir.org/mirex/wiki/2011:MIREX2011_Results`

	Accuracy	**Precision**	**Recall**
Results	0.574	0.637	0.683
Chroma results	0.629	0.700	0.754

Table 4.10: MIREX 2011 multiple-F0 estimation results for the submitted system.

Participants	Acc	Acc_c
Yeh and Roebel	0.683	0.702
Dressler	0.634	0.664
Benetos and Dixon	0.574	0.629
Reis et al.	0.492	0.550
Lee et al.	0.474	0.557

Table 4.11: MIREX 2011 multiple-F0 estimation results in terms of accuracy and chroma accuracy for all submitted systems.

is a reported improvement of +10.6% in terms of Acc, using the same data and evaluation.

Note tracking results are displayed in Table 4.12, where the submitted system ranked 2nd out of the 4 groups that submitted for the task. For the note tracking task, each system must return as an output a list of active notes in MIDI-like format. It can be seen that for all systems, the note-based onset-offset results are significantly lower than the onset-only ones.

4.6 Discussion

This chapter proposed models for decomposing sound spectrograms which can be used for automatic music transcription and instrument identification. The first model expands upon the shift-invariant probabilistic latent component analysis (SI-PLCA) method [SRS08b], and represents an input music signal as a series of templates per pitch and instrument, which can also be shifted across log-frequency. The second model utilises sound state templates and introduces temporal constraints for modeling the temporal evolution of notes. The third and final system builds upon the previous methods and proposes a model for multiple-pitch and multiple-instrument sound state templates which is able to model the temporal evolution of notes in a polyphonic scenario. All proposed systems have been published in international conferences and a journal paper.

Participants	$\mathcal{F}_{on}$	$\mathcal{F}_{of}$
Yeh and Roebel	0.5601	0.3493
Benetos and Dixon	0.4506	0.2077
Lee et al.	0.3862	0.2076
Reis et al.	0.4078	0.1767

Table 4.12: MIREX 2011 note tracking results for all submitted systems.

One system was also publicly evaluated in the MIREX 2011 contest.

Evaluation results showed that the proposed spectrogram factorization-based transcription systems of this chapter outperform the proposed audio feature-based systems of Chapter 3 and also outperform in most cases state-of-the-art systems in the transcription literature. In addition, the proposed spectrogram factorization-based systems can easily be modified for transcribing different instruments or for instrument-specific transcription, through the use of appropriate templates. Also, they offer a mathematically grounded and transparent way of operation, without resulting to ad hoc solutions or heuristics, which can be found in several transcription systems in the literature. In addition, the time-pitch representation that is the output of the proposed systems can also be used for pitch visualization purposes, as in [Kla09b].

Specific aspects of the proposed models which help improve transcription performance are a high log-frequency resolution in the front-end; incorporating sparsity constraints for the pitch activation and source contribution in the model; incorporating temporal constraints for the evolution of notes in the model; and performing note smoothing in the back-end.

Although the performance of the proposed systems is better than past approaches in the literature, the overall accuracy is still well below that of a human expert. The proposed systems can however be used as a basis for creating a yet richer model. For example, instead of using temporal constraints for sound state templates, whole-note templates can be used, with an additional parametrisation on note durations. Also, a joint note tracking step along with the multi-pitch detection step could possibly improve performance. The postprocessing module could also be expanded, by introducing information on key or chord transitions. Also, the number of sound states could also be made instrument-dependent by performing slight modifications to the model. To that end, an analysis of the number of sound states needed to approximate each instrument source is needed. It should be noted however, that creating more

complex models also signifies the need to introduce additional constraints in order to control the convergence of the model. Also, computational speed is another issue, especially in convolutive models; to that end, sparse representations (e.g. [LYC12, ONP12]) can be used, substituting for the EM algorithm.

As far as instrument identification in polyphonic music is concerned, although results outperformed the state-of-the-art for the same experiment, additional work needs to be done in order to improve the current instrument recognition performance of the proposed systems. This can be achieved by utilizing the information provided by the source contribution matrix $P_t(s|p)$, combined with features for characterising music timbre [Pee04].

Chapter 5

Transcription Applications

This chapter presents proposed applications of produced transcription systems to computational musicology, music information retrieval, and computational auditory scene analysis. Also included is a short piano piece created from the output of a transcription system. Thus, the aim of this chapter is to demonstrate the impact that automatic transcription has in music technology as well as in other audio processing applications.

Firstly, a system for automatically detecting key modulations from J.S. Bach chorale recordings is presented. A comparison between an audio input and a symbolic input is made for the key modulation detection task, showing that transcribed recordings reach almost the same accuracy as the symbolic data for that task. This work was published in [MBD11] (joint work with Lesley Mearns) and to the author's knowledge, this is the first study which utilises polyphonic music transcription for systematic musicology research.

In Section 5.2, a system for estimating the temperament of harpsichord recordings is presented, which is based on a harpsichord-specific transcription front-end. The measured temperaments are compared with the specified temperament found in CD sleeve notes of harpsichord recordings. This work was published in [DTB11] (joint work with Simon Dixon and Dan Tidhar).

A method for score-informed transcription for automatic piano tutoring is presented in Section 5.3. The method takes as input a recording made by a student which may contain mistakes along with a reference score and estimates the mistakes made by the student. This work was published in [BKD12] (joint work with Anssi Klapuri).

Finally, in Section 5.4, the proposed transcription models based on temporally-

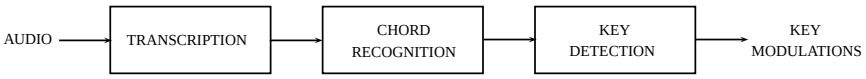

Figure 5.1: Key modulation detection diagram.

constrained shift-invariant probabilistic latent component analysis presented in Chapter 4 are utilised in the context of computational auditory scene analysis [WE06], specifically for the characterization of acoustic scenes in train station recordings. This work was published in [BLD12] (joint work with Mathieu Lagrange).

5.1 Automatic Detection of Key Modulations in J.S. Bach Chorales

In this section, experiments for the automatic detection of key modulations in J.S. Bach chorale recordings are presented. Transcribed audio is processed into vertical notegroups, and the groups are automatically assigned chord labels. For comparison, MIDI representations of the chorales are also processed. HMMs are used to detect key change in the chord sequences, based upon two approaches to chord and key transition representations. The initial hypothesis is that key and chord values which are derived from pre-eminent music theory will produce the most accurate models of key and modulation. The music theory models are tested against models resulting from perceptual experiments about chords and harmonic relations. Experiments show that the music theory models produce better results than the perceptual data. The transcribed audio gives encouraging results, with the key detection outputs ranging from 79% to 97% of the MIDI ground truth results. The diagram for the proposed key modulation detection system can be seen in Fig. 5.1.

It should be noted that for this work the author contributed in the collection of the dataset, the transcription experiments using the proposed system, and the implementation of the HMMs for key detection.

5.1.1 Motivation

The aims of this work are to test the possibility of obtaining musicological information directly from audio, which if successful, has the potential to open up new opportunities for musicological research based on musical recordings,

	BWV	Title
1	1.6	Wie schön leuchtet der Morgenstern
2	2.6	Ach Gott, vom Himmel sieh' darein
3	40.6	Schwing dich auf zu deinem Gott
4	57.8	Hast du denn, Liebster, dein Angesicht gänzlich verborgen
5	85.6	Ist Gott mein Schild und Helfersmann
6	140.7	Wachet auf, ruft uns die Stimme
7	253	Danket dem Herrn heut und allzeit
8	271	Herzlich tut mich verlangen
9	359	Jesu meiner Seelen Wonne
10	360	Jesu, meiner Freuden Freude
11	414	Danket dem Herrn, heut und allzeit
12	436	Wie schön leuchtet der Morgenstern

Table 5.1: The list of J.S. Bach chorales used for the key modulation detection experiments.

and to ascertain whether perceptual or music theory data is more effective in the modelling of harmony. To the author's knowledge, this is the first study which utilises AMT for systematic musicology research. Although key detection could also be achieved using an audio-based chord or key detection system, thus skipping the transcription step, we claim that fully transcribing audio is appropriate, as it provides a framework for extracting information from a music piece that is not limited to a specific music information retrieval (MIR) task.

5.1.2 Music Transcription

12 J.S. Bach chorales are randomly selected for experiments from `www.jsbchorales.net`, which provides organ-synthesized recordings along with aligned MIDI reference files. The list of the chorales employed for the key detection experiments can be seen in Table 5.1. Sample excerpts of original and transcribed chorales are available online[1].

Firstly, the chorale recordings are transcribed into MIDI files using a modified version of the automatic transcription system of Section 3.4, which is based on joint multiple-F0 estimation and note onset/offset detection. Since the application of the transcription system concerns chorale recordings, the pitch range was limited to C2-A#6 and the maximum polyphony level was restricted to 4 voices. Since the recordings are synthesized, tempo is constant and it can be computed using the onset detection functions from Section 3.4. The estimated pitches in the time frames between two beats are averaged, resulting in a series

[1] `http://www.eecs.qmul.ac.uk/~emmanouilb/chorales.html`

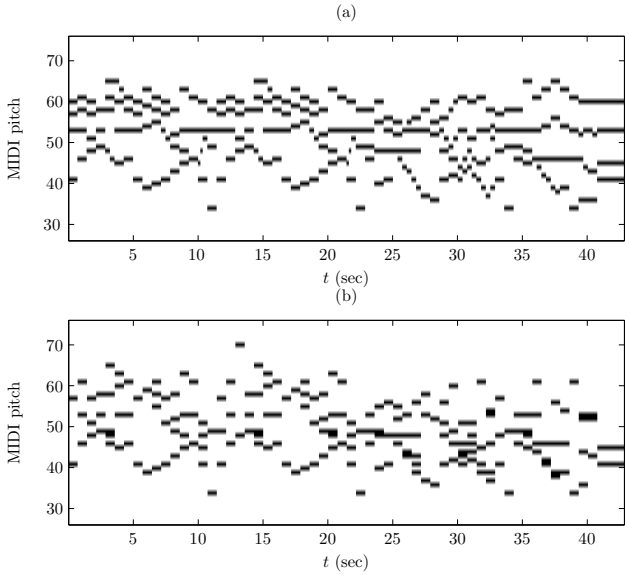

Figure 5.2: (a) The pitch ground-truth of BWV 2.6 '*Ach Gott, vom Himmel sieh' darein*'. (b) The transcription output of the same recording.

of chords per beat. Transcription accuracy is 33.1% using the Acc_2 metric. An example of the transcription output of BWV 2.6 '*Ach Gott, vom Himmel sieh' darein*' is given in Fig. 5.2.

5.1.3 Chord Recognition

Transcribed audio, and for comparison, ground truth MIDI files, are segmented into a series of vertical notegroups according to onset times. The algorithm, which was proposed by Lesley Mearns, can be seen in detail in [MBD11].

To measure the competence of the chord labelling process, the automatically generated chord sequences are compared to hand annotated sequences. Due to the laboriousness of hand annotation, six files in the set have been annotated with ground truth chord sequences (annotations done by Lesley Mearns). It should be noted that all 12 recordings were annotated for key modulations. Each pair of chord index values in the sequences is compared, and a basic difference measure is calculated by counting the number of matches. The final counts are normalised, resulting in a proportional measure of matched or mismatched values between the two files (Table 5.2). If two index values differ, the Levenshtein distance is calculated for the two pitch class sets represented as strings, to

Transcribed Audio		**Ground Truth Midi**	
Match	Levenshtein	Match	Levenshtein
0.56	0.64	0.85	0.15

Table 5.2: Chord match results for the six transcribed audio and ground truth MIDI against hand annotations.

find out the degree of difference between the pitch class sets. The Levenshtein distances calculated for each file are summed and normalised by the length of sequence to produce a combined measure of accuracy and distance.

A greater quantity of label mismatches are found with the transcribed files than the ground truth MIDI files, depicting some of the pitch and timing errors resulting from the automatic transcription. Total chord mismatches between the transcribed data and the hand annotated data (i.e. where there are no pitches in common between the two pitch class sets), indicate an error in timing or quantisation. The greatest difficulty posed to the chord recognition algorithm by the transcribed data however is the frequent presence of diads rather than triads in the groups. The transcription algorithm has a low false alarm error rate and a high missed detection rate, consequently the transcription process produces an output which assists the chord recognition method where the MIDI data poses problems; groups with suspended 9th and 13th notes, or other notegroups containing complex chord tones which are not defined in the chord dictionary, are captured from the transcribed data as simple triads whereas the MIDI data may result in a 'no chord' value. Complex chords such as 9ths and 13ths are less adaptable to the pitch class set match approach due to the fact that internal tones must be omitted from such chords to fit with four part harmony. Overall, the average accuracy levels for the ground truth files are in the upper range of accuracy results reported in [PB02]. The transcribed audio achieves an average of 65% correct of the ground truth result.

5.1.4 Key Modulation Detection

Key change detection is performed using a set of HMMs [Rab89]. The observation sequence $\mathcal{O} = \{\mathfrak{o}_t\}$, $t = 1, \ldots, T$ is given by the output of the chord recognition algorithm in the previous section. The observation matrix therefore defines the likelihood of a key given a chord. Likewise, the hidden state sequence which represents keys is given by $\mathcal{Q} = \{\mathfrak{q}_t\}$. Each HMM has a key transition matrix $P(\mathfrak{q}_t|\mathfrak{q}_{t-1})$ of size 24×24, (representing the 12 major and 12 minor keys)

which defines the probability of making a transition from one key to another. For a given chord sequence, the most likely key sequence is given by:

$$\hat{\mathcal{Q}} = \arg\max_{\mathfrak{q}} \prod_{t} P(\mathfrak{q}_t|\mathfrak{q}_{t-1}) P(\mathfrak{o}_t|\mathfrak{q}_t) \tag{5.1}$$

which can be estimated using the Viterbi algorithm [Rab89].

Five observation matrices and four key transition matrices are compared in total. Three of the observation matrices are derived from music theory, and are designed to represent and test Schönberg's theory with regard to the chord membership of the 24 major and minor modes [Sch11]. Two further observation matrices use data from Krumhansl's perceptual experiments [Kru90]. The four different versions of the key transition matrix are used in conjunction with all five of the observation matrices. For details on the observations and transition matrices, the reader is referred to [MBD11].

5.1.5 Evaluation

To provide a rigorous measure of accuracy of the outputs of the HMMs, each key value in the output sequences is compared to the corresponding hand-annotated key, and an error rate (*Err*) is calculated (definition can be found in [MBD11]).

For the triadic models of Schönberg, error rates range from 0.26 to 0.35 for the transcribed data and 0.20 to 0.33 for the ground truth MIDI data sets, using different transition and observation matrices (detailed results given at [MBD11]). The key output accuracy of the twelve transcribed audio recordings for all models is encouragingly high when compared to the ground truth MIDI, achieving an average of 79% of the accuracy of the ground truth accuracy, despite the higher quantity of chord recognition errors for the transcribed data. For the Sevenths Model, this more complex HMM containing 132 chords demonstrates a greater level of disparity from the hand annotated key sequences than the triad based models. For this model, the error rates for the transcribed data are very close to the MIDI data achieving a relative best accuracy of 97%.

5.1.6 Discussion

This approach to key detection and key modulation using automatic chord classification of transcribed audio and ground truth MIDI data showed that key error rates for the audio recordings are only slightly higher than the key error

rates for the ground-truth MIDI. Also, the key error rates are slightly higher for transcribed data using the triadic models, but the complex chord HMM exhibits remarkable alignment of results for both transcribed audio and MIDI data, suggesting that the quality of the transcribed chorales is of sufficiently high quality for the task. Results are considered promising for the use of automatic transcription research in computational musicology. By combining key outputs with chord sequences, functional harmony could be obtained for the chorales.

5.2 Harpsichord-specific Transcription for Temperament Estimation

In this section, a system for estimating the temperament of harpsichord recordings is described. Temperament refers to the compromise arising from the fact that not all musical intervals can be maximally consonant simultaneously. The front-end of the system is based on a conservative (high precision, low recall) harpsichord-specific transcription system. Over 500 harpsichord recordings, for which the temperament is specified on the CD sleeve notes, are transcribed and analysed. The measured temperaments are compared with the annotations and it is found that while this information is mostly correct, there are several cases in which another temperament matches the data more closely than the advertised one, thus raising an interesting issue about the nature of human annotations and their use as "ground truth".

It should be noted that for this work, the author proposed and implemented an efficient harpsichord-specific transcription system and performed transcription experiments on the dataset of over 500 harpsichord recordings.

5.2.1 Background

More information on temperament can be found in subsection 2.1.2. In [DTB11] it is mentioned that temperament models ignore the inharmonicity effect. However, although stringed instruments are slightly inharmonic, this effect on harpsichord is negligible [DMT12].

Precise frequency estimation is the main tool for estimating temperament. However, despite the vast literature on frequency and pitch detection (reviewed in [dC06, KD06]), there is no general purpose method suitable for all signals and applications. Only few papers address high-precision frequency estimation

to a resolution of cents, which is required for the present work. The highest precision is obtained using the FFT with quadratic interpolation and correction of the bias due to the window function [AS04], which outperforms instantaneous frequency estimation using phase information [TMD10].

5.2.2 Dataset

The dataset used for this study consists of 526 tracks from 22 CDs and 48 tracks from [TMD10]; details of the dataset can be found online[2]. The CDs present a rather balanced sample of recorded solo harpsichord music, including famous and less famous players, and a range of composers including J. S. Bach, D. Scarlatti, F. Couperin, M. Locke, and J. P. Sweelinck. The CDs also provide details of the temperament used for the recordings. A few CDs provide details of the reference frequency as well (e.g. 415Hz); there are also cases where the temperament information is precise and unambiguous or underspecified.

5.2.3 Harpsichord Transcription

For performing precise pitch estimation, the existence and timing of each note must be known. Therefore a transcription system for solo harpsichord is developed, using pre-extracted harpsichord templates, NMF with beta-divergence [Kom07] for multiple-F0 estimation, and HMMs [Rab89] for note tracking. As explained in subsection 2.3.3, NMF with beta-divergence is a computationally inexpensive method which has been used for piano transcription [DCL10]. It has been shown to produce reliable results for instrument-specific transcription, being highly ranked in the MIREX 2010 piano-only note tracking task.

Extracting Pitch Templates

Firstly, spectral templates are extracted from three different harpsichords, from the RWC musical instrument sounds database [GHNO03]. For extracting the note templates, the constant-Q transform (CQT) is computed with spectral resolution of 120 bins per octave. The standard NMF algorithm [LS99] with one component is employed for template extraction.

For template extraction, the complete harpsichord note range is used (E1 to E6). Thus, three spectral template matrices were extracted, $\mathbf{W}^{(1)}, \mathbf{W}^{(2)}, \mathbf{W}^{(3)} \in$

[2] `http://www.eecs.qmul.ac.uk/~simond/ismir11`

$\mathbb{R}^{\Omega \times 61}$, corresponding to each harpsichord model (where Ω is the log-spectrum length).

Multiple-F0 estimation

For the multiple-F0 estimation step, we use the NMF algorithm with beta-divergence [Kom07]. The basic model is the same as in the standard NMF algorithm as shown in (2.6). Since in our case the spectral template matrix is fixed, only the gains $\mathbf{H}$ are updated as:

$$\mathbf{h} \leftarrow \mathbf{h} \otimes \frac{\mathbf{W}^T((\mathbf{W}\mathbf{h})^{\beta-2} \otimes \mathbf{v})}{\mathbf{W}^T(\mathbf{W}\mathbf{h})^{\beta-1}} \tag{5.2}$$

where $\mathbf{v} \in \mathbb{R}^{\Omega \times 1}$ is a single frame from the test signal, $\beta \in \mathbb{R}$ the divergence parameter, set to 0.5 for this work, as in [DCL10], and $\otimes$ is the elementwise product. Although the update rule (Equation 5.2) does not ensure convergence, non-negativity is ensured [DCL10].

For the harpsichord transcription case, the spectral template matrix was created by concatenating the spectral templates from all instrument models:

$$\mathbf{W} = [\mathbf{W}^{(1)} \quad \mathbf{W}^{(2)} \quad \mathbf{W}^{(3)}] \tag{5.3}$$

thus, $\mathbf{W} \in \mathbb{R}^{\Omega \times 183}$. After the NMF update rule was applied to the input log-spectrum $\mathbf{V}$, the pitch activation matrix was created by summing the component vectors from $\mathbf{H}$ that correspond to the same pitch p:

$$\mathbf{H'}_{p,t} = \mathbf{H}_{p,t} + \mathbf{H}_{p+61,t} + \mathbf{H}_{p+122,t} \tag{5.4}$$

where $p = 1, \ldots, 61$ is the pitch index (corresponding to notes E1-E6) and t the time index.

Note tracking

As in the proposed automatic transcription systems of Chapters 3 and 4, note tracking is performed on the pitch activations using on/off pitch-wise HMMs. In this case, the pitch activation matrix is $\mathbf{H'}_{p,t}$. For details on the note tracking procedure, the reader is referred to subsection 4.2.4.

For setting the parameter λ in (4.14), a training dataset is used, that consists of the 7 harpsichord recordings present in the RWC classical music database

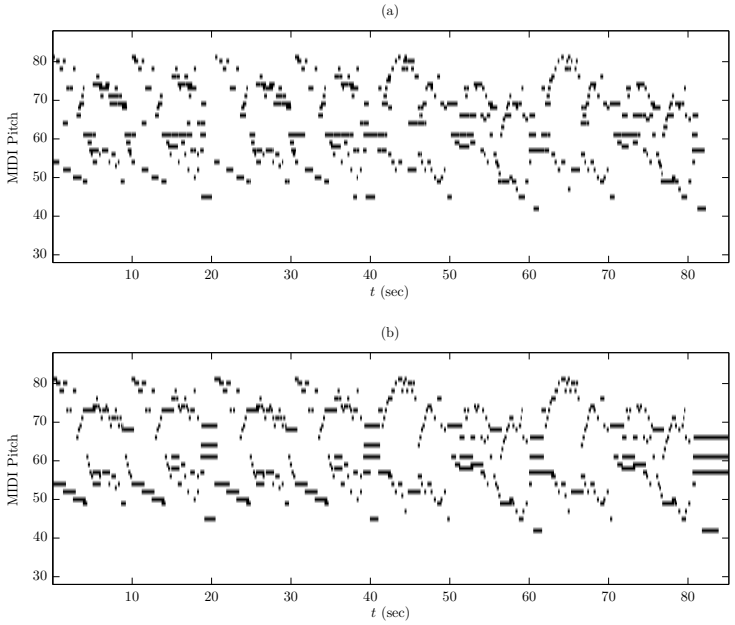

Figure 5.3: (a) The piano-roll transcription of J.S. Bach's *Menuet in G minor* (RWC MDB-C-2001 No. 24b). (b) The pitch ground truth of the same recording.

[GHNO03]. As a ground truth for the recordings, the syncRWC MIDI files are used[3]. Since for the present system a conservative transcription with high precision is favorable, λ is set to 0.25, which results in a false alarm error rate of 5.33% with a missed detection error rate of 46.49% (see section 2.5 for metric definitions). An example of the harpsichord transcription procedure is shown in Fig. 5.3, where the piano-roll transcription of recording RWC MDB-C-2001 No. 24b is seen along with its respective MIDI ground truth.

5.2.4 Precise F0 and Temperament Estimation

Based on the transcription results, we search for spectral peaks corresponding to the partials of each identified note. For identification of the correct peaks, the tuning reference frequency and inharmonicity of the tone also need to be estimated. For information on the precise F0 estimation algorithm along with the tuning and inharmonicity estimation procedure, the reader is referred to

[3] `http://staff.aist.go.jp/m.goto/RWC-MDB/AIST-Annotation/SyncRWC`

[DTB11]. The output of the precise F0 estimation step is a 12-dimensional temperament vector, which can be compared with the profiles of known theoretical temperaments.

The temperament classifier recognises the following temperaments: equal, fifth comma, Vallotti, quarter comma meantone (QCMT), fifth comma meantone (FCMT), sixth comma meantone (SCMT), Kellner, Werckmeister III, Lehman, Neidhardt (1,2 and 3), Kirnberger (2 and 3) and just intonation. It also recognises rotations of these temperaments, although this is not a typical tuning practice for all temperaments, as illustrated by the example of the Young II temperament, a rotation of the Vallotti temperament, which is considered a different temperament in its own right. For details on the temperament classification procedure the reader is referred to [DTB11]. It should be noted that in [DTB11], the proposed divergence between a temperament estimate and profile is weighted by the pitch activation $\mathbf{H'}_{p,t}$, which is the output of the harpsichord-specific transcription system.

5.2.5 Evaluation and Discussion

Detailed temperament estimation results can be found online[4] and in [DTB11]. The results for tuning show agreement with the ground truth values where they were available. The temperament estimation results vary from close agreement to the metadata (CDs 4,5,8,9,16,21,22) to moderate agreement (e.g. CDs 15, 18) to disagreement (e.g. CDs 12,13, 17).

Since a claim is made that CD sleeve notes are a questionable source of "ground truth", we need an independent means of ascertaining the reliability of our system. Thus, experiments are also made using the 4 pieces recorded with six different temperaments from [TMD10]. These tracks are all classified correctly from the set of 180 possible temperaments (15 temperaments by 12 rotations).

It was found that while temperament information provided in CD sleeve notes mostly matches the detected temperament, there were several cases in which another temperament matches the data more closely than the specified one. This raises an interesting issue about the nature of human annotations and their use as "ground truth", as well as a dichotomy between temperament as a mathematical system and temperament in performance practice, where a more pragmatic approach might be applied [DTB11].

[4] `http://www.eecs.qmul.ac.uk/~simond/ismir11`

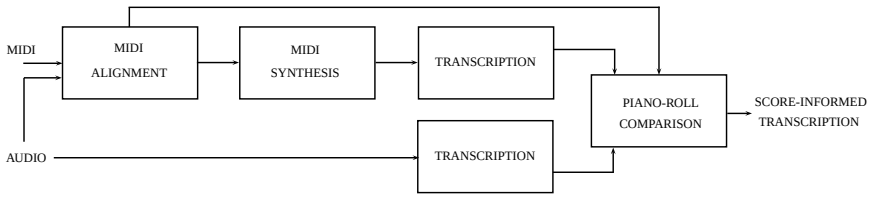

Figure 5.4: Diagram for the proposed score-informed transcription system.

5.3 Score-informed Transcription for Automatic Piano Tutoring

In contrast with unsupervised tasks such as automatic music transcription, certain applications can also incorporate score information. One such example is the emerging field of informed source separation (e.g. [HDB11]). One application that can exploit score information is automatic tutoring, where a system evaluates a student's performance based on a reference score. Thus, the problem that needs to be addressed is *score-informed transcription*. In the past, the problem of informed transcription has received limited attention, with the most notable work done in automatic violin tutoring in [WZ08], which fuses audio and video transcription with score information.

In this section, a score-informed transcription method for automatic piano tutoring is proposed. The method takes as input a recording made by a student which may contain mistakes, along with a reference score. The recording and the aligned synthesized score are automatically transcribed using the NMF algorithm [LS99], followed by pitch-wise HMMs [Rab89] for note tracking. By comparing the two transcribed recordings, common errors occurring in transcription algorithms such as extra octave notes can be suppressed. The result is a piano-roll description which shows the mistakes made by the student along with the correctly played notes. In Fig. 5.4, the diagram for the proposed score-informed transcription system is depicted.

5.3.1 MIDI-to-audio Alignment and Synthesis

For automatically aligning the reference MIDI score with the recording made by the student, the windowed time warping (WTW) alignment algorithm proposed in [MD10] is employed. This algorithm is computationally inexpensive, and can be utilised in a real-time automatic piano tutoring application. In the

experiments performed in [MD10], it was shown that the alignment algorithm can correctly align 97% of the audio note onsets in the test set employed, using a 2 sec tolerance (accuracy drops to 73.6% using a 100ms tolerance).

The result is an aligned MIDI file, which afterwards is synthesized using the TiMidity synthesizer using the *Merlin Vienna* soundfont library[5]. For comparative purposes, manually-aligned MIDI files are also produced and synthesized, which are described in subsection 5.3.5.

5.3.2 Multi-pitch Detection

As in the harpsichord-specific transcription system of Section 5.2, for transcribing piano recordings we employ the NMF algorithm with β-divergence [Kom07], using pre-extracted piano templates. As explained in the previous section, the NMF algorithm with β-divergence is computationally inexpensive and it has been shown to produce reliable results in piano-specific transcription [DCL10].

Firstly, spectral templates for the complete piano note range are extracted, corresponding to notes from A0 to C8. We use recordings from 3 chromatic scales from a Yamaha U3 Disklavier, which is also used for the test recordings. In addition, we employ isolated note samples from 3 piano models from the MAPS database [EBD10]. The fact that we are using training templates from the same piano source as in the test set is a reasonable assumption given the specific tutoring application, since the student can provide training examples in a setup stage. If templates from the same source are not available, general-purpose templates from e.g. the MAPS database can be used (related experiments shown in subsection 5.3.5). For extracting the templates, the CQT [SK10] is employed using a resolution of 120 bins/octave and lowest frequency 27.5 Hz. Next, the NMF algorithm [LS99] as shown in eq. (2.6) using a single component is employed for extracting the template from an isolated note recording.

For the multi-pitch detection step, the NMF model with β-divergence is employed [Kom07] (details of the algorithm are given in subsection 2.3.3). For the present experiments, we used $\beta = 0.5$, which was shown to produce the best results for piano transcription in [DCL10]. Since in our case the spectral template matrix is fixed, only the gain is iteratively updated (after random initialization) using eq. (5.2). Convergence is observed at 10-15 iterations.

For piano transcription, the spectral template matrix $\mathbf{W}$ is created by concatenating the spectral templates from either the 3 sets of the Disklavier or the

[5] `http://ocmnet.com/saxguru/Timidity.htm`

MAPS templates:

$$\mathbf{W} = [\mathbf{W}^{(1)} \;\; \mathbf{W}^{(2)} \;\; \mathbf{W}^{(3)}]. \tag{5.5}$$

Thus, $\mathbf{W} \in \mathbb{R}^{\Omega \times 264}$, where Ω is the log-spectrum size. After the NMF update rule of (5.2) is applied to the input log-spectrogram $\mathbf{V} \in \mathbb{R}^{\Omega \times T}$ (where T is the frame length), the pitch activation matrix is created by adding the component vectors from $\mathbf{H}$ that correspond to the same pitch:

$$\mathbf{H}'_{p,t} = \mathbf{H}_{p,t} + \mathbf{H}_{p+88,t} + \mathbf{H}_{p+176,t} \tag{5.6}$$

where $\mathbf{H}' \in \mathbb{R}^{88 \times T}$.

5.3.3 Note Tracking

As in the automatic transcription systems presented in Chapters 3 and 4, note tracking is performed on the pitch activations of the original and synthesized audio using on/off pitch-wise HMMs, using as input in the observation function of (4.14) the pitch activation $\mathbf{H}'$. For details on the note tracking procedure, the reader is referred to subsection 4.2.4.

In order to set the value of parameter λ in (4.14) for the original recording, we use one piece from the dataset for training (detailed in subsection 5.3.5). Also, two additional piano-rolls from the transcribed recording using different values for λ are extracted, thus creating a 'strict' transcription (with high precision and low recall) and a 'relaxed' transcription (with high recall and low precision), which will be utilised in the output of the proposed system. The values of λ that are used for the normal, strict, and relaxed transcription, are respectively $\{1.3, 1.0, 2.1\}$.

Finally, the resulting piano-rolls are processed in order to detect any repeated notes which might appear in the final piano-roll as a continuous event (e.g. trills). For the piano, detecting note onsets can be achieved by simply detecting energy changes. Thus, peak detection is performed using the activation matrix for each detected note. If a peak is detected at least 200ms after the onset, then the note is split into two.

5.3.4 Piano-roll Comparison

In order to compare the performance of the student with the aligned score, additional information is utilised using the transcribed synthesized score, as well

Algorithm 1 Piano-roll comparison for score-informed transcription

Input: $prStudent, prSynth, prGT$

```
1: for each onset(p, t) ∈ prGT do
2:    if onset(p, t) ∈ prStudent then
3:       prResult(p, t) = correct note
4:    else
5:       if onset(p, t) ∈ prSynth then
6:          prResult(p, t) = missed note
7:       else
8:          prResult(p, t) = correct note
9:       end if
10:   end if
11: end for
12: for each onset(p, t) ∈ prStudent do
13:   if onset(p, t) ∉ prGT ∪ prSynth then
14:      prResult(p, t) = extra played note
15:   end if
16: end for
17: return prResult
```

as the strict and relaxed transcriptions of the recording. The motivation is that automatic transcription algorithms typically contain false alarms (such as octave errors) and missed detections (usually in the case of dense chords). However, the transcribed synthesized score might also contain these errors. Thus, it can assist in eliminating any errors caused by the transcription algorithm instead of attributing them to the student's performance.

Two assumptions are made in the algorithm: firstly, the recording does not contain any structural errors. Thus, only local errors can be detected, such as missed or extra notes played by the student. Secondly, evaluation is performed by only examining note onsets, thus discarding note durations.

The process comparing the piano-roll for the transcribed recording ($prStudent$), the synthesized MIDI ($prSynth$), and the aligned MIDI ($prGT$) is given in Algorithm 1. The tolerance for $onset(p, t)$ is set to $\pm$200ms. In line 8, when an onset is present in the ground truth but is absent in both transcriptions, then we do not have enough knowledge to determine the existence of that note and it is set as correct.

After Algorithm 1 is completed, the extra and missed notes present in $prResult$ are re-processed using the 'strict' piano-roll $prStrict$ and the 'relaxed' piano-roll $prRelaxed$, respectively. The notion is that if that same extra note is not present in $prStrict$, then it is simply caused by a deficiency in the tran-

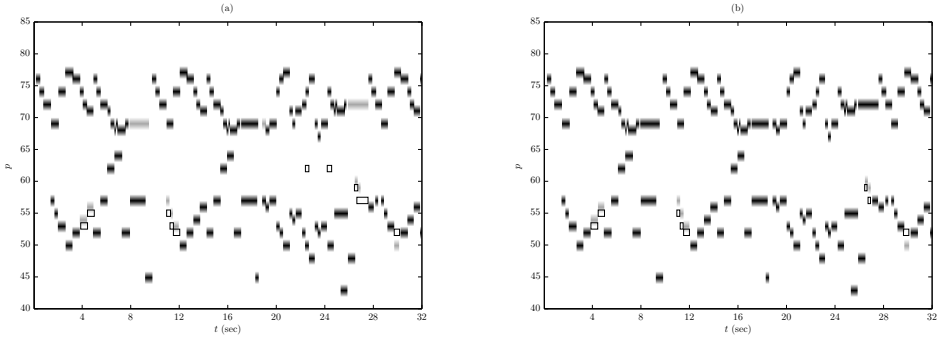

Figure 5.5: (a) The score-informed transcription of a segment from Johann Krieger's Bourrée. (b) The performance ground-truth. Black corresponds to correct notes, gray to missed notes and empty rectangles to extra notes played by the performer.

scription algorithm of the original recording. Likewise, if a missed note appears in *prRelaxed*, then it is taken that it was played but was not detected due to the transcription of the original recording.

The final output of the comparison step is the resulting piano-roll, which contains information on correct notes, missed notes, and extra played notes. In Fig. 5.5, the score-informed transcription of a piece can be seen, compared to the ground-truth of the student's performance.

5.3.5 Evaluation

Dataset

Since no dataset exists for score-informed piano transcription experiments, 7 recordings are made using a Yamaha U3 Disklavier. The piano is slightly out of tune, making the recording conditions more realistic. The recordings were selected from the Associated Board of the Royal Schools of Music 2011/12 syllabus for grades 1 and 2. A list of the recorded pieces can be seen in Table 5.3. Each recording contains mistakes compared to the original score and MIDI ground-truth was created detailing those mistakes. The first recording is used for development, whereas the other six recordings are used for testing. The dataset is available online at the Centre for Digital Music Research Data Repository[6].

[6] `http://c4dm.eecs.qmul.ac.uk/rdr/`

	Composer	Title
1	Josef Haydn	Andante from Symphony No. 94
2	James Hook	Gavotta, Op. 81
3	Pauline Hall	Tarantella
4	Felix Swinstead	A Tender Flower
5	Johann Krieger	Bourrée from Sechs musicalishe Partien
6	Johannes Brahms	The Sandman, WoO 31
7	Tim Richards (arr.)	Down by the Riverside

Table 5.3: The score-informed piano transcription dataset.

Metrics

Since the task of score-informed transcription is a relatively unexplored one, a set of metrics will be presented for evaluating the performance of the proposed method. Firstly, we will evaluate the method's efficiency for the task of automatic transcription by employing the onset-based note-level accuracy also used in [DCL10]. This evaluation will be performed on the transcribed recording and synthesized score. A returned note event is assumed to be correct if its onset is within a ± 100 ms range of a ground-truth onset. As in the metrics defined in Section 2.5, we define the number of correctly detected notes as N_{tp}, the number of false alarms as N_{fp} and the number of missed detections as N_{fn}. The accuracy metric is defined as:

$$Acc_{on} = \frac{N_{tp}}{N_{tp} + N_{fp} + N_{fn}} \tag{5.7}$$

In addition, the note-based precision (Pre_{on}), recall (Rec_{on}), and F-measure ($\mathcal{F}_{on}$), presented in Section 2.5, are also employed for evaluating the automatic transcription performance of the employed methods.

For the score-informed transcription experiments, each detected note from the student's recording can be classified as correct, or mistaken. Mistaken notes are treated as either missed notes or extra notes. Thus, for each piece, three layers of ground-truth exist, which are compared with the corresponding outputs of Algorithm 1. Using (5.7) we will define Acc_{corr} as the algorithm's accuracy for the notes that were correctly played by the student. Likewise, Acc_{mn} denotes the accuracy for the notes that the student omitted and Acc_{en} the accuracy for the extra notes produced. Using the F-measure, a similar set of metrics is defined for the score-informed transcription evaluation: $\mathcal{F}_{corr}$, $\mathcal{F}_{mn}$, $\mathcal{F}_{en}$.

Finally, we define weighted metrics joining all three layers of the ground-

	Acc_{on}	$\mathcal{F}_{on}$	Pre_{on}	Rec_{on}
Recording	83.88%	91.13%	93.34%	89.11%
Manual MIDI	84.73%	91.57%	93.56%	89.73%
Automatic MIDI	89.77%	94.55%	95.05%	94.09%

Table 5.4: Automatic transcription results for score-informed transcription dataset.

truth. Given that N_{corr} is the number of correctly played notes in the performance of the student, N_{mn} is the number of notes missed and N_{en} is the number of extra notes, the weighted accuracy is defined as:

$$Acc_w = \frac{N_{corr}Acc_{corr} + N_{mn}Acc_{mn} + N_{en}Acc_{en}}{N_{corr} + N_{mn} + N_{en}} \tag{5.8}$$

A similar definition can be made for a weighted F-measure, denoted as $\mathcal{F}_w$.

Results

In Table 5.4, the automatic transcription results for the original recording and the synthesized MIDI (using manual and automatic alignment) are shown. In all cases the performance of the NMF-based transcription algorithm is quite high, with the $\mathcal{F}_{on}$ always surpassing 90%. The performance difference between the transcription of the manual and automatic MIDI is due to the fact that the note velocities (dynamics) are preserved in the synthesized manually-aligned MIDI. It should be stressed that when transcribing the synthesized MIDI, templates from the MAPS database [EBD10] were used, whereas when transcribing the original recording, templates from the Disklavier were utilised. When using the MAPS templates for transcribing the recordings, $\mathcal{F}_{on}$ drops to 80.43%. When simple thresholding on $\mathbf{H}'$ is employed instead of the HMM-based note tracking procedure, the average $\mathcal{F}_{on}$ for the recordings drops to 84.92%.

In Table 5.5, score-informed transcription results are presented, using either manually-aligned or automatically-aligned MIDI. For the manually-aligned case, it can be seen that the method reaches very high accuracy for the correctly played notes by the student, while the detection performance for missed or extra notes is lower. However, the overall performance of the method in terms of $\mathcal{F}_w$ is quite high, reaching 96.76%. When automatically-aligned MIDI is used, the system performance is diminished, which is expected, as additional errors from imperfect alignment are introduced. The biggest decrease in performance

	$\mathcal{F}_w$	Acc_w	Acc_{corr}	Acc_{mn}	Acc_{en}
Manual MIDI	96.76%	94.38%	97.40%	70.63%	75.27%
Automatic MIDI	92.93%	88.20%	93.17%	49.16%	60.49%

Table 5.5: Score-informed transcription results.

can be observed for the missed notes by the student. This can be attributed to the fact that the alignment algorithm might place the non-played notes at different positions compared to the ground-truth. Still, the overall performance of the system using automatically-aligned MIDI files reaches an $\mathcal{F}_w$ of 92.93%.

In order to test the performance of different components of the proposed method, comparative experiments are performed by disabling the process for detecting repeated notes, using both manually-aligned and automatically-aligned MIDI. Using the manually-aligned score, $\mathcal{F}_w = 92.79\%$ while using the automatically-aligned score, $\mathcal{F}_w = 89.04\%$. Another experiment is performed using the templates from the MAPS dataset [EBD10] for transcribing the recording. Using the manually-aligned MIDI, $\mathcal{F}_w = 90.75\%$ while using the automatically-aligned MIDI, $\mathcal{F}_w = 85.94\%$. Without processing *prResults* with the 'strict' and 'relaxed' piano-rolls, the score-informed transcription results using manually-aligned scores reach $\mathcal{F}_w = 94.92\%$ and using automatically-aligned scores reach $\mathcal{F}_w = 90.82\%$. A final comparative experiment is performed by utilizing only the piano-roll of the aligned ground-truth for score information, instead of also using the piano-roll of the transcribed synthesized score. In this case, using the manually-aligned score $\mathcal{F}_w = 93.55\%$ and using the automatically-aligned score $\mathcal{F}_w = 89.47\%$, which demonstrates that transcribing the synthesized score can assist in improving performance for a score-informed transcription system.

5.3.6 Discussion

This section proposed a system for score-informed transcription which is applied to automatic piano tutoring. Results indicate that using manually-aligned scores, the proposed method can successfully analyze the student's performance, making it useful for real-life applications. Using automatically-aligned scores produces somewhat lower performance especially when the student deviates from the score.

Score-informed transcription is a relatively unexplored research field and several of its sub-problems could be improved, for example creating robust

instrument-specific transcription algorithms. Future directions include the creation of a MIDI-to-audio alignment algorithm specifically tailored for the piano alignment task, operating with higher precision as this was shown to be an important factor in the proposed method's performance. In addition, the detection of structural errors such as missed or replicated segments can be achieved through a more sophisticated alignment algorithm.

5.4 Characterisation of Acoustic Scenes using SI-PLCA

The temporally-constrained shift-invariant transcription model that was proposed in Section 4.4 can also be utilised in other audio modelling applications. In this section, the model of Section 4.4 is modified and applied to the field of computational auditory scene analysis (CASA) [WE06], and more specifically to the problem of acoustic scene characterization.

5.4.1 Background

The problem of modeling acoustic scenes is one of the most challenging tasks in the CASA field [WE06]. It is closely related to the problem of detecting and classifying acoustic events within a scene, and has numerous applications in audio processing. In the literature the problem is also called *context recognition* [EPT+06]. In the case of scene categorisation or characterization, we are interested in specifying the environment of the recording, which is informed by the types of events that are present within the scene of interest. The problem is especially challenging in the case of a real-world scenario with an unlimited set of events which could also overlap in time.

Regarding related literature, Mesaros et al. [MHK11] proposed a system for sound event detection which employed PLCA [SRS06] (also presented in subsection 2.3.3) for separating and detecting overlapping events. The system was tested in a supervised scenario using a dataset of 103 recordings classified into 10 different scenes, containing events from 61 classes. In [CE11], Cotton and Ellis utilised the NMD algorithm [Sma04a] (also presented in subsection 2.3.3) for non-overlapping event detection. A comparison was made between NMD with a frame-based approach using Mel-frequency cepstral coefficients (MFCCs). Experiments performed on a dataset collected under the CHIL project, consisting

of 16 different event classes, showed that a combination of the NMD system and the frame-based system yielded the best results.

In some cases, the salient events that characterise the scene are not known a priori, or may be hard to learn from training data due to the large discrepancy between two acoustic realizations of the same event. This leads to an unsupervised formulation of the scene description problem, where we want the algorithm to be able to extract in an unsupervised manner the events that describe the scene. Following this approach, Cauchi [Cau11] proposed a method for classifying auditory scenes in an unsupervised manner using sparse NMF. After extracting spectral basis vectors from acoustic scenes, each basis is converted into MFCCs for compactness. A distance metric is defined for measuring the difference between extracted dictionaries from different scenes. Evaluation is performed on a corpus of 66 recordings taken from several train stations [TSP+08], originally created for a perceptual study on acoustic scene categorisation, resulting in six acoustic scene classes. Experiments made by comparing the sparse NMF with a bag-of-features approach from [ADP07] showed that the NMF algorithm is able to successfully extract salient events within an acoustic scene.

5.4.2 Proposed Method

In this section, we build upon the work by Cauchi [Cau11] and propose a method for modeling and classifying acoustic scenes in an unsupervised manner using a temporally-constrained shift-invariant model. This level of temporality will control the appearance of the time-frequency patches in a recording and can be supported by using the proposed HMM-constrained SI-PLCA model presented in Section 4.4, also modified for supporting time-frequency patches instead of one-dimensional spectra. In the model, the component activation function would consist of zeros in case of inactivity and ones at the time instants where an event would appear. Each HMM in the model can represent a certain component, which would be represented using a two-state, on/off model. This on/off model would serve as an event indicator function, which would enforce temporal constraints in the auditory scene activation matrix. Fig. 5.6 shows the diagram for the proposed system.

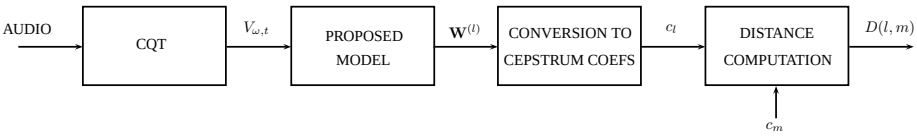

Figure 5.6: Diagram for the proposed acoustic scene characterisation system.

Formulation

This proposed temporally-constrained model takes as input a normalised spectrogram $V_{\omega,t}$ and approximates it as a series of time-frequency patches. Also produced is a component activation matrix, as well as component priors. The activation of each acoustic component is controlled via a 2-state on/off HMM. The model can be formulated as:

$$P(\omega,t) = \sum_z P(z) \sum_{q_t^{(z)}} P(\omega,\tau|z) *_\tau P(t|z) P(q_t^{(z)}|t) \tag{5.9}$$

where $q_t^{(z)}$ is the state sequence for the z-th component, $z = 1,\ldots,Z$. $P(\omega,\tau|z)$ is the time-frequency patch for the z-th component, $P(z)$ is the component prior, $P(t|z)$ is the activation for each component, and $P(q_t^{(z)}|t)$ the state activation for each component. Thus in the model, the desired source activation is given by $P(z|t)P(q_t^{(z)} = 1|t)$.

The activation sequence for each component is constrained using a corresponding HMM, which is based on the produced source activation $P(z,t) = P(z)P(t|z)$. In terms of the activations, the component-wise HMMs can be expressed as:

$$P(\bar{z}) = \sum_{\bar{q}^{(z)}} P(q_1^{(z)}) \prod_t P(q_{t+1}^{(z)}|q_t^{(z)}) \prod_t P_t(z_t|q_t^{(z)}) \tag{5.10}$$

where $\bar{z}$ refers to the sequence of activations for a given component z, $P(q_1^{(z)})$ is the prior probability, $P(q_{t+1}^{(z)}|q_t^{(z)})$ is the transition matrix for the z-th component, and $P_t(z_t|q_t^{(z)})$ is the observation probability. The observation probability for an active component is:

$$P_t(z_t|q_t^{(z)} = 1) = \frac{1}{1 + e^{-P(z,t)-\lambda}} \tag{5.11}$$

where a high value of λ will lead to a low observation probability, leading to

an 'off' state. The formulation of the observation function is similar to the one used for note tracking in subsection 4.2.4.

Parameter Estimation

As in the model of Section 4.4, the unknown parameters in the model can be estimated using the EM algorithm [DLR77]. For the *Expectation* step, we compute the posterior for all the hidden variables:

$$P(z,\tau,q_t^{(1)},\ldots,q_t^{(Z)}|\bar{z},\omega,t) = P(q_t^{(1)},\ldots,q_t^{(Z)}|\bar{z})P(z,\tau|q_t^{(1)},\ldots,q_t^{(Z)},\omega,t) \tag{5.12}$$

Since we are utilising independent HMMs, the joint probability for all hidden source states is given by:

$$P_t(q_t^{(1)},\ldots,q_t^{(Z)}|\bar{z}) = \prod_{z=1}^{Z} P_t(q_t^{(z)}|\bar{z}) \tag{5.13}$$

where

$$P_t(q_t^{(z)}|\bar{z}) = \frac{P_t(\bar{z},q_t^{(z)})}{\sum_{q_t^{(z)}} P_t(\bar{z},q_t^{(z)})} = \frac{\alpha_t(q_t^{(z)})\beta_t(q_t^{(z)})}{\sum_{q_t^{(z)}} \alpha_t(q_t^{(z)})\beta_t(q_t^{(z)})} \tag{5.14}$$

and $\alpha_t(q_t^{(z)})$, $\beta_t(q_t^{(z)})$ are the forward and backward variables for the z-th HMM [Rab89], which are computed recursively using (4.22)-(4.23).

The second term of (5.12) can be computed using Bayes' theorem:

$$P(z,\tau|q_t^{(1)},\ldots,q_t^{(Z)},\omega,t) = P(z,\tau|\omega,t) = \frac{P(z)P(\omega,\tau|z)P(t-\tau|z)}{\sum_z\sum_\tau P(z)P(\omega,\tau|z)P(t-\tau|z)|t)} \tag{5.15}$$

Finally, the posterior for the component transition matrix is given by:

$$P_t(q_t,q_{t+1}|\bar{z}) = \frac{\alpha_t(q_t)P(q_{t+1}|q_t)\beta_{t+1}(q_{t+1})P_t(z_{t+1}|q_{t+1})}{\sum_{q_t,q_{t+1}} \alpha_t(q_t)P(q_{t+1}|q_t)\beta_{t+1}(q_{t+1})P_t(z_{t+1}|q_{t+1})} \tag{5.16}$$

For the *Maximization* step, the update rules for estimating the unknown parameters are:

$$P(z) = \frac{\sum_{\omega,\tau,t}\overline{\sum}_{q_t^{(z)}} V_{\omega,t}P(z,\tau,q_t^{(1)},\ldots,q_t^{(Z)}|\omega,t)}{\sum_{z,\omega,\tau,t}\overline{\sum}_{q_t^{(z)}} V_{\omega,t}P(z,\tau,q_t^{(1)},\ldots,q_t^{(Z)}|\omega,t)} \tag{5.17}$$

$$P(\omega,\tau|z)=\frac{\sum_t \overline{\sum}_{q_t^{(z)}} V_{\omega,t} P(z,\tau,q_t^{(1)},\ldots,q_t^{(Z)}|\omega,t)}{\sum_{\omega,\tau,t} \overline{\sum}_{q_t^{(z)}} V_{\omega,t} P(z,\tau,q_t^{(1)},\ldots,q_t^{(Z)}|\omega,t)} \tag{5.18}$$

$$P(t|z)=\frac{\sum_{\omega,\tau} \overline{\sum}_{q_t^{(z)}} V_{\omega,t+\tau} P(z,\tau,q_t^{(1)},\ldots,q_t^{(Z)}|\omega,t+\tau)}{\sum_{t,\omega,\tau} \overline{\sum}_{q_t^{(z)}} V_{\omega,t+\tau} P(z,\tau,q_t^{(1)},\ldots,q_t^{(Z)}|\omega,t+\tau)} \tag{5.19}$$

$$P(q_{t+1}^{(z)}|q_t^{(z)})=\frac{\sum_t P(q_t^{(z)},q_{t+1}^{(z)}|\bar{z})}{\sum_{q_{t+1}^{(z)}} \sum_t P(q_t^{(z)},q_{t+1}^{(z)}|\bar{z})} \tag{5.20}$$

$$P(q_1^{(z)})=P_1(q_1^{(z)}|\bar{z}) \tag{5.21}$$

where $\overline{\sum}_{q_t^{(z)}}=\sum_{q_t^{(1)}}\cdots\sum_{q_t^{(Z)}}$. Eq. (5.21) updates the component prior using the posterior of eq. (5.14). The final event activation is given by the activation for each component given by the model and the probability for an active state for the corresponding component:

$$P(z,t,q_t^{(z)}=1)=P(z)P(t|z)P(q_t^{(z)}=1|t) \tag{5.22}$$

As in the model of Section 4.4, sparsity constraints are applied to $P(t|z)$ using the entropic prior of [Bra99] applied in the PLCA context in [Sma09] in order to obtain a sparse component activation. For all the experiments performed in this paper, the length of each basis has been set to 400ms.

Acoustic Scene Distance

For computing the distance between acoustic scenes, we first compute the CQT [SK10] of each 44.1 kHz recording with a log-frequency resolution of 5 bins per octave and an 8-octave span with 27.5 Hz set as the lowest frequency. The step size is set to 40 ms. Afterwards, time-frequency patches are extracted using the proposed HMM-constrained SIPLCA algorithm with $Z \in \{10, 25, 50\}$ bases and $\lambda = 0.005$ (the value was set after experimentation). Sparsity was enforced to $P(t|z)$ with sparsity parameter values $sH \in \{0, 0.1, 0.2, 0.5\}$. In all cases the length of each basis is set to 400 ms.

For each basis $\mathbf{W}_z = P(\omega,\tau|z)$, very small values ($< 0.001$) are replaced by the median value of $\mathbf{W}_z$. Afterwards, a vector of 13 cepstral coefficients is computed for each basis frame $\mathbf{w}[k] = \mathbf{W}_z[k,t],\ k = 1,\ldots,K$, in order to result in a compact representation for computational speed purposes. In order to convert a vector $\mathbf{w}[k]$ into cepstral coefficients, we employ the formula presented

in [Bro99]:

$$c_i = \sum_{k=1}^{K} \log(\mathbf{w}[k]) \cos\left(i\left(k - \frac{1}{2}\right)\frac{\pi}{K}\right) \tag{5.23}$$

where $i = 1, \ldots, 13$. Each vector of cepstral coefficients is then normalised to the [0,1] region. The first coefficient, which corresponds to the DC component of the signal, is dropped. Finally, for each time-frequency basis, the coefficients are summed together over time, thus resulting in a single vector representing a basis. This compressed basis vector is denoted as $\mathbf{w}_z$, where z denotes the component index.

For computing the distance between a scene l and a scene m, we employ the same steps as in [Cau11]. Firstly, we compute the elementwise distance between a basis $\mathbf{w}_z^{(l)}$, $z = 1, \ldots, Z$ and the nearest basis of dictionary $\mathbf{W}^{(m)}$ (which includes all vectors $\mathbf{w}_z^{(m)}$):

$$d_z(l, m) = \min_{j \in [1, Z]} ||\mathbf{w}_z^{(l)} - \mathbf{w}_j^{(m)}|| \tag{5.24}$$

The final distance between two acoustic scenes is defined as:

$$D(l, m) = \sum_{z=1}^{Z} d_z(l, m) + d_z(m, l) \tag{5.25}$$

Equation (5.25) is formulated in order for the distance measure between two scenes to be symmetric. In the end, the acoustic scene distance matrix D is used for evaluation.

It should be noted that quantifying the distance between two basis vectors by considering the Euclidean distance of their time average most probably leads to a loss of descriptive power of our model. This choice is made for tractability purposes. Indeed, for the corpus used in this study and 50 bases per item, building the matrix D involves making about 10^12 comparisons. Finding an efficient way of considering the time axis during the distance computation is left for future research.

5.4.3 Evaluation

Dataset

For the acoustic scene classification experiments we employ the dataset created by J. Tardieu [TSP+08]. The dataset was originally created for a perceptual

Scene	Platform	Hall	Corridor	Waiting	Ticket Office	Shop
No. Samples	10	16	12	13	10	5

Table 5.6: Class distribution in the employed dataset of acoustic scenes.

study on free- and forced-choice recognition of acoustic scenes by humans. It contains 66 44.1 kHz files recorded in 6 different train stations (Avignon, Bordeaux, Lille Flandres, Nantes, Paris Est, Rennes). Each file is classified into a 'space', which corresponds to the location this file was recorded: platforms, halls, corridors, waiting room, ticket offices, shops. The recordings contain numerous overlapping acoustic events, making even human scene classification a nontrivial task. In Table 5.6, the class distribution for the employed dataset can be seen. In addition to the ground truth included for each recording, an additional scene label is included as a result of the forced-categorisation perceptual study performed in [TSP+08].

Evaluation metrics

For evaluation, we employ the same set of metrics that were used in [Cau11] for the same experiment, namely the mean average precision (MAP), the 5-precision, and the classification accuracy of a nearest neighbour classifier. The MAP and 5-precision metrics are utilised for ranked retrieval results, where in this case the ranking is given by the values of the distance matrix D. MAP is able to provide a single-figure metric across recall levels and can describe the global behaviour of the system. It is computed using the average precision, which is the average of the precision obtained for the set of top n documents existing after each relevant document is retrieved. The 5-precision is the precision at rank 5, i.e. when the number of relevant samples is equal to 5. It corresponds to the number of samples in the smallest class, which describes the system performance at a local scale.

Regarding the classification accuracy metric, for each row of D we apply the k-nearest neighbour classifier with 11 neighbours, which corresponds to the average number of samples per class.

Results

Acoustic scene classification experiments are performed using the SI-PLCA algorithm of [SR07] and the proposed SI-PLCA algorithm with temporal constraints

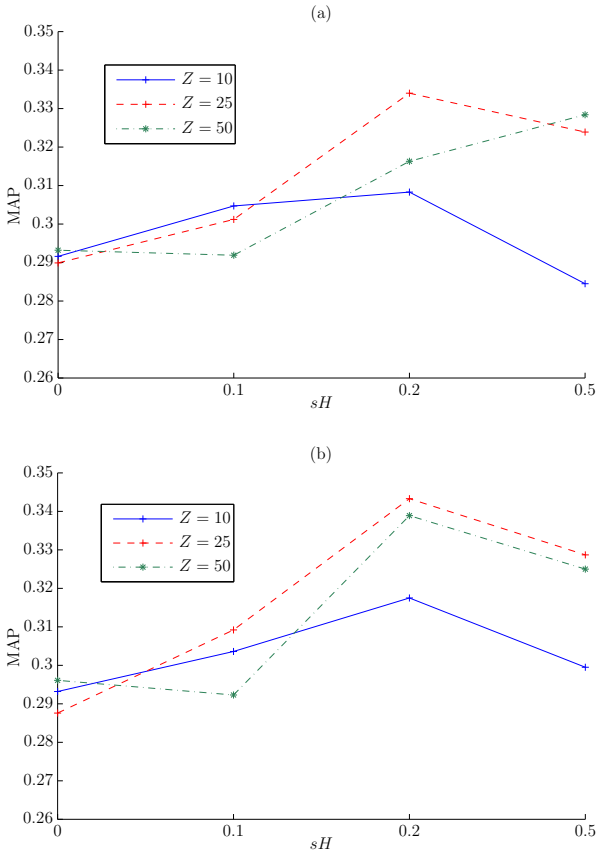

Figure 5.7: Acoustic scene classification results (MAP) using (a) the SI-PLCA algorithm (b) the TCSI-PLCA algorithm, with different sparsity parameter (sH) and dictionary size (Z).

(named TCSI-PLCA for brevity). Comparative results are also reported using a bag-of-frames (BOF) approach of [ADP07] reported in [Cau11]. The bag-of-frames method computes several audio features which are fed to a Gaussian mixture model classifier. The NMF method of [Cau11] is also implemented and tested. Results are also compared with the human perception experiment reported in [TSP+08]. Experiments are performed using different dictionary sizes Z and sparsity parameters sH (details on the range of values can be seen in the previous subsection).

The best results using each employed classifier are presented in Table 5.7. The proposed temporally-constrained SIPLCA model outperforms all other clas-

Model	MAP	5-Precision
Human Perception [TSP+08]	0.62	0.73
Random	0.25	0.18
BOF [ADP07]	0.24	0.18
NMF ($Z = 50, sH = 0.99$)	0.32	0.29
SI-PLCA ($Z = 25, sH = 0.2$)	0.33	0.35
TCSI-PLCA ($Z = 25, sH = 0.2$)	**0.34**	**0.36**

Table 5.7: Best MAP and 5-precision results for each model.

sifiers using both metrics, apart from the human forced categorisation experiment. The proposed method slightly outperforms the standard SI-PLCA algorithm, which in turn outperforms the NMF algorithm. It can also be seen that the BOF method is clearly not suitable for such an experiment, since the audio features employed in this method are more appropriate for non-overlapping events, whereas the dataset that is utilised contains concurrent events and a significant level of background noise. However, the human categorisation experiment from [TSP+08] outperforms all other approaches.

More detailed results for the SI-PLCA algorithm using different sparsity parameter values and different numbers of extracted bases (Z) can be seen in Fig. 5.7 (a). In all cases, enforcing sparsity improves performance. It can also be seen that the best performance is reported for $Z = 25$, although the performance of the system using $Z = 50$ improves when greater sparsity on $P(t|z)$ is encouraged. Detailed results for the proposed TCSI-PLCA method can be seen in Fig. 5.7 (b), using different dictionary sizes and sparsity values. It can be seen that the performance reaches a peak when $sH = 0.2$, for the case of $Z = 25$. When using a dictionary size of $Z = 50$, the performance of the proposed method is slightly decreased. Thus, selecting the appropriate number of components is important in the performance of the proposed method, since using too many components will lead to a parts-based representation which in the unsupervised case will lead to non representative dictionaries. Likewise, selecting too few bases will lead to a less descriptive model of the input signal.

Regarding classification accuracy using 11-nearest neighbours, results are shown in Table 5.8. Again, the TCSI-PLCA method outperforms all the other automatic approaches. In this case however, the non-negative matrix factorization approach from [Cau11] outperforms the SIPLCA algorithm by 0.5%. For the TCSI-PLCA algorithm, the best performance is again reported for $sH = 0.2$,

Classifier	**Accuracy** %
Human Perception [TSP+08]	54.8%
Random	16.6%
BOF [ADP07]	19.7%
NMF ($Z = 50, sH = 0$)	34.1%
SI-PLCA ($Z = 25, sH = 0.5$)	33.6%
TCSI-PLCA ($Z = 50, sH = 0.2$)	35.0%

Table 5.8: Best classification accuracy for each model.

while for the NMF approach the best performance is reported for $sH = 0$. Regarding dictionary size, the best results are reported for $Z = 50$.

Comparative experiments are performed by selecting only basis vectors that correspond to a sparse activation $P(t|z)$. In the PLCA domain, the sparseness criterion can be given by maximizing the l_2 norm as in [Sma11], due to the fact that all elements of the activation matrix take values between 0 and 1. However, the performance of the SI-PLCA and TCSI-PLCA algorithms in fact decreased slightly when selecting only the basis vectors that corresponded to the sparsest activations. This issue may be addressed in the future by enforcing sparsity only to certain components that represent salient events and keeping the rest of the components (which could represent noise) without enforcing sparsity.

5.4.4 Discussion

In this section we proposed a method for modeling and classifying acoustic scenes using a temporally-constrained shift-invariant model similar to the one proposed for automatic music transcription purposes in Section 4.4. In the classification stage, each extracted time-frequency basis is converted into a compact vector of cepstral coefficients for computational speed purposes. The employed dataset consisted of recordings taken from six types of scenes at different train stations. Comparative experiments were performed using a standard non-negative matrix factorization approach, as well as a bag-of-frames algorithm which is based on computing audio features. Results show that using shift-invariant models for learning time-frequency patches improves classification performance. Moreover, incorporating temporal constraints in the SI-PLCA model as well as enforcing sparsity constraints in the component activation result in improved classification performance.

However, the classification performance of the proposed computational methods is still significantly lower than the human forced categorisation task presented in [TSP+08]. We acknowledge that this performance is in our case an upper bound that may not even be reached by purely data-driven methods since humans most probably make extensive use of prior knowledge but the significant gap between the human and computational performances indicates that there is potentially room for improvement on the computational side.

In order to improve spectrogram factorization techniques such as NMF and SI-PLCA, additional constraints and knowledge need to be incorporated into the models. A hierarchical model which would consist of event classes and component subclasses would result in a richer model, but would also require prior information on the shape of each event in order to result in meaningful time-frequency patches. Prior information can be provided by utilising training samples of non-overlapping acoustic events. Also, an additional sparseness constraint could be imposed on the activation matrix, in order to control the number of overlapping components present in the signal (instead of enforcing sparsity as in the present work). In addition, instead of using a first-order Markov model for imposing temporal constraints, a more complex algorithm which would be able to model the duration of each event, such as a semi-Markov model [Yu10] could be employed. Finally, finding an efficient way of comparing extracted time frequency patches is also important. In this respect, we believe that lower bounding approaches to the dynamic time warping technique are of interest [Keo02, RCM+12].

5.5 Discussion

This chapter presented applications of proposed automatic music transcription systems. The first two systems were applications of AMT to computational musicology, namely for modulation detection and temperament estimation. For the system presented in Section 5.3, an algorithm for score-informed transcription was proposed, which was applied to the problem of automatic piano tutoring. Finally, in Section 5.4, the temporally-constrained shift-invariant model that was proposed for automatic music transcription in Section 4.4 was applied to the field of computational auditory scene analysis, namely for acoustic scene characterisation.

The applications of automatic music transcription presented in this chapter

are but a small subset of the potential applications of AMT to music technology. The creation of a robust AMT system can help in solving several problems in the field of music information retrieval (MIR), such as music genre classification, music similarity, cover song identification, and artist identification. It can also improve the performance of problems which are based on low-level descriptors, such as instrument identification and chord estimation. AMT can also bridge the gap in systematic and computational musicology between current symbolic music processing approaches and the use of audio recordings for addressing related problems. Interactive systems for automatic improvisation and accompaniment as well as for automatic tutoring can also benefit from automatic transcription methods. Finally, the techniques developed for automatic transcription such as the ones presented in Chapter 4 can also be used for other problems which require the analysis and decomposition of time series data, such as the case of acoustic scene characterisation that was presented in this chapter.

Chapter 6

Conclusions and Future Perspectives

In this thesis, several methods for automatic music transcription have been proposed using audio feature-based techniques and spectrogram factorization-based techniques, in an attempt to exploit characteristics of the temporal evolution of sounds. In addition, several applications of automatic transcription systems were proposed, demonstrating the impact of AMT research in music technology and audio processing. The majority of the work presented in this thesis has been presented in international peer-reviewed journals and conferences, as shown in Section 1.4. In this chapter, the main contributions of the thesis are summarised and directions for future work are presented.

6.1 Summary

6.1.1 Audio feature-based AMT

In Chapter 3, methods for audio feature-based automatic music transcription were proposed and evaluated. Initial work consisted of a system for multiple-F0 estimation of isolated piano sounds, which used pitch candidate selection and rule-based refinement steps (Section 3.2). Contributions of that system were a pitch salience function in the log-frequency domain which supported inharmonicity and tuning changes; a feature measuring spectral irregularity which is robust to overlapping partials; and a feature based on the common ampli-

tude modulation assumption for eliminating octave errors. Experimental results showed that the proposed system outperforms several state-of-the-art systems for the task of multiple-F0 estimation of isolated piano sounds. A variant of the proposed system for supporting complete recordings instead of isolated sounds was publicly evaluated in the MIREX 2010 multiple-F0 estimation task [MIR].

Afterwards, a joint multiple-F0 estimation system was proposed for AMT, followed by note tracking (Section 3.3). Contributions of that work were a noise suppression algorithm based on a pink noise assumption; an overlapping partial treatment procedure using the harmonic envelopes of pitch candidates; a pitch set score function which incorporated several spectral and temporal features; an algorithm for spectral envelope estimation in the log-frequency domain; and a note tracking procedure using conditional random fields [LMP01]. The system was evaluated using several datasets commonly used in AMT literature, where it was shown that the proposed system outperforms several state-of-the-art AMT systems for the same experiments. It was also shown that the joint multiple-F0 estimation algorithm of Section 3.3 performs better than the iterative multiple-F0 estimation algorithm of Section 3.2, at the expense of increased computational cost. In addition, it was shown that the note tracking procedures using hidden Markov models [Rab89] and conditional random fields [LMP01] helped improve transcription performance compared to simple thresholding.

Finally, an extension of the joint multiple-F0 estimation system was proposed, by explicitly incorporating information about note onsets and offsets (Section 3.4). Contributions of this work include a note onset detection procedure which incorporates tuning and pitch information from the pitch salience function and a note offset detection procedure using pitch-wise hidden Markov models [Rab89]. This system was evaluated using the same datasets as the system of Section 3.3, and results demonstrate an improved transcription performance using note-based metrics (instead of frame-based metrics), since this system explicitly models note events. Also, in cases where hard onsets are present, is was shown that explicitly incorporating note onset information improves transcription performance.

6.1.2 Spectrogram factorization-based AMT

In Chapter 4, methods for automatic music transcription using spectrogram factorization techniques were proposed and evaluated. Proposed systems extended the shift-invariant probabilistic latent component analysis (SI-PLCA)

model [SRS08b], for supporting multiple templates per pitch and instrument, as well as for introducing temporal constraints for sound evolution, while at the same time being able to model frequency modulations as shifts in the log-frequency domain. Additionally, the proposed spectrogram factorization models can be modified easily for instrument-specific transcription by changing instrument templates.

The first proposed system consisted of a model based on SI-PLCA which supported the use of multiple spectral templates per pitch, as well as per musical instrument (Section 4.2). The contribution of each source is time- and pitch-dependent, making the model also suitable for instrument identification in polyphonic music. Finally, the high-resolution time-pitch representation that is the output of the system can also be used for pitch visualization purposes. The system was evaluated using the same set of recordings as in Chapter 3, where it was shown that the proposed model outperformed the audio feature-based approaches in most cases. It was shown that a convolutive model can help improve transcription accuracy compared to a non-convolutive linear model (e.g. using PLCA [SRS06] or NMF [LS99]). Also, incorporating sparsity constraints in the pitch and source activations improved transcription performance. The system of Section 4.2 was also publicly evaluated in the MIREX 2011 contest, where it ranked 2nd in the multiple-instrument note tracking task [MIR].

In Section 4.3, temporal constraints were incorporated within a single-source SI-PLCA model using hidden Markov models [Rab89] for modelling the temporal evolution of notes. The proposed model expressed the evolution of monophonic music sounds as a sequence of sound state templates, shifted across log-frequency. Experimental results on pitch detection showed that the temporally-constrained shift-invariant model outperformed a non-temporally-constrained model for the same experiment, indicating that incorporating temporal constraints in multiple-instrument multi-pitch detection can further improve transcription performance.

Finally, the temporal constraints of Section 4.3 were combined with the multiple-instrument multi-pitch model of Section 4.2 in the proposed model of Section 4.4. Thus, the contribution of this section was a system for multi-pitch detection and multiple instrument assignment, supporting also multiple sets of sound state templates per source. At the same time, the model supported tuning changes and frequency modulations due to its shift-invariant nature. Experiments showed that the proposed model outperforms the non-temporally constrained model of Section 4.2, both for automatic transcription and instru-

ment assignment, and also outperforms state-of-the-art transcription systems in the literature for the same experiments.

6.1.3 Transcription Applications

In Chapter 5 applications of the proposed AMT systems were presented, in order to demonstrate the potential impact of automatic music transcription research in music technology and audio processing.

In Section 5.1, the AMT system of Section 3.4 was utilised as front-end for an automatic modulation detection system for J.S. Bach chorales. To the author's knowledge, this is the first study which utilised AMT for systematic musicology research. Results comparing an audio input and a symbolic input showed that although there are many differences between the transcribed audio and the original score, the performance of the two systems for key detection is similar, showing that AMT can be used as an audio front-end for certain tasks in the systematic musicology field.

A computationally efficient harpsichord-specific transcription system was proposed in Section 5.2 as a front-end for estimating temperament in harpsichord recordings. The system was used to transcribe over 500 complete harpsichord recordings taken from 22 CDs. The measured temperaments are compared with the annotations found in CD sleeve notes and it was found that while this information is mostly correct, there were several cases where a discrepancy in temperament was found, raising an interesting issue about the nature of "ground truth".

A method for score-informed transcription was proposed in Section 5.3 and was applied to automatic piano tutoring, in an effort to detect mistakes made by piano students. It should be noted that the problem of score-informed transcription is relatively unexplored, and a contribution of this work is the transcription of the synthesized score along with the original recording. A score-informed piano transcription dataset was created by the author and is available online. Results indicated that using manually-aligned scores, the proposed method can successfully analyze the student's performance. Also, it was shown that transcribing the synthesized score helped improve score-informed transcription performance.

Finally, in Section 5.4, the temporally-constrained shift-invariant transcription model of Section 4.4 was modified for the problem of acoustic scene characterisation in an unsupervised manner. Experimental results using train station

recordings showed that the proposed model outperforms NMF-based models and that temporal constraints help improve classification accuracy. It was also shown that the proposed transcription models can be used in non-music audio processing applications.

6.2 Future Perspectives

Although the proposed systems outperform state-of-the-art systems, the overall transcription performance is still considerably below that of a human expert, and will most likely continue to be for some years, as the transcription problem is inherently complex and the field has only recently started to grow.

As shown in this work, signal processing-based systems are computationally inexpensive and have demonstrated encouraging transcription results, but have problems with respect to generalisation (e.g. to different instrument sources). Thus, signal processing-based systems cannot straightforwardly be used as a basis for a more general system for analysing music signals, which could additionally address the problems of instrument identification, source separation, extraction of rhythmic information, etc. On the other hand, spectrogram factorisation models produced competitive results, offering at the same time a transparent model of operation which helps in extending these models for the creation of more complex systems for music signal analysis. The main drawback of spectrogram factorisation models is that they are computationally expensive.

It was also shown that AMT systems can effectively be used in other music technology applications. Current tasks in music information retrieval (MIR) such as genre classification, music similarity, and chord detection typically employ low-level features instead of utilising information from the transcribed score. Although transcription-based techniques for MIR will most likely be more computationally demanding compared to low-level feature-based techniques, they can also offer a more complete framework for analysing music signals. This framework can be used as a basis for addressing many tasks (instead of proposing task-specific MIR techniques) and can also be used for the extraction of high-level musicological features for music analysis. Another field where AMT systems can be used is computational musicology; current applications use symbolic data as input, whereas using an AMT system, research could be performed from an audio front-end.

Proposed systems can be used as a basis for creating improved transcription

systems as well as systems for music signal analysis. In the process of carrying out research and writing for the thesis, many ideas for future research emerged regarding automatic transcription, note tracking, and instrument identification, which will be detailed below.

Regarding improving transcription performance, the temporally-constrained model of Section 4.4 can be modified to support whole-note templates instead of a series of spectra for each sound state, resulting in a more constrained model, albeit more demanding computationally. Since the duration of each note event is arbitrary, each whole-note template can be scaled over time using dynamic time warping techniques (e.g. [MD10]).

Different time-frequency representations can also be used as input to the proposed AMT systems, in an effort to further improve transcription performance. For example, the auditory models by Yang et al. [YWS92] can be used instead of the constant-Q transform. Also, the use of spectral reassignment was shown to outperform the short-time Fourier transform for automatic transcription in [Hai03] and could be tested using the proposed systems. Another avenue of research would be the use of several time-frequency representations, using e.g. different window sizes. This would result in a tensorial input, which could be transcribed by modifying currently proposed techniques for SI-PLCA to probabilistic latent tensor factorization (PLTF) [CŞS11].

Another way of improving transcription performance would be fusing different AMT systems at the decision level (late fusion). In [HS10], it was shown that combining several conservative onset detectors (with high precision and low recall), an improvement can be achieved in onset detection; the same idea can be utilised in the context of automatic transcription.

Computational efficiency is another issue, especially in the convolutive transcription models of Chapter 4, which employ the EM algorithm. One way of addressing this issue would be to keep the same model formulation but to utilise a different algorithm for parameter estimation, which would be more computationally efficient, e.g. convolutive sparse coding [Vir04].

For further improving the SI-PLCA-based models of Chapter 4, in [DCL10] it was shown that the NMF algorithm with β-divergence performed better than the standard NMF algorithm. Since in [SRS08a] it was shown that the NMF algorithm using the KL divergence is equivalent to the PLCA algorithm, introducing β-divergences in the PLCA and SI-PLCA models could also further improve transcription performance.

Regarding note tracking, all proposed transcription systems in Chapters 3

and 4 performed multiple-F0 estimation and note tracking separately. Transcription performance could potentially improve by proposing a joint model for multiple-F0 estimation and note tracking (similar to the one in [KNS07]), which however would be less computationally efficient. One other way to improve transcription performance with respect to the note tracking process would be to utilise a key induction procedure which would assist in assigning priors and transition probabilities using training data in the same key (instead of having one transition matrix for all keys). Also, the present 2-state on/off models for note tracking could be further extended by incorporating a musicological model of note transitions at one level and chord transitions at a higher level, as in [ROS09b].

Current note tracking models however do not explicitly model note durations, but only express note or chord transitions. Instead of using a first-order Markov model for imposing temporal constraints, a more complex algorithm which would be able to model the duration of each event, such as a semi-Markov model [Yu10] can be employed. Such a development would also be of interest for the acoustic scene characterisation experiments of Section 5.4, for modelling the duration of specific events.

Finally, regarding instrument assignment, although the proposed model of Section 4.4 outperformed other approaches for the same experiment, instrument identification performance is still poor. However, the proposed spectrogram factorization-based models could potentially improve upon instrument assignment performance by utilizing the information provided by the source contribution matrix $P_t(s|p)$, combined with features for characterizing music timbre (e.g. [Pee04]). Also, in the model of Section 4.4, the number of sound states can also be made instrument-dependent by performing slight modifications to the model, thus providing a more realistic model for each instrument.

Appendix A

Expected Value of Noise Log-Amplitudes

We present the derivation for the expected value of noise log-amplitudes, which is used in the proposed noise suppression algorithm for the joint multi-pitch detection system of Section 3.3. We assume that the noise amplitude follows an exponential distribution. In order to find the expected value of the noise log amplitudes $E\{\log(|N_c(\hat{\omega})|)\}$, we adopt a technique similar to [Yeh08]. Let $\Theta = \log(N_c(\bar{\omega})) = \Phi(N)$:

$$\begin{aligned} E\{\Theta\} &= \int_{-\infty}^{+\infty} \theta P(\theta) d\theta = \int_{-\infty}^{+\infty} \theta P(\Phi^{-1}(\theta)) \left| \frac{d\Phi^{-1}(\theta)}{d\theta} \right| \\ &= \int_{-\infty}^{+\infty} \chi \theta e^{-\chi e^{\theta}} e^{\theta} d\theta = \int_{0}^{+\infty} \chi \log(\psi) e^{-\chi\psi} d\psi \\ &= -\gamma - \chi \log(\chi) \cdot \int_{0}^{+\infty} e^{-\chi\psi} d\psi \\ &= \log(\chi^{-1}) - \gamma \end{aligned} \tag{A.1}$$

where γ is the Euler constant:

$$\gamma = -\int_{0}^{+\infty} e^{-\psi} \log(\psi) d\psi \approx 0.57721. \tag{A.2}$$

Appendix B

Log-frequency spectral envelope estimation

An algorithm for posterior-warped log-frequency regularized spectral envelope estimation is proposed, which is used in the joint multi-pitch detection system of Section 3.3. Given a set of harmonic partial sequences (HPS) in the log-frequency domain, the algorithm estimates the log-frequency envelope using linear regularized discrete cepstrum estimation. In [DR03] a method for estimating the spectral envelope using discrete cepstrum coefficients in the Mel-scale was proposed. The superiority of discrete cepstrum over continuous cepstrum coefficients and linear prediction coefficients for spectral envelope estimation was argued in [SR99]. Other methods for envelope estimation in the linear frequency domain include a weighted maximum likelihood spectral envelope estimation technique in [BD08], which was employed for multiple-F0 estimation experiments in [EBD10]. The proposed algorithm can be outlined as follows:

1. Extract the harmonic partial sequence $HPS[p, h]$ and corresponding log-frequency bins $\omega_{p,h}$ for a given pitch p and harmonic index $h = 1, \ldots, 13$.

2. Convert the log-frequency bins $\omega_{p,h}$ to linear angular frequencies $\tilde{\omega}_{p,h}$ (where the sampling rate is $f_s = 44.1$ kHz and the lowest frequency for analysis is $f_{low} = 27.5$ Hz):

$$\tilde{\omega}_{p,h} = 27.5 \cdot \frac{2\pi}{f_s} \cdot 2^{\frac{\omega_{p,h}}{120}} \tag{B.1}$$

3. Perform spectral envelope estimation on $HPS[p,h]$ and $\tilde{\omega}_{p,h}$ using the linear regularized discrete cepstrum. Coefficients $\mathbf{c}_p$ are estimated as:

$$\mathbf{c}_p = (\mathbf{M}_p^T \mathbf{M}_p + \rho \mathbf{K})^{-1} \mathbf{M}_p^T \mathbf{a}_p \tag{B.2}$$

where $\mathbf{a}_p = [\ln(HPS[p,1]), \ldots, \ln(HPS[p,H])]$, $\mathbf{K} = \text{diag}([0, 1^2, 2^2, \cdots, (K-1)^2])$, K is the cepstrum order, ρ is the regularization parameter, and

$$\mathbf{M}_p = \begin{bmatrix} 1 & 2\cos(\tilde{\omega}_{p,1}) & \cdots & 2\cos(K\tilde{\omega}_{p,1}) \\ \vdots & \vdots & & \vdots \\ 1 & 2\cos(\tilde{\omega}_{p,H}) & \cdots & 2\cos(K\tilde{\omega}_{p,H}) \end{bmatrix} \tag{B.3}$$

4. Estimate the vector of log-frequency discrete cepstral coefficients $\mathbf{d}_p$ from $\mathbf{c}_p$. In order to estimate $\mathbf{d}_p$ from $\mathbf{c}_p$, we note that the function which converts linear angular frequencies into log-frequencies is given by:

$$g(\tilde{\omega}) = 120 \cdot \log_2\left(\frac{f_s \cdot \tilde{\omega}}{2\pi \cdot 27.5}\right) \tag{B.4}$$

which is defined for $\tilde{\omega} \in [\frac{2\pi \cdot 27.5}{f_s}, \pi]$. Function $g(\tilde{\omega})$ is normalized using $\bar{g}(\tilde{\omega}) = \frac{\pi}{g(\pi)} g(\tilde{\omega})$, which becomes:

$$\bar{g}(\tilde{\omega}) = \frac{\pi}{\log_2(\frac{f_s}{2 \cdot 27.5})} \cdot \log_2\left(\frac{f_s \cdot \tilde{\omega}}{2\pi \cdot 27.5}\right) \tag{B.5}$$

The inverse function, which converts angular log-frequencies into angular linear frequencies is given by:

$$\bar{g}^{-1}(\hat{\omega}) = \frac{2\pi \cdot 27.5}{f_s} \cdot 2^{\frac{\bar{\omega} \log_2(\frac{f_s}{2 \cdot 27.5})}{\pi}} \tag{B.6}$$

which is defined in $[0, \pi] \rightarrow [\frac{2\pi \cdot 27.5}{f_s}, \pi]$. From [DR03], it can be seen that:

$$\mathbf{d}_p = \mathbf{A} \cdot \mathbf{c}_p \tag{B.7}$$

where

$$\mathbf{A}_{m+1,l+1} = \frac{(2 - \delta_{0l})}{\Omega} \sum_{\omega=0}^{\Omega-1} \cos\left(l \bar{g}^{-1}(\frac{\pi\omega}{\Omega})\right) \cos\left(\frac{\pi \omega m}{\Omega}\right) \tag{B.8}$$

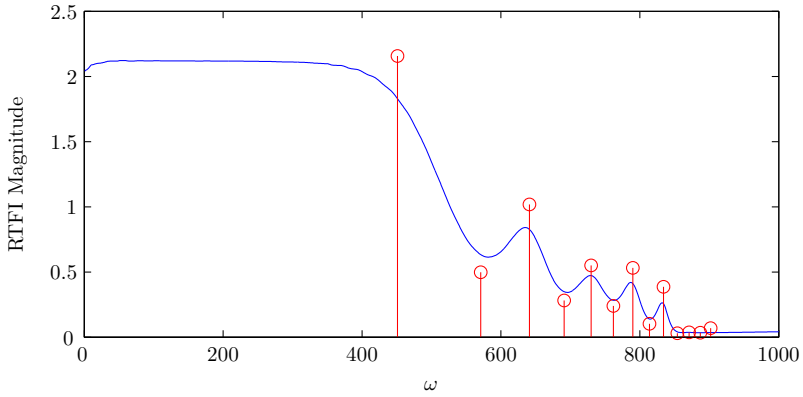

Figure B.1: Log-frequency spectral envelope of an F#4 piano tone with $P = 50$. The circle markers correspond to the detected overtones.

where Ω is the size of the spectrum in samples, and m, l range from 0 to $P - 1$.

5. Estimate the log-frequency spectral envelope SE from $\mathbf{d}_p$. The log-frequency spectral envelope is defined as:

$$SE_p(\hat{\omega}) = \exp\left(d_{0p} + 2\sum_{i=1}^{P-1} d_{ip}\cos(i\hat{\omega})\right). \tag{B.9}$$

In Fig. B.1, the warped log-frequency spectral envelope of an F#4 note produced by a piano (from the MAPS dataset) is depicted.

Appendix C

Derivations for the Temporally-constrained Convolutive Model

In this appendix, the derivations for the temporally-constrained model of Section 4.3 are presented. The derivations follow closely the one in [Mys10]. As mentioned in Section 4.3, the parameters of the model are as follows:

1. Sound state templates $P(\mu_t|q_t) = P(\omega_t - f_t|q_t)$
2. Pitch shift per sound state $P_t(f_t|q_t)$
3. Sound state transition matrix $P(q_{t+1}|q_t)$
4. Initial state probabilities $P(q_1)$

The parameters are estimated using the EM algorithm [DLR77], by maximizing the log-likelihood of the data. The posterior distribution of the model is given by:

$$P(\bar{f}, \bar{q}|\bar{\omega}) \tag{C.1}$$

where $\bar{f}$ is the sequence of draws of f.

C.1 Log likelihood

The complete data log likelihood is given by:

$$\log P(\bar{f}, \bar{q}, \bar{\omega}) = \log P(q_1) + \sum_{t}^{T-1} \log P(q_{t+1}|q_t) + \sum_{t}^{T} \sum_{v}^{V_t} \log P(\omega_{t,v} - f_{t,v}|q_t) + \sum_{t}^{T} \sum_{v}^{V_t} \log P_t(f_{t,v}|q_t) \tag{C.2}$$

where $V_t = \sum_{\omega} V_{\omega,t}$ and $\omega_{t,v}, f_{t,v}$ denote draw v at frame t of random variables ω, f, respectively.

The expected value of the complete data log likelihood wrt to the posterior distribution is given by:

$$\begin{aligned}
\mathcal{L} &= E_{\bar{f},\bar{q}|\bar{\omega}} \log P(\bar{f}, \bar{q}, \bar{\omega}) \\
&= \sum_{\bar{q}} \sum_{\bar{f}} P(\bar{f}, \bar{q}|\bar{\omega}) \log P(\bar{f}, \bar{q}, \bar{\omega}) \\
&= \sum_{\bar{q}} \sum_{\bar{f}} P(\bar{f}, \bar{q}|\bar{\omega}) \log P(q_1) \\
&+ \sum_{t}^{T-1} \sum_{\bar{q}} \sum_{\bar{f}} P(\bar{f}, \bar{q}|\bar{\omega}) \log P(q_{t+1}|q_t) \\
&+ \sum_{t}^{T} \sum_{v}^{V_t} \sum_{\bar{q}} \sum_{\bar{f}} P(\bar{f}, \bar{q}|\bar{\omega}) \log P(\omega_{t,v} - f_{t,v}|q_t) \\
&+ \sum_{t}^{T} \sum_{v}^{V_t} \sum_{\bar{q}} \sum_{\bar{f}} P(\bar{f}, \bar{q}|\bar{\omega}) \log P_t(f_{t,v}|q_t)
\end{aligned} \tag{C.3}$$

By marginalizing certain variables in $\mathcal{L}$:

$$\begin{aligned}
\mathcal{L} &= \sum_{q_1} P(q_1|\bar{\omega}) \log P(q_1) \\
&+ \sum_{t}^{T-1} \sum_{q_t} \sum_{q_{t+1}} P_t(q_t, q_{t+1}|\bar{\omega}) \log P(q_{t+1}|q_t) \\
&+ \sum_{t=1}^{T} \sum_{v}^{V_t} \sum_{q_t} \sum_{f_{t,v}} P_t(f_{t,v}, q_t|\bar{\omega}) \log P(\omega_{t,v} - f_{t,v}|q_t) \\
&+ \sum_{t=1}^{T} \sum_{v}^{V_t} \sum_{q_t} \sum_{f_{t,v}} P_t(f_{t,v}, q_t|\bar{\omega}) \log P_t(f_{t,v}|q_t) \qquad \text{(C.4)}
\end{aligned}$$

We change the summations to be over frequencies rather than draws:

$$\begin{aligned}
\mathcal{L} &= \sum_{q_1} P(q_1|\bar{\omega}) \log P(q_1) \\
&+ \sum_{t}^{T-1} \sum_{q_t} \sum_{q_{t+1}} P_t(q_t, q_{t+1}|\bar{\omega}) \log P(q_{t+1}|q_t) \\
&+ \sum_{t}^{T} \sum_{q_t} \sum_{f_t} \sum_{\omega_t} V_{\omega,t} P_t(f_t, q_t|\omega_t, \bar{\omega}) \log P(\omega_t - f_t|q_t) \\
&+ \sum_{t}^{T} \sum_{q_t} \sum_{f_t} \sum_{\omega_t} V_{\omega,t} P_t(f_t, q_t|\omega_t, \bar{\omega}) \log P(f_t|q_t) \qquad \text{(C.5)}
\end{aligned}$$

We incorporate constraints using Lagrange multipliers $\zeta^{(1)}, \zeta^{(2)}_{q_t}, \zeta^{(3)}_{f,q}, \zeta^{(4)}_{q_t}$

$$\begin{aligned}
\mathcal{L} &= \sum_{q_1} P(q_1|\bar{\omega}) \log P(q_1) \\
&+ \sum_{t}^{T-1} \sum_{q_t} \sum_{q_{t+1}} P_t(q_t, q_{t+1}|\bar{\omega}) \log P(q_{t+1}|q_t) \\
&+ \sum_{t}^{T} \sum_{q_t} \sum_{f_t} \sum_{\omega_t} V_{\omega,t} P_t(f_t, q_t|\omega_t, \bar{\omega}) \log P(\omega_t - f_t|q_t) \\
&+ \sum_{t}^{T} \sum_{q_t} \sum_{f_t} \sum_{\omega_t} V_{\omega,t} P_t(f_t, q_t|\omega_t, \bar{\omega}) \log P(f_t|q_t) \\
&+ \zeta^{(1)} \left(1 - \sum_{q_1} P(q_1)\right) + \sum_{q_t} \zeta^{(2)}_{q_t} \left(1 - \sum_{q_{t+1}} P(q_{t+1}|q_t)\right) \\
&+ \sum_{f} \sum_{q} \zeta^{(3)}_{f,q} \left(1 - \sum_{\omega} P(\omega - f|q)\right) \\
&+ \sum_{t}^{T} \sum_{q_t} \zeta^{(4)}_{q_t} \left(1 - \sum_{f_t} P_t(f_t|q_t)\right) \qquad \text{(C.6)}
\end{aligned}$$

We need to estimate the parameters that maximize the above equation. For the **E-step**, we compute the following marginalizations:

1. Marginalized posterior for state priors: $P(q_1|\bar{\omega})$
2. Marginalized posteriors for state transitions: $P_t(q_t, q_{t+1}|\bar{\omega})$
3. Marginalized posteriors for state templates and pitch shift: $P_t(f_t, q_t|\omega_t, \bar{\omega})$

C.2 Expectation Step

The marginalized posteriors for state templates and pitch track is computed as follows:

$$\begin{aligned}
P_t(f_t, q_t|\bar{\omega}) &= \frac{P_t(f_t, q_t, \bar{\omega})}{P(\bar{\omega})} \\
&= P_t(f_t|\bar{\omega}, q_t) \frac{P_t(\bar{\omega}, q_t)}{P(\bar{\omega})} \\
&= P_t(f_t|\omega_t, q_t) P_t(q_t|\bar{\omega}) \qquad \text{(C.7)}
\end{aligned}$$

$P_t(q_t|\bar{\omega})$ is computed using (4.20) and (4.21), which utilize the forward and backward variables $\alpha_t(q_t)$ and $\beta_t(q_t)$, defined in (4.22) and (4.23), respectively.

For the computation of $\alpha_t(q_t)$ and $\beta_t(q_t)$ we also need the likelihoods $P(\bar{\omega}_t|q_t)$ which are computed as:

$$\begin{aligned} P(\bar{\omega}_t|q_t) &= \prod_{v}^{V_t} P_t(\omega_{t,v}|q_t) \\ &= \prod_{\omega_t} P_t(\omega_t|q_t)^{V_{\omega,t}} \end{aligned} \tag{C.8}$$

where $P_t(\omega_t|q_t)$ is computed using (4.17).

We also need to compute $P_t(f_t|\omega_t, q_t)$, which using Bayes' theorem and the notion that $P(\omega_t|f_t, q_t) = P(\omega_t - f_t|q_t)$ is:

$$\begin{aligned} P_t(f_t|\omega_t, q_t) &= \frac{P(\omega_t|f_t, q_t)P_t(f_t|q_t)}{\sum_{f_t} P(\omega_t|f_t, q_t)P_t(f_t|q_t)} \\ &= \frac{P(\omega_t - f_t|q_t)P_t(f_t|q_t)}{\sum_{f_t} P(\omega_t - f_t|q_t)P_t(f_t|q_t)} \end{aligned} \tag{C.9}$$

The marginalized posterior for the sound state transitions is computed as:

$$\begin{aligned} P_t(q_t, q_{t+1}|\bar{\omega}) &= \frac{P_t(\bar{\omega}, q_t, q_{t+1})}{P(\bar{\omega})} \\ &= \frac{P_t(\bar{\omega}, q_t, q_{t+1})}{\sum_{q_t}\sum_{q_{t+1}} P_t(\bar{\omega}, q_t, q_{t+1})} \end{aligned} \tag{C.10}$$

where

$$\begin{aligned} &P_t(\bar{\omega}, q_t, q_{t+1}) \\ &= P(q_{t+1}, \bar{\omega}_{t+1}, \ldots, \bar{\omega}_T|\bar{\omega}_1, \ldots, \bar{\omega}_t, q_t)P(\bar{\omega}_1, \ldots, \bar{\omega}_t, q_t) \\ &= P(q_{t+1}, \bar{\omega}_{t+1}, \ldots, \bar{\omega}_T|q_t)\alpha_t(q_t) \\ &= P(\bar{\omega}_{t+1}, \ldots, \bar{\omega}_T|q_{t+1})P(q_{t+1}|q_t)\alpha_t(q_t) \\ &= P(\bar{\omega}_{t+1}|q_{t+1})\beta_{t+1}(q_{t+1})P(q_{t+1}|q_t)\alpha_t(q_t) \end{aligned} \tag{C.11}$$

which leads to the computation of the marginalized posterior for the sound state transitions using (4.24).

The marginalized posterior for the state priors is given by $P(q_1|\bar{\omega})$, computed from (4.20).

C.3 Maximization Step

In order to estimate the sound state spectral templates $P(\mu|q)$ we take the derivative of (C.6) wrt μ, q, which gives the set of equations:

$$\frac{\sum_{f_t}\sum_t V_{\omega,t} P_t(f_t, q_t|\omega_t, \bar{\omega})}{P(\omega_t - f_t|q_t)} - \zeta^{(3)}_{f,q} = 0 \tag{C.12}$$

By eliminating the Lagrange multiplier:

$$P(\omega - f|q) = \frac{\sum_{f,t} V_{\omega,t} P_t(f, q|\omega, \bar{\omega})}{\sum_{\omega,f,t} V_{\omega,t} P_t(f, q|\omega, \bar{\omega})} \tag{C.13}$$

For estimating the pitch track $P_t(f_t|q_t)$, we take the derivative of (C.6) wrt f, q:

$$\frac{\sum_{\omega_t} V_{\omega,t} P_t(f_t, q_t|\omega_t, \bar{\omega})}{P_t(f_t|q_t)} - \zeta^{(4)}_{q_t} = 0 \tag{C.14}$$

By eliminating the Lagrange multiplier:

$$P_t(f_t|q_t) = \frac{\sum_{\omega_t} V_{\omega,t} P_t(f_t, q_t|\omega_t, \bar{\omega})}{\sum_{f_t,\omega_t} V_{\omega,t} P_t(f_t, q_t|\omega_t, \bar{\omega})} \tag{C.15}$$

For estimating the sound state transitions $P(q_{t+1}|q_t)$, we take the derivative of (C.6) wrt q_{t+1}, q_t, which gives the set of equations:

$$\frac{\sum_{t=1}^{T-1} P_t(q_t, q_{t+1}|\bar{\omega})}{P(q_{t+1}|q_t)} - \zeta^{(2)}_{q_t} = 0 \tag{C.16}$$

By eliminating the Lagrange multiplier:

$$P(q_{t+1}|q_t) = \frac{\sum_{t=1}^{T-1} P_t(q_t, q_{t+1}|\bar{\omega})}{\sum_{q_{t+1}}\sum_{t=1}^{T-1} P_t(q_t, q_{t+1}|\bar{\omega})} \tag{C.17}$$

For estimating the state priors $P(q_1)$ we take the derivative of (C.6) wrt q_1, which gives the set of equations:

$$\frac{P_1(q_1|\bar{\omega})}{P(q_1)} - \zeta^{(1)} = 0 \tag{C.18}$$

By eliminating the Lagrange multiplier:

$$P(q_1) = \frac{P_1(q_1|\bar{\omega})}{\sum_{q_1} P_1(q_1|\bar{\omega})} = P_1(q_1|\bar{\omega}) \tag{C.19}$$

Bibliography

[Abd02] S. A. Abdallah. *Towards Music Perception by Redundancy Reduction and Unsupervised Learning in Probabilistic Models*. PhD thesis, Department of Electronic Engineering, King's College London, 2002.

[ADP07] J.J. Aucouturier, B. Defreville, and F. Pachet. The bag-of-frames approach to audio pattern recognition: a sufficient model for urban soundscapes but not for polyphonic music. *Journal of the Acoustical Society of America*, 122(2):881–891, 2007.

[AEB05] M. Aharon, M. Elad, and A. Bruckstein. K-SVD and its non-negative variant for dictionary design. In *SPIE Conference on Wavelet Applications in Signal and Image Processing*, San Diego, USA, July 2005.

[ANP11] F. Argenti, P. Nesi, and G. Pantaleo. Automatic transcription of polyphonic music based on the constant-Q bispectral analysis. *IEEE Transactions on Audio, Speech, and Language Processing*, 19(6):1610–1630, August 2011.

[AP04] S. A. Abdallah and M. D. Plumbley. Polyphonic transcription by non-negative sparse coding of power spectra. In *International Conference on Music Information Retrieval*, pages 318–325, Barcelona, Spain, October 2004.

[AP06] S. A. Abdallah and M. D. Plumbley. Unsupervised analysis of polyphonic music by sparse coding. *IEEE Transactions on Neural Networks*, 17(1):179–196, January 2006.

[AS04] M. Abe and J. Smith. CQIFFT: Correcting bias in a sinusoidal parameter estimator based on quadratic interpolation of FFT

magnitude peaks. Technical Report STANM-117, CCRMA, Dept of Music, Stanford University, 2004.

[AS05] B. E. Anderson and W. J. Strong. The effect of inharmonic partials on pitch of piano tones. *Journal of the Acoustical Society of America*, 117(5):3268–3272, May 2005.

[Bar51] J.M. Barbour. *Tuning and Temperament: A Historical Survey*. Dover Publications, Mineola, NY, USA, 2004/1951.

[BBFT10] A. M. Barbancho, I. Barbancho, J. Fernandez, and L. J. Tardón. Polyphony number estimator for piano recordings using different spectral patterns. In *Audio Engineering Society 128th Convention*, London, UK, May 2010.

[BBJT04] I. Barbancho, A. M. Barbancho, A. Jurado, and L. J. Tardón. Transcription of piano recordings. *Applied Acoustics*, 65:1261–1287, September 2004.

[BBR07] N. Bertin, R. Badeau, and G. Richard. Blind signal decompositions for automatic transcription of polyphonic music: NMF and K-SVD on the benchmark. In *IEEE International Conference on Acoustics, Speech, and Signal Processing*, pages 65–68, Honolulu, USA, April 2007.

[BBST11] A. M. Barbancho, I. Barbancho, B. Soto, and L. J. Tardón. SIC receiver for polyphonic piano music. In *IEEE International Conference on Audio, Speech and Signal Processing*, pages 377–380, Prague, Czech Republic, May 2011.

[BBV09] N. Bertin, R. Badeau, and E. Vincent. Fast Bayesian NMF algorithms enforcing harmonicity and temporal continuity in polyphonic music transcription. In *2009 IEEE Workshop Applications of Signal Processing to Audio and Acoustics*, October 2009.

[BBV10] N. Bertin, R. Badeau, and E. Vincent. Enforcing harmonicity and smoothness in Bayesian non-negative matrix factorization applied to polyphonic music transcription. *IEEE Transactions on Audio, Speech, and Language Processing*, 18(3):538–549, March 2010.

[BD04] T. Blumensath and M. Davies. Unsupervised learning of sparse and shift-invariant decompositions of polyphonic music. In *IEEE International Conference on Acoustics, Speech, and Signal Processing*, volume 5, pages 497–500, Montreal, Canada, May 2004.

[BD08] R. Badeau and B. David. Weighted maximum likelihood autoregressive and moving average spectrum modeling. In *IEEE International Conference on Acoustics, Speech, and Signal Processing*, pages 3761–3764, Las Vegas, USA, April 2008.

[BD10a] E. Benetos and S. Dixon. Multiple-F0 estimation of piano sounds exploiting spectral structure and temporal evolution. In *ISCA Tutorial and Research Workshop on Statistical and Perceptual Audio Processing*, pages 13–18, Makuhari, Japan, September 2010.

[BD10b] E. Benetos and S. Dixon. Multiple fundamental frequency estimation using spectral structure and temporal evolution rules. In *Music Information Retrieval Evaluation eXchange*, Utrecht, Netherlands, August 2010.

[BD11a] E. Benetos and S. Dixon. Joint multi-pitch detection using harmonic envelope estimation for polyphonic music transcription. *IEEE Journal of Selected Topics in Signal Processing*, 5(6):1111–1123, October 2011.

[BD11b] E. Benetos and S. Dixon. Multiple-F0 estimation and note tracking using a convolutive probabilistic model. In *Music Information Retrieval Evaluation eXchange*, Miami, Florida, USA, October 2011.

[BD11c] E. Benetos and S. Dixon. Multiple-instrument polyphonic music transcription using a convolutive probabilistic model. In *8th Sound and Music Computing Conference*, pages 19–24, Padova, Italy, July 2011.

[BD11d] E. Benetos and S. Dixon. Polyphonic music transcription using note onset and offset detection. In *IEEE International Conference on Audio, Speech and Signal Processing*, pages 37–40, Prague, Czech Republic, May 2011.

[BD11e] E. Benetos and S. Dixon. A temporally-constrained convolutive probabilistic model for pitch detection. In *IEEE Workshop on Applications of Signal Processing to Audio and Acoustics*, pages 133–136, New Paltz, USA, October 2011.

[BD12a] E. Benetos and S. Dixon. A shift-invariant latent variable model for automatic music transcription. *Computer Music Journal*, 36(4):81–94, Winter 2012.

[BD12b] E. Benetos and S. Dixon. Temporally-constrained convolutive probabilistic latent component analysis for multi-pitch detection. In *International Conference on Latent Variable Analysis and Signal Separation*, pages 364–371, Tel-Aviv, Israel, March 2012.

[BDA+05] J. P. Bello, L. Daudet, S. Abdallah, C. Duxbury, M. Davies, and M. Sandler. A tutorial on onset detection of music signals. *IEEE Transactions on Audio, Speech, and Language Processing*, 13(5):1035–1047, September 2005.

[BDG+12] E. Benetos, S. Dixon, D. Giannoulis, H. Kirchhoff, and A. Klapuri. Automatic music transcription: breaking the glass ceiling. In *13th International Society for Music Information Retrieval Conference*, pages 379–384, Porto, Portugal, October 2012.

[BDS06] J. P. Bello, L. Daudet, and M. B. Sandler. Automatic piano transcription using frequency and time-domain information. *IEEE Transactions on Audio, Speech, and Language Processing*, 14(6):2242–2251, November 2006.

[BED09a] R. Badeau, V. Emiya, and B. David. Expectation-maximization algorithm for multi-pitch estimation and saparation of overlapping harmonic spectra. In *IEEE International Conference on Acoustics, Speech, and Signal Processing*, pages 3073–3076, Taipei, Taiwan, April 2009.

[BED09b] M. Bay, A. F. Ehmann, and J. S. Downie. Evaluation of multiple-F0 estimation and tracking systems. In *10th International Society for Music Information Retrieval Conference*, pages 315–320, Kobe, Japan, October 2009.

[Bel03] J. P. Bello. *Towards the Automated Analysis of Simple Polyphonic Music: a Knowledge-Based Approach*. PhD thesis, Department of Electronc Engineering, Queen Mary, University of London, 2003.

[BG10] P. Bunch and S. Godsill. Transcription of musical audio using Poisson point process and sequential MCMC. In *7th International Symposium on Computer Music Modeling and Retrieval*, pages 99–105, Malaga, Spain, June 2010.

[BG11] P. Bunch and S. Godsill. Point process MCMC for sequential music transcription. In *IEEE International Conference on Audio, Speech and Signal Processing*, pages 5936–5939, Prague, Czech Republic, May 2011.

[BJ05] F. Bach and M. Jordan. Discriminative training of hidden Markov models for multiple pitch tracking. In *IEEE International Conference on Audio, Speech and Signal Processing*, pages 489–492, Philadelphia, USA, March 2005.

[BKD12] E. Benetos, A. Klapuri, and S. Dixon. Score-informed transcription for automatic piano tutoring. In *European Signal Processing Conference*, pages 2153–2157, Bucharest, Romania, August 2012.

[BKTB12] A.M. Barbancho, A. Klapuri, L.J. Tardon, and I. Barbancho. Automatic transcription of guitar chords and fingering from audio. *IEEE Transactions on Audio, Speech, and Language Processing*, 20(3):915–921, March 2012.

[BLD12] E. Benetos, M. Lagrange, and S. Dixon. Characterisation of acoustic scenes using a temporally-constrained shift-invariant model. In *International Conference on Digital Audio Effects*, pages 317–323, York, UK, September 2012.

[BLW07] J. G. A. Barbedo, A. Lopes, and P. J. Wolfe. High time-resolution estimation of multiple fundamental frequencies. In *8th International Conference on Music Information Retrieval*, pages 399–402, Vienna, Austria, September 2007.

[BMS00] J. P. Bello, G. Monti, and M. Sandler. Techniques for automatic music transcription. In *International Conference on Music Information Retrieval*, Plymouth, Massachusetts, USA, October 2000.

[BP92] J. C. Brown and M. S. Puckette. An efficient algorithm for the calculation of a constant Q transform. *Journal of the Acoustical Society of America*, 92(5):2698–2701, November 1992.

[BQ07] L. I. Ortiz Berenguer and F. J. Casajús Quirós. Approaching polyphonic transcription of piano sounds. In *154th Meeting of the Acoustical Society of America*, volume 2, pages 212–216, November 2007.

[BQGB04] L. I. Ortiz Berenguer, F. J. Casajús Quirós, M. Torres Guijarro, and J. A. Beracoechea. Piano transcription using pattern recognition: aspects on parameter extraction. In *International Conference on Digital Audio Effects*, pages 212–216, Naples, Italy, October 2004.

[Bra99] M. Brand. Pattern discovery via entropy minimization. In *Uncertainty '99: Int. Workshop Artificial Intelligence and Statistics*, Fort Lauderdale, Florida, USA, January 1999.

[Bro91] J. C. Brown. Calculation of a constant Q spectral transform. *Journal of the Acoustical Society of America*, 89(1):425–434, January 1991.

[Bro92] J. C. Brown. Musical fundamental frequency tracking using a pattern recognition method. *Journal of the Acoustical Society of America*, 92(3):1394–1402, September 1992.

[Bro99] J. C. Brown. Computer identification of musical instruments using pattern recognition with cepstral coefficients as features. *Journal of the Acoustical Society of America*, 105(3):1933–1941, March 1999.

[Bro06] P. Brossier. *Automatic Annotation of Musical Audio for Interactive Applications*. PhD thesis, Quen Mary University of London, UK, August 2006.

[BS12] S. Böck and M. Schedl. Polyphonic piano note transcription with recurrent neural networks. In *IEEE International Conference on Audio, Speech and Signal Processing*, pages 121–124, Kyoto, Japan, March 2012.

[Cau99] G. Cauwenberghs. Monaural separation of independent acoustical components. In *IEEE International Symposium on Circuits and Systems*, volume 5, pages 62–65, Orlando, USA, May 1999.

[Cau11] B. Cauchi. Non-negative matrix factorisation applied to auditory scenes classification. Master's thesis, ATIAM (UPMC / IRCAM / TELECOM ParisTech), August 2011.

[CDW07] A. Cont, S. Dubnov, and D. Wessel. Realtime multiple-pitch and multiple-instrument recognition for music signals using sparse non-negative constraints. In *International Conference on Digital Audio Effects*, Bordeaux, France, October 2007.

[CE11] C. Cotton and D. Ellis. Spectral vs. spectro-temporal features for acoustic event detection. In *IEEE Workshop on Applications of Signal Processing to Audio and Acoustics*, pages 69–72, New Paltz, USA, October 2011.

[Cem04] A. T. Cemgil. *Bayesian music transcription*. PhD thesis, Radboud University Nijmegen, Netherlands, September 2004.

[Chu92] C. K. Chui. *An Introduction to Wavelets*. Academic Press, San Diego, USA, 1992.

[CJ02] Y.R. Chien and S.K. Jeng. An automatic transcription system with octave detection. In *IEEE International Conference on Acoustics, Speech, and Signal Processing*, volume 2, pages 1865–1868, Orlando, USA, May 2002.

[CJAJ04] M. G. Christensen, S. H. Jensen, S. V. Andersen, and A. Jakobsson. Subspace-based fundamental frequency estimation. In *European Signal Processing Conference*, pages 637–640, Vienna, Austria, September 2004.

[CJJ06] M. G. Christensen, A. Jakobsson, and S. H. Jensen. Multi-pitch estimation using harmonic MUSIC. In *Asilomar Conference on Signals, Systems, and Computers*, pages 521–525, 2006.

[CJJ07] M. G. Christensen, A. Jakobsson, and S. H. Jensen. Joint high-resolution fundamental frequency and order estimation. *IEEE Transactions on Audio, Speech, and Language Processing*, 15(5):1635–1644, July 2007.

[CK11] N. Cho and C.-C. Jay Kuo. Sparse music representation with source-specific dictionaries and its application to signal separation. *IEEE Transactions on Audio, Speech, and Language Processing*, 19(2):337–348, February 2011.

[CKB03] A. T. Cemgil, B. Kappen, and D. Barber. Generative model based polyphonic music transcription. In *2003 IEEE Workshop Applications of Signal Processing to Audio and Acoustics*, New Paltz, New York, USA, October 2003.

[CKB06] A. T. Cemgil, H. J. Kappen, and D. Barber. A generative model for music transcription. *IEEE Transactions on Audio, Speech, and Language Processing*, 14(2):679–694, March 2006.

[CLLY07] C. Cao, M. Li, J. Liu, and Y. Yan. Multiple F0 estimation in polyphonic music. In *3rd Music Information Retrieval Evaluation eXchange*, volume 5, September 2007.

[CM60] G. Cooper and L.B. Meyer. *The rhythmic structure of music*. University of Chicago Press, 1960.

[Con06] A. Cont. Realtime multiple pitch observation using sparse non-negative constraints. In *7th International Conference on Music Information Retrieval*, Victoria, Canada, October 2006.

[CPT09] G. Costantini, R. Perfetti, and M. Todisco. Event based transcription system for polyphonic piano music. *Signal Processing*, 89(9):1798–1811, September 2009.

[CQ98] P. Fernandez Cid and F.J. Casajus Quirós. Multi-pitch estimation for polyphonic musical signals. In *IEEE International Conference on Acoustics, Speech, and Signal Processing*, pages 3565–3568, Seattle, USA, May 1998.

[CQRSVC+10] F.J. Canadas Quesada, F. Rodriguez Serrano, P. Vera Candeas, N.R. Reyes, and J. Carabias Orti. Improving multiple-F0 estimation by onset detection for polyphonic music transcription. In

IEEE International Workshop on Multimedia Signal Processing (MMSP), pages 7–12, October 2010.

[CRV+10] F. Canadas, F. Rodriguez, P. Vera, N. Ruiz, and J. Carabias. Multiple fundamental frequency estimation & tracking in polyphonic music for MIREX 2010. In *Music Information Retrieval Evaluation eXchange*, Utrecht, Netherlands, August 2010.

[CSJJ07] M. G. Christensen, P. Stoica, A. Jakobsson, and S. H. Jensen. The multi-pitch estimation problem: some new solutions. In *IEEE International Conference on Acoustics, Speech, and Signal Processing*, pages 1221–1224, Honolulu, USA, April 2007.

[CSJJ08] M. G. Christensen, P. Stoica, A. Jakobsson, and S. H. Jensen. Multi-pitch estimation. *Elsevier Signal Processing*, 88(4):972–983, April 2008.

[CŞS11] A. T. Cemgil, U. Şimşekli, and U. C. Sübakan. Probabilistic latent tensor factorization framework for audio modeling. In *IEEE Workshop on Applications of Signal Processing to Audio and Acoustics*, pages 137–140, New Paltz, USA, October 2011.

[CST00] N. Cristianini and J. Shawe-Taylor. *Support Vector Machines and other kernel-based learning methods*. Cambridge University Press, Cambridge, United Kingdom, 2000.

[CSY+08] W.-C. Chang, A. Su, C. Yeh, A. Röbel, and X. Rodet. Multiple-F0 tracking based on a high-order HMM model. In *International Conference on Digital Audio Effects*, Espoo, Finland, September 2008.

[CTS11] G. Costantini, M. Todisco, and G. Saggio. A sensor interface based on sparse NMF for piano musical transcription. In *4th IEEE International Workshop on Advances in Sensors and Interfaces*, pages 157–161, June 2011.

[dC98] A. de Cheveigné. Cancellation model of pitch perception. *Journal of the Acoustical Society of America*, 103(3):1261–1271, March 1998.

[dC06] A. de Cheveigné. Multiple F0 estimation. In D. L. Wang and G. J. Brown, editors, *Computational Auditory Scene Analysis, Algorithms and Applications*, pages 45–79. IEEE Press/Wiley, New York, 2006.

[dCK02] A. de Cheveigné and H. Kawahara. YIN, a fundamental frequency estimator for speech and music. *Journal of the Acoustical Society of America*, 111(4):1917–1930, April 2002.

[DCL10] A. Dessein, A. Cont, and G. Lemaitre. Real-time polyphonic music transcription with non-negative matrix factorization and beta-divergence. In *11th International Society for Music Information Retrieval Conference*, pages 489–494, Utrecht, Netherlands, August 2010.

[DDR11] J. Durrieu, B. David, and G. Richard. A musically motivated mid-level representation for pitch estimation and musical audio source separation. *IEEE Journal of Selected Topics in Signal Processing*, 5(6):1180–1191, October 2011.

[Der06] O. Derrien. Multi-scale frame-based analysis of audio signals for musical transcription using a dictionary of chromatic waveforms. In *IEEE International Conference on Acoustics, Speech, and Signal Processing*, volume 5, pages 57–60, Toulouse, France, May 2006.

[DG03] M. Davy and S. J. Godsill. Bayesian harmonic models for musical signal analysis. In *Bayesian Statistics VII*, pages 305–314. Oxford University Press, 2003.

[DGI06] M. Davy, S. Godsill, and J. Idier. Bayesian analysis of western tonal music. *Journal of the Acoustical Society of America*, 119(4):2498–2517, 2006.

[DHP09] Z. Duan, J. Han, and B. Pardo. Harmonically informed multi-pitch tracking. In *10th International Society for Music Information Retrieval Conference*, pages 333–338, Kobe, Japan, October 2009.

[DHP10] Z. Duan, J. Han, and B. Pardo. Song-level multi-pitch tracking by heavily constrained clustering. In *IEEE International Con-*

ference on Audio, Speech and Signal Processing, pages 57–60, Dallas, USA, March 2010.

[Dix00] S. Dixon. On the computer recognition of solo piano music. In *2000 Australasian Computer Music Conference*, pages 31–37, July 2000.

[dL97] L. de Lathauwer. *Signal processing based on multilinear algebra*. PhD thesis, K. U. Leuven, Belgium, 1997.

[DLR77] A. P. Dempster, N. M. Laird, and D. B. Rubin. Maximum likelihood from incomplete data via the EM algorithm. *Journal of the Royal Statistical Society*, 39(1):1–38, 1977.

[DMT12] S. Dixon, M. Mauch, and D. Tidhar. Estimation of harpsichord inharmonicity and temperament from musical recordings. *Journal of the Acoustical Society of America*, 131(1):878–887, January 2012.

[DPZ10] Z. Duan, B. Pardo, and C. Zhang. Multiple fundamental frequency estimation by modeling spectral peaks and non-peak regions. *IEEE Transactions on Audio, Speech, and Language Processing*, 18(8):2121–2133, November 2010.

[DR93] B. Doval and X. Rodet. Fundamental frequency estimation and tracking using maximum likelihood harmonic matching and HMMs. In *IEEE International Conference on Acoustics, Speech, and Signal Processing*, pages 221–224, Minneapolis, USA, April 1993.

[DR03] W. D'haes and X. Rodet. Discrete cepstrum coefficients as perceptual features. In *International Computer Music Conference*, September 2003.

[Dre11] K. Dressler. Multiple fundamental frequency extraction for MIREX 2011. In *Music Information Retrieval Evaluation eXchange*, Miami, Florida, USA, October 2011.

[DTB11] S. Dixon, D. Tidhar, and E. Benetos. The temperament police: The truth, the ground truth and nothing but the truth. In *12th International Society for Music Information Retrieval Conference*, pages 281–286, Miami, Florida, USA, October 2011.

[DZZS07] Z. Duan, D. Zhang, C. Zhang, and Z. Shi. Multi-pitch estimation based on partial event and support transfer. In *IEEE International Conference on Multimedia and Expo*, pages 216–219, July 2007.

[EBD07] V. Emiya, R. Badeau, and B. David. Multipitch estimation of quasi-harmonic sounds in colored noise. In *International Conference on Digital Audio Effects*, Bordeaux, France, September 2007.

[EBD08] V. Emiya, R. Badeau, and B. David. Automatic transcription of piano music based on HMM tracking of jointly estimated pitches. In *European Signal Processing Conference*, Lausanne, Switzerland, August 2008.

[EBD10] V. Emiya, R. Badeau, and B. David. Multipitch estimation of piano sounds using a new probabilistic spectral smoothness principle. *IEEE Transactions on Audio, Speech, and Language Processing*, 18(6):1643–1654, August 2010.

[EM11] S. Ewert and M. Müller. Estimating note intensities in music recordings. In *IEEE International Conference on Audio, Speech and Signal Processing*, pages 385–388, Prague, Czech Republic, May 2011.

[EP06] D. P. W. Ellis and G. E. Poliner. Classification-based melody transcription. *Machine Learning*, 65:439–456, 2006.

[EPT+06] A.J. Eronen, V.T. Peltonen, J.T. Tuomi, A.P. Klapuri, S. Fagerlund, T. Sorsa, G. Lorho, and J. Huopaniemi. Audio-based context recognition. *IEEE Transactions on Audio, Speech, and Language Processing*, 14(1):321–329, January 2006.

[ES06] M. R. Every and J. E. Szymanski. Separation of synchronous pitched notes by spectral filtering of harmonics. *IEEE Transactions on Audio, Speech, and Language Processing*, 14(5):1845–1856, September 2006.

[FBR11] B. Fuentes, R. Badeau, and G. Richard. Adaptive harmonic time-frequency decomposition of audio using shift-invariant PLCA. In *IEEE International Conference on Audio, Speech*

and Signal Processing, pages 401–404, Prague, Czech Republic, May 2011.

[FCC05] D. FitzGerald, M. Cranitch, and E. Coyle. Generalized prior subspace analysis for polyphonic pitch transcription. In *International Conference on Digital Audio Effects*, pages 39–45, Madrid, Spain, September 2005.

[FF09] N. Fonseca and A. Ferreira. Measuring music transcription results based on a hybrid decay/sustain evaluation. In *7th Triennial Conference of European Society for the Cognitive Sciences of Music*, pages 119–124, Jyväskylä, Finland, August 2009.

[FHAB10] M. O. Faruqe, M. A.-M. Hasan, S. Ahmad, and F. H. Bhuiyan. Template music transcription for different types of musical instruments. In *2nd International Conference on Computer and Automation Engineering*, pages 737–742, Singapore, February 2010.

[FK11] X. Fiss and A. Kwasinski. Automatic real-time electric guitar audio transcription. In *IEEE International Conference on Audio, Speech and Signal Processing*, pages 373–376, Prague, Czech Republic, May 2011.

[Fon08] N. Fonseca. Fragmentation and frontier evolution for genetic algorithms optimization in music transcription. In *Lecture Notes in Computer Science*, volume 5290, pages 305–314. October 2008.

[FR98] N. F. Fletcher and T. D. Rossing. *The Physics of Musical Instruments*. Springer, New York, 2nd edition, 1998.

[GB03] R. Gribonval and E. Bacry. Harmonic decomposition of audio signals with matching pursuit. *IEEE Transactions on Audio, Speech, and Language Processing*, 51(1):101–111, January 2003.

[GBHL09] R. Gang, M. F. Bocko, D. Headlam, and J. Lundberg. Polyphonic music transcription employing max-margin classification of spectrographic features. In *IEEE Workshop on Applications of Signal Processing to Audio and Acoustics*, pages 57–60, New Paltz, USA, October 2009.

[GBL+11] R. Gang, G. Bocko, J. Lundberg, S. Roessner, D. Headlam, and M.F. Bocko. A real-time signal processing framework of musical expressive feature extraction using MATLAB. In *12th International Society for Music Information Retrieval Conference*, pages 115–120, Miami, Florida, USA, October 2011.

[GD02] S. Godsill and M. Davy. Bayesian harmonic models for musical pitch estimation and analysis. In *IEEE International Conference on Acoustics, Speech, and Signal Processing*, pages 1769–1772, Orlando, USA, May 2002.

[GE09] G. Grindlay and D. Ellis. Multi-voice polyphonic music transcription using eigeninstruments. In *IEEE Workshop on Applications of Signal Processing to Audio and Acoustics*, New Paltz, USA, October 2009.

[GE10] G. Grindlay and D. Ellis. A probabilistic subspace model for multi-instrument polyphonic transcription. In *11th International Society for Music Information Retrieval Conference*, pages 21–26, Utrecht, Netherlands, August 2010.

[GE11] G. Grindlay and D. Ellis. Transcribing multi-instrument polyphonic music with hierarchical eigeninstruments. *IEEE Journal of Selected Topics in Signal Processing*, 5(6):1159–1169, October 2011.

[GHNO03] M. Goto, H. Hashiguchi, T. Nishimura, and R. Oka. RWC music database: music genre database and musical instrument sound database. In *International Conference on Music Information Retrieval*, pages 229–230, Baltimore, USA, October 2003.

[GJ97] Z. Ghahramani and M. Jordan. Factorial hidden Markov models. *Machine Learning*, 29:245–273, 1997.

[GMSV98] I. Guyon, J. Makhoul, R. Schwartz, and V. Vapnik. What size test set gives good error estimates? *IEEE Transactions on Pattern Analysis and Machine Intelligence*, 20(1):52–64, January 1998.

[Got00] M. Goto. A robust predominant-F0 estimation method for real-time detection of melody and bass lines in CD recordings. In

IEEE International Conference on Acoustics, Speech, and Signal Processing, volume 2, pages 757–760, Istanbul, Turkey, June 2000.

[Got04] M. Goto. A real-time music-scene-description system: predominant-F0 estimation for detecting melody and bass lines in real-world audio signals. *Speech Communication*, 43:311–329, 2004.

[Gro08] M. Groble. Multiple fundamental frequency estimation. In *2008 Music Information Retrieval Evaluation eXchange*, September 2008.

[GS07a] Z. Guibin and L. Sheng. Automatic transcription method for polyphonic music based on adaptive comb filter and neural network. In *2007 IEEE International Conference on Mechatronics and Automation*, pages 2592–2597, August 2007.

[GS07b] D. Gunawan and D. Sen. Identification of partials in polyphonic mixtures based on temporal envelope similarity. In *AES 123rd Convention*, October 2007.

[Hai03] S. W. Hainsworth. *Techniques for the automated analysis of musical audio*. PhD thesis, University of Cambridge, UK, December 2003.

[HBD10] R. Hennequin, R. Badeau, and B. David. NMF with time-frequency activations to model non stationary audio events. In *IEEE International Conference on Audio, Speech and Signal Processing*, pages 445–448, Dallas, USA, March 2010.

[HBD11a] R. Hennequin, R. Badeau, and B. David. NMF with time-frequency activations to model non stationary audio events. *IEEE Transactions on Audio, Speech, and Language Processing*, 19(4):744–753, May 2011.

[HBD11b] R. Hennequin, R. Badeau, and B. David. Scale-invariant probabilistic latent component analysis. In *IEEE Workshop on Applications of Signal Processing to Audio and Acoustics*, pages 129–132, New Paltz, USA, October 2011.

[HDB11] R. Hennequin, B. David, and R. Badeau. Score informed audio source separation using a parametric model of non-negative spectrogram. In *IEEE International Conference on Audio, Speech and Signal Processing*, pages 45–48, Prague, Czech Republic, May 2011.

[HM03] S. W. Hainsworth and M. D. Macleod. The automated music transcription problem. Technical report, Engineering Department, Cambridge University, UK, 2003.

[Hof99] T. Hofmann. Probabilistic latent semantic analysis. In *Uncertainty in AI*, pages 289–296, Stockholm, Sweden, July 1999.

[HS10] A. Holzapfel and Y. Stylianou. Three dimensions of pitched instrument onset detection. *IEEE Transactions on Audio, Speech, and Language Processing*, 18(6):1517–1527, August 2010.

[Joh03] M. Johansson. Automatic transcription of polyphonic music using harmonic relations. Master's thesis, Royal Institute of Technology, Sweden, April 2003.

[JVV08] H. Järveläinen, T. Verma, and V. Välimäki. The effect of inharmonicity on pitch in string instrument sounds. In *International Computer Music Conference*, pages 237–240, Berlin, Germany, August 2008.

[KCZ09] A. Kobzantsev, D. Chazan, and Y. Zeevi. Automatic transcription of piano polyphonic music. In *4th International Symposium on Image and Signal Processing and Analysis*, pages 414–418, Zagreb, Croatia, September 2009.

[KD06] A. Klapuri and M. Davy, editors. *Signal Processing Methods for Music Transcription*. Springer-Verlag, New York, 2006.

[KdCP98] H. Kawahara, A. de Cheveigné, and R.D. Patterson. An instantaneous-frequency-based pitch extraction method for high quality speech transformation: revised TEMPO in the STRAIGHT-suite. In *5th International Conference on Spoken Language Processing*, Sydney, Australia, December 1998.

[KDK12] H. Kirchhoff, S. Dixon, and A. Klapuri. Shift-invariant non-negative matrix deconvolution for music transcription. In *IEEE International Conference on Audio, Speech and Signal Processing*, pages 125–128, Kyoto, Japan, March 2012.

[KEA06] A.P. Klapuri, A.J. Eronen, and J.T. Astola. Analysis of the meter of acoustic musical signals. *IEEE Transactions on Audio, Speech, and Language Processing*, 14(1):342–355, January 2006.

[Keo02] E. Keogh. Exact indexing of dynamic time warping. In *28th Int. Conf. Very Large Data Bases*, pages 406–417, Hong Kong, China, August 2002.

[Kla01] A. Klapuri. Multipitch estimation and sound separation by the spectral smoothness principle. In *IEEE International Conference on Acoustics, Speech, and Signal Processing*, Salt Lake City, USA, May 2001.

[Kla03] A. Klapuri. Multiple fundamental frequency estimation based on harmonicity and spectral smoothness. *IEEE Transactions on Speech and Audio Processing*, 11(6):804–816, November 2003.

[Kla04a] A. Klapuri. Automatic music transcription as we know it today. *Journal of New Music Research*, 33(3):269–282, 2004.

[Kla04b] A. Klapuri. *Signal processing methods for the automatic transcription of music*. PhD thesis, Tampere University of Technology, Finland, 2004.

[Kla05] A. Klapuri. A perceptually motivated multiple-F0 estimation method. In *2005 IEEE Workshop on Applications of Signal Processing to Audio and Acoustics*, New Paltz, USA, October 2005.

[Kla06] A. Klapuri. Multiple fundamental frequency estimation by summing harmonic amplitudes. In *7th International Conference on Music Information Retrieval*, Victoria, Canada, October 2006.

[Kla08] A. Klapuri. Multipitch analysis of polyphonic music and speech signals using an auditory model. *IEEE Transactions on Audio, Speech, and Language Processing*, 16(28):255–266, February 2008.

[Kla09a] A. Klapuri. A classification approach to multipitch analysis. In *6th Sound and Music Computing Conference*, Porto, Portugal, July 2009.

[Kla09b] A. Klapuri. A method for visualizing the pitch content of polyphonic music signals. In *10th International Society for Music Information Retrieval Conference*, pages 615–620, Kobe, Japan, October 2009.

[KNKT98] K. Kashino, K. Nakadai, T. Kinoshita, and H. Tanaka. Application of Bayesian probability network to music scene analysis. In D. F. Rosenthal and H. G. Okuno, editors, *Computational Auditory Scene Analysis*, pages 115–137. Lawrence Erlbaum Associates, Publishers, Hillsdale, USA, 1998.

[KNS04] H. Kameoka, T. Nishimoto, and S. Sagayama. Extraction of multiple fundamental frequencies from polyphonic music using harmonic clustering. In *the 5th International Symposium on Independent Component Analysis and Blind Signal Separation*, pages 59–62, Granada, Spain, April 2004.

[KNS07] H. Kameoka, T. Nishimoto, and S. Sagayama. A multipitch analyzer based on harmonic temporal structured clustering. *IEEE Transactions on Audio, Speech, and Language Processing*, 15(3):982–994, March 2007.

[Kom07] R. Kompass. A generalized divergence measure for nonnegative matrix factorization. *Neural Computation*, 19(3):780–791, 2007.

[Kru90] C. L. Krumhansl, editor. *Cognitive Foundations of Musical Pitch*. Oxford University Press, 1st edition, 1990.

[KT99] M. Karjalainen and T. Tolonen. Multi-pitch and periodicity analysis model for sound separation and auditory scene analysis. In *IEEE International Conference on Acoustics, Speech, and Signal Processing*, Phoenix, USA, March 1999.

[KT11] A. Koretz and J. Tabrikian. Maximum a posteriori probability multiple pitch tracking using the harmonic model. *IEEE Transactions on Audio, Speech, and Language Processing*, 19(7):2210–2221, September 2011.

[LMP01] J. Lafferty, A. McCallum, and F. Pereira. Conditional random fields: Probabilistic models for segmenting and labeling sequence data. In *18th International Conference on Machine Learning*, pages 282–289, San Francisco, USA, June 2001.

[LNK87] M. Lahat, R. Niederjohn, and D. Krubsack. A spectral autocorrelation method for measurement of the fundamental frequency of noise-corrupted speech. *Acoustics, Speech and Signal Processing, IEEE Transactions on*, 35(6):741–750, June 1987.

[LRPI07] T. Lidy, A. Rauber, A. Pertusa, and J. M. Iñesta. Improving genre classification by combination of audio and symbolic descriptors using a transcription system. In *8th International Conference on Music Information Retrieval*, Vienna, Austria, September 2007.

[LS99] D. D. Li and H. S. Seung. Learning the parts of objects by non-negative matrix factorization. *Nature*, 401:788–791, October 1999.

[Lu06] D. Lu. Automatic music transcription using genetic algorithms and electronic synthesis. Technical report, University of Rochester, USA, 2006.

[LW07] Y. Li and D. L. Wang. Pitch detection in polyphonic music using instrument tone models. In *IEEE International Conference on Acoustics, Speech, and Signal Processing*, volume 2, pages 481–484, Honolulu, USA, April 2007.

[LWB06] A. Loscos, Y. Wang, and W. J. J. Boo. Low level descriptors for automatic violin transcription. In *7th International Conference on Music Information Retrieval*, Victoria, Canada, October 2006.

[LWW09] Y. Li, J. Woodruff, and D. L. Wang. Monaural musical sound separation based on pitch and common amplitude modulation. *IEEE Transactions on Audio, Speech, and Language Processing*, 17(7):1361–1371, September 2009.

[LYC11] C.-T. Lee, Y.-H. Yang, and H. Chen. Automatic transcription of piano music by sparse representation of magnitude spec-

tra. In *IEEE International Conference on Multimedia and Expo (ICME)*, July 2011.

[LYC12] C.-T. Lee, Y.-H. Yang, and H. Chen. Multipitch estimation of piano music by exemplar-based sparse representation. *IEEE Transactions on Multimedia*, 14(3):608–618, June 2012.

[LYLC10] C.-T. Lee, Y.-H. Yang, K.-S. Lin, and H. Chen. Multiple fundamental frequency estimation of piano signals via sparse representation of Fourier coefficients. In *Music Information Retrieval Evaluation eXchange*, Utrecht, Netherlands, August 2010.

[Mar04] M. Marolt. A connectionist approach to automatic transcription of polyphonic piano music. *IEEE Transactions on Multimedia*, 6(3):439–449, June 2004.

[Mar07] M. Marolt. Gaussian mixture models for extraction of melodic lines from audio recording. In *International Conference on Music Information Retrieval*, pages 80–83, Barcelona, Spain, October 2007.

[Mar12] M. Marolt. Automatic transcription of bell chiming recordings. *IEEE Transactions on Audio, Speech, and Language Processing*, 20(3):844–853, March 2012.

[MBD11] L. Mearns, E. Benetos, and S. Dixon. Automatically detecting key modulations in J.S. Bach chorale recordings. In *8th Sound and Music Computing Conference*, pages 25–32, Padova, Italy, July 2011.

[McK03] C. McKay. Using blackboard systems for polyphonic transcription: a literature review. Technical report, Faculty of Music, McGill University, Canada, 2003.

[MD10] R. Macrae and S. Dixon. Accurate real-time windowed time warping. In *11th International Society for Music Information Retrieval Conference*, pages 423–428, Utrecht, Netherlands, August 2010.

[MEKR11] M. Müller, D.P.W. Ellis, A. Klapuri, and G. Richard. Signal processing for music analysis. *IEEE Journal of Selected Topics in Signal Processing*, 5(6):1088–1110, October 2011.

[MH92] R. Meddis and M. J. Hewitt. Modeling the identification of concurrent vowels with different fundamental frequencies. *Journal of the Acoustical Society of America*, 91(1):233–245, 1992.

[MHK11] A. Mesaros, T. Heittola, and A. Klapuri. Latent semantic analysis in sound event detection. In *European Signal Processing Conference*, Barcelona, Spain, August 2011.

[MID] Musical Instrument Digital Interface. `http://www.midi.org/`.

[MIR] Music Information Retrieval Evaluation eXchange (MIREX). `http://music-ir.org/mirexwiki/`.

[MKT+07] K. Miyamoto, H. Kameoka, H. Takeda, T. Nishimoto, and S. Sagayama. Probabilistic approach to automatic music transcription from audio signals. In *IEEE International Conference on Acoustics, Speech, and Signal Processing*, pages 697–700, Honolulu, USA, May 2007.

[MO97] Ray Meddis and Lowel O'Mard. A unitary model of pitch perception. *Journal of the Acoustical Society of America*, 102(3):1811–1820, 1997.

[MS06] M. Mørup and M. N. Schmidt. Sparse non-negative matrix factor 2D deconvolution. Technical report, Technical University of Denmark, 2006.

[MS09] G. Mysore and P. Smaragdis. Relative pitch estimation of multiple instruments. In *IEEE International Conference on Acoustics, Speech, and Signal Processing*, pages 313–316, Taipei, Taiwan, April 2009.

[MSH08] M. Mørup, M. N. Schmidt, and L. K. Hansen. Shift invariant sparse coding of image and music data. Technical report, Technical University of Denmark, 2008.

[MSR10] G. Mysore, P. Smaragdis, and B. Raj. Non-negative hidden Markov modeling of audio with application to source separation. In *9th International Conference on Latent Variable Analysis and Signal Separation*, pages 140–148, St. Malo, France, September 2010.

[Mys10] G. Mysore. *A non-negative framework for joint modeling of spectral structure and temporal dynamics in sound mixtures*. PhD thesis, Stanford University, USA, June 2010.

[NEOS09] M. Nakano, K. Egashira, N. Ono, and S. Sagayama. Sequential estimation of multiple fundamental frequency through harmonic-temporal clustering. In *Music Information Retrieval Evaluation eXchange (MIREX)*, October 2009.

[Nie08] B. Niedermayer. Non-negative matrix division for the automatic transcription of polyphonic audio. In *9th International Conference on Music Information Retrieval*, pages 544–549, Philadelphia, USA, September 2008.

[NLRK+11] M. Nakano, J. Le Roux, H. Kameoka, T. Nakamura, N. Ono, and S. Sagayama. Bayesian nonparametric spectrogram modeling based on infinite factorial infinite hidden Markov model. In *IEEE Workshop on Applications of Signal Processing to Audio and Acoustics*, pages 325–328, New Paltz, USA, October 2011.

[NM65] J. A. Nelder and R. Mead. A simplex method for function minimization. *Computer Journal*, 7:308–313, 1965.

[NNLS11] J. Nam, J. Ngiam, H. Lee, and M. Slaney. A classification-based polyphonic piano transcription approach using learned feature representations. In *12th International Society for Music Information Retrieval Conference*, pages 175–180, Miami, Florida, USA, October 2011.

[Nol67] M. Noll. Cepstrum pitch determination. *Journal of the Acoustical Society of America*, 41(2):293–309, 1967.

[NPA09] P. Nesi, G. Pantaleo, and F. Argenti. Automatic transcription of polyphonic music based on constant-Q bispectral analysis for MIREX 2009. In *Music Information Retrieval Evaluation eXchange*, Kobe, Japan, October 2009.

[NR07] E. Nichols and C. Raphael. Automatic transcription of music audio through continuous parameter tracking. In *8th International Conference on Music Information Retrieval*, Vienna, Austria, September 2007.

[NRK+10] M. Nakano, J. Le Roux, H. Kameoka, Y. Kitano, N. Ono, and S. Sagayama. Nonnegative matrix factorization with Markov-chained bases for modeling time-varying patterns in music spectrograms. In *9th International Conference on Latent Variable Analysis and Signal Separation*, pages 149–156, St. Malo, France, September 2010.

[NRK+11] M. Nakano, J. Le Roux, H. Kameoka, N. Ono, and S. Sagayama. Infinite-state spectrum model for music signal analysis. In *IEEE International Conference on Audio, Speech and Signal Processing*, pages 1972–1975, Prague, Czech Republic, May 2011.

[OBBC10] A. Ortiz, A. M. Barbancho, I. Barbancho, and R. Cruz. Lightweight pitch detector for embedded systems using neural networks. In *7th International Symposium on Computer Music Modeling and Retrieval*, pages 195–203, Malaga, Spain, June 2010.

[OCQR10] J. J. Carabias Orti, P. Vera Candeas, F. J. Cañadas Quesada, and N. Ruiz Reyes. Music scene-adaptive harmonic dictionary for unsupervised note-event detection. *IEEE Transactions on Audio, Speech, and Language Processing*, 18(3):473–486, March 2010.

[OCR+08] J. J. Carabias Orti, P. Vera Candeas, N. Ruiz Reyes, R. Mata Campos, and F. J. Cañadas Quesada. Polyphonic piano transcription based on spectral separation. In *Audio Engineering Society 124th Convention*, Amsterdam, Netherlands, May 2008.

[OCR+09a] J. J. Carabias Orti, P. Vera Candeas, N. Ruiz Reyes, F. J. Cañadas Quesada, and R. Mata Campos. Overlapped event-note separation based on partials amplitude and phase estimation for polyphonic music transcription. In *European Signal Processing Conference*, pages 943–947, Glasgow, Scotland, August 2009.

[OCR+09b] J. J. Carabias Orti, P. Vera Candeas, N. Ruiz Reyes, F. J. Cañadas Quesada, and P. Cabañas Molero. Estimating instrument spectral envelopes for polyphonic music transcrip-

tion in a music scene-adaptive approach. In *Audio Engineering Society 126th Convention*, Munich, Germany, May 2009.

[OF97] Bruno A. Olshausen and David J. Field. Sparse coding with an overcomplete basis set: A strategy employed by V1? *Vision Research*, 37(23):3311 – 3325, 1997.

[OKS12] K. Ochiai, H. Kameoka, and Shigeki Sagayama. Explicit beat structure modeling for non-negative matrix factorization-based multipitch analysis. In *IEEE International Conference on Audio, Speech and Signal Processing*, pages 133–136, Kyoto, Japan, March 2012.

[ONP12] K. O'Hanlon, H. Nagano, and Mark Plumbley. Structured sparsity for automatic music transcription. In *IEEE International Conference on Audio, Speech and Signal Processing*, pages 441–444, Kyoto, Japan, March 2012.

[OP11] K. O'Hanlon and M. Plumbley. Structure-aware dictionary learning with harmonic atoms. In *European Signal Processing Conference*, Barcelona, Spain, September 2011.

[OS03] N. Orio and M. S. Sette. An HMM-based pitch tracker for audio queries. In *International Conference on Music Information Retrieval*, pages 249–250, Baltimore, USA, October 2003.

[OVC+11] J. J. Carabias Orti, T. Virtanen, P. Vera Candeas, N. Ruiz Reyes, and F. J. Cañadas Quesada. Musical instrument sound multi-excitation model for non-negative spectrogram factorization. *IEEE Journal of Selected Topics in Signal Processing*, 5(6):1144–1158, October 2011.

[PAB+02] M. Plumbley, S. Abdallah, J. P. Bello, M. Davies, G. Monti, and M. Sandler. Automatic music transcription and audio source separation. *Cybernetics and Systems*, 33(6):603–627, 2002.

[PB02] B. Pardo and W.P. Birmingham. Algorithms for chordal analysis. *Computer Music Journal*, 26(2):22–49, 2002.

[PCG10] P. H. Peeling, A. T. Cemgil, and S. J. Godsill. Generative spectrogram factorization models for polyphonic piano transcrip-

tion. *IEEE Transactions on Audio, Speech, and Language Processing*, 18(3):519–527, March 2010.

[PE07a] G. Poliner and D. Ellis. A discriminative model for polyphonic piano transcription. *EURASIP Journal on Advances in Signal Processing*, (8):154–162, January 2007.

[PE07b] G. Poliner and D. Ellis. Improving generalization for polyphonic piano transcription. In *2007 IEEE Workshop on Applications of Signal Processing to Audio and Acoustics*, New Paltz, USA, October 2007.

[Pee04] G. Peeters. A large set of audio features for sound description (similarity and classification) in the CUIDADO project. Technical report, CUIDADO I.S.T. Project, 2004.

[Pee06] G. Peeters. Music pitch representation by periodicity measures based on combined temporal and spectral representations. In *IEEE International Conference on Acoustics, Speech, and Signal Processing*, volume 5, pages 53–56, Toulouse, France, May 2006.

[PEE+07] G. Poliner, D. Ellis, A. F. Ehmann, E. Gómez, S. Streich, and B. Ong. Melody transcription from music audio: approaches and evaluation. *IEEE Transactions on Audio, Speech, and Language Processing*, 15(4):1247–1256, May 2007.

[Per10] A. Pertusa. *Computationally efficient methods for polyphonic music transcription.* PhD thesis, Universidad de Alicante, Spain, 2010.

[PG11] P.H. Peeling and S.J. Godsill. Multiple pitch estimation using non-homogeneous Poisson processes. *IEEE Journal of Selected Topics in Signal Processing*, 5(6):1133–1143, October 2011.

[PGSMR12] Peter P. Grosche, B. Schuller, M. Müller, and G. Rigoll. Automatic transcription of recorded music. *Acta Acustica united with Acustica*, 98(2):199–215, March 2012.

[PHC06] A. Paradzinets, H. Harb, and L. Chen. Use of continuous wavelet-like transform in automated music transcription. In *Eu-*

ropean Signal Processing Conference, Florence, Italy, September 2006.

[PI04] A. Pertusa and J. M. Iñesta. Pattern recognition algorithms for polyphonic music transcription. In *Pattern Recognition in Information Systems*, pages 80–89, Porto, Portugal, 2004.

[PI05] A. Pertusa and J. M. Iñesta. Polyphonic monotimbral music transcription using dynamic networks. *Pattern Recognition Letters*, 26(12):1809–1818, September 2005.

[PI07] A. Pertusa and J. M. Iñesta. Multiple fundamental frequency estimation based on spectral pattern loudness and smoothness. In *Music Information Retrieval Evaluation eXchange*, Vienna, Austria, 2007.

[PI08] A. Pertusa and J. M. Iñesta. Multiple fundamental frequency estimation using Gaussian smoothness. In *IEEE International Conference on Acoustics, Speech, and Signal Processing*, pages 105–108, Las Vegas, USA, April 2008.

[PI12] A. Pertusa and J. M. Iñesta. Efficient methods for joint estimation of multiple fundamental frequencies in music signals. *EURASIP Journal on Advances in Signal Processing*, 2012.

[PLG07] P. Peeling, C. Li, and S. Godsill. Poisson point process modeling for polyphonic music transcription. *Journal of the Acoustical Society of America*, 121(4):168–175, March 2007.

[QCR+08] F.J. Cañadas Quesada, P. Vera Candeas, N. Ruiz Reyes, R. Mata Campos, and J. J. Carabias Orti. Multipitch estimation of harmonically-related note-events by improving harmonic matching pursuit decomposition. In *Audio Engineering Society 124th Convention*, Amsterdam, Netherlands, May 2008.

[QCR+09] F.J. Cañadas Quesada, P. Vera Candeas, N. Ruiz Reyes, J. J. Carabias Orti, and D. Martínez Muñoz. A joint approach to extract multiple fundamental frequency in polyphonic signals minimizing Gaussian spectral distance. In *Audio Engineering Society 126th Convention*, Munich, Germany, May 2009.

[QCRO09] F.J. Cañadas Quesada, P. Vera Candeas, N. Ruiz Reyes, and J. J. Carabias Orti. Polyphonic transcription based on temporal evolution of spectral similarity of Gaussian mixture models. In *European Signal Processing Conference*, pages 10–14, Glasgow, Scotland, August 2009.

[QRC+10] F.J. Cañadas Quesada, N. Ruiz Reyes, P. Vera Candeas, J. J. Carabias Orti, and S. Maldonado. A multiple-F0 estimation approach based on Gaussian spectral modelling for polyphonic music transcription. *Journal of New Music Research*, 39(1):93–107, April 2010.

[Rab77] L. Rabiner. On the use of autocorrelation analysis for pitch detection. *IEEE Transactions on Acoustics, Speech, and Signal Processing*, 25(1):24–33, February 1977.

[Rab89] L. R. Rabiner. A tutorial on hidden Markov models and selected applications in speech recognition. *Proceedings of the IEEE*, 77(2):257–286, February 1989.

[Rap02] C. Raphael. Automatic transcription of piano music. In *International Conference on Music Information Retrieval*, pages 15–19, Paris, France, October 2002.

[RCM+12] T. Rakthanmanon, B. Campana, A. Mueen, G. Batista, B. Westover, Q. Zhu, J. Zakaria, and E. Keogh. Searching and mining trillions of time series subsequences under dynamic time warping. In *18th ACM SIGKDD Int. Conf. Knowledge Discovery and Data Mining*, pages 262–270, Beijing, China, August 2012. ACM.

[RFdVF08] G. Reis, N. Fonseca, F. F. de Vega, and A. Ferreira. Hybrid genetic algorithm based on gene fragment competition for polyphonic music transcription. In *EvoWorkshops*, volume 4974 of *Lecture Notes in Computer Science*, pages 305–314. Springer, 2008.

[RFF11] G. Reis, F. Fernandéz, and A. Ferreira. A genetic algorithm for polyphonic transcription of piano music. In *Music Information Retrieval Evaluation eXchange*, Miami, Florida, USA, October 2011.

[RK05] M. Ryynänen and A. Klapuri. Polyphonic music transcription using note event modeling. In *2005 IEEE Workshop on Applications of Signal Processing to Audio and Acoustics*, pages 319–322, New Paltz, USA, October 2005.

[RK08] M. Ryynänen and A. Klapuri. Automatic transcription of melody, bass line, and chords in polyphonic music. *Computer Music Journal*, 32(3):72–86, Fall 2008.

[ROS07] S. A. Raczyński, N. Ono, and S. Sagayama. Multipitch analysis with harmonic nonnegative matrix approximation. In *8th International Conference on Music Information Retrieval*, pages 381–386, Vienna, Austria, September 2007.

[ROS09a] S. A. Raczyński, N. Ono, and S. Sagayama. Extending nonnegative matrix factorization - a discussion in the context of multiple frequency estimation of music signals. In *European Signal Processing Conference*, pages 934–938, Glasgow, Scotland, August 2009.

[ROS09b] S. A. Raczyński, N. Ono, and S. Sagayama. Note detection with dynamic Bayesian networks as a postanalysis step for NMF-based multiple pitch estimation techniques. In *IEEE Workshop on Applications of Signal Processing to Audio and Acoustics*, pages 49–52, New Paltz, USA, October 2009.

[RSC+74] M. Ross, H. Shaffer, A. Cohen, R. Freudberg, and H. Manley. Average magnitude difference function pitch extractor. *IEEE Transactions on Acoustics, Speech, and Signal Processing*, 22(5):353–362, October 1974.

[RVBS10] S. A. Raczyński, E. Vincent, F. Bimbot, and S. Sagayama. Multiple pitch transcription using DBN-based musicological models. In *11th International Society for Music Information Retrieval Conference*, pages 363–368, Utrecht, Netherlands, August 2010.

[RVPK08] M. Ryynänen, T. Virtanen, J. Paulus, and A. Klapuri. Accompaniment separation and karaoke application based on automatic melody transcription. In *IEEE International Conference on Multimedia and Expo*, pages 1417–1420, Hannover, Germany, June 2008.

[Ryy08] M. Ryynänen. *Automatic transcription of pitch content in music and selected applications*. PhD thesis, Tampere University of Technology, Finland, 2008.

[SB03] P. Smaragdis and J. C. Brown. Non-negative matrix factorization for polyphonic music transcription. In *2003 IEEE Workshop on Applications of Signal Processing to Audio and Acoustics*, pages 177–180, New Paltz, USA, August 2003.

[SC09] C. Santoro and C. Cheng. Multiple F0 estimation in the transform domain. In *10th International Society for Music Information Retrieval Conference*, pages 165–170, Kobe, Japan, October 2009.

[ŞC10] U. Şimşekli and A. T. Cemgil. A comparison of probabilistic models for online pitch tracking. In *7th Sound and Music Computing Conference*, Barcelona, Spain, July 2010.

[ŞC11] U. Şimşekli and A. T. Cemgil. Probabilistic models for real-time acoustic event detection with application to pitch tracking. *Journal of New Music Research*, 40(2):175–185, 2011.

[Sch11] A. Schönberg. *Theory of Harmony*. University of California Press, 1911.

[Sch86] R. O. Schmidt. Multiple emitter location and signal parameter estimation. *IEEE Transactions on Antennas and Propagation*, 34(3):276–280, March 1986.

[Sha07] M. Shashanka. *Latent variable framework for modeling and separating single-channel acoustic sources*. PhD thesis, Department of Cognitive and Neural Systems, Boston University, USA, August 2007.

[SIOO12] D. Sakaue, K. Itoyama, T. Ogata, and H. G. Okuno. Initialization-robust multipitch estimation based on latent harmonic allocation using overtone corpus. In *IEEE International Conference on Audio, Speech and Signal Processing*, pages 425–428, Kyoto, Japan, March 2012.

[SK10] C. Schörkhuber and A. Klapuri. Constant-Q transform toolbox for music processing. In *7th Sound and Music Computing Conf.*, pages 322–329, Barcelona, Spain, July 2010.

[SKT+08] S. Saito, H. Kameoka, K. Takahashi, T. Nishimoto, and S. Sagayama. Specmurt analysis of polyphonic music signals. *IEEE Transactions on Audio, Speech, and Language Processing*, 16(3):639–650, March 2008.

[SL90] M. Slaney and R.F. Lyon. A perceptual pitch detector. In *IEEE International Conference on Acoustics, Speech, and Signal Processing*, pages 357–360, Albuquerque, New Mexico, April 1990.

[SM06] M. Schmidt and M. Mørup. Sparse non-negative matrix factor 2-D deconvolution for automatic transcription of polyphonic music. In *6th International Symposium on Independent Component Analysis and Blind Signal Separation*, Paris, France, May 2006.

[Sma04a] P. Smaragdis. Discovering auditory objects through non-negativity constraints. In *ISCA Tutorial and Research Workshop on Statistical and Perceptual Audio Processing*, Jeju, Korea, October 2004.

[Sma04b] P. Smaragdis. Non-negative matrix factor deconvolution; extraction of multiple sound sources from monophonic inputs. In *5th International Conference on Independent Component Analysis*, pages 494–499, Granada, Spain, September 2004.

[Sma09] P. Smaragdis. Relative-pitch tracking of multiple arbitary sounds. *Journal of the Acoustical Society of America*, 125(5):3406–3413, May 2009.

[Sma11] P. Smaragdis. Polyphonic pitch tracking by example. In *IEEE Workshop on Applications of Signal Processing to Audio and Acoustics*, pages 125–128, New Paltz, USA, October 2011.

[Son] Sonic Visualiser 1.7.1. `http://www.sonicvisualiser.org/`.

[SP07] D. Stowell and M. Plumbley. Adaptive whitening for improved real-time audio onset detection. In *International Computer Mu-*

sic Conference, pages 312–319, Copenhagen, Denmark, August 2007.

[SR99] D. Schwarz and X. Rodet. Spectral envelope estimation and representation for sound analysis-synthesis. In *International Computer Music Conference*, Beijing, China, October 1999.

[SR07] P. Smaragdis and B. Raj. Shift-invariant probabilistic latent component analysis. Technical report, Mitsubishi Electric Research Laboratories, December 2007. TR2007-009.

[SRS06] P. Smaragdis, B. Raj, and Ma. Shashanka. A probabilistic latent variable model for acoustic modeling. In *Neural Information Processing Systems Workshop*, Whistler, Canada, December 2006.

[SRS08a] M. Shashanka, B. Raj, and P. Smaragdis. Probabilistic latent variable models as nonnegative factorizations. *Computational Intelligence and Neuroscience*, 2008. Article ID 947438.

[SRS08b] P. Smaragdis, B. Raj, and M. Shashanka. Sparse and shift-invariant feature extraction from non-negative data. In *IEEE International Conference on Acoustics, Speech, and Signal Processing*, pages 2069–2072, Las Vegas, USA, April 2008.

[SS04] P. Stoica and Y. Selén. Cyclic minimizers, majorization techniques, and the expectation maximization algorithm: a refresher. *IEEE Signal Processing Magazine*, 21(1):112–114, January 2004.

[Sun00] X. Sun. A pitch determination algorithm based on subharmonic-to-harmonic ratio. In *6th International Conference on Spoken Language Processing*, Beijing, China, October 2000.

[Ter77] E. Terhardt. The two-component theory of musical consonance. In E. Evans and J. Wilson, editors, *Psychophysics and Physiology of Hearing*, pages 381–390. Academic, 1977.

[TK00] T. Tolonen and M. Karjalainen. A computationally efficient multipitch analysis model. *IEEE Transactions on Speech and Audio Processing*, 8(6):708–716, November 2000.

[TL05] H. D. Thornburg and R. J. Leistikow. A new probabilistic spectral pitch estimator: exact and MCMC-approximate strategies. In *Lecture Notes in Computer Science*, volume 3310, pages 41–60. Springer, 2005.

[TMD10] D. Tidhar, M. Mauch, and S. Dixon. High precision frequency estimation for harpsichord tuning classification. In *IEEE International Conference on Audio, Speech and Signal Processing*, pages 61–64, Dallas, USA, March 2010.

[TS09] M. Triki and D.T.M. Slock. Perceptually motivated quasi-periodic signal selection for polyphonic music transcription. In *IEEE International Conference on Acoustics, Speech, and Signal Processing*, pages 305–308, Taipei, Taiwan, March 2009.

[TSP+08] J. Tardieu, P. Susini, F. Poisson, P. Lazareff, and S. McAdams. Perceptual study of soundscapes in train stations. *Applied Acoustics*, 69(12):1224–1239, 2008.

[UDMS12] J. Urbano, J. S. Downie, B. McFee, and M. Schedl. How significant is statistically significant? the case of audio music similarity and retrieval. In *13th International Society for Music Information Retrieval Conference*, pages 181–186, Porto, Portugal, October 2012.

[Uhl10] C. Uhle. An investigation of low-level signal descriptors characterizing the noiselike nature of an audio signal. In *Audio Engineering Society 128th Convention*, London, UK, May 2010.

[VBB07] E. Vincent, N. Bertin, and R. Badeau. Two nonnegative matrix factorization methods for polyphonic pitch transcription. In *Music Information Retrieval Evaluation eXchange*, September 2007.

[VBB08] E. Vincent, N. Bertin, and R. Badeau. Harmonic and inharmonic nonnegative matrix factorization for polyphonic pitch transcription. In *IEEE International Conference on Acoustics, Speech, and Signal Processing*, pages 109–112, Las Vegas, USA, April 2008.

[VBB10] E. Vincent, N. Bertin, and R. Badeau. Adaptive harmonic spectral decomposition for multiple pitch estimation. *IEEE Transactions on Audio, Speech, and Language Processing*, 18(3):528–537, March 2010.

[Ver09] C. Di Veroli. *Unequal Temperaments: Theory, History, and Practice*. Bray Baroque, Bray, Ireland, 2009.

[Vir04] T. Virtanen. Separation sound sources by convolutive sparse coding. In *ISCA Tutorial and Research Workshop on Statistical and Perceptual Audio Processing*, Jeju, Korea, October 2004.

[VK02] T. Virtanen and A. Klapuri. Separation of harmonic sounds using linear models for the overtone series. In *IEEE International Conference on Acoustics, Speech, and Signal Processing*, volume 2, pages 1757–1760, Orlando, USA, May 2002.

[VM07] M. Varewyck and J.-P. Martens. Assessment of state-of-the-art meter analysis systems with an extended meter description model. In *8th International Conference on Music Information Retrieval*, Vienna, Austria, September 2007.

[VMR08] T. Virtanen, A. Mesaros, and M. Ryynänen. Combining pitch-based inference and non-negative spectrogram factorization in separating vocals from polyphonic music. In *ISCA Tutorial and Research Workshop on Statistical And Perceptual Audition*, Brisbane, Australia, September 2008.

[VR04] E. Vincent and X. Rodet. Music transcription with ISA and HMM. In *5th International Symposium on Independent Component Analysis*, pages 1197–1204, Granada, Spain, September 2004.

[Wag03] A. Wagstaff. Automatic music transcription. Master's thesis, Cranfield University, UK, June 2003.

[WE06] D. L. Wang and G. J. Brown (Eds.). *Computational auditory scene analysis: Principles, algorithms and applications*. IEEE Press/Wiley-Interscience, 2006.

[Wel04] J. Wellhausen. Towards automatic music transcription: extraction of MIDI-data out of polyphonic piano music. In *8th World Multi-Conference on Systemics, Cybernetics and Informatics*, pages 39–45, Orlando, USA, July 2004.

[WL06] C. Weihs and U. Ligges. Parameter optimization in automatic transcription of music. In M. Spiliopoulou, R. Kruse, C. Borgelt, A. Nürnberger, and W. Gaul, editors, *Studies in Classification, Data Analysis, and Knowledge Organization*, pages 740–747. Springer, Berlin, 2006.

[WRK+10] J. Wu, S. A. Raczynski, Y. Kitano, T. Nishimoto, N. Ono, and S. Sagayama. Statistical harmonic model with relaxed partial envelope constraint for multiple pitch estimation. In *Music Information Retrieval Evaluation eXchange*, Utrecht, Netherlands, August 2010.

[WS05] X. Wen and M. Sandler. Partial searching algorithm and its application for polyphonic music transcription. In *6th International Conference on Music Information Retrieval*, pages 690–695, London, UK, September 2005.

[WVR+11a] J. Wu, E. Vincent, S. Raczyński, T. Nishimoto, N. Ono, and S. Sagayama. Polyphonic pitch estimation and instrument identification by joint modeling of sustained and attack sounds. *IEEE Journal of Selected Topics in Signal Processing*, 5(6):1124–1132, October 2011.

[WVR+11b] J. Wu, E. Vincent, S. A. Raczyński, T. Nishimoto, N. Ono, and S. Sagayama. Multipitch estimation by joint modeling of harmonic and transient sounds. In *IEEE International Conference on Audio, Speech and Signal Processing*, pages 25–28, Prague, Czech Republic, May 2011.

[WZ08] Y. Wang and B. Zhang. Application-specific music transcription for tutoring. *IEEE MultiMedia*, 15(3):70–74, July 2008.

[Yeh08] C. Yeh. *Multiple fundamental frequency estimation of polyphonic recordings*. PhD thesis, Université Paris VI - Pierre at Marie Curie, France, June 2008.

[YG10] K. Yoshii and M. Goto. Infinite latent harmonic allocation: a nonparametric approach to multipitch analysis. In *11th International Society for Music Information Retrieval Conference*, pages 309–314, Utrecht, Netherlands, August 2010.

[YG12a] K. Yoshii and M. Goto. A nonparametric Bayesian multipitch analyzer based on infinite latent harmonic allocation. *IEEE Transactions on Audio, Speech, and Language Processing*, 20(3):717–730, March 2012.

[YG12b] K. Yoshii and M. Goto. Unsupervised music understanding based on nonparametric Bayesian models. In *IEEE International Conference on Audio, Speech and Signal Processing*, pages 5353–5356, Kyoto, Japan, March 2012.

[YR04] C. Yeh and A. Röbel. A new score function for joint evaluation of multiple F0 hypotheses. In *International Conference on Digital Audio Effects*, Naples, Italy, October 2004.

[YRR05] C. Yeh, A. Röbel, and X. Rodet. Multiple fundamental frequency estimation of polyphonic music signals. In *IEEE International Conference on Audio, Speech and Signal Processing*, volume 3, pages 225–228, Philadelphia, USA, March 2005.

[YRR10] C. Yeh, A. Röbel, and X. Rodet. Multiple fundamental frequency estimation and polyphony inference of polyphonic music signals. *IEEE Transactions on Audio, Speech, and Language Processing*, 18(6):1116–1126, August 2010.

[YSWJ10] T.-Y. Hu Y.-S. Wang and S.-K. Jeng. Automatic transcription for music with two timbres from monaural sound source. In *IEEE International Symposium on Multimedia*, pages 314–317, Taichung, Taiwan, December 2010.

[YSWS05] J. Yin, T. Sim, Y. Wang, and A. Shenoy. Music transcription using an instrument model. In *IEEE International Conference on Audio, Speech and Signal Processing*, volume 3, pages 217–220, Philadelphia, USA, March 2005.

[Yu10] S. Z. Yu. Hidden semi-Markov models. *Artificial Intelligence*, 174(2):215 – 243, 2010.

[YWS92] X. Yang, K. Wang, and S. A. Shamma. Auditory representations of acoustic signals. *IEEE Transactions on Information Theory*, 38(2):824–839, March 1992.

[ZCJM10] J. X. Zhang, M. G. Christensen, S. H. Jensen, and M. Moonen. A robust and computationally efficient subspace-based fundamental frequency estimator. *IEEE Transactions on Audio, Speech, and Language Processing*, 18(3):487–497, March 2010.

[Zho06] R. Zhou. *Feature extraction of musical content for automatic music transcription.* PhD thesis, École Polytechnique Fédérale de Lausanne, October 2006.

[ZLLX08] X. Zhang, W. Liu, P. Li, and B. Xu. Multipitch detection based on weighted summary correlogram. In *6th International Symposium on Chinese Spoken Language Processing*, Kunming, China, December 2008.

[ZR07] R. Zhou and J. D. Reiss. A real-time frame-based multiple pitch transcription system using the resonator time-frequency image. In *3rd Music Information Retrieval Evaluation eXchange*, September 2007.

[ZR08] R. Zhou and J. D. Reiss. A real-time polyphonic music transcription system. In *4th Music Information Retrieval Evaluation eXchange*, September 2008.

[ZRMZ09] R. Zhou, J. D. Reiss, M. Mattavelli, and G. Zoia. A computationally efficient method for polyphonic pitch estimation. *EURASIP Journal on Advances in Signal Processing*, 2009. Article ID 729494.